CONTINUITY DEVELOPMENT BETWEEN PRECAST BEAMS USING PRESTRESSED SLABS, AND ITS EFFECT ON FLEXURE AND SHEAR

By

ALUTHJAGE DON CHANDRATHILAKA JAYANANDANA

A Thesis Submitted in Fulfilment of the Requirements

for the Degree of Doctor of Philosophy

Department of Civil Engineering

The University of Leeds

January 1989

To My Parents

ABSTRACT

Development of continuity between precast prestressed bridge girders by post-tensioning the insitu top slab in the regions of hogging moment is a relatively new technique which forms the basis for this research study. Compared to the more conventional method of using reinforcing steel in the slab over the interior supports, prestressed slabs will ensure a crack free more durable bridge deck, and will therefore reduce the maintenance costs.

The effect that such a slab has on flexural and shear behaviour of the bridge deck has been studied both analytically and experimentally by considering composite beams based on M-8 standard precast beam section. Comparison of the design of bridge decks with a prestressed slab and a reinforced concrete slab indicated that a partially prestressed slab with a prestress considering up to 50% of the live load will ensure the slab remains crack free under total service load. Although secondary effects and the two stage construction of such a slab tend to increase the prestress requirement for the slab, the same two effects considerably reduce the positive midspan moments, resulting in a decrease in the prestress required in the precast beams (and thus a possible increase in the span range) for given standard precast beam sections.

The experimental investigation consisted of testing eleven 1/3-scale M-8 continuous composite beams in two series, Series-A and Series-B. Series A, in which three beams were tested as double cantilevers was planned to study the effects of prestressed slab on overall flexural behaviour. A considerable improvement in crack control under service loads and a higher ratio of measured to calculated ultimate moment capacity was obtained in beams with a prestressed slab. The continuity developed using insitu prestressed slabs was very effective at all levels of loading. Recommendations have been made for the flexural design of continuous bridge decks with this type of prestressed slabs.

In Series B, effect of prestressed slabs on shear strength at the continuity connection has been studied. A considerable increase in web shear cracking load was obtained for beams with prestressed slabs, resulting in a decrease in the amount of shear reinforcement required for such beams. The different methods of predicting web shear cracking strength and web crushing strength according to current design codes were compared with experimental values, and based on the results, recommendations for the design for vertical shear of composite beams subjected to hogging moments have been made.

ACKNOWLEDGEMENTS

I would like to thank Professor A.R. Cusens, Head of the Department of Civil Engineering of the University of Leeds for the opportunity to carry out this project. I wish to express my gratitude and sincere thanks to Mr. A.E. Gamble for his invaluable suggestions, encouragement and helpful supervision throughout the course of this research work.

I would like to thank the technical staff of the Department for their ready assistance in the preparation and testing of specimens, and photography.

I wish to express my gratitude to the Commonwealth Scholarship Commission (U.K.) for the scholarship and the University of Moratuwa (Sri Lanka) for the study leave which enabled me to complete this work.

I would like to extend my thanks to Dr. N. Gowripalan for checking the manuscript of this thesis. Thanks are also due to my friends who helped me in the preparation of the thesis.

Finally, I am greatly indebted to my parents and sisters for their patience and encouragement.

TABLE OF CONTENTS

LIST OF TABLES

LIST OF PLATES

PRINCIPAL NOTATION

A	Cross sectional area of beam
Aps	Area of prestressing steel
A_s	Area of non-prestressed tension reinforcement
A_{sv}	Cross sectional area of the two legs of a link
a_v	Shear span
b	Breadth of the beam
b_w	Breadth of the web
d	Effective depth
E_c	Modulus of elasticity of concrete
E_s	Modulus of elasticity of steel
e	Eccentricity
f_c	Concrete stress
f_{cp}	Prestress at the centroid
f_{cu}	Compressive strength of concrete cubes
f_c'	Compressive strength of concrete cylinders
f_{pe}	Effective prestress
f_{pu}	Characteristic strength of prestressing steel
f_r	Modulus of rupture of concrete
f_s	Steel stress
f_t	Tensile strength of concrete
f_y	Yield stress of tension reinforcement
f_{yv}	Yield stress of shear reinforcement

h	Overall depth
h_f	Flange thickness
L	Span
L_t	Transmission length
M	Bending moment
M_{cr}	Flexural cracking moment
M_o	Decompression moment
M_p	Prestressing moment due to prestress in the slab
M_u	Ultimate moment
P	Effective prestressing force
r	Shear reinforcement ratio ($r = A_{sv}/b\ s$)
s	Spacing of shear reinforcement
V	Shear force
V_c	Shear force carried by concrete
V_{co}	Web shear cracking load
V_{cr}	Flexural shear cracking load
V_p	Vertical component of prestressing force of inclined tendons
V_s	Shear force carried by stirrups
V_u	Ultimate shear force
v_c	Shear strength of concrete
w	Crack width
x	Neutral axis depth
α	Ratio of length of prestressed portion of slab to overall span

γ_{fl}	Partial safety factors applied to loads
γ_{f3}	Partial safety factors applied to load effects
γ_m	Partial safety factors applied to material strength
ε_c	Concrete strain
ε_s	Steel strain
ν	Poisson's ratio
ρ	Tensile steel ratio ($\rho = A_s/b\ d$)
ϕ	Curvature

CHAPTER 1

INTRODUCTION

1.1 General

Composite beams made with prestressed concrete girders and in-situ concrete slabs have been used in medium span bridges for many years. Although different methods of construction and different shapes of girders have been used, they are all constructed to carry loads as monolithic beams. In the most commonly used construction, precast girders of 'I' or inverted 'T' are placed side by side and then connected by an insitu cast concrete slab. This form of construction became very popular and standardised precast sections have been developed in U.K. [1] and USA leading to better economy in construction. This type of construction can be used for simple span decks or even made continuous. This thesis is concerned with continuity of composite beams consisting, in this instance, of precast 'M' beams, which are normally spaced at 1.0 m centres and an insitu concrete top slab[2].

Composite beams have many advantages over monolithic beams. They offer all the advantages of factory fabrication of precast girders, such as economy, good quality control, reuse of forms etc. and when some types of composite beams are used, external formwork is not necessarily required to cast the top insitu slab. This results in a very economical solution when the headroom becomes high. Composite beams use a smaller area for the precast section but the overall stiffness and strength are not reduced as a top slab is added later. This results in a lighter, and yet structurally efficient, section. Since prestress is applied only to the precast girder the required prestressing force is relatively small and will not be too critical at transfer due to the intrinsic shape of the

precast section.

As long as separation between precast beam and insitu slab is prevented, the two parts of the composite beam behave as a monolithic unit in carrying applied loads. When loaded, horizontal shear stresses will develop at the interface, but these can be resisted by ensuring a good bond between the precast beam and the slab, which can be achieved by making the top surface of the precast beam as rough as possible and providing steel stirrups extending from the precast beam into the slab[3].

1.2. Continuity Between Precast Girders

1.2.1 Importance of Continuity

Continuous composite beams offer many advantages over a series of simple spans, if site conditions allow their use in bridge decks. In this type of construction, the top slab is cast continuously over the supports making that part of the bridge deck joint-free. Leakage of water and de-icing salts through these joints in simple span beams, at the piers, can cause the deterioration of cross heads and piers. This is a serious problem affecting the durability and maintenance costs of many bridges in Great Britain and USA, however well these joints are made[4]. Continuity is adopted as an effective solution to this problem[5]. In addition to improving durability it also provides a smooth riding surface for motorists.

The other advantages of continuous composite beams are related to the structural behaviour. When the same section is used, a continuous beam can carry a higher load than a simple beam, with mid-span moments and deflections being reduced and allowing the use of smaller sections in continuous beams. This, in turn, will result in economy of materials and reduction in dead weight. In the

case of an overload, redistribution of stresses can take place in continuous beams and failure will occur only when moment capacity at two or more sections has been exceeded. This means that a higher factor of safety against collapse can be achieved[3,6].

Although fully continuous insitu prestressed beams have all the above advantages, and may also save the cost of anchorages at the supports, they have some draw backs. Developing full continuity over all the spans is not easy and involves complicated tendon profiles, and difficult stressing operations. Higher friction loss due to curved profiles, secondary stresses and shortening of long members due to prestress etc. are some of the disadvantages in achieving full continuity insitu. These effects are not so predominant in partially continuous beams in which continuity is effective in carrying only a part of the total load applied on the beam, mainly the superimposed dead load and live load, as prestressing or non-prestressed steel used to develop partial continuity is provided only in the region of internal supports. Consequently, the main attention of this study is focussed on the development of partial continuity between precast girders using a new technique involving prestressing the top slab in the region of negative(hogging) moments and its practical and economic viability. The details of this new method and some of the other methods used to develop partial continuity will be considered later.

1.2.2 Different Methods of Developing Partial Continuity

Some of the methods used for developing partial continuity between precast girders are illustrated in Fig. 1.1 and 1.2.

Fig. 1.1.(a) shows the use of cap cables to establish continuity between precast beams over the supports[7]. Although stressing of these cables is not

difficult, the curvature of the cables makes the fictional losses very high and the use of rods difficult.

In Fig. 1.1.(b) is shown a system using post-tensioned bolts. These bolts are straight and therefore the frictional loss is small but difficult to stress. An alternative arrangement is to locate the bolts horizontally near the top of the beam by increasing the height of the beams in the support region.

It is also possible to establish continuity between precast beams by applying a transverse prestress as shown in Fig. 1.1(c). Additional reinforced or prestressed concrete planks are placed between the ends of adjoining beams as tying elements. Transverse prestress is applied after erection of girders and tying elements. Alternatively, the precast girders themselves can be tapered and overlap each other over the supports for applying prestress. The transverse prestress then holds the beam together and effectively makes them continuous for subsequent loading.

Fig. 1.2 illustrates the methods of developing continuity using an in-situ cast top slab. The added slab acts compositely with the precast beams in carrying the loads applied after the development of continuity.

Fig. 1.2 (a) shows a method in which non-prestressed reinforcing bars are placed in the top slab in the region of the supports to resist the hogging moments. The advantage of this method over the methods shown in Fig 1.1 is that no stressing is involved. The feasibility of this method was studied at Portland Cement Association Laboratories in 1960's [8,9] and this is the widely used method at present to connect precast beams for partial continuity.

Fig. 1.2(b) shows another method similar in concept to the previous one. In this case, precast prestressed concrete rods are used instead of reinforcing bars[10]. It is also possible to use them in combination with reinforcing steel. It is expected that the prestressed rods, in addition to resisting

negative moments, have a restraining effect on secondary insitu concrete to delay the cracking and thereby increase the cracking moment. Although this method also does not involve stressing at the site, the bond between the prefabricated prestressed rods and in-situ concrete could cause problems.

Another method of developing continuity between precast beams is shown in Fig. 1.2(c). In this method, the ends of the precast beams from adjacent spans are embedded in a concrete crosshead which is cast while the precast beams are being supported by temporary scaffolding. Reinforcing bars are provided in the insitu crosshead to carry negative moments. The spans of the bridge is increased by the inclusion of a crosshead. However, this method requires scaffolding which is not necessary in other methods described above. This method has been used in bridge construction in U.K [11].

Very few research studies have been undertaken to study these different methods. The method using non-prestressed reinforcement in the in-situ slab (Fig.1.2(a)) has received the most attention from investigators[8,9,13,14]. The application of this method in connecting double T beams in building construction has also been studied[15].

1.2.3 Proposed New Method for Developing Partial Continuity

The research work outlined in this thesis was undertaken to study a new proposal for developing partial continuity in beam and slab bridges. In this method, the slab near the interior supports is prestressed by post-tensioning straight tendons between points of contraflexure. As in methods shown in Fig.1.2.(a) and 1.2.(b), previously, the precast beams are erected first, then the top slab is cast in the region where negative moments develop under service loads and post-tensioned with straight tendons to create a partially prestressed

composite section near the support. After post-tensioning, the rest of the slab is cast.

The sequence of construction for a two span bridge using this technique is shown in Fig.1.3. The aim of prestressing the slab is to eliminate cracking of the slab under service loads and if cracks appear under high live loads, enable them to close after load is reduced, keeping the slab in compression. In other words, to maintain a crack free slab under service loads while developing continuity between precast beams in adjacent spans. This is a great advantage over the most commonly used method of reinforced slab which is designed as a cracked section under service loads.

1.2.4 Advantages of the New Method

The new method offers many advantages over the other conventional methods of developing continuity, the most important one being the crack free slab under service loads as mentioned in previous section. Therefore, the prestressed slab is expected to improve durability of bridge decks. Bridge decks are subjected to very unfavourable exposure and the action of de-icing salts, freezing of water etc. A recent study has shown that the durability of deck slabs can be improved by prestressing [16,17]. In that study, durability of both prestressed and reinforced slabs was investigated comparatively by subjecting both types of slab to aggressive de-icing salt exposure conditions. Both types of slabs were loaded until cracking occurred, prior to being subjected to such exposure conditions. During the exposure test these slabs were loaded to open up the cracks at regular intervals. The results of these tests showed that prestressing had significantly reduced the chloride penetration and incidence of corrosion of steel at the cracks compared to the reinforced slab. The main reason

for the improvement in durability is that when cracks are not wide and close after unloading, chlorides, water and oxygen cannot penetrate easily into the slab, thereby reducing the risk of corrosion. It also reduces frost damage. Therefore, prestressing the slab will improve the durability of bridge deck and reduce the maintenance cost. Although prestressed rods [10] are expected to delay cracking and close cracks when loading is removed, they are not very effective as the whole slab is not in compression.

In addition to the improvement in durability, a prestressed slab improves the structural behaviour of the composite beam at the connection as the cracking moment and stiffness are increased. A favourable stress distribution is created in the composite section by the prestress in the top slab at the support where otherwise, prestress in the pretensioned beams would be very small at their ends due to the build up of prestress along the transmission length. Since additional prestress is added to the precast girders, we can expect increased shear capacity in addition to the improved flexural behaviour of the joint. These improvements in the flexural and shear behaviour will be studied in detail, both analytically and experimentally, in later chapters.

Another advantage of this new method is that it eases the congestion of reinforcement in the top slab at the continuous support. Unlike other methods described in Section 1.2.2, stressing is easier and simple anchorages can be used. Also, as strands are straight, frictional losses are small.

In this method, the top slab is cast in two stages, and thus a greater part of the self weight of the top slab is added to the beam after continuity has been developed, effectively reducing the mid-span moment due to self weight of the slab.

Although the ultimate moment capacity of the slab may be the same as a reinforced concrete slab, there are many improvements under service load

conditions inherent in this method. These together with improved durability and reduced maintenance cost should offset any additional cost incurred in prestressing.

In recent years, there has been increased attention by research workers to the use of prestressed slabs in composite bridges. Already several research reports have been published on the application of prestressed slabs in negative moment regions of composite bridge beams consisting of steel girders and insitu cast concrete slab [18,19,20]. They have shown that prestressing the slab is very satisfactory and increases the cracking load and stiffness considerably. The same technique should be used with more benefits in concrete composite beams.

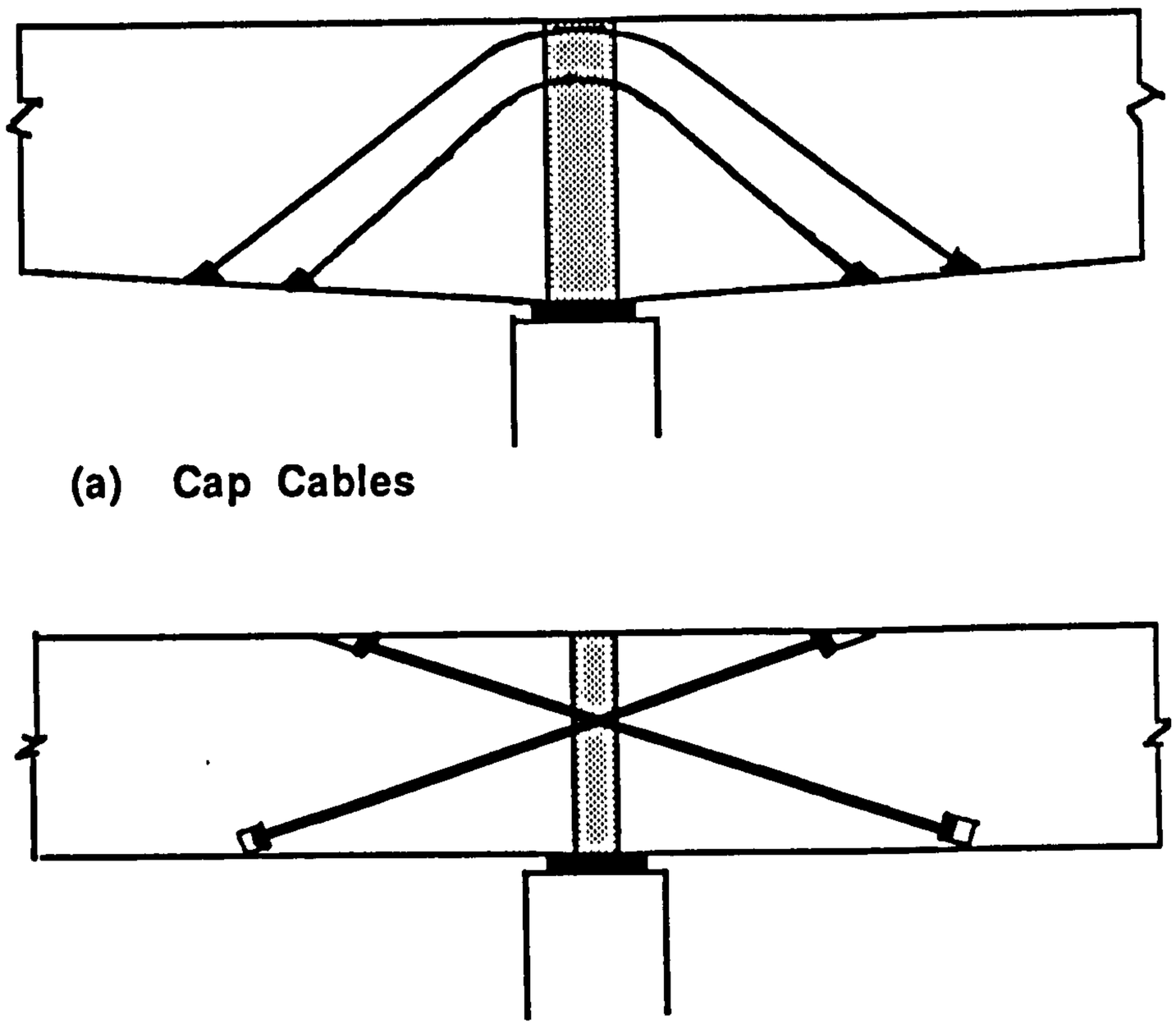

(a) Cap Cables

(b) Post-Tensioned Bolts

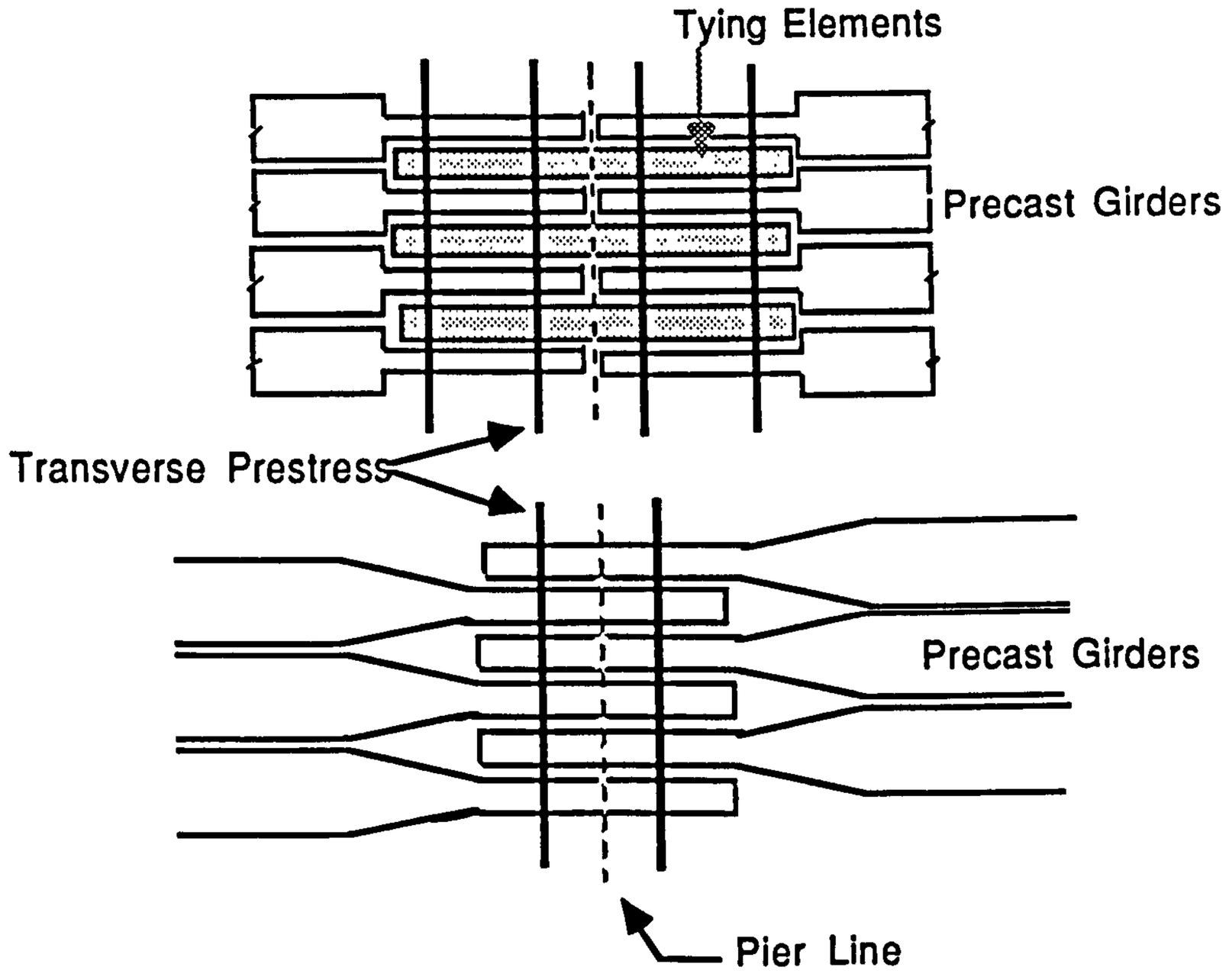

(c) Transverse Prestress

Fig. 1.1 Methods of Developing Continuity Between Precast Beams

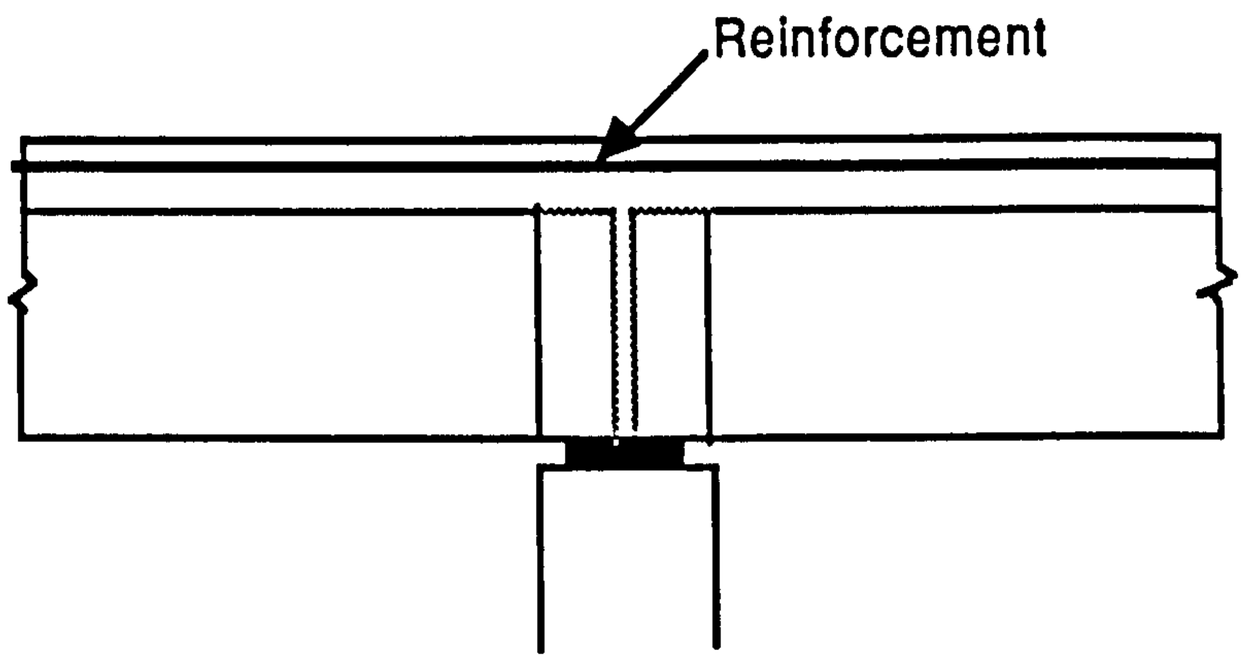

(a) Reinforcement in the Deck Slab

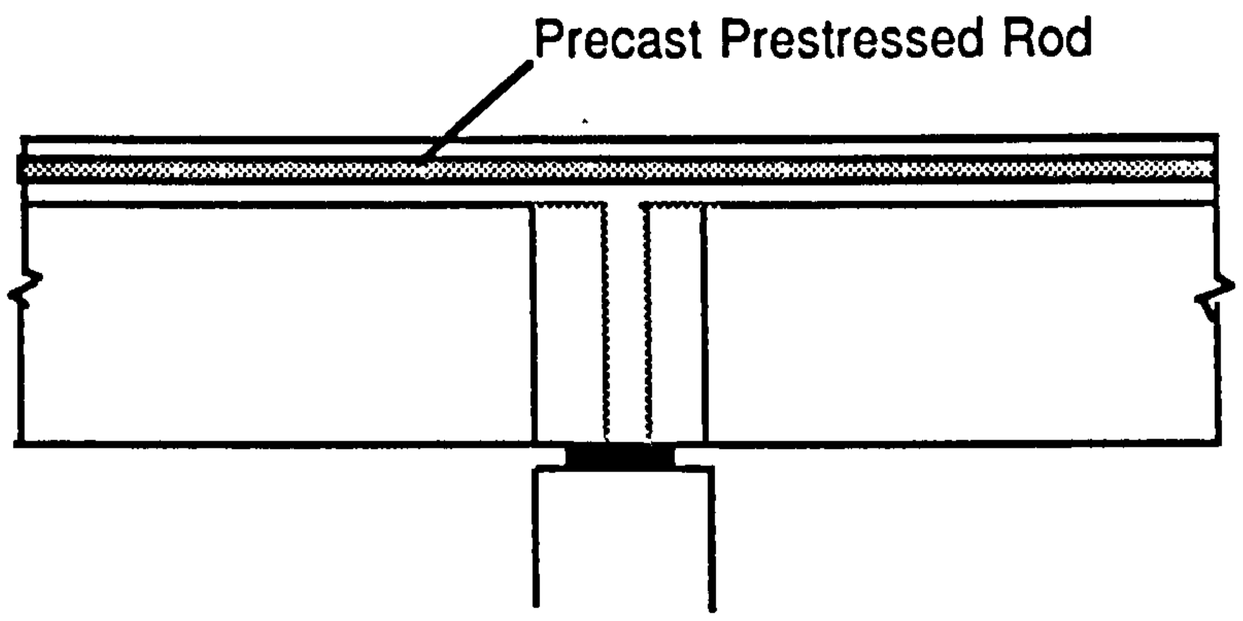

(b) Precast Prestressed Rod Reinforcement in the Top Slab

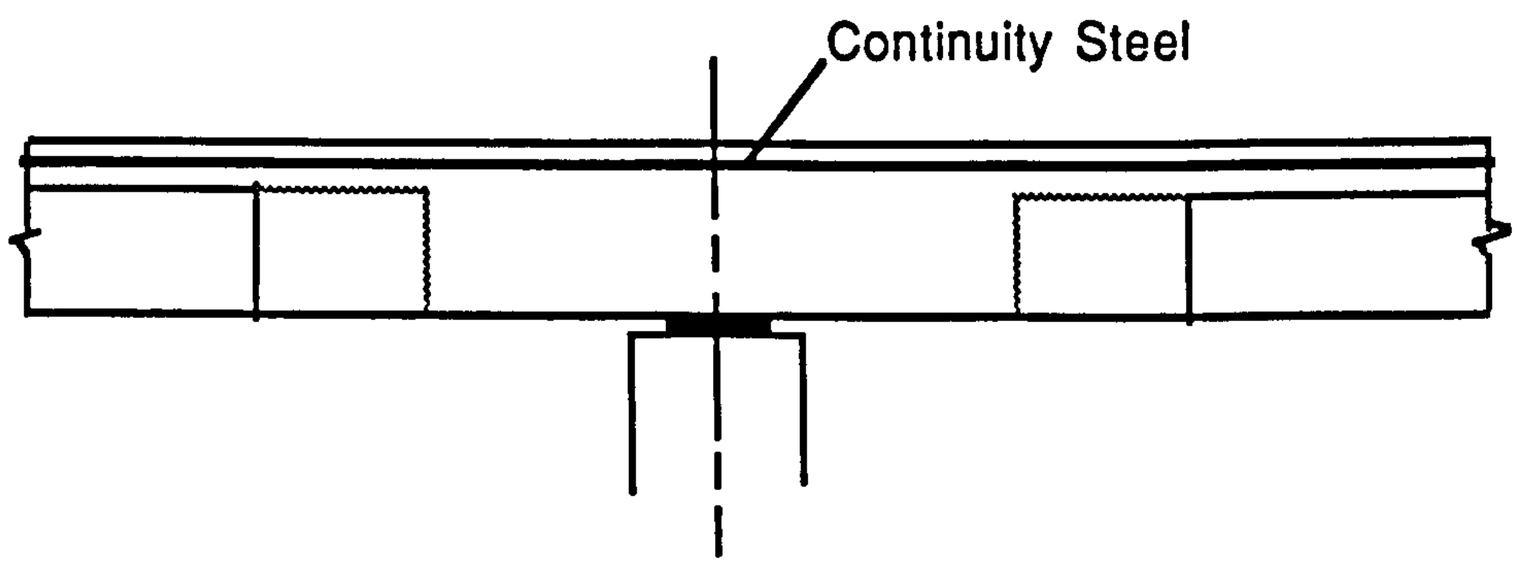

(c) Beams Embedded in Crosshead

Fig. 1.2 Types of Continuity Connections for Precast Beams Using In-Situ Concrete Top Slab

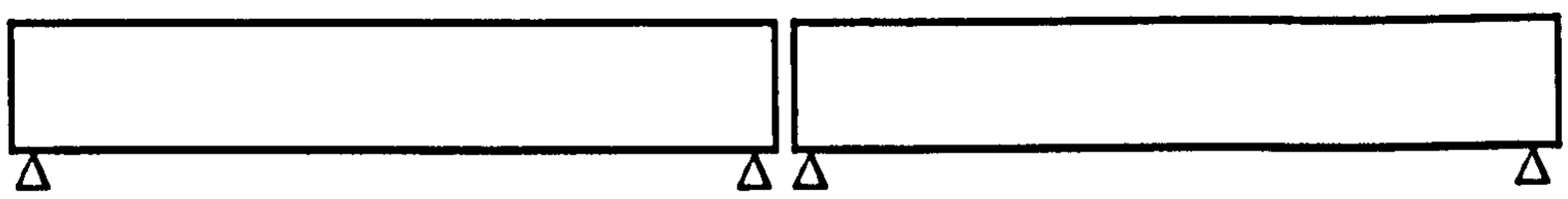

(a) Stage 1: Precast Prestressed Girders are Placed on Supports

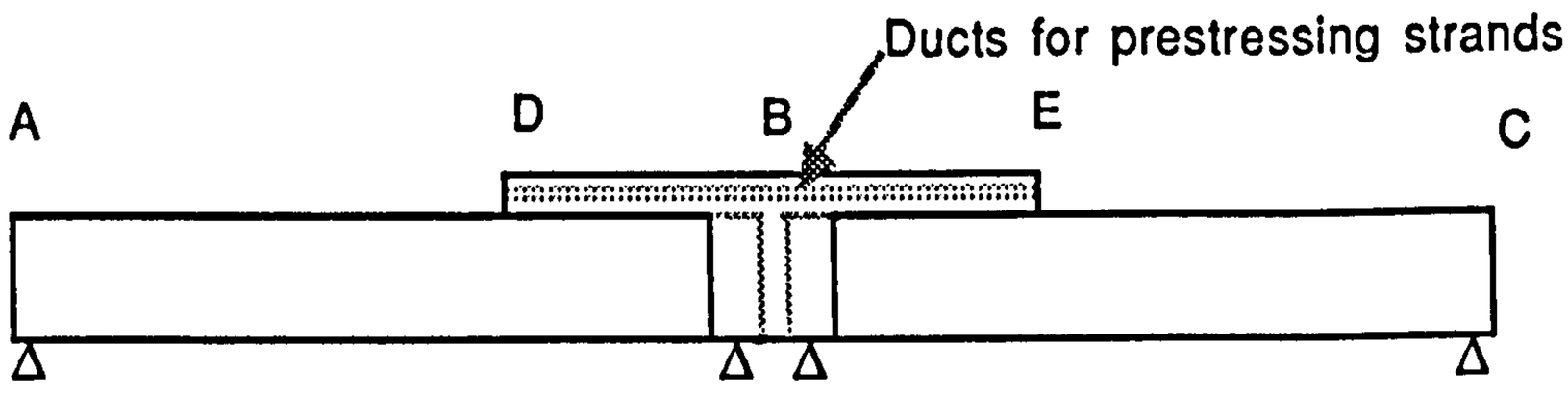

(b) Stage 2 : Casting of In-Situ Concrete Top Slab and Diaphragm

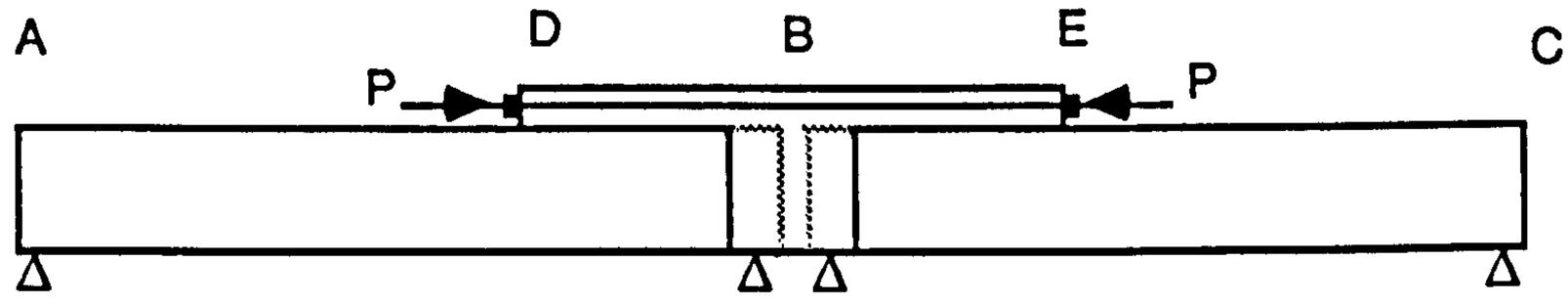

(c) Stage 3 : Post-Tensioning of Top Slab

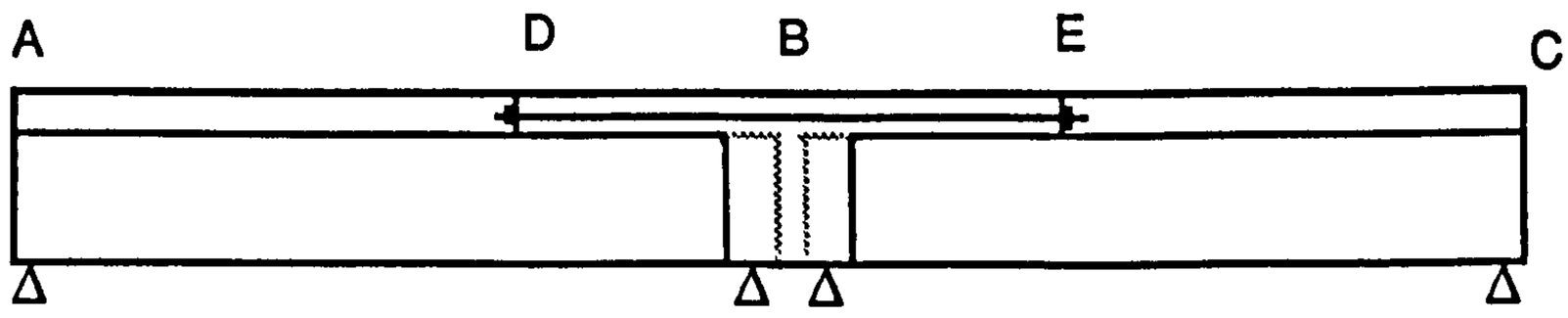

(d) Stage 4 : Casting of the Remainder of the Slab

Fig. 1.3. Sequence of Construction for the Proposed Method

CHAPTER 2

REVIEW OF PREVIOUS WORK ON CONTINUITY OF COMPOSITE BEAMS

2.1 General

Although the concept of establishing continuity between precast beams of composite section has gained popularity and has been adopted in many bridge construction works over the last two or three decades, there is little available literature on the strength and behaviour of continuous composite beams subjected to negative moments. Much research has been published on the subject of the behaviour of monolithic reinforced and prestressed beams in negative bending, but the continuous composite beams is a much more complex problem. Even though a number of methods are available for developing continuity between precast members in bridge construction, only a few have been studied experimentally. The most widely used method, that of developing continuity by placing non-prestressed reinforcement in the top slab, has attracted the attention of most researchers. There was also an experimental investigation to study the effectiveness of precast prestressed rods as tension reinforcement for negative moments [10]. In recent years, there has been a considerable interest in using prestressed slabs in negative moment regions of steel-concrete composite beams. In this chapter, though, only research work related to the continuous composite beams subjected to negative moments will be reviewed briefly.

2.2 Portland Cement Association Tests [8,21-25]

In the early 1960's, an extensive experimental programme was carried out at the PCA laboratories in the USA to study the feasibility of establishing

partial continuity by placing reinforcing bars in the top slab and at the same time obtain additional information required in the design of such bridges in practice. At that time, the use of precast prestressed beams had been well established in bridge construction and interest was growing in this method of developing continuity between girders, mainly due to its simplicity of construction operations at the site and the advantages of continuity at the interior supports. The experimental programme was completed in several stages and covered many aspects of continuity connection. They were

(1) Pilot tests to study the feasibility of establishing live load continuity by using deformed bars.

(2) A study on horizontal shear transfer between precast girders and in-situ deck slab.

(3) Design of a typical two span continuous bridge using this type of continuity connection.

(4) Flexural strength of continuous composite beams.

(5) Shear strength of continuous composite beams subjected to negative moments.

(6) Behaviour of the continuity connection under repeated loading and reverse bending.

(7) Effects of creep and shrinkage on continuity behaviour.

(8) Tests on 1/2 scale continuous bridge.

The results of the different stages of the experimental programme were published in a series of PCA Laboratories Development Department bulletins[8,21-25]. In this thesis, the main attention is given to the flexural and shear strength of the continuous beams. Therefore, only results of tests relevant to those two areas in particular will be discussed here.

2.2.1 Pilot Tests on Continuous Composite Girders [8]

As the first stage of the PCA laboratory investigation, a series of pilot tests were carried out on composite beams to study the feasibility of developing continuity by providing deformed bars in the top slab over the support. Fifteen T-shaped composite beams were tested in three groups. In Group 1, three composite beams, each consisting of a single precast girder and top slab were tested as double cantilevers. These beams did not have any joint. Nine beams were tested in Group 2 in a similar manner, but each beam consisted of two short precast girders connected by a top slab and diaphragm. Group 3 beams were made from two short girders connected to one long precast girder by the top slab and two diaphragms and were tested as continuous beams. The details of these beams and loading arrangements are shown in Fig 2.1.

One of the main objectives of the pilot tests was to study the effects of girder prestress and slab reinforcement on the ultimate strength of the continuity connection. These two parameters were selected as the main variables. Three different percentages of deck reinforcement (0.83%, 1.66% and 2.49%) were used together with three different percentages of girder prestress (zero, 0.6% and 0.9%). It was thought that the ultimate moment capacity of the composite beams in negative bending would be limited by the compressive stresses in the bottom flange of the precast girders which already had a prestress. Group 1 and Group 2 beams were tested as double cantilevers to study this effect. To produce the most severe case, straight prestressing strands were used in all beams. Group 1 beams, with continuous prestressing strands over the support, had the highest compressive stress in the bottom flange at the critical section.

The theoretical ultimate flexural strength of these beams was calculated using a rectangular stress block for concrete. In the calculations, two separate

cases were considered. In one case, prestress in the girder was included and in the other, it was neglected. In the first case, it was assumed that prestress was fully effective along the entire length of beam (i.e. transmission length is zero). When the prestress was considered, the ultimate moment capacity was reduced due to the reduction of the internal compressive force as a result of prestressing forces in the compressive zone. This effect was more predominant at higher slab reinforcement percentages (greater than 0.8%). When the slab reinforcement percentage was low, there was a slight increase in the ultimate moment capacity when prestressed steel was considered. This was due to the fact that some strands could be found located above the centroid of the compressive force in the concrete. For practical range of slab reinforcement (between 0.5% and 1.5%) the difference between the two cases was small and can be neglected in the design calculations if the amount of prestress is not too high.

The ultimate moments obtained from tests of Group 1 and Group 2 beams were compared to moments calculated by both considering and neglecting the prestressing steel on the girders. The average ratio of measured moment to calculated moment (neglecting prestress) decreased from 1.23 to 0.83 when slab reinforcement increased from 0.83% to 2.49%. When the prestressing steel was considered, the corresponding ratios were 1.23 and 1.02. This confirmed the conclusion drawn from the results of the analysis that prestress effects may be significant when slab reinforcement percentages are high.

All the beams with a deck reinforcement percentage of 0.83% failed due to yielding of steel. The beams with low girder prestress and 1.66% of slab reinforcement failed in a similar manner. The beams with 1.66% slab reinforcement and high prestress and beams with 2.49% slab reinforcement and low prestress behaved as balanced section at failure. Only in beams with high prestress and the highest percentage of slab reinforcement (2.49%) was failure controlled by compression. From these results it was concluded that compression

in the bottom flange is not critical for the practical range of slab reinforcement from 0.5% to 1.5%. In all tests the failure occurred out side the diaphragm but very close to it. It was also observed that the balanced percentage of slab reinforcement reduced when prestress in the girders was increased. Also, the horizontal shear stresses were well resisted by the rough surface of the precast girders and projecting shear stirrups.

Three beams in Group 3 were subjected to equal negative moments at the two supports and a positive moment at the mid-span by the loading arrangement shown in Fig. 2.1. This made it possible to study whether the continuity connection allowed any redistribution of moments as in other continuous structures. The main variable was the percentage of slab reinforcement (0.83% and 1.66%). The results of the three tests showed that when flexural cracks developed at the supports well below the working load, the moment of inertia of the section was affected resulting in a change of moment distribution along the beam. Up to cracking, the ratio between negative and positive moments remained approximately constant and once the section at the supports cracked, the ratio changed, depending on the relative amount of positive and negative reinforcement. In all three beams yielding of negative moment steel took place before failure.

The results of the pilot tests showed that negative moments could be carried successfully by this type of continuity connection in composite beams. The compressive stress at the bottom of the beams becomes critical only if a very high percentage of slab reinforcement is used together with high girder prestress. At the ultimate stage, the prestressing forces reduce, due to the high compression at the bottom of girders, and also the prestress is not fully effective at the ends of pretensioned girders. Normally, in practice, strands are debonded or deflected. Therefore, the conditions are not so unfavourable and full ultimate moment capacity of the negative steel could be developed in most cases. The test results of Group 3 beams indicated that the continuity connection developed by

the fact that deformed bars allowed considerable redistribution of moments at the ultimate load.

After these pilot tests of the PCA investigation, a similar experimental study was carried out to investigate the use of a similar method of developing partial continuity between precast beams in building construction [15]. A number of double -T beams were tested. The actual experimental investigation carried out and the results obtained were very similar to the PCA Pilot tests and therefore will not be discussed here. It was concluded that this method can also be used satisfactorily in building construction to develop continuity between precast prestressed beams.

2.2.2 Bridge Design Studies (PCA Tests) [22]

In Part 3 of the PCA experimental programme, a two span continuous composite bridge was designed according to the existing American specifications at that time. The objective of this was to study the application of the method of developing continuity by using deformed bars in a more practical case and to understand the problems associated with the design of continuous highway bridges. The two span was selected because it was considered to represent the more critical case in many aspects. After designing a two lane bridge consisting of five precast girders to carry self weight and live loads including impact loads, it was decided to test half scale model beams to study the behaviour of a bridge under such loading. The model beams were fabricated and tested in a manner to simulate as close as possible the conditions that would exist in the full scale highway bridge by careful scaling of dimensions, loads and moments.

In the first part of the experimental study a half scale two span beam was tested to check the general behaviour of a continuous bridge girder subjected to design loads and subsequent higher overloads. The beam was subjected to three

tests. In the first test, the load was increased up to the design load and then unloaded. In the second, up to twice the design load and the third test was continued up to the failure. Reactions, deflections and also crack widths were measured. The applied moment and the ratio of support moment to mid span moment were compared with those obtained by elastic theory assuming constant stiffness along the beam. Flexural cracks appeared in the slab before the load reached the design load in the first test. From this stage onwards, the measured bending moments deviated from the elastic moments. When the load was increased above the design load, cracking became more extensive and the effects of the reduced stiffness at the support section were reflected on the measured support moment and mid-span moment. The ratio of support moment to mid-span moment reduced considerably when loading was continued in the third cycle. The deflection readings at the mid-span showed that the residual deflection increased in the second and third tests as expected in any reinforced concrete structure. The beam underwent a considerable deflection to give ample warning before final failure occurred. The cracks opened very early in the second and third tests and became wider as load and steel strain increased.

At the ultimate load, yielding of steel and crushing of the concrete was observed both at mid-span and support, although the final failure was at the support. The beam had an ultimate moment capacity greater than that calculated according to the limit state design. No moment redistribution was considered in determining the theoretical moment and this could have been one of the reasons for the greater flexural strength at the support. The behaviour at the ultimate state was considered to be satisfactory. At service load also, measured deflections and crack widths satisfied the requirements for reinforced concrete members. Several questions arose at the design phase of the highway bridge, concerning such aspects as the shear strength of composite beams subjected to negative moments, the strength of the connection under repeated loads and the effects of

creep and shrinkage on the behaviour of the beam etc. To find solutions to these, more model beams were tested.

2.2.3 Shear Tests of Continuous Girders [23]

One of the areas where uncertainty existed during the design of continuous prestressed highway bridge, in Part 3 of the PCA investigation, was the design criterion for sections subjected to both negative moments and shear forces. No test data was available on the shear strength of composite beams subjected to such loading conditions. Due to this lack of information in an important aspect of design like shear, Mattock and Kaar [23] carried out a series of shear tests on half scale composite beams similar to those used in previous tests of the PCA study.

Fifteen half scale composite beams with a continuity connection were tested to study the shear strength of beams subjected to negative moments. There was a considerable concern before these tests about the influence of any flexural cracks appearing in the top slab on the shear strength of the composite section.

The major variables for this test series were the influence of shear reinforcement (varied from 0.38% to 1.14%) and the location of the applied vehicle loads. The details of the test beams and the loading arrangement are as shown in Fig. 2.2. The ratio of shear span(x) to effective depth(d) varied from 1.0 to 4.5.

Thirteen beams in the test series failed in shear with a typical mode of failure being a diagonal compression failure of the web. Web crushing, in all beams, started in the lower quarter of the web depth, near the support, and spread along the beam at the ultimate load. Although there were many flexural cracks near the support, they were too close to the support or too steeply inclined to lead to a shear failure. There were some flexural cracks which merged

with diagonal cracks but they were not critical. When diagonal cracks first appeared, the crack widths were from 0.075 mm to 0.10 mm. The crack widths near to failure were between 1.3 mm and 1.8 mm. Although the load deflection curves had the same shape, the length of curve increased when the shear reinforcement percentage was increased. Therefore, it was concluded that the ductility increases with the increase in the shear reinforcement. Stirrup strain measurements taken during the tests indicated that stirrup strain was very small until the diagonal cracks had appeared, and increased rapidly in tension afterwards. Stirrups in the region of diagonal cracking yielded immediately after the inclined cracking.

The test results showed that the diagonal cracking load and the ultimate shear strength increased when shear span/effective depth ratio was reduced, especially when the ratio was less than 3.0. The ultimate shear strength also increased when the percentage of shear reinforcement was increased.

To explain the mode of failure of the test beams, the authors put forward a hypothesis. Mattock and Kaar explained that web crushing at the end of struts between diagonal cracks was not due to axial compression but due to combined axial compression and bending. Their hypothesis was based on the observations that failure always started at the bottom of the web and the ultimate shear strength of beams was influenced by the amount of shear reinforcement. Fig.2.3 shows the forces acting on a single compression strut according to this hypothesis. Two forces are present in the strut which is connected to the compression flange at the bottom. They are a compression force (C) and shear force (S). Magnitudes of these two depend on the amount of shear reinforcement and the angle of inclination of the strut, which is influenced by the shear span/effective depth ratio. The force polygon indicates that when the stirrup force(F) increases, S becomes smaller and struts carry higher compressive force before failure. There is a limit for the increase of F beyond which struts

fail in compression. This means that shear reinforcement percentage cannot be increased indefinitely to increase the shear capacity of the beams. On the other hand, if no shear reinforcement is provided, the shear force S would be very large relative to C and strut will fail in tension at one face at the bottom immediately after cracking.

It is also clear from the force polygon that for a given amount of stirrup reinforcement, any change in the angle of inclination of struts will change C and S. For shorter shear spans, this angle increases with the decrease of shear span/effective depth ratio, resulting in an increase of C which in turn will increase the shear strength. This was confirmed by the test results. In all test beams, ultimate shear strength increased when x/d ratio was reduced. Mattock and Kaar also concluded that the contribution of stirrups to the ultimate shear strength of beams will decrease when the shear span/effective depth ratio is increased.

Based on the observations made, Mattock and Kaar put forward an expression to calculate ultimate shear strength as shown below.

$$\frac{(V_u - V_c)}{b\,d\,\text{Sin}\,\beta} = \frac{6.24\,(r\,f_{yv})}{\sqrt{f_c'}} - \frac{0.44\,(r\,f_{yv})^2}{f_c'} \quad \text{(psi)} \quad \text{..Eqn . 2.1}$$

where V_u = Ultimate shear force

V_c = Shear at inclined cracking

r = ratio of shear reinforcement

β = Angle of inclination of straight line drawn from load point to support

This expression assumes that the shear strength of the beam is the sum of shear strength of concrete (V_c) and shear strength provided by stirrups. This

equation was simplified to

$$A_{sv} = \frac{(V_u - V_c)\, s_v}{3.5\, d\, f_{yv}\, \text{Sin}\, \beta} \qquad \text{...Eqn. 2.2}$$

It was concluded that ductile failure could be ensured if a girder was designed in such a way that the load required to cause shear failure was at least 80% of the load required to cause flexural failure.

2.3 Burns (University of Texas)[10]

After the PCA laboratory tests, another experimental investigation was undertaken at the University of Texas during 1964-65, to study the use of a new type of tension reinforcement to carry negative moments at the supports of continuous composite beams. In this method, precast prestressed concrete rods were used in place of, or in combination with, deformed bars in the top slab. Improvements in controlling cracks in the deck slab were expected with this method , which was considered as a modification of the method of developing continuity by reinforcing bars, as the construction procedure was almost identical to the latter. Both these methods do not involve any stressing operation in the field.

Burns carried out an experimental programme similar to the pilot tests of the PCA laboratories to study the effectiveness of prestressed rods in continuous beams. Seven beams were tested, four as double cantilevers and three as two span continuous beams. In these beams, the type of reinforcement varied, viz, deformed bars, combination of deformed bars and prestressed rods and prestressed rods only. In two beams, post-tensioned strands of curved profile were included. The details of the test beams and loading arrangements are shown in Fig. 2.4.

It was expected that the cracking in the top slab would be restrained due to the fact that concrete in the slab was bonded to the prestressed rods which were in compression. When cracks have appeared at a higher load than that for a reinforced concrete slab, the prestressing force in the strands of precast rods would close the cracks after unloading. These predictions on behaviour of beams were confirmed to a certain extent by the observations made during testing of double cantilever beams. The load deflection curves for all three beams (beam A,B and C) showed a linear relationship up to cracking load and became non-linear as more cracks developed and reinforcement yielded at the support. These three beams were designed to have the same ultimate strength. The cracking load for the beam A having only reinforcing bars was about 25% of the ultimate load. The beam C with only prestressed rods had a cracking load of about half the ultimate load, showing a significant increase. the beam B with a combination of prestressed rods and deformed bars fell in between the limiting curves of A and C. It was also observed that the cracks tended to close when beams with prestressed rods were unloaded. The double cantilever beam with post-tensioning(Fig. 2.4(c)) showed similar behaviour to that of beams with prestressed rods. The only difference was that it could sustain a larger deflection before failure.

The two span beams (D and E) were identical in many aspects and exhibited very similar load-deflection response. The curves were linear even after the first cracking at the support up to cracking at mid-span. The beam D developed a weaker bond between precast rods and concrete causing the failure at a slightly lower ultimate load. The beam E failed after developing plastic hinges at the sections subjected to both positive and negative moments. The two span beam with post-tensioned strands failed at a higher load after following a very similar behaviour to the other two up to the cracking. This was mainly due to the higher moment capacity given by the post-tensioned strands.

The observations made during the tests led to the conclusion that precast

prestressed rods acted satisfactorily in restraining the cracking in the top slab. It was also shown that there could be difficulties in developing a good bond between prestressed rods and surrounding concrete which is very important for the performance of this connection.

2.4 Gamble (University of Illinois)[13,14]

At the University of Illinois, two three span continuous composite beams of 1/8-scale were tested in two stages after a study of long-term effects of continuous composite beams. The objective of the first stage, reported by Anderson et al.[13] was to study the effectiveness of continuity connection developed by providing reinforcement in the top slab at low load levels. The influence lines for reactions and mid span deflections were obtained experimentally by applying a small point load of 815 N (equivalent to a concentrated load of 52 kN in the prototype beam) at different locations along one of the beams. The experimental influence lines for reactions and deflections agreed very closely with the theoretical values obtained assuming full continuity and constant moment of inertia. These results indicated that this type of continuity connection is very effective at low load levels.

In the second stage which was reported by Gamble[14], two composite beams were subjected to overloads. The beams were tested in seven loading stages in which the location three point loads was changed to produce either maximum sagging moment in one of the spans or relatively high shear force and large hogging moment at one of the supports. Even though high shear forces were applied, shear behaviour was not considered due to the small scale of the test beams. Due to the limitations of the loading capacity of the rig, beams could not be loaded up to the failure. Therefore, the study was limited to the comparison of experimental cracking loads, deflections and reactions at high overloads with those

calculated using elastic theory.

It was discussed that the observed cracking moments were greater than those calculated using elastic theory. A reasonable agreement between theoretical and experimental values was obtained for reactions but measured deflections showed some deviations from the theoretical values.

Although the results indicated that the flexural behaviour of the continuous beams could be predicted with reasonable accuracy using elastic theory at overload conditions, the reliability of the results were affected by the use of very small scale model beams.

2.5 Prestressed Slabs in Steel-Concrete Continuous Composite Beams

Composite beams made of steel girders and in-situ cast concrete slab are still used in bridge construction. These also are best used as continuous beams, where the negative moments are resisted by reinforcing bars in the top deck slab. The reinforced concrete slab develops cracks under service loads, thereby reducing the effectiveness of the slab and composite action of the beam at the supports in carrying negative moments. It also causes reduction of moment capacity and stiffness of the section. In addition, the cracking exposes reinforcement bars for corrosion. Prestressing of the deck in the negative moment region has been under consideration as a possible solution to these problems.

It is expected that prestressed slabs would lead to crack free, more durable decks as well as to an increase in moment capacity of the support section. Already, several research works have been carried out in Canada and USA to study the application of prestressed deck slab in steel-concrete composite beams[18,19,20]. Although prestressing is used mainly as a means of controlling cracking in the deck slab in continuous steel-concrete composite beams (and such

beams made of two materials greatly differ in strength and other properties do not have the same characteristics of continuous prestressed composite beam at interior supports), the practical application of prestressed slabs in bridge decks and its effect on the cracking and structural behaviour are of interest to the research work outlined in this thesis. Therefore, some of the research studies on the use of prestressed slabs in composite beams will be discussed briefly.

2.5.1 Basu et al [18,19]

Analytical and experimental investigations were carried out by Basu et al[18,19] on the behaviour of partially prestressed composite beams consisting of a concrete slab supported by a steel beam .

In Part 1 of the study [18], the possible methods of applying prestress to the concrete slab were considered. One of the methods considered was jacking the interior supports upwards or stressing the steel girders before casting the slab and releasing them after concrete has hardened. Although this could induce some prestress to the slab, it was considered to be difficult and ineffective. Post-tensioning of the slab in the region of negative moment by prestressing strands in the slab was regarded as the most effective and adopted for the investigation. At the time of stressing, composite action must have developed and both slab and steel girders are stressed. After stressing, the rest of the slab is cast.

In the analytical investigation, the factors influencing the length of portion of the slab to be prestressed were considered. The compressive stress created in the concrete slab by the prestressing force is considered as the sum of axial compressive stress and stress due to prestressing moment. The positive primary moment at the support due to prestressing force acting at an eccentricity on the section is reduced by the negative secondary moment induced due to the

reactions of the indeterminate structure. This secondary moment increases when the length of the prestressed part of the slab is increased. This effect was found to be less significant when the number of spans is increased. Normally, the length of the prestressed part of the slab depends on the locations of the points of contraflexure of the bending moment envelope.

A two span composite beam with a prestressed slab subjected to two point loads on each span at one third points was analysed up to collapse. The case of a non-prestressed slab was also considered for comparison purposes. The ratio of prestressed length of the slab to span length was taken as 0.25. Theoretical moment-curvature relationships, load-deflection curves etc. were developed for both elastic and plastic stages. Theoretical cracking loads and ultimate moments were also calculated.

The results of the analysis showed that prestressing of the slab prevents cracking up to a load about 42% of the collapse load. It also increased the ultimate capacity by about 20% compared to the case without prestressing. The deflections of the beam without prestressing were about 30% greater than the deflections of beam with prestressed slab. These results indicated that smaller sections can be used for steel girders if slab is prestressed.

In Part 2 of the study [19], a two span composite beam was tested to verify the results of the analysis by experimental results. The details of the beam tested were identical to those of the beam used in the analysis. The testing was completed in two stages. In the first stage, the load was increased up to cracking of the slab at the interior support and then the beam was unloaded. In the second stage, the load was increased up to the maximum capacity of the loading system in a number of increments.

The results of the tests showed a close agreement with analytical results. The measured cracking load was almost equal to the calculated value. After unloading at the end of first stage, cracks closed completely. The load-deflection

curve of the second stage followed the curve of the first cycle very closely up to the cracking load, indicating that prestressing the slab had prevented the loss of stiffness of the section due to cracking in the first cycle, in addition to the increase in cracking load. The beam behaved linearly in the initial stages of loading.

Although the beam could not be loaded to failure due to the limitations of the capacity of the loading system, and occurrence of local buckling in the bottom flange of the steel girder, the other measured properties such as curvature at interior support, redistribution of moments, strains in the steel girder etc. showed a close resemblance to the theoretical values. The advantages of prestressed slabs predicted in the analysis were confirmed by the experimental results.

2.5.2 Kennedy and Grace (University of Windsor) [20]

Another research study on prestressed slabs in continuous composite bridges carried out at the University of Windsor, Canada [20], yielded similar results to those obtained by Basu et al[18,19]. It also confirmed the advantages of prestressing the concrete slab in negative moment regions of the slab and thereby preventing the loss of stiffness and composite action.

Kennedy and Grace[20] developed a theoretical solution to analyse composite bridge decks as a whole consisting of longitudinal and transverse steel beams and in-situ cast concrete slab, using equivalent orthotropic plate theory. Using this method they analysed a two span continuous composite bridge deck for two cases.

(a) Reinforced concrete deck slab over the entire length of the bridge deck.

(b) Prestressed slab in the region of negative moments and reinforced concrete slab for the rest of the bridge deck.

The bridge deck considered had five longitudinal steel girders and five steel beams as diaphragms. The length of the prestressed part of the slab was 0.27 of the span length.

To verify the results of theoretical analysis, two $1/8^{th}$ scale models of the two span composite bridge were tested. Model 1 had a reinforced concrete deck while the concrete deck of model 2 was post-tensioned longitudinally in the region of the intermediate support. Steel angles were used as shear connectors. Each model was subjected to two tests.

In the first test, a point load was applied successively to the mid-spans of the exterior girder, the first interior girder and the middle girder. The objective of this test was to check whether the analytical method predicted the distribution of moments, deflections etc. accurately when a point load is applied on the bridge deck. The measured moments and deflections of the bridge models agreed well with the theoretical values. Therefore the method of analysis was found to be satisfactory in analysing composite bridge decks.

In the second stage, the model bridge decks were subjected to two point loads at the mid-span of the middle girders. The load was increased to a load close to the calculated ultimate load. The following observations were made during the testing.

(1) In model 1, which had not been prestressed, the first cracks developed at a load of about 13% of the designed failure load whereas no cracks were detected at about 26% of the failure load in model 2.

(2) Very severe cracks developed in model 1 at about 55% of failure load. Some cracks were about 0.3mm in width. At the same load, cracks in model 2 were not so severe.

(3) When cracks appeared in model 1 at low loads, mid-span deflection of the model 1 was about 15% greater than that of model 2.

Based on the these observations and the results of the analysis, it could be concluded that prestressing the top slab could prevent cracking of the slab under service loads and increase the cracking load as well as the stiffness considerably.

2.6 Comments

The review of the available literature shows that the structural behaviour of continuous composite beams has not been fully investigated. Research on the most widely used method of developing continuity by reinforcing bars in the top slab in hogging moment regions has established that the continuity developed by this method is effective under small load levels as well as under overloads[8,14,22]. However, the serviceability conditions, specially cracking, and shear strength at the continuity connection have not received sufficient attention. Although shear tests of the PCA investigation looked into some aspects of shear behaviour of composite beams in hogging moment regions, the lack of data on the shear strength of continuous composite beams is clearly reflected from the insufficient guidance given in the design codes in this respect.

The research outlined in this thesis will deal with the serviceability conditions in flexure and shear strength of continuity connection developed using prestressed slabs in the hogging moment regions. The investigations on the application of prestress to the slab of composite bridge decks consisting of steel girders and concrete slab have indicated that considerable improvement in crack control and durability by this prestressing. The present investigation will be directed to study the effects of the prestressed slab on the flexural and shear behaviour of continuous composite beams consisting of precast concrete beams and in-situ concrete slab.

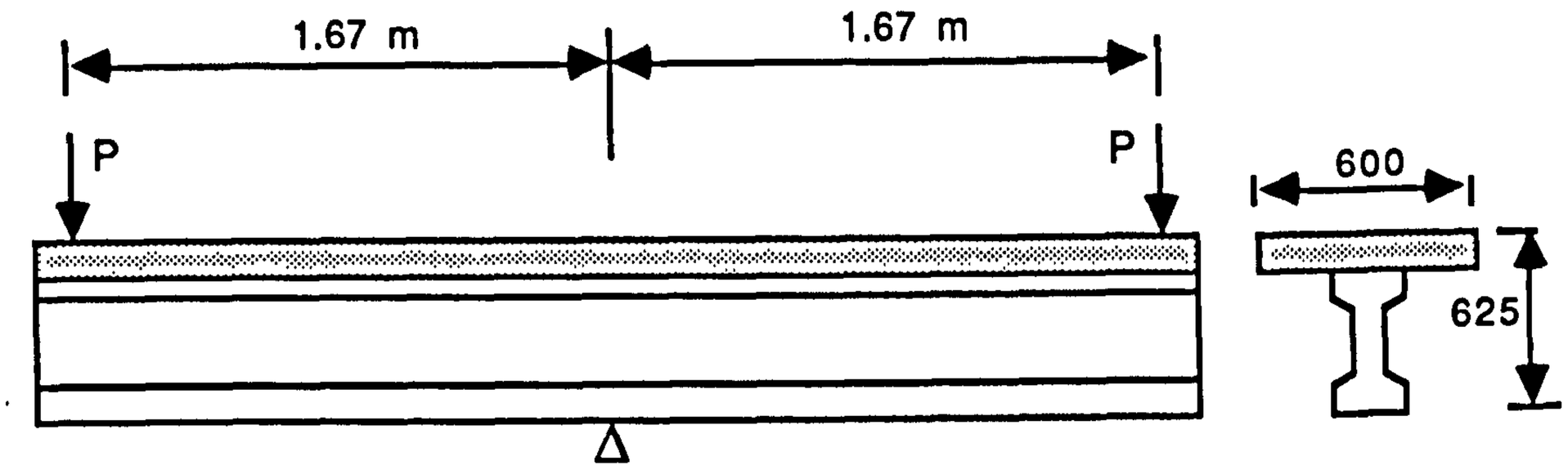

(a) Group-1 Girders

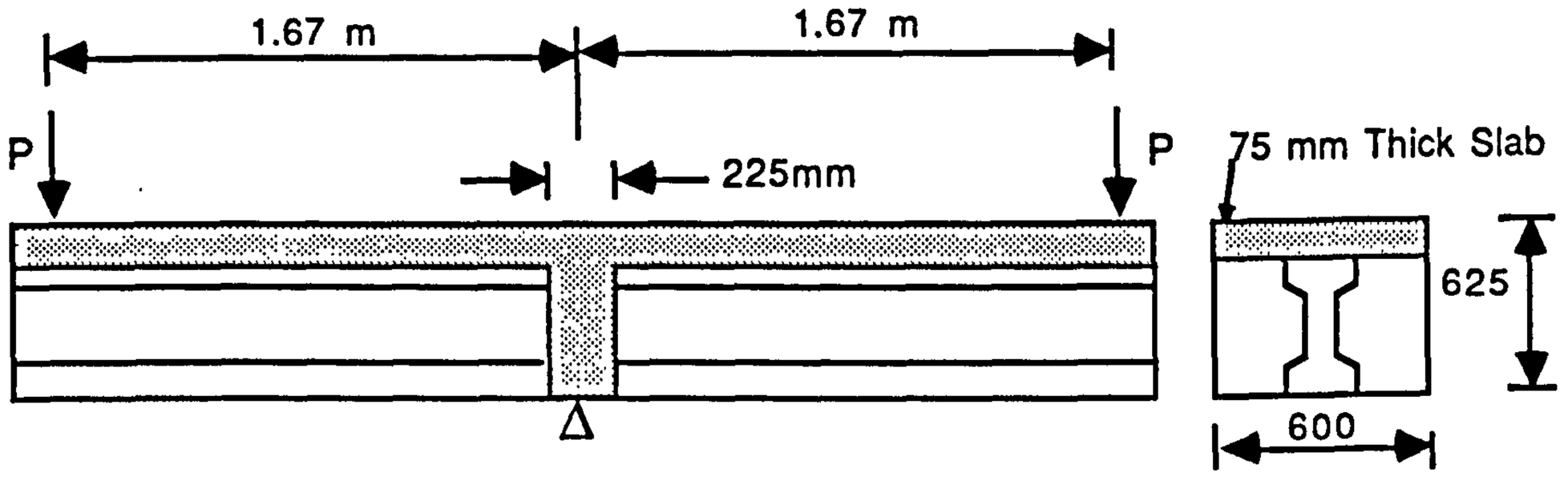

(b) Group-2 Girders

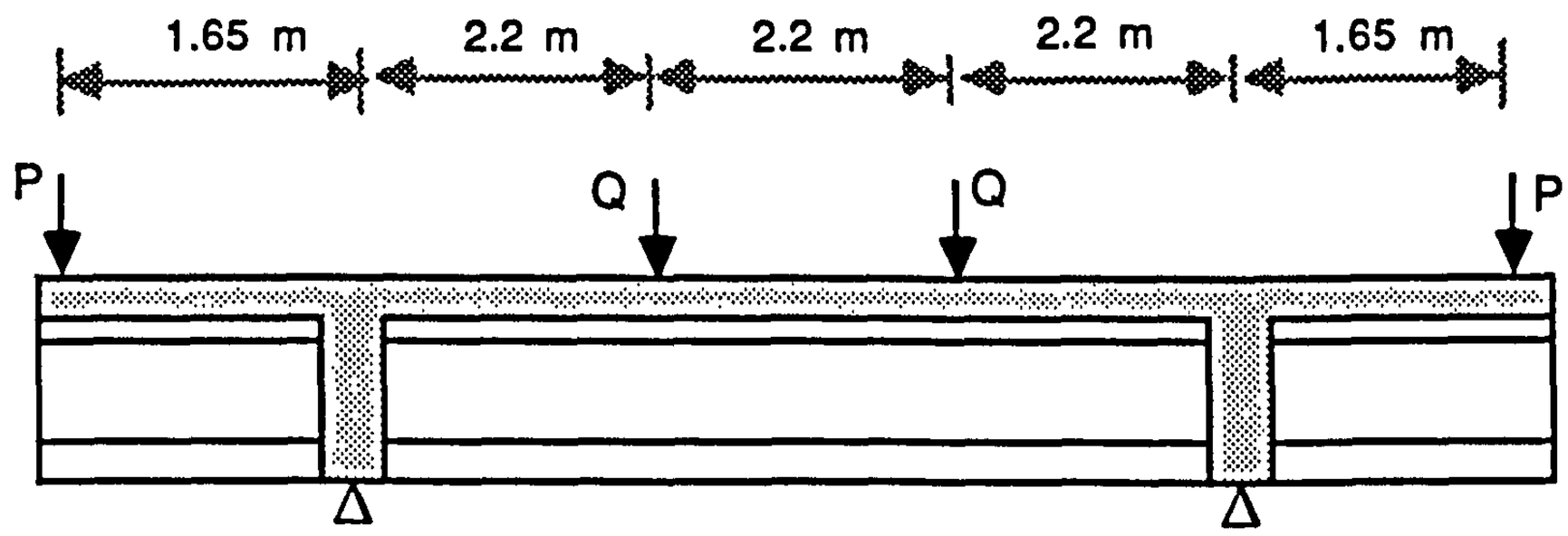

(c) Group-3 Girders

Fig. 2.1 Loading Arrangements of Girders of PCA Pilot Tests[8]

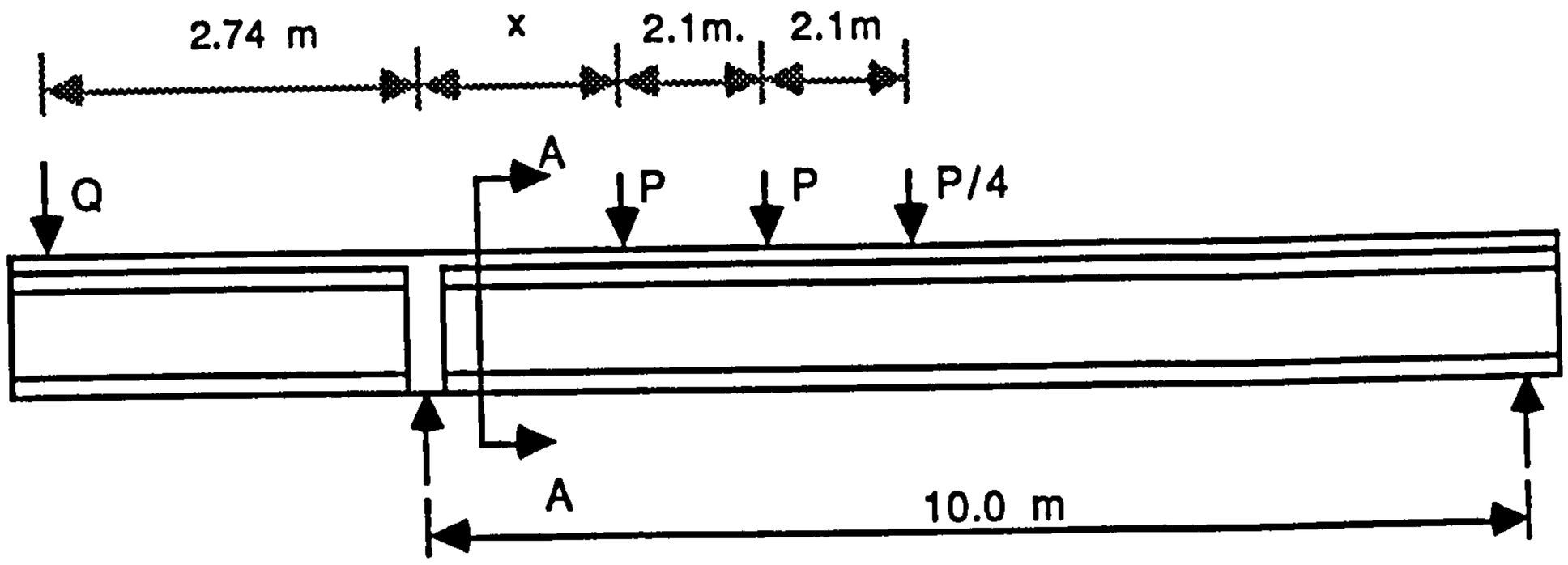

(a) Elevation

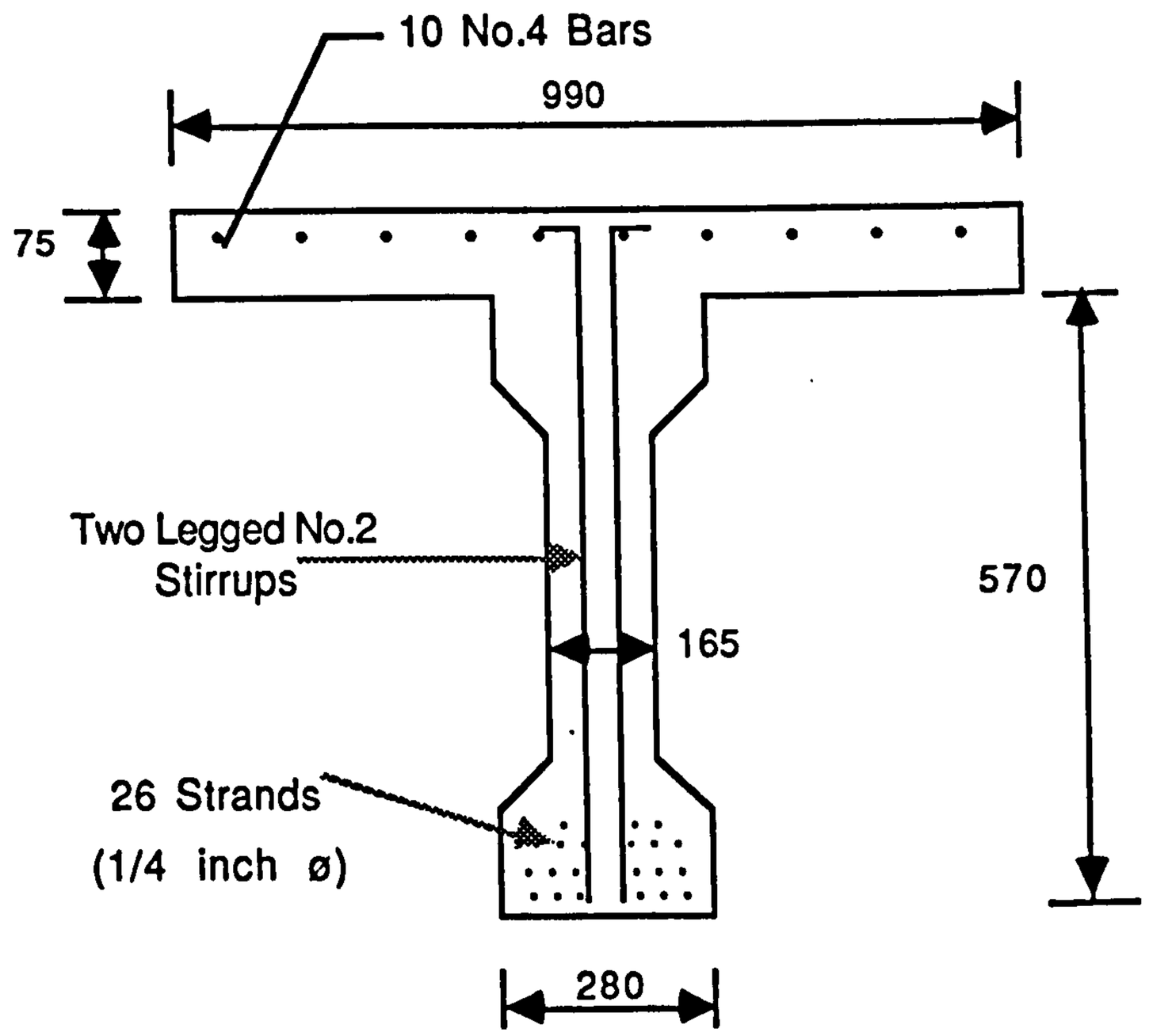

(Note : All dimensions are in mm)

(b) Section A-A

Fig. 2.2 Details of Beams in PCA Shear Tests (Mattock and Kaar[23])

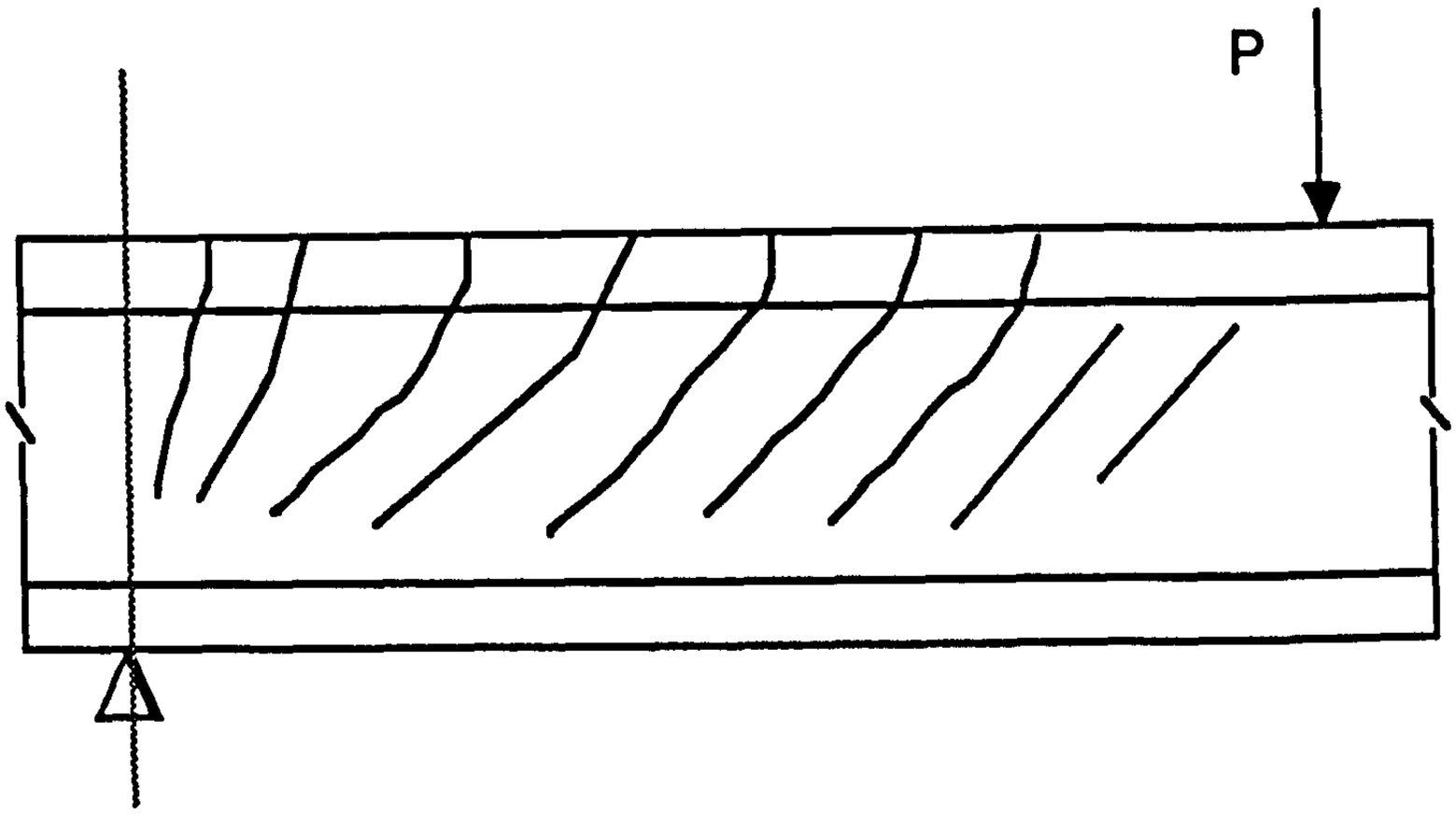

(a) Typical Crack Pattern Before Failure

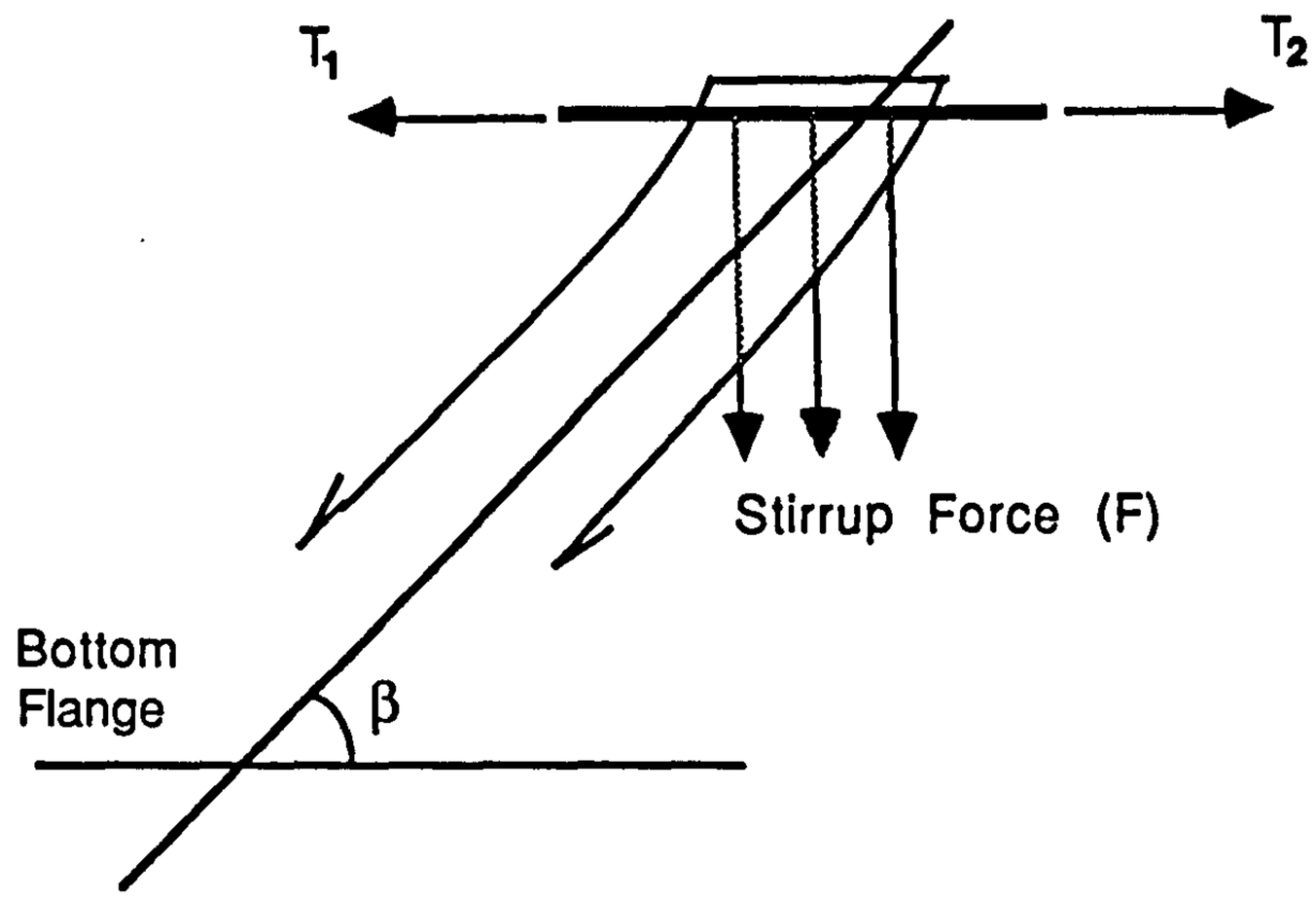

(b) Forces Acting on a Single Compression Strut Formed by Concrete Between Two Inclined Cracks

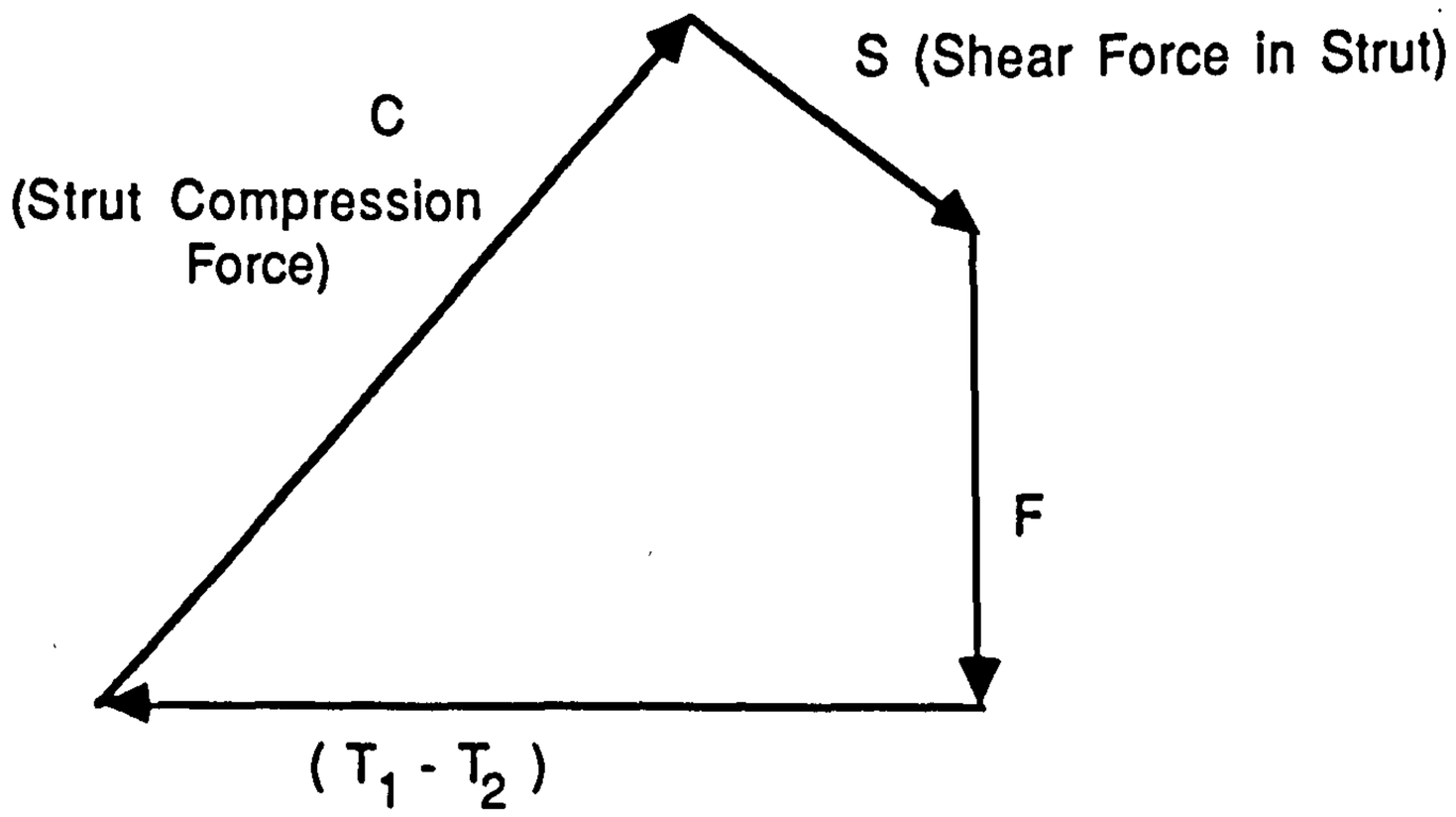

(c) Polygon of Forces Acting at Top of Compression Strut

Fig. 2.3 Diagonal Compression Failure of Composite Beams (Mattock and Kaar[23])

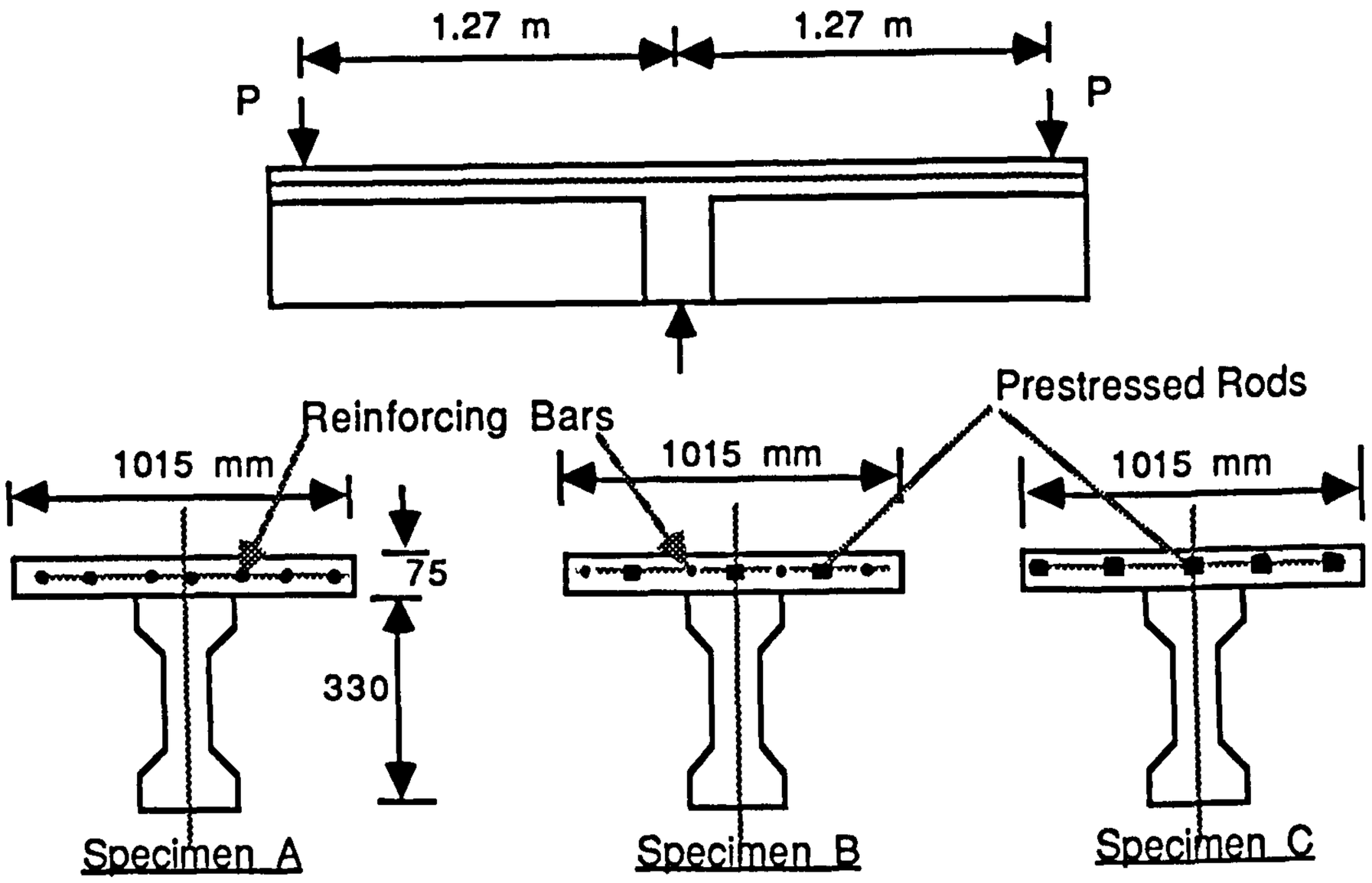

(a) Details of Double Cantilever Beams

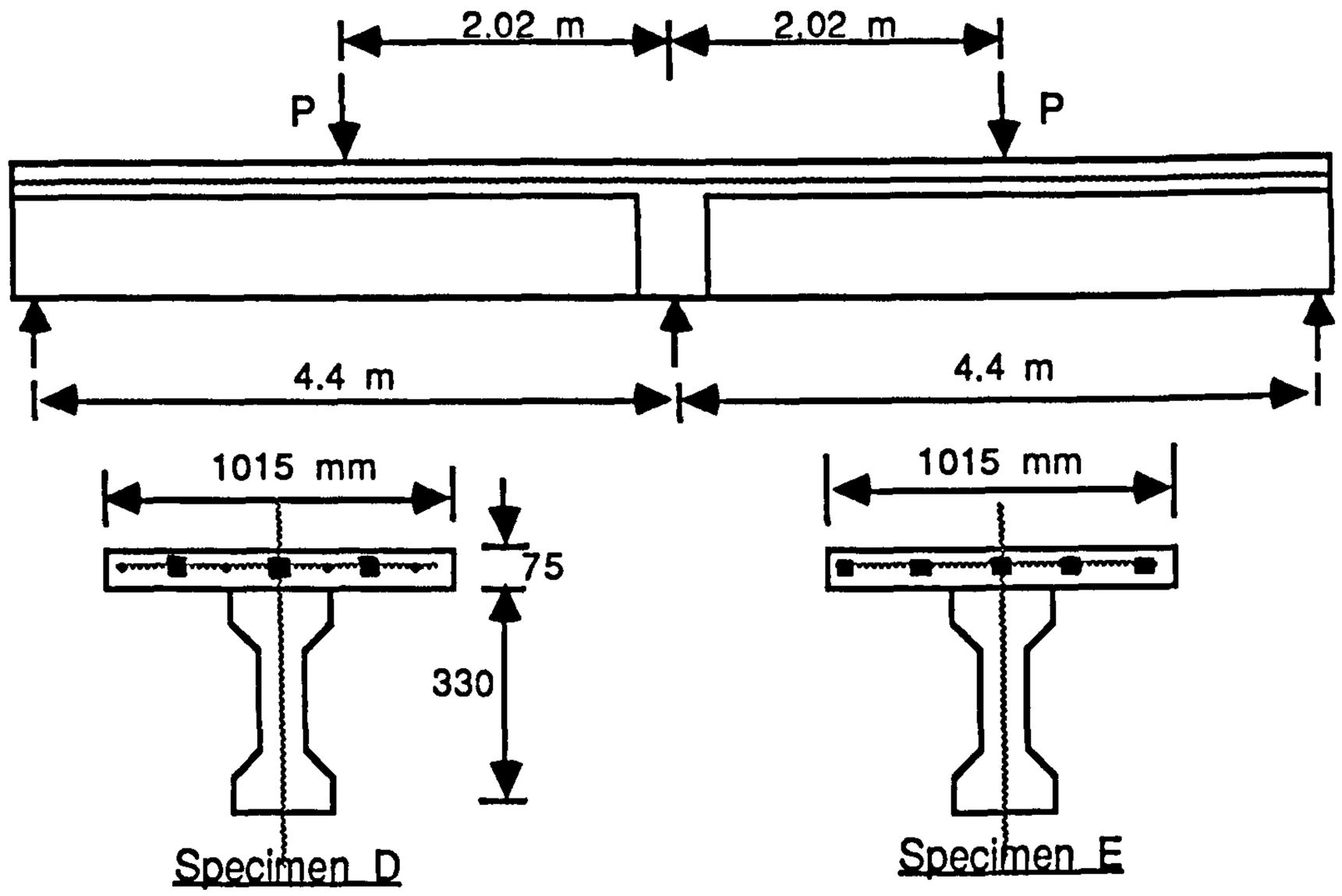

(b) Details of Two Span Girders

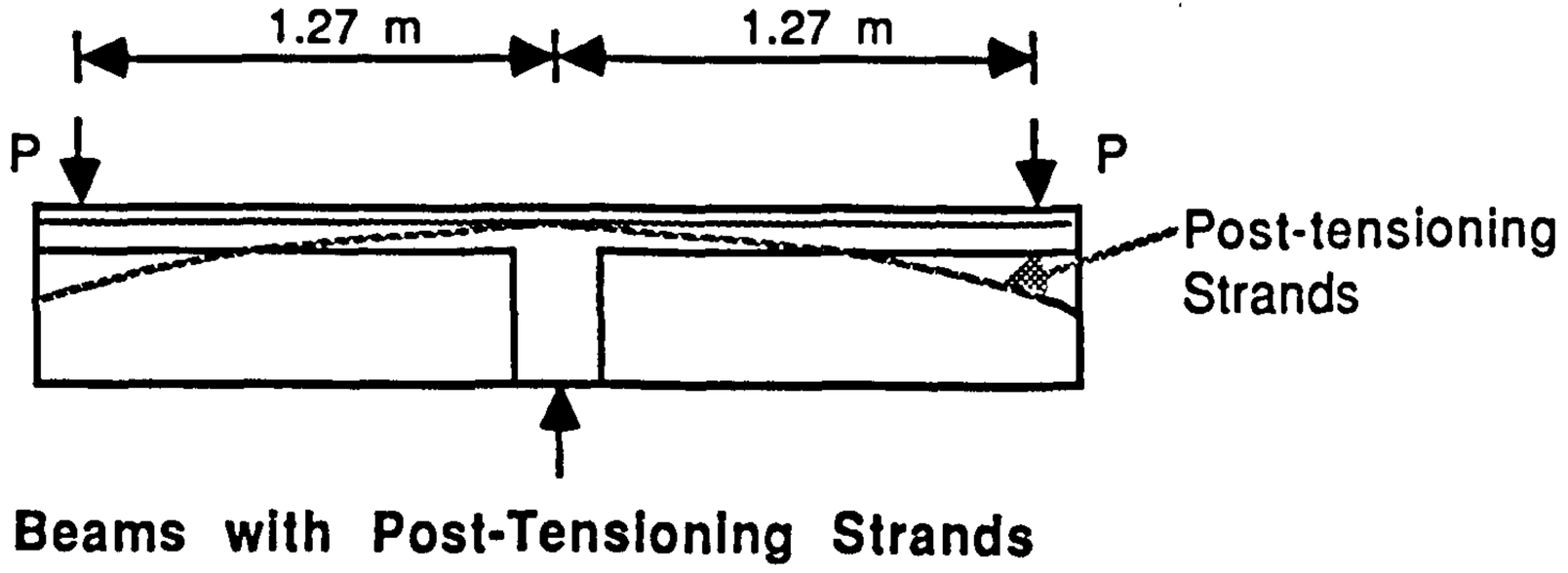

(c) Beams with Post-Tensioning Strands

Fig. 2.4 Details of Test Beams and Loading Arrangements (Burns[10])

CHAPTER 3

ANALYSIS OF PROTOTYPE BRIDGE DECK

3.1 Main Objective of the Study

The proposed method of developing continuity between precast beams by prestressing the composite top deck slab is a relatively new technique in bridge deck construction. Although there have been a few research studies carried out in recent years on the use of a prestressed slab in hogging moment regions of steel composite beams-mainly for controlling cracking in the top slab[18,19,20]-no research literature is available on the use of this technique with prestressed composite beams. Also, continuity between composite precast beams has received less attention from researchers. Therefore, before a method like this is used in practice, it is necessary to study all the important features of bridge decks which could use this method. It is considerably different from the conventional method of developing continuity in which no stress is applied to the top slab. Only the most important changes in the structural behaviour brought about by the application of prestress to the top slab will be studied in the research work outlined in this thesis.

The main objective of prestressing the slab at the interior support is not only to develop continuity but also to create a positive prestressing moment which together with the axial effects of prestressing force would keep the top slab in compression under total or part of the service moments applied after the development of continuity. This will ensure a crack free, more durable slab in the hogging moment region and increase the prestress in the precast girders near the joint. This can increase the web shear cracking strength and the flexural shear cracking strength at the support. In this study, the improvement in the behaviour

of the continuous composite beam in flexure and shear will be given the main points of consideration.

To study the above mentioned changes in the structure due to the prestressed slab, analytical and experimental studies involving this type of construction will be carried out. In the analytical study, a full scale continuous composite bridge deck with a prestressed slab in the hogging moment will be analysed and designed according to the BS 5400 for concrete bridges [26,27]. The size and the type of sections and layout of the bridge deck will be chosen to be similar to those commonly used in medium span bridge construction in Great Britain. The objective of this analytical study is to evaluate effects of the prestressed slab using a continuous bridge model and to obtain necessary data for the design of reduced scale model beams for an experimental investigation which will be carried out to study the effectiveness of the prestressed slab in developing continuity and controlling the negative moment cracking at the support. Flexural and shear behaviour will be the main topics studied in this programme. In both the analytical and the experimental studies, comparisons will be made between continuous bridges with reinforced slab (conventional method) and continuous bridges with prestressed slabs(proposed method). Also, the difference between bridges with a fully prestressed slab and a partially prestressed slab will be considered.

This research work will also study the adverse effects of applying prestress to the slab. One of such effects is the secondary moments induced by the application of prestressing moment to a continuous structure. This will cause a reduction in the applied prestressing moment at the support. The two stage construction of the slab which is necessary in this new method creates additional negative moment at the support due to weight of the slab. Although these two effects will increase the prestressing steel requirement for the slab at the interior supports, they have a desirable effect in mid-span region reducing the positive moment applied on the

beam. These effects will be evaluated in the analysis and the design of the prototype bridge deck. Also, the effects of increasing the compressive stress at the bottom of precast beams as a result of the post-tensioning of the slab will be studied.

3.2 The Effect of Prestress in the Slab on Bending Moment Distribution In Composite Beams

The use of a prestressed slab to develop continuity in composite bridge beams involves two stages of construction for the top slab and the application of a prestressing force to it. Both processes produce changes particularly in the bending moment distribution along the beam, compared with the conventional method of using a reinforced slab over the support. The most important effects are the inducement of a prestressing moment over the prestressed segment of slab and a change in the beams's behaviour in carrying the weight of the top slab. These effects will be discussed here with a prestressed slab. The span and the length of the prestressed portion of the slab in each span are L and αL respectively. Later, these will be numerically evaluated when a two span M-beam bridge deck is studied as a design model.

3.2.1 The Effect of Two-Stage Construction of the Top Slab

The top slab of a continuous composite beam has to be cast in two stages. First, the portion of the slab to be post-tensioned is cast. The weight of this slab is carried by two simply supported precast beams (see Fig. 3.1(a)). The maximum positive bending moment due to the weight of this slab occurs close to the interior support. As the bending moments due to the weight of the girders is smaller in this region, the moment due to the weight of the prestressed slab is not

significant.

When the remaining portions of the slab in the two spans are cast, continuity between the two spans has already been established. Therefore, the weight of the slab cast in the second stage is carried by a continuous beam with a composite section at the interior support and precast beam section in the remainder of the span (Fig. 3.1(b)). The composite section in the hogging moment region has a greater stiffness than the precast section along the rest of the beam. This difference in stiffness results in the support section carrying a greater portion of the load due to the weight of the slab than in the case where the beam has a uniform stiffness. The bending moment diagram is shown in Fig. 3.1(c).

Although the continuity and the variation of stiffness creates an additional bending moment at the interior support due to the weight of the slab, it considerably reduces the mid-span moment due to self weight of the slab. Also, the location of the section where bending moment due to the weight of the slab is maximum shifts from mid-span towards the end support. As a result, the maximum positive moment carried by the precast beam alone is reduced. In a beam with a reinforced slab, the maximum moment due to both self weight of girder and the slab occurs at the mid-span. This reduction in the span moment is very useful as prestressing steel required at the mid-span has to be provided for the entire length. This fact partly offsets the disadvantages of having an additional moment at the support where the amount of prestressing steel provided in the hogging moment region of the slab is relatively small. Also, any reduction in the span moment would allow an increase in the span range for a particular section of precast beam.

3.2.2 Secondary Effects of Prestress in the Top Slab

Post-tensioning of the portion of the top slab at the interior support

creates a compressive stress in the top slab to help overcome tensile stresses due to applied loads. This compressive stress, due to the prestressing force, is made up of two components, viz. component due to axial force and component due to the prestressing moment. When a prestressing force P is applied to the slab, it creates a positive uniform bending moment over the length of the prestressed slab as shown in Fig. 3.2.(a) and (b). This moment is equal to the product of the prestressing force P and the eccentricity e, and is called the primary moment due to prestressing.

At the time when prestress is applied to the slab, continuity has already been established, even though any significant hogging moment would only be carried after prestressing. The application of primary prestressing moment on an indeterminate structure such as a continuous beam, induces reactions at the supports, which in turn, produce negative bending moment along the entire beam (see Fig. 3.2(c)). These are considered as secondary moments due to prestressing. The reactions and secondary moments can be determined by using any method of linear elastic analysis taking into consideration the difference in stiffness of the beam AD(precast girders) and BD (composite section). The secondary moment at the support for this beam can be expressed as

$$M_s = \frac{3\alpha(2-\alpha)}{2R(1-\alpha)^3 + 2\alpha(\alpha^2 - 3\alpha + 3)} \times Pe \qquad \text{.....Eqn. 3.1}$$

where R is the ratio of second moment of area of composite section to that of precast beam and α is the ratio of the length of the prestressed slab to the span.

As a result of the secondary moments induced along the beam, the prestressing moment at the interior support is reduced. The resultant moment over the interior support due to prestressing force in the slab is equal to the algebraic sum of primary and secondary moments. This also can be expressed in

terms of R, α, P and e as shown below.

$$M = \frac{2R(1-\alpha)^3 + 2\alpha^3 - 3\alpha^2}{2R(1-\alpha)^3 + 2\alpha(\alpha^2-3\alpha+3)} \times Pe \quad \text{....Eqn.3.2}$$

The resultant bending moment diagram due to prestress for the two span beam is shown in Fig. 3.2(d). The values given in the diagram are for R=2.46 and α=0.225, which refer to the prototype bridge deck consisting of M-8 beams which will be considered later.

3.2.3 Factors Affecting Secondary Moment due to Prestress in the Slab

The Eqn.3.1 indicates that the secondary moment depends on the ratio of the length of prestressed segment of the slab to span (α), the ratio of stiffness (R) and the primary prestressing moment (P e). It is also clear that the length of the span has no direct effect on secondary moment.

3.2.3.1 Ratio of Length of Prestressed Slab to Span

For a given span and beam section, when the length of prestressed segment of the slab is increased, the secondary moment due to prestress increases causing a corresponding decrease in the applied prestressing moment at the support. The secondary moment and resultant moment at the support given by Eqns. 3.1 and 3.2 respectively have been plotted against α, the ratio of length of prestressed slab to span in Fig.3.3. Therefore, it is important that the length of the prestressed portion of the slab is kept to the smallest possible value as required by the

bending moment envelope due to applied loads.

Basu et al[18] have shown that in composite beams made of steel girders and prestressed concrete slab at the interior support region, the effect of increasing α becomes less critical when the number of spans is increased from two to four. The same effect is applicable to prestressed composite beams.

3.2.3.2 Stiffness Ratio Between Composite Section and Precast Beam

This is a parameter which remains fixed for a given section of precast beam and top slab. However, if different sizes of beams are considered, the secondary moments reduce when the stiffness ratio R is increased. The influence of this ratio over secondary moment reduces when the number of spans is increased[18].

If the difference in stiffness of precast beam and composite section for a two span beam is ignored (i.e. the value of R is taken as 1.0), the secondary moment effects will be much more significant than when the difference in stiffness is considered. The equation for resultant prestressing moment then becomes,

$$M = (1.5\alpha^2 - 3\alpha + 1) P e \qquad \text{....Eqn. 3.3}$$

For α=0.2, this represents 34% reduction in the resultant prestressing moment at the support. Fig. 3.3 also shows the variation of prestressing moment at the interior support of the two span beam for R=1.0 and R=2.46.

3.2.4 The Effects of Secondary Moments on Other Parts of the Beam

Although the secondary moments due to prestress in the top slab have an adverse effect on the prestressing moment at the interior support, it can be

beneficial in other parts of a continuous beam which are subject to sagging moment. As the secondary effects induces a negative moment throughout the beam (see Fig.3.2.(c)), it reduces the positive moment acting in the beam. This beneficial effect is enhanced by the fact that secondary moments are applied on the precast beam. Although the secondary moment in the mid-span region is small, any reduction in the span moment is very advantageous due to the reasons given in Section 3.2.1. As for the two stage construction of the slab, the secondary moments due to prestress in the top slab will be quantitatively analysed in the design of prototype M-beam bridge deck later in the report.

3.2.5 Selection of Length of Prestressed Segment of Slab

The length of the prestressed portion of the top slab can be decided by considering the locations of the inflection points of the bending moment envelope which depend on the applied loading. By slightly increasing the length of the prestressed segment of the slab beyond these inflection points into the span, it is possible to ensure that the entire portion of the slab remains in compression. Any increase in the length of the slab more than absolutely necessary for the applied loading will result in an increase in the secondary effects, thereby reducing the effectiveness of prestress in the slab. Both these factors must be considered in selecting the ratio α for a continuous composite bridge.

A value of α between 0.20 and 0.25 will be suitable for most cases. The resultant moment at the support due to post-tensioning the slab for these two values of α (and R=2.46) are 0.7 Pe and 0.6 Pe respectively.

3.2.6 Resultant Bending Moment due to Prestress in the Slab and Service Loads

The resultant bending moment diagram due to both prestress and service loads can be obtained by superimposing one on the other. This is illustrated in Fig.3.4. For a two span continuous beam, a smooth continuous bending moment envelope is assumed as shown in Fig. 3.4.(a). The prestressing moment diagram as shown in Fig. 3.2.(d) is superimposed on this to produce the resulting bending moment envelope (Fig. 3.4.(b)). In an actual bridge , the bending moment envelope will not be a continuous curve as assumed in Fig.3.4.(a) and therefore the negative moment peaks at the end of the prestressed segment of the slab will not be significant.

3.3 Details of Prototype Bridge

3.3.1 Type of Beams

Of the many forms of standard precast beams used in bridge construction, M-beams introduced by C & CA/MoT[1] have become the most widely used type for short and medium span bridges in U.K. Therefore, it was decided to consider an M-beam bridge deck for the study of the application of prestressed slabs in continuous bridges. The present standard M-beam range[2] from M2 to M10, when positioned at the normal spacing of 1.0 m, can be used for spans from 16 m to 29 m. Since the advantages of post-tensioning the slab are more predominant for longer spans, an M-8 section was chosen for the study. It was assumed that the prototype beams were pretensioned with 15.2 mm low relaxation strands which were deflected at the ends.

3.3.2 Span and Layout of Beams

A two-span continuous bridge deck has been considered. This case was considered as it normally represents the more critical case for many effects of continuous beams such as the hogging moment and the shear forces at interior supports. Although it is possible to have a sagging moment at the interior support due to live load acting on remote spans in bridges with three or more spans, it was not included in this research study.

Although the span range for M-8 beam is from 25m to 27 m[2], this was increased to 30 m to see whether the effects of post-tensioning the slab would allow an increase in span range. The M-beams, when they were first introduced, were intended to be spaced at 1.0m centre to centre but it is now common practice to have this spacing increased to more than 1.0 m. By increasing the spacing to 2.0 m, it is possible to save up to 25% in the cost of the bridge deck[30]. It will also allow the economic use of M-beams for spans shorter than 16 m. For the bridge under consideration in this study, a spacing of 1.25 m was adopted.

The thickness of the in-situ top slab was taken as 200 mm. The increase in the slab thickness from the standard 160 mm was made to have a sufficient slab thickness to accommodate ducts for post-tensioning in smaller scale model beams which were to be subsequently tested. However, the standard slab thickness of 160 mm will be sufficient for full scale beams. Fig. 3.5 shows the details of the M-8 beam with the top slab.

In the prototype design model, seven M8 precast beams were provided in the deck to support a two lane carriageway. The width of each traffic lane was 3.65 m. Transverse diaphragm beams were provided at the two abutments and the interior support. The details of the bridge deck are illustrated in Fig.3.6.

3.3.3 Length of Prestressed Segment of Slab

The value of the ratio of the length of prestressed portion of the slab to span was chosen as 0.225. The resultant prestressing moment at the interior support is 0.643 Pe for two-span composite beams made of M-8 precast section and 200 mm thick top slab which has a stiffness ratio of 2.46. For 30 m span bridge, this value of α requires a 6.75 m long portion of slab in each span to be prestressed at the interior support.

3.4 Loadings on Prototype Bridge

3.4.1 General

Only permanent loads due to self weight of components of the deck, finishes, surfacing etc. and live loads as specified by BS 5400: Part 2 [26] were considered in the analysis of prototype bridge deck. The loading and analysis of partially continuous composite bridge beams are more complicated than monolithically cast fully continuous beams. This is mainly due to the fact that several loading stages are involved and the beam's response to these loads can be either as a precast beam alone or a composite section after development of composite action and continuity. The following are the loads considered for the two span continuous composite bridge with prestressed slab in the negative region, as they come into effect in sequential order.

3.4.2 Dead Loads

3.4.2.1 Self Weight of Precast Beams

This was calculated on the basis of a concrete density of 24 kN/m^3. The uniformly distributed load due to self weight was 9.45 kN/m and was carried by

the precast beams as simply supported.

3.4.2.2 Self Weight of Top Slab

Assuming the same concrete density, the UDL due to weight of slab was 6.25 kN/m. In bridge decks with a prestressed portion of the slab, this is cast in two stages. The portion of the slab to be post-tensioned is cast first and the weight of the slab is carried by precast beams which are still simply supported. When the remaining portions of the slab in two spans are cast, continuity between the precast beams has developed due to post-tensioning of the previously cast slab. The weight of the slab is carried by a continuous composite section at the interior support and continuous precast section at mid-span.

3.4.2.3 Finishes and Surfacing

A uniformly distributed load of intensity 2.2 kN/m^2 was considered for finishes and surfacing of the bridge deck. This load is considered as a superimposed dead load and carried by the continuous composite beams.

3.4.3 Live loads

The live loads were applied to the continuous composite bridge deck. According to BS 5400: Part 2[26], two types of live loads have to be considered for highway bridges in Great Britain. They are HA loading which represents normal traffic loads and HB loading which represents an abnormally heavy vehicle load on bridges. For the application of both types of loadings, notional lanes were considered. These are the notional parts of the carriageway used solely for the purpose of applying the live loads. In the present case, two notional lanes were

considered and they had the same width of 3.65 m as the traffic lanes.

3.4.3.1 HA Loading

HA loading consists of either a uniformly distributed load (UDL) and a knife edge load (KEL) or a single wheel load of magnitude 100 kN. The magnitude of UDL depends on the loaded length of bridge deck. The loaded length is taken as the base of the positive or negative portion of the influence line for a particular effect at the section under consideration. The knife edge load is 120 kN/lane.

The following are the values of the UDL for the two span bridge deck under consideration.

For span moment and shear force at interior support:

Loaded length = 30 m

UDL of HA loading = 30 kN/m/lane

For interior support moment:

Loaded length = 60 m

UDL of HA loading = 21.6 kN/m/lane

3.4.3.2 HB Loading

HB loading consists of a four axle vehicle with four equally spaced wheels per axle as shown in Fig. 3.7. The spacing between the two inner axles can be varied from 6 m to 26 m so that the four axles can be positioned to produce the most critical case for any particular effect such as support moment, mid-span moment etc. HB loading is applied as units with each unit representing 10 kN axle load. For all highway bridges in Great Britain, a minimum of 25 units must be considered. The number can be increased up to 45 units if so desired by the appropriate authority.

For the two span prototype bridge, 37.5 units were considered. Therefore the total load per axle was 375 kN (93.75 kN/wheel). The critical position of the HB vehicle for the negative moment at the interior support, shear force at the same support and positive span moment were determined using the influence lines of two span continuous beam for those effects.

3.4.4 Application of HA and HB Loading

The application of HA and HB loads on the two span two lane bridge deck was undertaken according to the specifications of BS 5400: Part 2. The bridge deck must be analysed for HA loading alone or HB loading alone or a combination of HA and HB loadings.

When HA loading alone is considered, the full HA UDL and KEL are applied to two notional lanes at the appropriate parts and 0.6 times these loads to all other lanes. Since a two-lane bridge deck was considered, full HA loading was applied to both lanes.

When HB loading is considered, only one HB vehicle needs to be considered for a bridge deck. It can be wholly in one lane or can straddle two lanes. In either case, no other live load(i.e. HA loading) is considered for 25 m in front of and 25 m behind the HB vehicle. When the HB vehicle occupies only one lane, one other lane is loaded with full HA loading and all other lanes with 0.6 times HA loading.

The case in which the HB vehicle straddles two lanes was considered as the critical one for the individual beams of the two lane bridge deck of study. The middle beam was subjected to the maximum effects of loading. The largest axle spacing (26 m) was used in the critical case for interior support moment in which axles were positioned in peaks of influence line ordinates of the two spans. For span moment and shear force at the interior support, only one span had to be loaded for the critical case and therefore, the smallest axle spacing (6.0 m) was

used.

3.5 Analysis of Bridge Deck for Loads

3.5.1 Analysis of Bridge Deck for Permanent Loads

Except for live loads, for which the entire bridge deck was analysed, a simply supported or continuous individual beam consisting of an M8 precast beam with or without the top slab (as relevant to the stage of loading) was considered in the analysis of two span bridge. The beam and loads were chosen to represent an interior beam of the two span bridge deck. The difference in stiffness of different parts of the beam, when its length was made up of both precast portion and composite portion, was taken into consideration in the analysis of the beam. The analysis of the two span continuous beam was carried out using elastic theory available for the analysis of statically indeterminate beams.

The following partial safety factors (γ_{fl}) as specified in BS 5400: Part 2 were applied to the loads to obtain design loads.

Type of Load		Partial Safety Factor(γ_{fl})	
		Serviceability	Ultimate
(1) Dead loads (Concrete)		1.00	1.20
(2) Superimposed dead load		1.20	1.75
(3) Live loads	HA alone	1.20	1.50
	HB alone	1.10	1.30

The results of the analysis for dead load and superimposed dead load are given in Table 3.1.

3.5.2 Analysis of Bridge Deck for Live Loads

The two-span bridge deck was analysed for live loads by grillage analysis. Grillage analysis is one of the most widely used methods in the analysis of bridges. It can be used to analyse most types of bridge deck with any type of support conditions and is cheaper than the finite element to run on computers[31,32,33].

In using the grillage analogy, the bridge deck has to be idealised into a two-dimensional grillage consisting of rigidly connected longitudinal and transverse beams. Therefore, the grillage analogy is ideally suited for M-beam bridge decks as considered in this study because they can be conveniently idealised into a grid consisting of longitudinal precast beams and transverse beams made of insitu cast top slab [31]. It can also accommodate continuity. Each beam of the grillage is considered to have both a flexural stiffness and a torsional stiffness.

In the analysis of the two span bridge deck for HA and HB loading, the computer programme for grillage analysis called 'HECB /B/9 Grids' by the Highway Engineering Computer Branch of Department of Environment in United Kingdom[34] was used.

3.5.2.1 Idealisation of Bridge Deck for Grillage Analysis

The first step in the analysis of a bridge deck is to idealise it into a suitable grillage. In the idealisation of the two span M beam bridge deck, the recommendations of West [32] were followed. For beam and slab bridges, the longitudinal members of the grid are positioned to coincide with the actual beams. Usually, an odd number of beams are preferred so that there is a member on the centre line of the bridge. The top slab is divided into a number of transverse strips which are orthogonal to the longitudinal beams to form the members of the grillage in other direction.

For the analysis of the bridge deck considered in this study, the longitudinal members of the grillage were positioned to coincide with seven M-8 beams which are at 1.25 m spacing. The top slab was divided into transverse beams at a spacing of 3.0 m giving a total number of 21 beams in two spans. A part of the idealised grillage layout for the two span bridge is shown in Fig. 3.8.

3.5.2.2 Flexural and Torsional Inertias of Members

After idealisation of the bridge deck, the flexural and torsional stiffness of longitudinal and transverse members was evaluated following the guidance given by West [32]. In the evaluation of torsional stiffness, non-rectangular parts of the composite section were idealised to rectangles and torsional inertia of the section was considered as the sum of the inertias of individual rectangles. Only half of the torsional inertia of the top slab was considered in each direction.

3.5.2.3 Application of HA and HB Loading to Grillage

The bridge deck was analysed using HECB B/9/ GRIDS programme[34] for different loading arrangements of HA and HB loading separately, for critical cases of span moment, interior support moment and shear force at the interior support. Several positions of the HB vehicle were considered as indicated by influence lines for above effects. For the cases in which the wheel loads of HB vehicle did not coincide with nodes of the grillage, they were apportioned to the nearest nodes[31,32].

Results of the grillage analysis for live loads are given in Table 3.2. The partial safety factors for loads have been included in the values.

3.6 Design Moments and Shear Forces In the Prototype Bridge Beams with a Prestressed Slab

The design moments and shear forces of the prototype bridge were obtained by considering the load combination of permanent loads and primary live loads acting together on the structure. The results of the analysis which are given in Table 3.1 and Table 3.2 were combined to determine the total value at a particular section. Wind loads were neglected. The final design moments and shear forces were obtained by multiplying the results of the analysis by a partial safety factor γ_{f3} [26] . γ_{f3} values for serviceability limit state and ultimate limit state are 1.0 and 1.1 respectively [26]. The critical design moments and shear forces for the two span composite bridge beams with prestressed slab are given in Table3.3.

3.7. Design of Prototype Beams with Prestressed Slab

The design of the prototype bridge beams for bending and shear are given below. Attention was primarily given to the design of the section at the interior support. As the sequence of construction and prestress in the slab affect the positive span moments, the design of the beams for the maximum positive bending moments was also included. The design was carried out according to the specifications of BS 5400: Part 4 [27].

3.7.1 Design of Interior Support

At the interior support, two types of sections have to be considered. They are the rectangular section of the diaphragm and the composite section consisting of an M8 precast beam with insitu, composite top slab. The same maximum design

moment was considered for both sections. The prestressing steel requirements in the precast beam and the top slab were determined for service moments. The section was then checked for the ultimate moment and shear forces. Any additional non-prestressed steel was provided if necessary to satisfy the ultimate limit state check.

3.7.1.1 Serviceability Limit State

The stresses in the composite beam and the diaphragm due to service moments are given below. A modular ratio of 0.91 was considered in evaluating stiffness to account for the difference in concrete strength of the precast beam and the top slab.

	Composite Section	Diaphragm
Top of the Slab	-7.90	-5.70
Top of the Precast Beam	-6.25	-4.30
Soffit of the Beam	10.40	5.70

(All stresses are in N/mm^2)

Although the stresses in the diaphragm were low, the greater cross sectional area and section modulus make it uneconomical to design prestressing steel for the slab based on the requirements of the diaphragm section. As the length of the diaphragm is also very short, it was decided to consider only the composite section for the determination of prestressing steel requirement for top slab.

The ends of the precast M beams were designed as Class 1 members. By deflecting and debonding the strands provided for positive span moments, a satisfactory prestress distribution can be created at the end of precast beams. The arrangement of prestressing strands shown in Fig. 3.9 (a) was considered. 15mm diameter Bridon Drawn Dyform L-R type prestressing strands of 300 kN

breaking load were used and assumed to be stressed up to 70% of breaking load. The same type of strand and the same level of stress will be used throughout the design of prototype bridge. After a calculated prestress loss of 20%, a prestress distribution with a 5.0 N/mm^2 at the top as shown in Fig. 3.9.(b) resulted. This prestress will be sufficient to ensure a Class 1 precast beam for composite beams with fully prestressed, partially prestressed or reinforced concrete slab. For beams with a prestressed slab, the remainder of the prestress required will be provided by the prestress in the slab.

3.7.1.1.1 Fully Prestressed Slab

The top slab was designed to avoid tension developing under service moment (Class 1). The prestressing strands were assumed to be located 70 mm below the top of slab providing adequate cover for strands. The compressive stress at the top of slab due to both axial force and moment due to prestressing force in the slab (considering secondary effects also) can be written in the general form,

$$f_p = P\,(1/A + 0.643\,e / Z_{tc})\times 0.91 \qquad \text{.....Eqn. 3.4}$$

where Z_{tc} is the section modulus of the composite section.

Seventeen prestressing strands of 15.2 mm diameter and Bridon Drawn Dyform L-R were found to be sufficient to create the required prestress. This was after a prestress loss of 19%. The prestress distribution due to prestress in the top slab is shown in Fig. 3.10 (a) and the total prestress in the composite section due to prestress in precast beam and slab is shown in Fig. 3.10(b)

3.7.1.1.2 Partially Prestressed Slab

In this case, the prestress was applied to the slab to keep it in compression up to about 50% of the live load moment at the interior support.

From the values of moments given in Tables 3.2 and 3.3, the required prestress was found to be 5.9 N/mm^2. Using the same type of prestressing strands as in the fully prestressed slab, it was found that 12 strands stressed up to 70% of their breaking load would produce a prestress distribution with compressive stress of 5.8 N/mm^2 at the top of the slab and approximately zero stress at the soffit of the beam. The prestress losses were calculated to be about 16%. This prestress at the top of the slab represents a degree of prestress [37] of 0.73 for the composite section. The prestress distribution due to prestress in the top slab alone and combined prestress distribution due to prestress in top slab and precast beam are also shown in Fig. 3.10.

With the applied prestress of 5.8 N/mm^2 to the top slab, the maximum tensile stress in the slab under service loads was limited to 2.1 N/mm^2. According to British codes BS 5400 [27] and BS 8110 [28], this type of section can be classified as Class 2. With 12 strands, although tensile stresses can develop under service loads, they will not be enough to cause cracking in the top slab.

3.7.1.2 Ultimate Moment Capacity of Composite Beams at the Interior Support

The ultimate moment at the interior support of beams with a prestressed slab was 3250 kNm. This was obtained by multiplying moments given in Table 3.1 and Table 3.2 by the load factor γ_{f3}. The two composite sections designed in Section.3.7.1.1 with two levels of prestress in the slab were checked for ultimate moment by using design formula given in BS 5400 [27]. Both sections were found to have a greater moment capacity than the ultimate moment due to applied loads and hence no additional non-prestressed steel was necessary. This was mainly due to the fact that a greater area of prestressing steel was required in the top slab of both types of sections due to secondary effects. Even though not required for

flexure, it would be better to provide a small amount of reinforcing bars to resist stresses in the slab due to shrinkage.

3.7.1.3 Ultimate Shear of Composite Beams with Prestressed Slabs

Vertical shear of composite beams is considered at the ultimate limit state. The sequence of loading has to be considered as the shear forces at the interior support are applied to the precast section and the composite section at different stages. BS 5400 does not specify a definite method for the design of prestressed composite sections for shear other than that the same procedure for prestressed concrete beam could be followed by the assuming that the ultimate shear force is resisted by the precast section or by composite section. For this design model, the composite section was designed for vertical shear by considering the appropriate section at different stages of loading [38].

The ultimate shear forces on the precast beam and composite section due to permanent loads and live loads were 247 kN and 716 kN respectively. The shear strength was checked at a section 850 mm from the support which is at the end of the transmission length of strands. Due to high prestress at the top of the precast beams, the shear strength of the section cracked in flexure was not critical and only web shear strength was considered in the design. Considering the entire composite section, and limiting the principal tensile stress to $0.24\sqrt{f_{cu}}$ at the centroid of the composite section, the shear force to cause web shear cracking (V_{co}) was determined for beams with two levels of prestress in the slab. The values of V_{co} were 680 kN and 640 kN for beam with fully prestressed slab and with partially prestressed slab respectively. Accordingly, shear reinforcement was designed in the form of 8 mm diameter high yield stirrups at spacings of 140 mm and 125 mm.

3.7.2 Design of Composite Section Subjected to Maximum Positive Moment

As a result of the two stage construction of the top slab, the location of the critical section for the positive moment shifts from its usual midspan position towards the end support. From the analysis the location of the critical section for the design of the two span prototype bridge beams was found to be 12.0 m from the end support. Only the design of the most critical section is given here.

3.7.2.1 Serviceability Limit State

The prestress in the precast M beams is governed by the total tensile stress at the soffit of the beam due to the service moments (first applied on the precast section alone and later on the composite section). In Britain, most bridge beams are designed to be Class 1 prestressed members and therefore M beams of the model bridge deck were designed to be similar.

At the section under consideration, the tensile stress at the bottom of the beam due to self weight of beam and top slab which are carried by precast section alone is 9.65 N/mm^2 and the stress due to subsequent loads which are applied on the composite section is 7.44 N/mm^2. As a result of the negative moment due to secondary effects of the prestress in the top slab, the stress in the bottom fibres was reduced by 1.60 N/mm^2 and 1.15 N/mm^2 in beams with fully prestressed and partially prestressed slab respectively. The M-beams were provided with a prestress of not less than the resultant tensile stress at the bottom of beam due to service moment by 15.2 mm diameter Bridon Drawn Dyform L-R type prestressing strands located at standard positions given in the PCA publication[2]. The beam with fully prestressed slab required 19 strands while the beam with

partially prestressed slab required 21 strands. Details of the two beams are given in Table 3.4.

3.7.2.2 Ultimate Moment Capacity of the Composite Section Subjected to Positive Moment

The total ultimate moment at the critical section for positive moment was calculated to be 4150 kNm. When checked using design formula given in the code, prestressing steel provided in both types of beams were found to have a greater ultimate moment capacity than 4150 kNm. Therefore no additional steel was necessary.

3.8 Design of Composite Bridge Beam with Reinforced Concrete Slab

To compare the design details of continuous composite beams with a prestressed slab and beams with a reinforced concrete slab and evaluate numerically the changes brought about by new method compared to the conventional method, a two span composite beam made with the same M8 section and with a reinforced concrete top slab was analysed and designed. The only difference in the analysis was that the entire weight of the top slab is carried by the precast section before the development of continuity, and the corresponding absence of any secondary moments. The slab is assumed to be cast span by span. As in the design of beams with prestressed slab, only bending and shear at the interior support and positive moment at the mid-span will be discussed here.

3.8.1. Ultimate Moment at Interior Support

The ultimate moment at the support due to loads applied after the

development of continuity is 2185 kNm. The area of reinforcing bars required in the slab to resist this moment was calculated using code formulae and found to be 4350 mm^2. This can be provided by 14 bars of 20 mm diameter high yield reinforcement which have a steel area of 4398 mm^2.

3.8.2 Ultimate Shear at Interior Support

The composite beam section with a reinforced concrete slab was checked for ultimate shear using the same procedure adopted for beams with prestressed slab. The total ultimate shear force was 930 kN of which 326 kN was carried by the precast beam alone and 604 kN by the composite section. While there is a small reduction in the total shear force(3.4%) compared to the beams with prestressed slab, the shear carried by precast beam alone has increased by 32% due to the construction sequence.

To calculate the shear capacity, the same prestress distribution in the precast beam (Fig. 3.9) was assumed. For beams with a reinforced concrete slab also, it was web shear cracking force which was critical. The shear strength of composite section uncracked in flexure (V_{co}) was 500 kN. The spacing of 8 mm diameter high yield stirrups required at the interior support was 100 mm. This means the beam requires 20% more shear reinforcement than that is required for beam with a partially prestressed slab.

3.8.3 Design of Mid-Span Section

In the two span composite beam with the reinforced concrete slab at the interior support, the maximum positive service moment in the mid-span region is considerably greater than that of the beam with a partially prestressed slab. The moment carried by the precast beam is 1765 kNm while that carried by the

composite section is 1575 kNm. As a result of the increase in service moment, the tensile stress at the soffit of the beam increased to 19.6 N/mm^2. Prestressing strands of 15.2 diameter were provided in the bottom flange at standard positions to make the beam a Class 1 member with no tensile stress under service loads. For that, 29 strands were required, increasing then prestressing steel requirement by about 38% compared with the beam with partially prestressed slab. The prestress provided at the bottom after losses of 35% is 20.3 N/mm^2. The area of prestressing steel was sufficient to resist the moment at ultimate limit state.

3.9 Comments on the Results of the Analysis

The analysis and design of the two span prototype bridge decks produce several important design criteria for the design of the model beams in the experimental programme. It also made it possible to have a direct comparison between the bridge decks with prestressed slab and bridge decks with reinforced concrete slab at the interior support. The comparison of the results of three types of slabs considered in the study are summarised in Table 3.5.

It is clear from the results that the bridge decks with the slab having two levels of prestress will remain uncracked under service loads while that with reinforced concrete slab will be cracked in the negative moment region under service loading. This is one of the main advantages of developing continuity with prestressed slabs, especially as the top slab of the bridge decks is subjected to very severe exposure conditions. When the two levels of prestress used in the study are considered, the partially prestressed slab with a degree of prestress of 0.73 is more economical than the fully prestressed slab. Neither of which develops cracks under service loads.

The results also indicated that adverse effects such as secondary moments associated with the use of prestressed slab become advantageous in the mid-span

region. These effects reduce the positive span moment. Savings of up to 34% and 28% in the amount of prestressing steel required in the precast beam can be achieved when the slab at the interior support is fully prestressed and partially prestressed to a degree of 0.73 respectively. This decrease is due to the reduction in the tensile stress at the bottom fibres of the precast beam as a result of effects of prestress in the top slab at the interior support.

The prestressing steel required in the precast beam in the mid-span region has to be provided for the entire length of the beam. Most of these are not needed at the ends and have to be debonded. Therefore, any reduction in the amount of prestress required in the precast beam is a great advantage. It also causes a reduction in prestressing losses, especially those due to elastic deformation and creep.

Another beneficial effect of the prestressed slab is the reduction in shear reinforcement required near the interior support. The reductions in shear reinforcement for beams with the fully prestressed slab and partially prestressed slab are 40% and 25% respectively.

These points generated from the design comparisons for the full scale bridge, can now be investigated in more detail in the programmed investigation using a 1/3 scale model M8 beams in the laboratory, and are reported in the later chapters.

Table 3.1 Results of the Analysis of the Two Span Composite Beam with Prestressed Slab for Permanent Loads

	Type of Section	Service. Limit State	Ultimate Limit State
(1) Moment at midspan (kNm))			
(a) Due to self weight of girders	P	1062.0	1221.0
(b) Due to weight of slab (first stage)	P	71.0	82.0
(c) Due to weight of slab (second stage)	P	246.0	295.0
(d) Due to superimposed dead load	C	185.0	270.0
(2) Moment at the section where span moment is maximum (12m from end) (kNm)			
(a) Due to self weight of girder	P	1019.0	1172.0
(b) Due to weight of slab(first stage)	P	57.0	65.0
(c) Due to weight of slab (second stage)	P	308.0	354.0
(d) Due to superimposed dead load	C	207.0	302.0
(3) Moment at the interior support (kNm)			
(a) Due to weight of slab (second stage)	C	-770.0	-885.0
(b) Due to superimposed dead load	C	-371.0	-541.0
(4) Shear force at the interior support (kN)			
(a) Due to selfweight of girder	P	283.0	325.0
(b) Due to weight of slab (first stage)	P	37.0	43.0
(c) Due to weight of slab (second stage)	C	82.0	94.0
(d) Due to superimposed dead load	C	62.0	91.0

Note : P - Precast Section

C - Composite Section

Table 3.2 Results of Grillage Analysis for Live Loads

Loading Arrangement	Serviceability	Ultimate
1. Loading arrangement for maximum interior support moment		
(a) Support moment HA Loading	-1088.0	-1360.0
HB Loading	-960.0	-1134.0
(b) Span moment HA Loading	696.0	870.0
HB Loading	748.0	884.0
(c) Shear force at interior support		
HA Loading	193.0	241.0
HB loading	171.0	203.0
2. Loading arrangement for maximum span moment		
(a) Support moment HA Loading	-783.0	-979.0
HB Loading	-882.0	-1042.0
(b) Span moment HA Loading	1224.0	1530.0
HB Loading	1390.0	642.0
(c) Shear force at interior support		
HA Loading	220.0	276.0
HB Loading	202.0	239.0
3. Loading arrangement for maximum shear force at interior support		
(a) Support moment HB Loading	628.0	742.0
(b) Span moment HB loading	788.0	931.0
(c) Shear force at the support		
HB Loading	367.0	434.0

Note : All bending moments in kNm

All shear forces in KN

Table 3.3 Design Moments And Shear Forces For Composite Bridge Deck With Prestressed Slab

	Serviceability	Ultimate
1. Bending moment at mid-span section (kNm)		
(a) Precast beam alone	1380.0	1825.0
(b) Composite Section	1440.0	2017.0
2. Bending moment at a section 12.0 m from end (kNm)		
(a) Precast beam alone	1385.0	1018.0
(b) Composite section	1598.0	2236.0
3. Bending moment at interior support (composite section only) kNm	-2230.0	-3250.0
4 Shear force at interior support (kN)		
(a) Precast beam alone	179.0	247.0
(b) Composite section	511.0	716.0

Table3.4. Details of the Precast M-Beams for Positive Moments

	Fully Prestressed	Partially Prestressed
1. Total Tensile stress at the bottom of beam due to permanent and live loads	-17.1	-17.1
2. Compressive stress at the bottom due to secondary effects	1.60	1.16
3. Resultant tensile stress at the bottom	-15.5	-15.9
4. Number of 15.2 mm diameter prestressing strands	19	21
5. Prestress at the bottom after losses	15.6	16.3
6. Prestress at the top sfter losses	5.3	5.5

(Note : All stresses are in N/mm^2)

Table 3.5 Summary of Results of Analysis

	Fully P.C. Slab	Partially P.C. slab	Reinforced Concrete Slab
(1) Interior support			
(a) Service moment (kNm)	-2230.0	-2230.0	-1460.0
(b) Stress at the top of slab (N/mm^2)	-7.9	-7.0	-5.7
(c) Number of 15.2 mm strands in the slab	17	12	-
(d) Prestress at the top of slab (N/mm^2)	7.93	5.8	-
(e) Design ultimate moment (kNm)	-3250.0	-3250.0	- 2185.0
(f) Non-prestressed steel required	Nil	Nil	14 T20
(g) Shear force on M-beam (kN)	247.0	247.0	326.0
(h) Shear force on composite beam (kN)	716.0	716.0	604.0
(j) A_{sv} / s_v required (%)	0.70	0.78	1.0
(2) Span section			
(a) Service moment on precast beam (kNm)	1157.0	1219.0	1765.0
(b) Service moment on composite section (kNm)	1598.0	1598.0	1565.0
(c) Stress at the bottom of beam (N/mm^2)	-15.5	-15.9	-19.6
(d) Number of prestressing strands (15.2 mm) required	19	21	29
(e) Prestress Losses	25.0 %	28.0 %	35.0%
(f) Prestress at the bottom (N/mm^2)	15.6	16.3	20.0
(g) Ultimate design moment (kNm)	4150.0	4150.0	4636.0
(h) Non-prestressed steel required	Nil	Nil	Nil

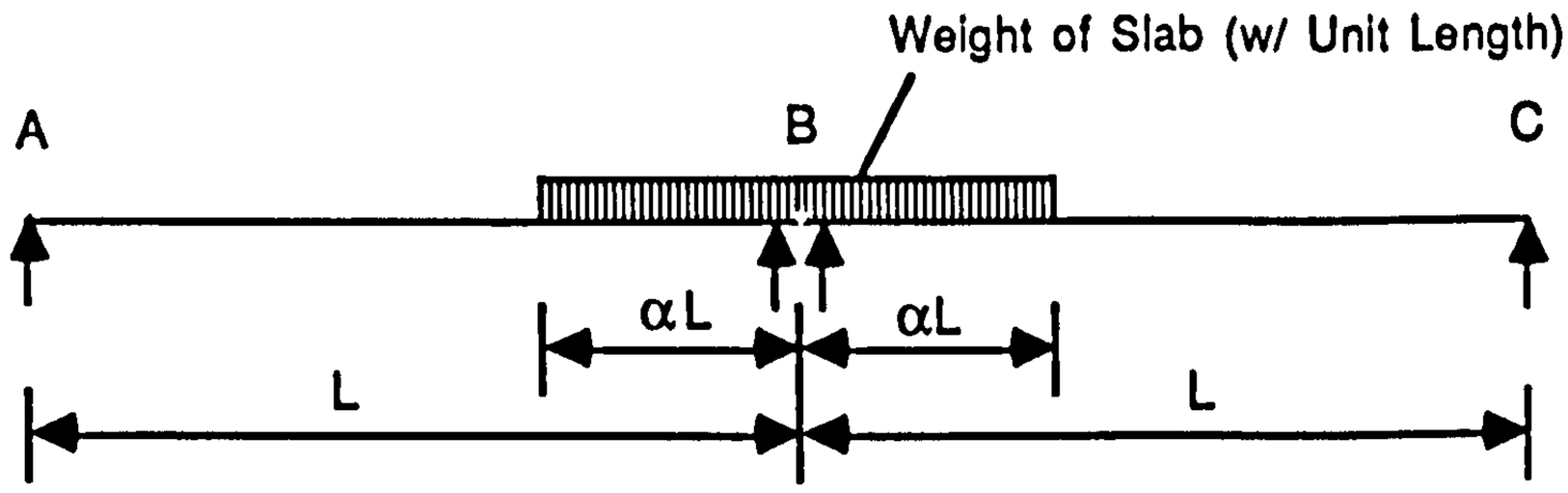

Bending Moment Diagram

(a) Two Simply Supported Beams Carrying the Weight of the Top Slab Cast in the First Stage

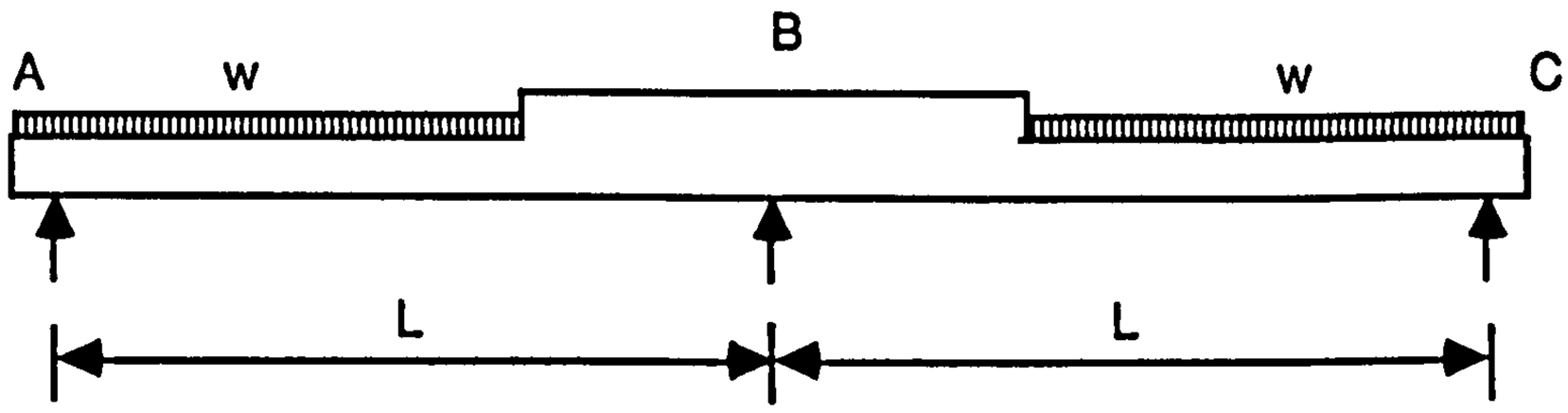

(b) Continuous Composite Slab Carrying the Weight of the Remaining Parts of Top Slab

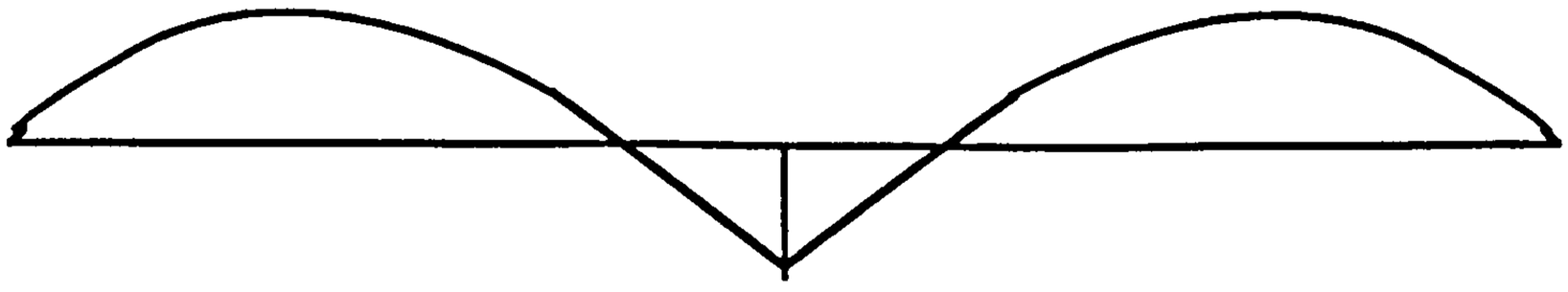

(c) Bending Moment Diagram Due to Weight of Slab Cast in Second Stage

Fig. 3.1. Bending Moment Due to Construction of Top Slab

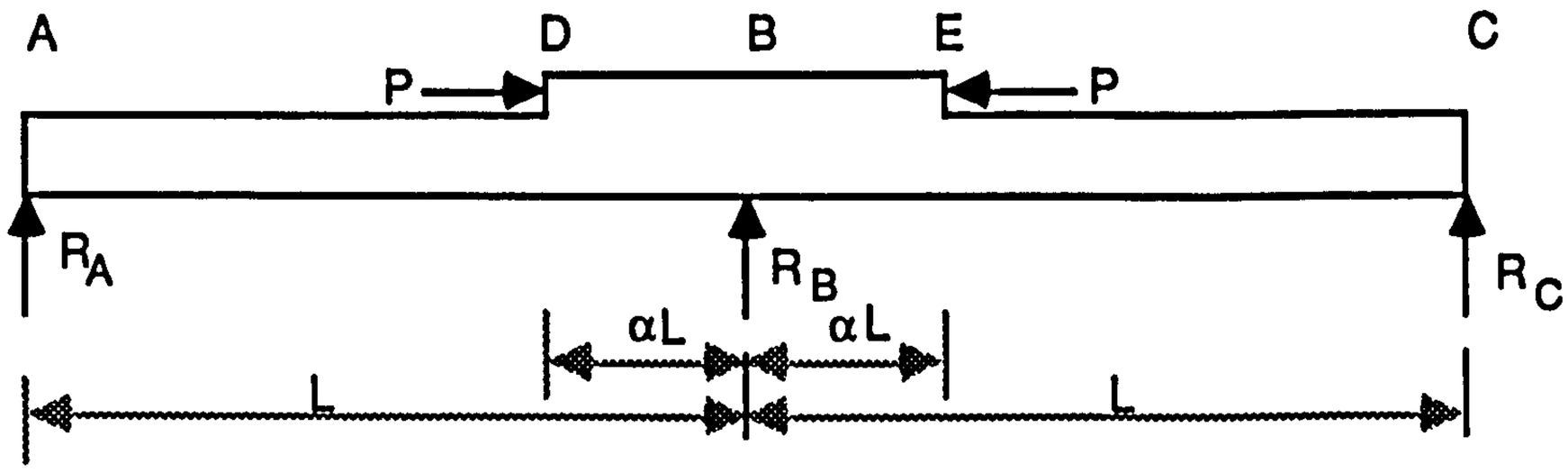

(a) Application of Prestress to the Top Slab

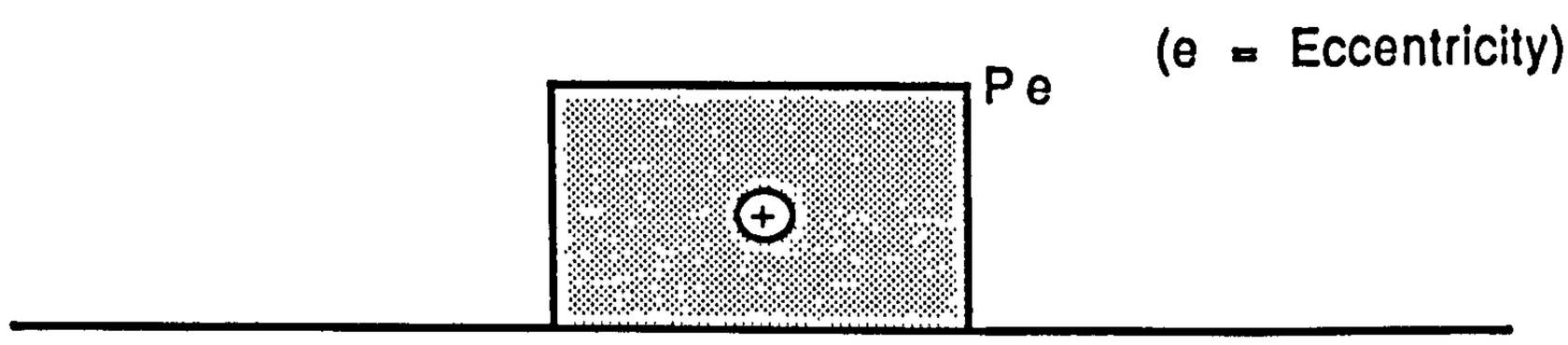

(b) Primary Bending Moment due to Prestress

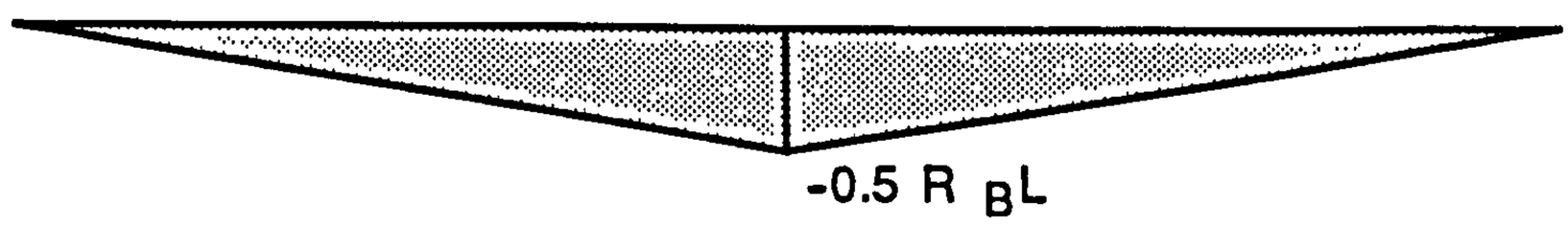

(c) Secondary Bending Moment due to Prestress

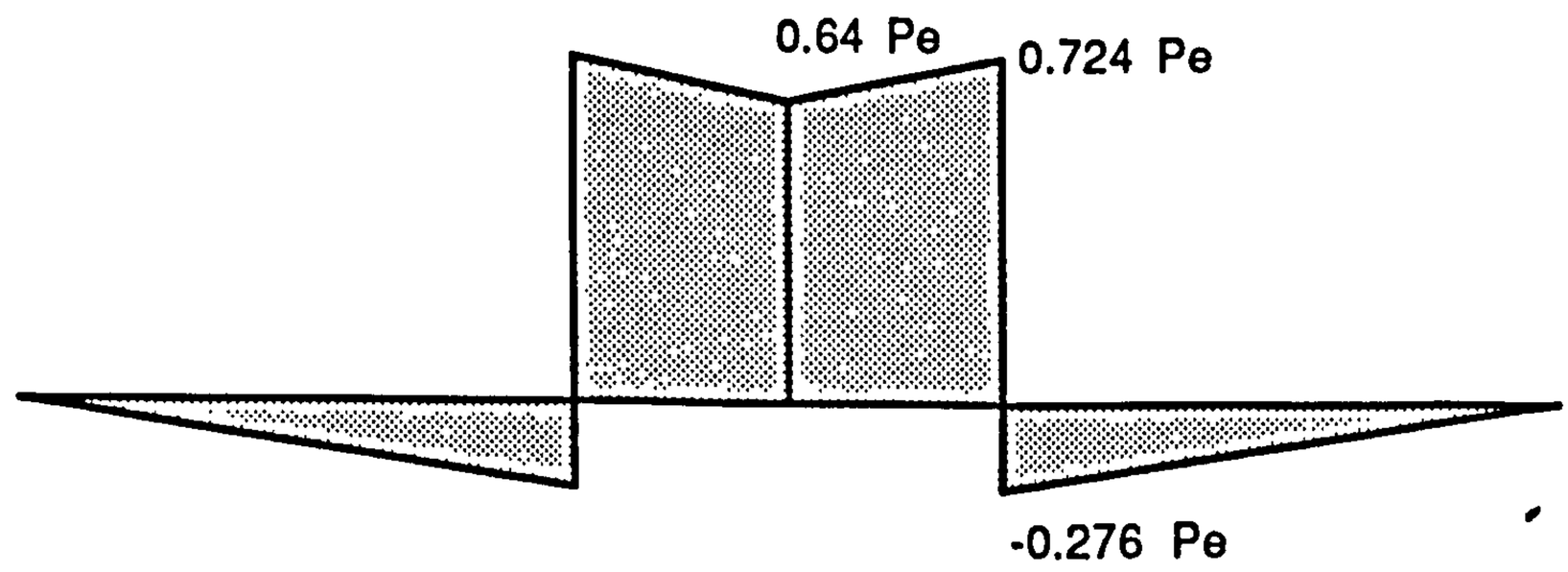

(d) Final Bending Moment Diagram Due to Prestress

(α = 0.225 and R = 2.46)

Fig. 3.2 Bending Moments Due to Prestress in the Top Slab

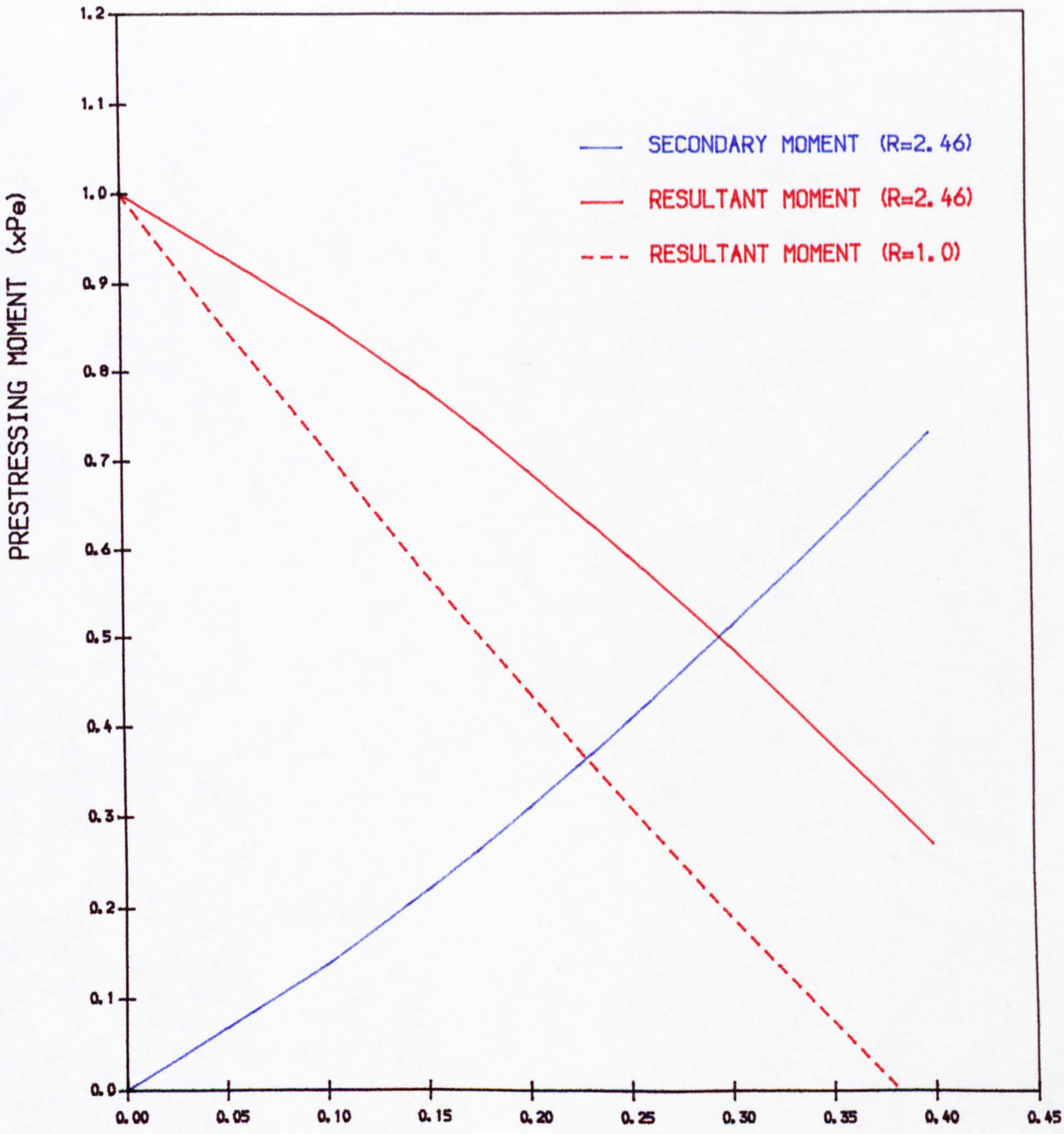

FIG. 3.3 : VARIATION OF PRESTRESSING MOMENT WITH LENGTH OF PRESTRESSED SEGMENT OF SLAB

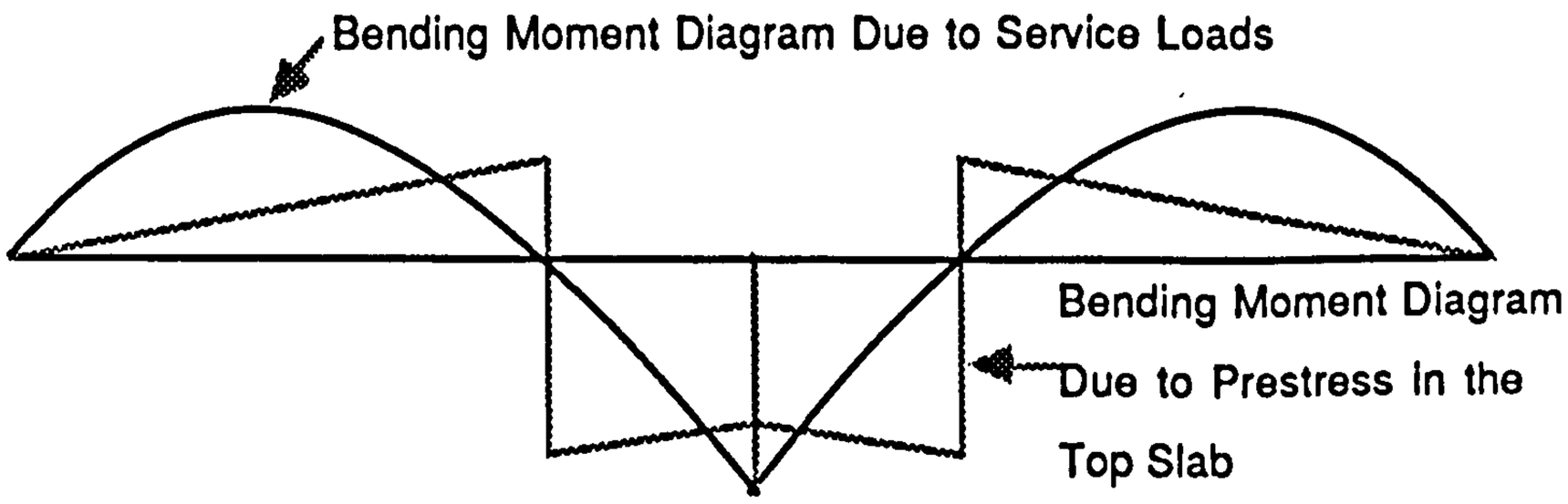

Fig. 3.4. Bending Moment Due to Prestress in the Slab and Service Loads

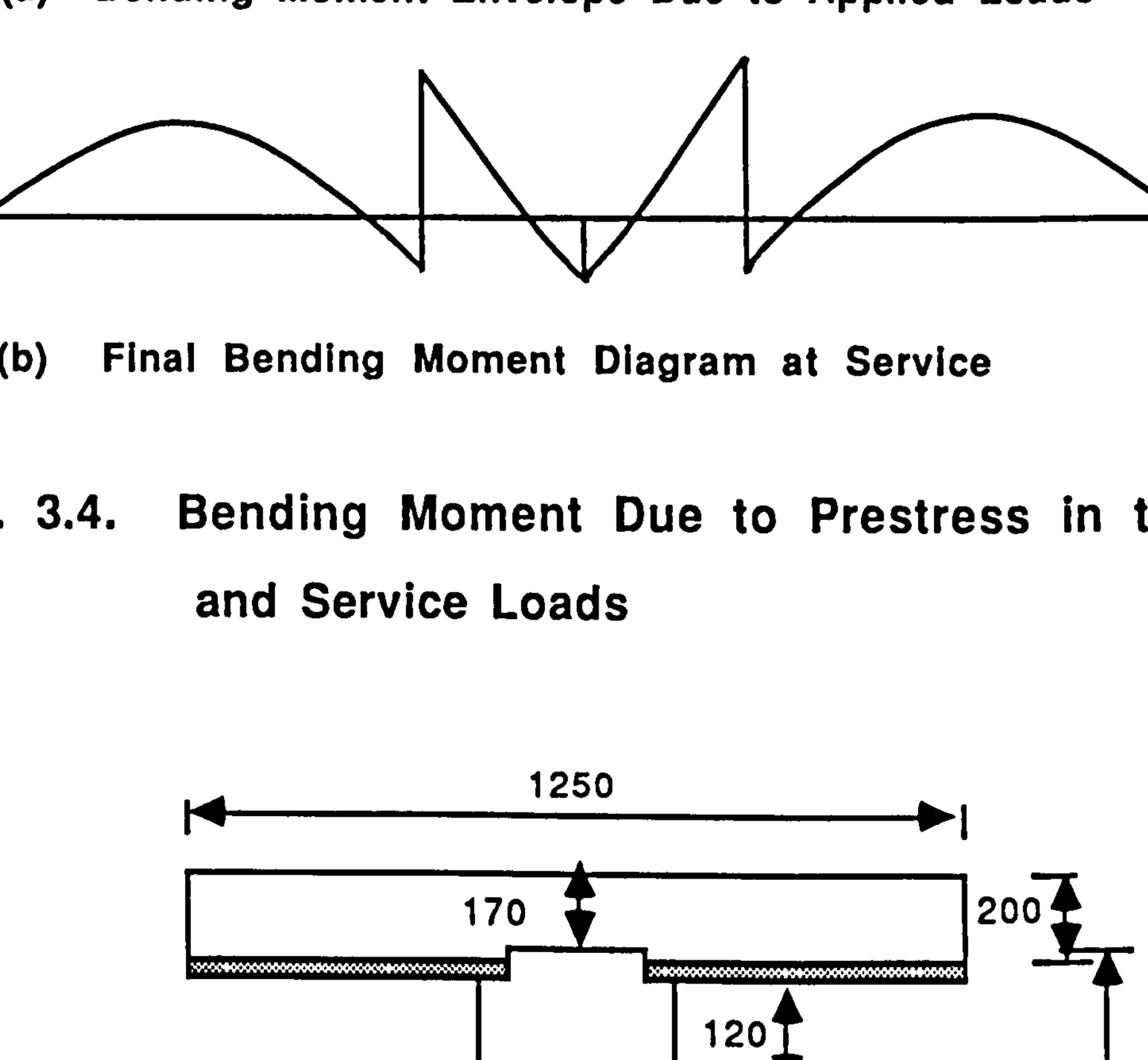

Fig. 3.5 Details of Precast M-8 Beam with Top Slab

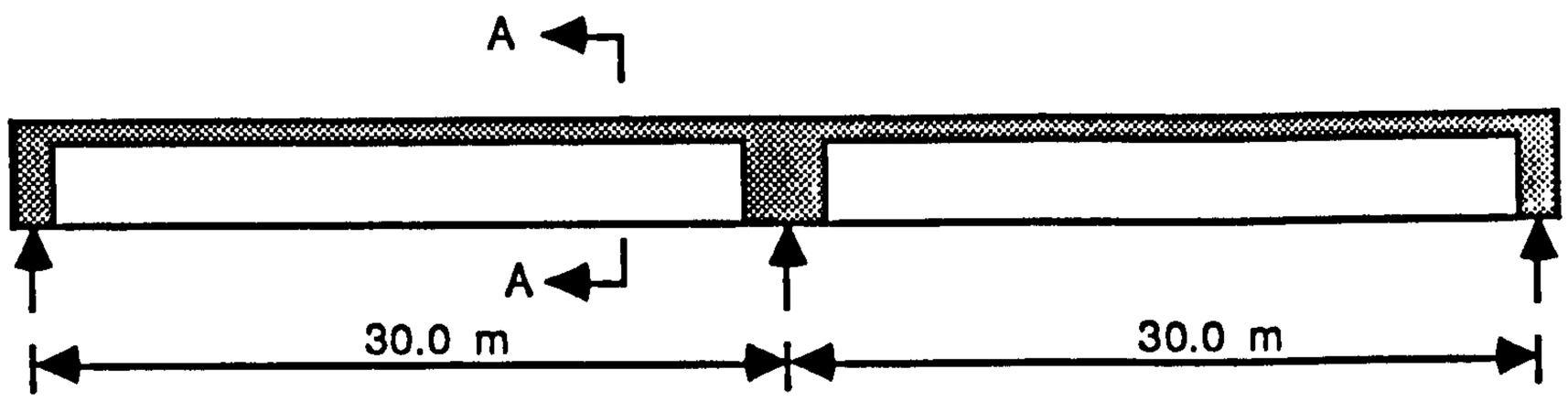

Longitudinal Section

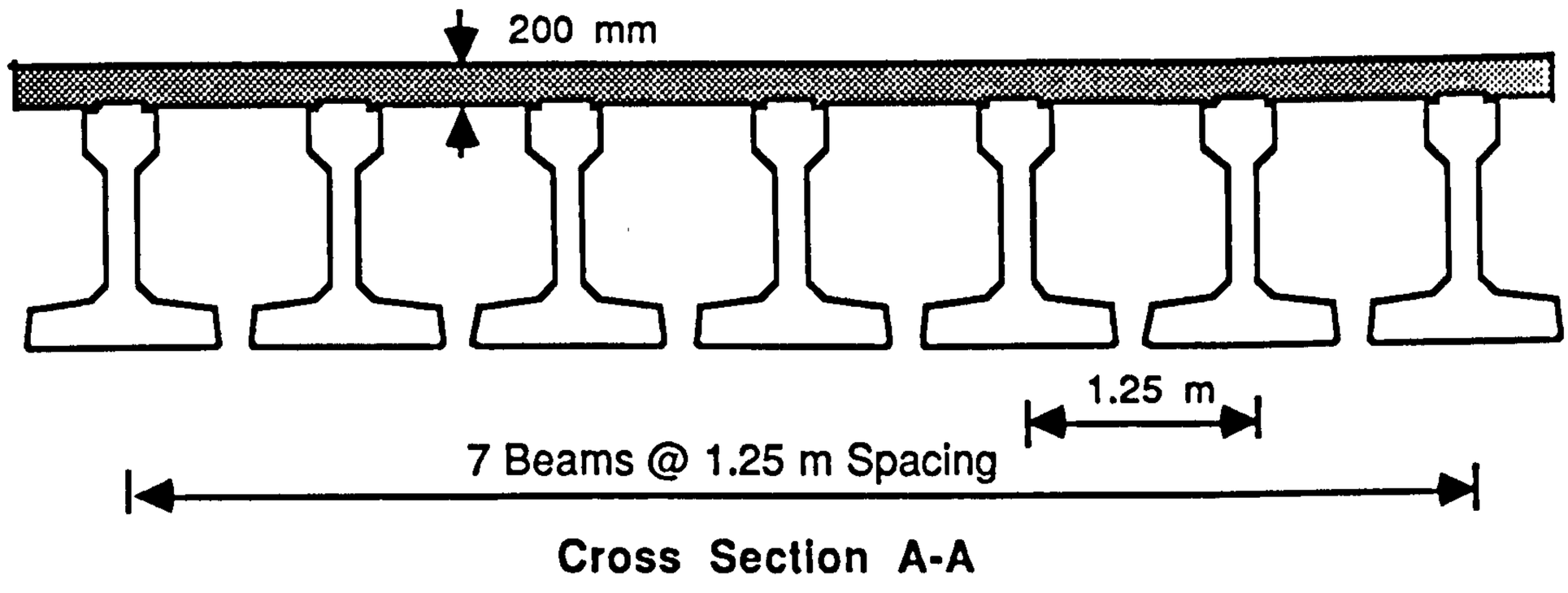

Cross Section A-A

Fig. 3.6 Details of the M-Beam Bridge Deck Condsidered for Analysis

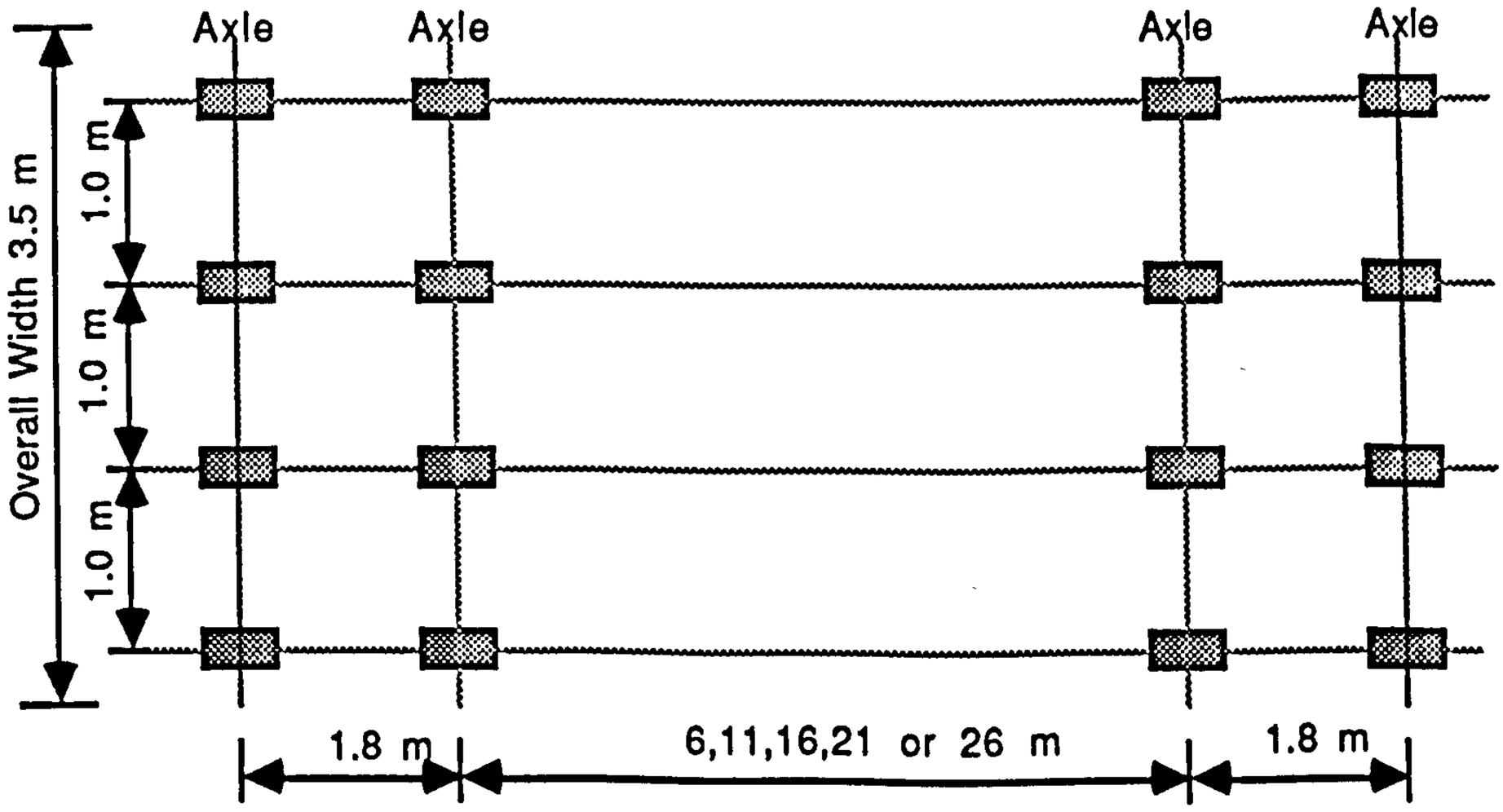

Fig. 3.7 HB Vehicle

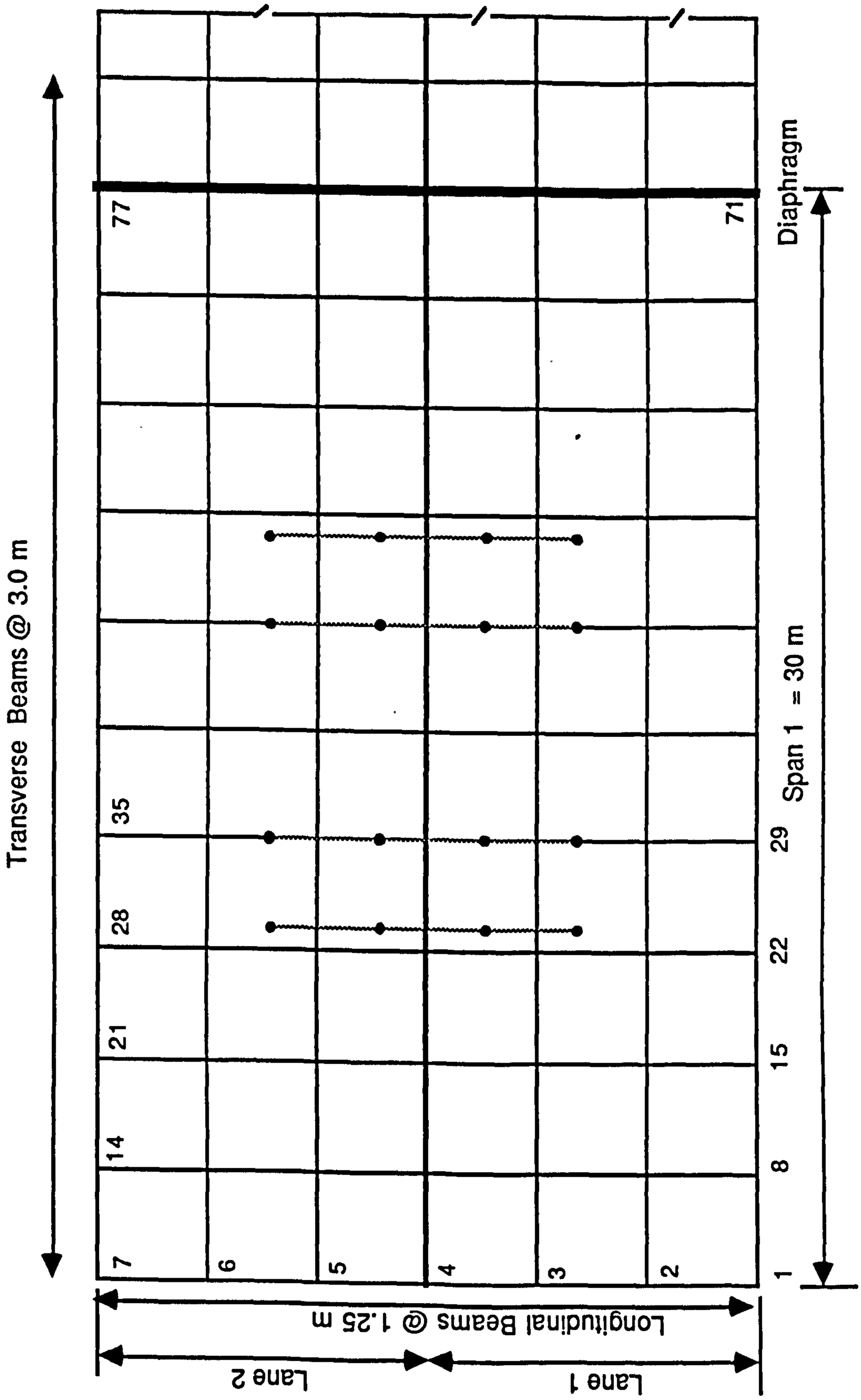

Fig. 3.8 A Part of the Grillage Layout with HB Vehicle Positioned for Maximum Positive Moment

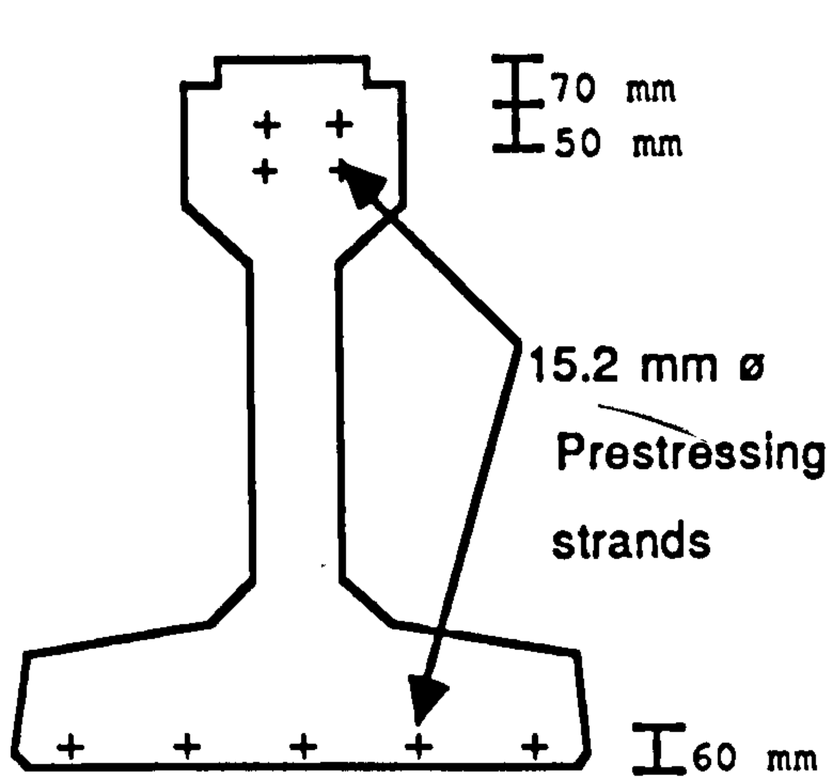

(a) Positions of strands at the end of precast M-beam

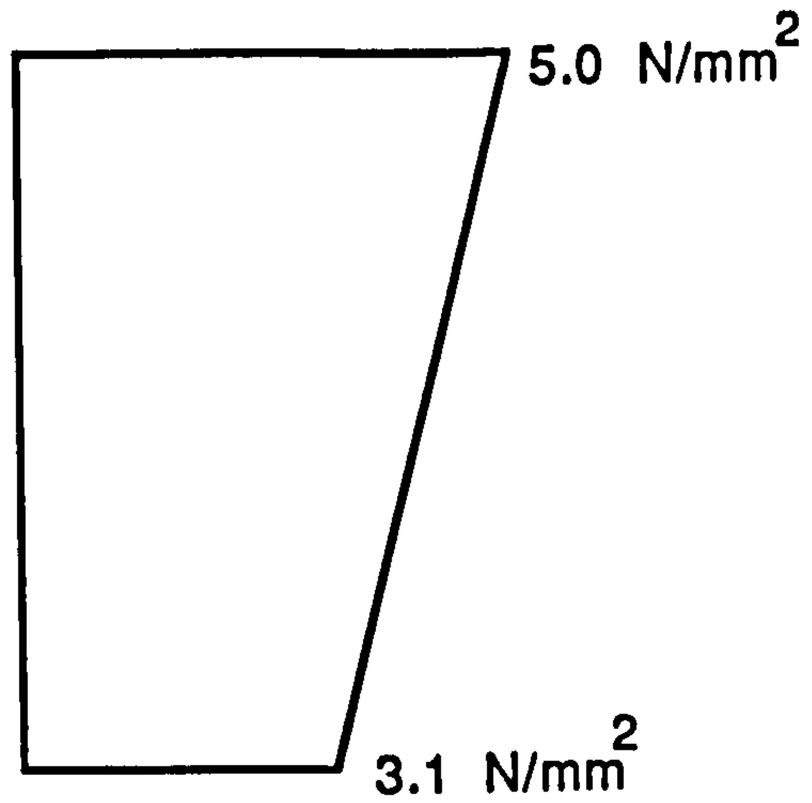

(b) Prestress distribution in precast M-beam at the end

Fig. 3.9 Prestress in Precast M-Beams at the Interior Support

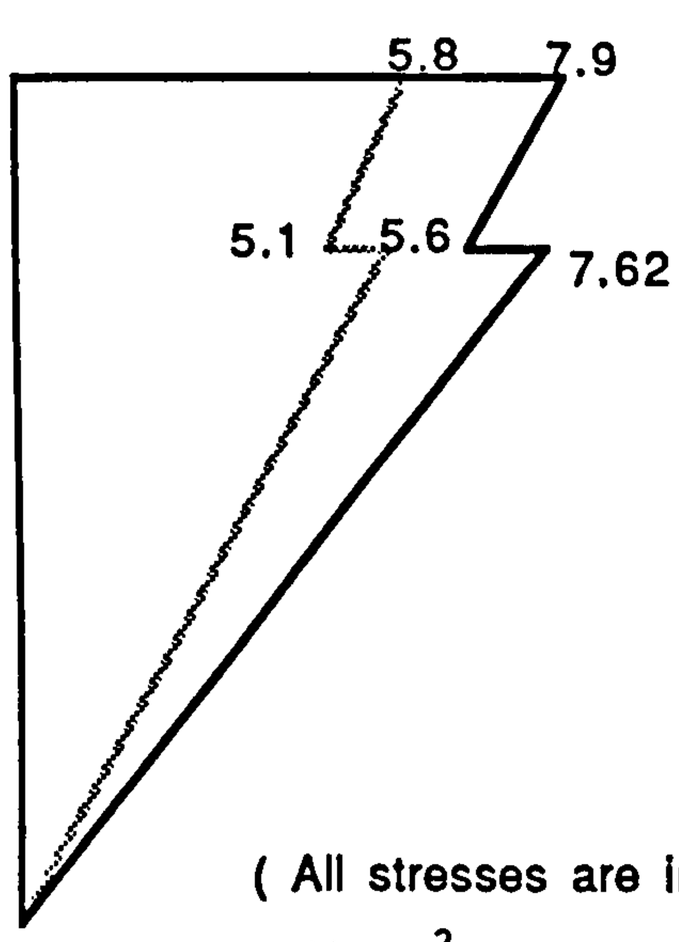

(a) Prestress in composite beam due to prestress in top slab

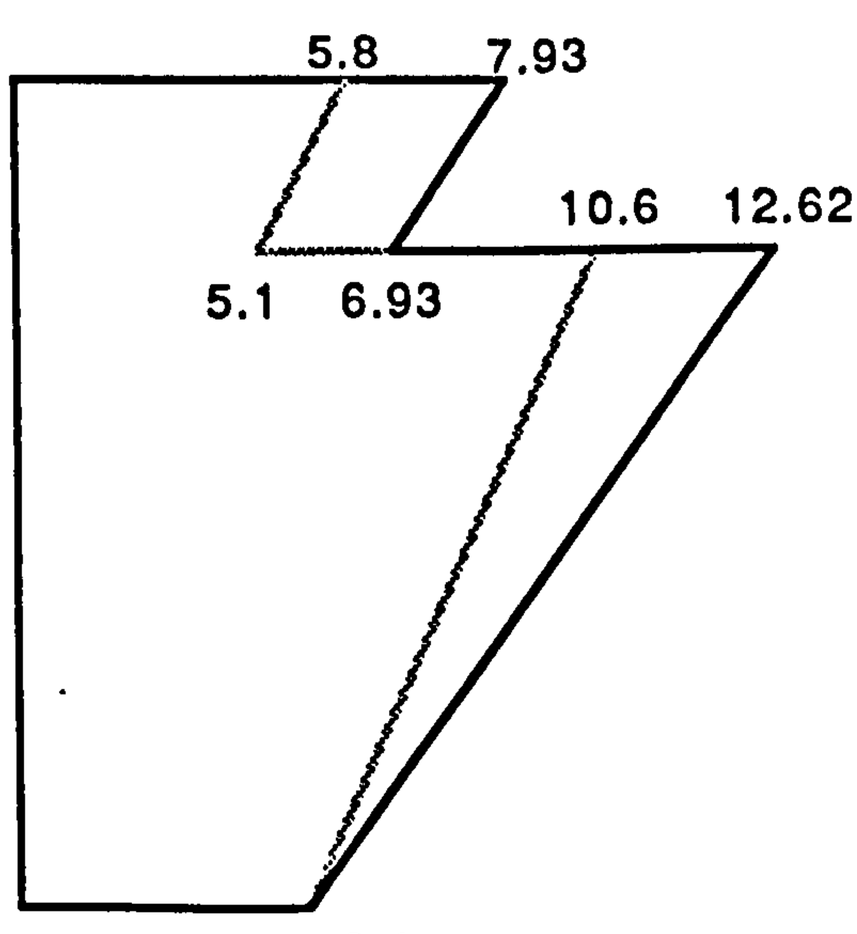

(b) Combined prestress distribution in the composite section due to prestress in the slab and the precast beam

..... Partially prestressed slab

——— Fully prestressed slab

Fig. 3.10. Prestress Distribution in the Composite Section at the Interior Support of Beams with Prestressed Slab

CHAPTER 4

TEST PROGRAMME, DESIGN AND FABRICATION OF MODEL BEAMS

4.1 Modelling of Beams for the Study

4.1.1 Scale and Details of Model Beams

The scale and length of the model beams was selected after giving due consideration to the practical problems associated with fabricating and testing beams in the laboratory. Although the test results of full scale structures are the most reliable and accurate, it is not practically possible to test a full size two span continuous bridge or even an individual beam in the laboratory. Considering the testing facilities available in the laboratory, it was decided to use 1/3 -scale model beams of M-8 standard section and to simulate in the test only the portion of the bridge subjected to negative moments of the interior support. Also, this research is mainly concerned with the behaviour of the continuity connection under hogging bending moment and shear forces. The maximum length of precast beams used in the tests was thus limited to 2.6 m.

The cross section of the model beams is shown in Fig 4.1. All dimensions of the M-8 section were reduced to 1/3 scale in the model beam. The height of the model beams was 400 mm (without the top slab). Smaller sizes of materials were used to suit the reduced scale of beams. The selected scale also provided a top slab of sufficient depth (67 mm) for the use of inflated ducts for the post-tensioning of the slab.

The horizontal scale had to be slightly modified to keep the length of beams to a more practical value. This was considered to be acceptable as only a small portion of the span was adopted in the study and the model beams were tested as statically determinate structures subjected to negative bending moments. For

beams with a post-tensioned slab, the entire length of the slab was prestressed. The length of the model beams was relatively short for the inclusion of a reinforced concrete portion of the slab.

All test beams consisted of two 1/3-scale precast beams connected by a 67 mm thick top slab and 200 mm long diaphragm of rectangular section. The slab and the diaphragm had the same width (417 mm). At the diaphragm where the connection was made, the two beam ends were embedded to a length of 82.5 mm in the diaphragm. The beams were separated by 35 mm (see Fig.4.2).

4.1.2 Design of Model Beams

The model beams were designed to have, as close as possible, the same stresses due to prestress and applied loads as in the prototype bridge at the interior support. The design moments and shear forces for the model beams were obtained from the analysis of the prototype bridge in the previous chapter by using the appropriate scale factors. The scale factors for bending moment and shear force were 1/27 and 1/9 respectively. The model beams were designed as Class 1 prestressed members according to BS 5400 : Part 4 [27].

4.2 Experimental Programme

Although there are many aspects of this new technique to be investigated, it is impossible to take all parameters in to consideration in a research study of this nature with limited time. Therefore, only the most important aspects have been selected for the present study. The experimental programme was designed to study the behaviour of the continuity connection between precast beams made with a prestressed slab, when it is subjected to negative bending moment and shear forces. The test programme was carried out in two series, Series A and Series B.

The flexural behaviour of the continuity connection was studied in Series A in which beams were designed to fail in flexure whilst Series B was designed to study effects of prestressing the top slab on the shear strength in the negative moment region. The cross section of the model beams in both series was the same. For better comparison of test results, continuous beams with a conventional reinforced slab were included in both series A and B. A total of eleven continuous composite model beams were tested throughout the two series.

4.2.1 Series A - Flexural Tests

4.2.1.1 Details of Model Beams in Series A

Three 1/3-scale composite beams with different levels of prestress in the top insitu slab were tested in this series. The main objectives of Series A tests were to study the structural efficiency of the use of a post-tensioned slab in developing partial continuity, and in controlling cracks in the slab, and to study the influence of varying levels of prestress in the slab on the flexural behaviour of the connection. The level of prestress in the slab was considered as the main variable. The other properties of the model beam were the same in all three cases.

The three levels of prestress used in the slab were

(1) Zero prestress (Reinforced concrete slab)

(2) Partially Prestressed slab

(3) Fully Prestressed slab

The reinforced concrete slab had seven high yield deformed bars of 12mm diameter as longitudinal reinforcement. In the partially prestressed slab, three prestressing strands (9.6 mm diameter) were used in combination with four 8mm diameter deformed bars, whereas the fully prestressed slab was post-tensioned with five prestressing strands (9.6 mm diameter). The three beams were designed for a negative moment determined from scaling the interior

support moment of the prototype bridge.

Each model beam consisted of two 2.6 m long pretensioned beams connected by the top slab and diaphragm. The precast beams were pretensioned with seven high tensile wires of 7 mm diameter of which the bottom three were straight and the other four were deflected from one end to the other. (The angle of inclination was 4.7^0.) The reinforcement details of the model beams in Series A are shown in Figs. 4.2 and 4.3. The designation of beams and the properties are given in Tables 4.1 and 4.2.

The post-tensioning strands and non prestressed reinforcement in the slab were provided for the full length of the connected beam, and to prevent shear failure occurring before flexural failure, the precast beams were provided with shear reinforcement of 6 mm diameter high yield deformed bars at a spacing of 75 mm. These stirrups extended into the top slab, providing resistance against horizontal shear stresses.

4.2.1.2 Design Moments and Shear Forces for Model Beams

From the results of the analysis of the prototype bridge deck, the design moment and shear forces were obtained for the model beams at the joint between them. The negative service moment was 83.5 kNm and the stress at the top slab was 7.9 N/mm^2 while the stress at the top of precast girder was 6.6 N/mm^2. The ultimate moment of model beams was 121 kNm.

4.2.1.3. Applied Prestress to the Model Beams In Series A

4.2.1.3.1 Prestress In Precast Beams

The precast beams in the flexural test series were prestressed with seven 7 mm diameter high tensile wires as shown in Fig 4.3. These wires were initially

stressed up to a force of 42 kN in each wire. It was not possible to fix any strain gauges to the beam surface before the transfer of prestress and therefore, the prestress losses were calculated according to the Code. After a total loss of 19%, the prestress at the top of the precast beam was 8.60 N/mm^2 at section X-X (see Fig.4.2). The prestress distribution in the precast beams at this section is shown in Fig 4.4.

4.2.1.3.2 Prestress in the Slab

As illustrated in Fig 4.2, the top slab of beam A-2 was post-tensioned with three 9.6 mm strands with a force of 70 kN each, whilst the beam A-3 was provided with five strands. The prestress at the top of the slab in beams A-2 and A-3 were 5.7 N/mm^2 and 9.3 N/mm^2 respectively. The prestress distribution due to the post-tensioning of the top slab and the resultant prestress distribution in the composite section at the joint is shown in Fig. 4.5.

4.2.1.4. Loading Arrangement for Series A

The three beams in Series A were made and tested as double cantilever as shown in Fig 4.6. Such an arrangement created a high negative bending moment with moderate shear forces. The shear span /effective depth ratio was 5.65.

However, it was decided that for ease of testing the same effect could be achieved by reversing the position of beam which was thus inverted and supported at the two ends whilst two closely spaced point loads were applied at the diaphragm. This arrangement, as seen in Fig 4.7, was less complicated than the double cantilever arrangement, and provided a stable test set up. A typical beam in Series A under test is shown in Plate 4.2.

4.2.1.5 Test Procedure

When the beam was in the test rig, additional strain gauges were fixed to measure vertical strain distribution at sections along the beam. The strain gauges fixed to the steel and the concrete surface were then connected to the data logger. Deflection gauges were positioned at the diaphragm and 800 mm away from the diaphragm on both beams.

The point load at the middle (diaphragm) was increased until the first crack appeared in the top slab. At regular load intervals, deflection and strain gauge readings were taken. When the cracking load was reached, the beam was unloaded in several steps. The beam was loaded again and the load at which the crack reappeared was recorded. The loading was continued up to the failure. The deflection and strain gauge readings were also taken as in the first loading cycle and in addition, crack widths were measured.

4.2.2 Series B - Shear Tests

4.2.2.1 General

In Series B, eight composite model beams were tested. The main objectives of the shear test series were to study the effects of prestress in the top slab on shear strength of the continuous composite beams in the negative moment region and to study the influence of shear reinforcement percentage and shear span/effective depth ratio on the shear strength of composite beams with prestressed slabs.

Each test beam was made up of two 1/3-scale precast beams of 2.6 m and 1.0 m long which were connected by the top slab and diaphragm. During the test the long beam was simply supported and the shorter beam cantilevered from the joint .

4.2.2.2 Design of Model Beams for Shear Test

The design of shear force and bending moment at the joint were obtained from the analysis of the prototype bridge. The case of maximum shear force at the interior support and the corresponding bending moment were considered. Only the portion of bridge girders subjected to negative moment was simulated in the test. The precast beams were pretensioned with five 9.3 mm prestressing strands which were arranged so that the bottom three strands were straight and the other two deflected at an angle of 4.7^0. The two precast beams were cast simultaneously using the same prestressing bed and it was possible to make the profile of strands in both beams on either side of the joint the same. The precast beams were designed as Class 1 members.

The main variable in the test series were the level of prestress in the slab, the percentage of shear reinforcement and the shear span. The effect of each variable was studied by choosing appropriate values for other variables and keeping them constant.

4.2.2.3. Range of Variables

4.2.2.3.1 Level of Prestress in the Slab

This was considered as the most important parameter in the study. The stress distribution created by the post tensioning in the slab gives an additional prestress to the precast beam. This can affect the inclined cracking load. Also, the prestress induced in the slab and top of precast beam will influence the flexural shear cracking.Therefore, a change in the shear strength of the composite section at the support can be expected after prestressing the top slab.

The same three levels of prestress used in the top slab of flexural series

(Series A) were used in the first three model beams of shear test series. The reinforcement details of these three beams were identical to those of A-1, A-2 and A-3. The use of the three levels of prestress, viz., zero prestress (reinforced concrete), partial prestress and full prestress should help to understand the effect of prestress on shear behaviour. The other details of the three beams were the same. The beams were provided with a shear reinforcement of 0.84 % .

Since it was thought that the partially prestressed slab would be the more practicable of the two types of prestressed slabs, it was used when the effect of other variables were studied.

4.2.2.3.2 Percentage of Shear Reinforcement

The total shear capacity at a section of a prestressed concrete beam is considered to be a combination of the resistance provided by both the concrete and shear reinforcement in the design codes[27,28,35,40]. The increase in shear strength produced by an increase in shear reinforcement is limited by the compressive stress in the web. When this happens, the beam will fail in a diagonal compression mode before the shear reinforcement has yielded. This is more visible in thin webbed sections.

To study how the additional prestress due to the post tensioned slab affects the shear strength of the composite beams, three different amounts of reinforcement were used in the model beams with a partially prestressed slab. The three shear reinforcement percentages used in the series were 0.42%, 0.53% and 0.84%. Two of these percentages (0.53% and 0.84%) were also used in model beams with a reinforced concrete slab for comparison between the two types.

In each test beam, a constant spacing of stirrups was maintained in both precast beams. High yield bars of 6 mm diameter were used for stirrups with

spacings of 125 mm, 200 mm and 250 mm for the three percentages, 0.84%, 0.53% and 0.42% respectively.

4.2.2.3.3. Shear Span / Effective Depth Ratio

Shear span is also considered as a factor having considerable influence on the failure mode of beams. When the ratio of shear span/effective depth is greater than 6.0, flexural failure could normally be expected .

It has been found that this ratio has a significant influence on shear strength of beams when it is less than 3.0. Mattock and Kaar[23] found that the shear strength of continuous composite beams increased when the ratio of shear span/effective depth is reduced.

To study the influence of shear span/effective depth ratio on composite beams in negative moment regions,two shear span/effective depth ratio of 2.35 and 3.5 were used for test beams with firstly a reinforced concrete slab and secondly a partially prestressed slab.

4.2.2.4. Designation of Test Beams in Series B

The beams in this series are designated as B1 ,B2, B3. . . . .,B8. The details of the beams are shown in Table 4.3. Since only one variable was changed for each beam, one model beam is used to study more than one aspect in the laboratory investigation .

The details of test beams in Series B are shown in Figs. 4.8 and 4.9.

4.2.2.5 Prestress in Model Beams for the Shear Test Series

The same design moments and stresses of the model beams of Series A (see

Section 4.2.1.2.) were considered for model beams of Series B, and the design shear force at the ultimate limit state was taken as 107 kN. The precast beams were pretensioned with five 9.3 mm diameter strands to produce a prestress at the top of precast beams of 6.7 N/mm^2 at section Y-Y (see Fig.4.8). The prestress losses were calculated to be 14%. The stress distribution due to prestress in the precast beams at this section is given in Fig 4.10 (a).

The two levels of prestress in the slab for the beams in Series B were the same as that of Series A and the same prestressing steel arrangements were used.(see Fig 4.2). The resultant prestress distribution in the composite section, near the joint, for the two types of prestress slabs are shown in Fig 4.10(b).

4.2.2.6. Loading Arrangements for Shear Tests

All beams in Series B were tested as simply supported beam with a cantilever overhang as shown in Fig.4.11. The loading arrangement, with two point loads P and Q, created high shear forces on both sides of the joint and small positive span moment in span BC. The two point loads P and Q were applied through a spreader beam with a hydraulic jack. The ratio between P and Q was selected to create a higher shear force in the shear span BC and to produce failure in that span. For the shear span (BC) of 1.0m, the ratio of P/Q was 0.73. For the last two tests (B-7 and B-8) in which the shear span was 1.5m, the P/Q ratio was changed to 0.54 to keep the relative values of bending moment and shear forces as close as possible to the previous six tests.

4.2.3.7 Test Procedure

After placing the beam on supports in the test rig, strain rosettes were fixed on the beam at required points. The electrical resistance gauges inside the

beam and on the beam surface were connected to the data logger which was used to read all the gauges. Two deflection dial gauges were placed one at the end of the cantilever and the other at the loading point on the long beam.

The beams were tested by static loading. The two point loads were increased to the failure of beam while maintaining a constant ratio between them. At regular load intervals, readings of the strain gauges and deflection gauges were taken. Also, the load at which cracks first appeared in the slab, in the short shear span and also in the long shear span were recorded. The crack widths were also measured using a hand microscope.

4.3 Fabrication of Model Beams

4.3.1 Materials

4.3.1.1 Prestressing Steel

In three flexural test beams, 7 mm diameter high tensile wires were used to pretension the precast beams. The prestressing wires were used so that the stress in the prestressing steel during the test could be measured easily by fixing strain gauges to the wires. The high tensile wires had a 0.2% proof stress of 1526 N/mm^2 and a tensile strength of 1670 N/mm^2. The modulus of Elasticity was 198 kN/mm^2.

In Series B (shear tests), 9.3 mm low-relaxation 7-wire prestressing strands (Bridon L-R) were used in the precast beams. The nominal area and the breaking load of the strands were 52.0 mm^2 and 102 kN respectively.

Low relaxation 7-wire strands (Bridon Supa 7 L-R) of 9.6 mm diameter were used in the model beams to post-tension the top slab. These had a cross sectional area of 55 mm^2 and a breaking load of 111 kN. The maximum relaxation of both sizes of strands was 2.5% after 1000 hours.

The stress-strain curves of the prestressing steel used in the model

beams are shown in Fig. 4.12(a), (b) and (c).

4.3.1.2 Non-prestressed Steel

Cold worked high yield deformed bars of 6mm diameter were used for shear reinforcement in the precast beams and transverse steel in top slab. The yield stress was 585 N/mm^2. Deformed bars of 8 mm and 12 mm diameter were used as longitudinal reinforcement in the top slab. In the beams with partially prestressed slabs, 8 mm diameter bars were used in combination with post-tensioned strands whilst in beams with reinforced concrete slabs, 12 mm diameter bars were used as main tensile reinforcement.

The stress-strain curves of 6 mm, 8 mm and 12 mm diameter bars are shown in Figs. 4.12 (d), (e) and (f).

In addition to deformed bars, 6 mm mild steel bars were used in the slab in the form of helices around the post-tensioned strands at the two ends of the beams to resist any bursting stresses induced by the prestressing forces.

Horizontal shear resistance was mainly provided by the bond between the top surface of the precast beams and top slab and by shear stirrups. To avoid horizontal shear failure, additional links made of 6 mm diameter high yield steel were tied to the alternative stirrups at the level of interface.

4.3.1.3 Concrete Mixes

Two concrete mixes were used for the precast beams and top slab. The materials used in both mixes were the same, only the mix proportions were different. Ordinary Portland cement was used without any admixtures and the coarse aggregate comprised uncrushed gravel with a maximum nominal size of 10mm. This was considered to be acceptable for 1/3 - scale model beams. In

deciding the mix proportions, the emphasis was given to the workability of the mix. Since no admixtures were used, a relatively high water cement ratio was used in the mixes to obtain sufficient workability for thin webbed beams with a shear reinforcement cage.

The mix proportions for the precast beam and top slab are as follows.

Precast Beam

Aggregate/cement ratio	=	4.8
Coarse aggregate/Fine aggregate ratio	=	1.47
Water/Cement ratio	=	0.54

The measured slump was about 100 mm and the concrete cube strength at the time of testing the beam was 55 - 65 N/mm^2.

Top Slab

Aggregate/Cement ratio	=	5.3
Coarse/Fine aggregate ratio	=	1.31
Water/Cement ratio	=	0.53

This mix gave a slump of about 75 mm and concrete cube strength at the time of testing of 50 - 60 N/mm^2.

4.3.2 Moulds and Prestressing Bed

The precast beams were cast in a prestressing bed consisting of heavy longitudinal steel channel sections connected together to form a horizontal bed with two side channels holding the total prestressing force before it was transferred to concrete beams. The mould for the precast beam was formed from metal sheets which were bent to form the shape of beam. The two sides of the mould were mounted onto steel channel sections using timber connectors. The two

steel channels were bolted to the prestressing bed to form the complete mould and also carried steel rollers which were positioned during the erection of the mould to deflect the prestressing strands.

In the shear test series (Series B), the two beam components of each model beam were cast simultaneously using two moulds in the prestressing bed. This was not possible for series A beams, which consisted of two long beams, and therefore necessitated two beams being cast separately.

4.3.3 Pretensioning of Strands of Precast Beams

First, one side of the mould was placed on the prestressing bed and then the shear reinforcement cage was placed followed by the prestressing wires or strands being threaded through the cage and end plates. The other side of the mould was then placed on the bed and both were bolted down. CCL wedge type anchorages were used and these were held by steel end plates. Load cells were provided between the anchorages and end plates to measure the prestressing force in the strands. All the strands or wires were stressed simultaneously by pulling the end plate at one end using two 200 kN jack. Details of the pretensioning arrangement for Series B beams are shown in Fig. 4.13.

Before the stressing operation, each strand was individually stressed up to 5 kN to take up any slack. During the pretensioning of the strands, the force was checked by load cells together with the extension of the strands while the total jacking force was measured by the scale of the loading machine. In addition to these, readings of the strain gauges on the high tensile wires were also taken for beams in Series A. The strands and wires were stressed up to 70% of their breaking load. After the required stress has been achieved, the load was transferred from the jacks to the prestressing bed by tightening the bolts.

4.3.4 Concreting the Precast Beams

Concreting took place on the day after stressing the strands. The mould was filled in layers of concrete each of which was compacted using external vibrators mounted on top of the mould. Control specimens (100 mm cubes, prisms and 150 mm cylinders) were made from the same concrete batch at the time of concreting. After concreting the beam was covered with wet hessian.

Prestress was normally transferred to the beam after seven days when the cube strength at transfer was 40 - 45 N/mm^2. The moulds were stripped only after the transfer and the beams were kept in a curing room until they were taken out to be connected by the insitu top slab and diaphragm.

4.3.5 Fabrication of Top Slab and Diaphragm

All the model beams tested in series A and B consisted of two precast beams connected by the diaphragm and top slab. This was done in the main laboratory using a separate mould. The two precast beams to be connected were placed end to end with a gap of 35 mm between them. Longitudinal and transverse reinforcement was placed in the mould, and in the beams where the slab was to be post-tensioned, 20 mm inflated rubber ducts were positioned in the slab and mild steel reinforcement in the form of helices were provided around the ducts to resist any bursting stresses which might develop at the two ends due to post-tensioning. The details of the joint before casting the top slab is shown in Plate 4.1.

Concreting commenced by filling the diaphragm section first followed by the slab. Control specimens were also made from the same mix. After concreting, the top surface of the slab was covered with hessian.

The ducts were deflated and removed from the slab about three days after

casting and the moulds were stripped after about five days.

4.3.6 Post-tensioning of the Top Slab

Throughout the experimental programme, only two arrangements of prestressing strands were used in the top slab (three strands and five strands). The slab was post-tensioned at between 7-10 days after casting. Before stressing, strain gauges were fixed to the concrete surface in the region of the joint to measure concrete strain induced by prestressing.

The slab was post-tensioned while the beams were being supported throughout their length. Prestressing strands of 9.6 mm diameter were threaded through the duct holes and a single steel plate of 25 mm thickness with the same area as the slab was used as an anchor plate at each end of the slab. These plates carried all the anchorages for the strands used in the beam. Load cells were placed between the CCL anchorages and the anchor plate to measure prestressing force. Before applying any stress, strain gauge and load cell readings were recorded.

The strands were stressed individually up to 70% of the breaking load in three stages by a CCL jack. The three stages were 25 kN, 50 kN and the final force 70 kN. Stressing began by stressing the middle strand to 25 kN followed by strands on the left and right being stressed alternately until all strands were stressed to same level. This sequence was repeated until the final jacking force was reached for all strands. Throughout the stressing operation, the forces in the strands were monitored by load cells and the pressure gauge scale of the jack. To take into account any slip that may take place during the locking off operation, the strands were slightly overstressed before releasing the jack. Finally, strain gauge readings were retaken immediately after prestressing. At the time of post-tensioning, the concrete cube strength of the slab was 38-42 N/mm^2.

4.3.7 Grouting

After completing the stressing of the strands in the slab, the duct holes were washed by water injection and then dried by sending air under pressure. During the concreting of the slab, small PVC tubes were placed in the slab in contact with the surface of ducts to provide access for grouting at the two ends. A grout mix consisting of 2 : 1 cement - water was thoroughly mixed and sent in at one end at a pressure of about 0.35 N/mm^2 until it was running freely from the other end.

4.4 Instrumentation

4.4.1 Strain Measurements

4.4.1.1 Steel Strain

Strains in the prestressing wires and high yield reinforcement were measured by using TML PL-5 electrical resistance gauges(gauge length-5mm) which were also used in the load cells.

Strain gauges on the longitudinal reinforcement in the slab were located at the two faces of the diaphragm. Stirrup strains were measured at a level of approximately the centroid of the composite section. The location of the strain gauges on prestressing wires in the precast beam was 300 mm from the end embedded in the diaphragm.

Before fixing strain gauges on high yield deformed bars, the surface had to be made smooth. The ribs of the bars over a length of about 40 mm were removed and smoothed with a fine abrasive paper. The surface was then cleaned with acetone before applying acidic conditioner to steel surface, followed by a neutraliser. The strain gauges were fixed to the steel with P 2 adhesive resin which was left to cure under uniform pressure for about 12 hours. PTFE type lead

wires which have a good water proofing resistance were soldered to the strain gauges.

To prevent mechanical damage during the fabrication of the model beam and moisture penetration to the gauges, they were covered with an epoxy compound which formed a flexible covering. Before this, the gauges and electrical connections were covered with M-Coat D layer to provide insulation against any electrical leakage. Finally, a coat of bitumen paint was applied on the covering to provide extra protection against moisture penetration.

4.4.1.2. Strain Measurement on Concrete Surface

Two types of strain gauges, mechanical and electrical, were used to measure concrete strains. The mechanical gauges used were Demec gauges which were made up of small metal discs fixed to the concrete surface with AMCO F 88 cement mixed with Dichloromethane. The strain between the Demec points was measured by a Demec extensometer. Three gauge lengths were used; 100 mm, 150 mm and 200 mm. The gauge resolution for these three gauge lengths were 14.8, 10.8 and 8.1 microstrain respectively. The main type of electrical resistance gauges used was 60 mm TML PL 60 gauges. Before fixing the electrical gauges, a thin layer of Araldite epoxy resin was applied. After it had cured, the surface was made smooth with a fine grain sand paper prior to being cleaned and fixing the gauges with Superglue adhesive.

The Demec gauges and electrical resistance gauges were used to measure two types of strains. These were the longitudinal linear strain and the principal strain in the concrete. For linear strain measurement, only a single gauge was sufficient, whereas for measuring principal concrete strains in the web, strain rosettes were used. Each rosette consisted of three gauges arranged in horizontal, vertical and 45^0 directions. For this, electrical strain rosettes (TML PR 20)

which had preset 20 mm gauges in three directions, were used. Strain rosettes made up of three PL 60 electrical resistance gauges or Demec gauges were also used.

4.4.2 Measurement of Electrical Resistance Gauges

All electrical resistance gauges which were both inside and on the surface of the beams were connected to an Intercole Compulog data logging system. The data logger used has a maximum input capacity of 99 channels and the system was programmed to read the strain to an accuracy of one microstrain at a speed of 33 channels per second. The strain gauges were connected to form a quarter bridge. The circuit made a half bridge at the time of reading by connecting a common dummy which was identical to the actual strain gauges. Two dummy gauges were used, one for PL -5 gauges inside the concrete and the other for strain gauges on the surface of the beam.

The same data logging system was used to read load cells. The strain gauges on the load cells were connected to the data logger via Plessey 7-pin plugs to form a full bridge circuit.

4.4.3 Deflection

Deflection of the test beams was measured using mechanical dial gauges with an accuracy of 0.01 mm. In the flexural test series, the deflections were measured at the diaphragm and sections 800 mm away from it in both beams. In the shear tests, deflection was measured at the end of cantilever and at the loading point on the long beam.

4.4.4 Crack Width

A magnifying glass and a hand lamp for improved lighting were used for the visual detection of cracks. The loads at which the first flexural cracks and the first shear cracks appeared were recorded. The crack widths were measured with a hand microscope with an accuracy of 0.02 mm/division. Once the cracks had formed, the propagation of the cracks were marked on the surface as the load was increased.

4.4.5. Relative Displacement at the Interface between Slab and Precast Beam

A displacement type transducer was used to detect any relative movement between the top slab and precast beam during loading in the shear tests. The transducer used had a maximum displacement of ±1 mm. The transducer was mounted in a metal bracket which was fixed to the top flange of the precast beam (as close as possible to the interface) at a location 300 mm from the diaphragm. The transducer was connected to an amplifier which was calibrated to read 4000 divisions for a 1 mm displacement.

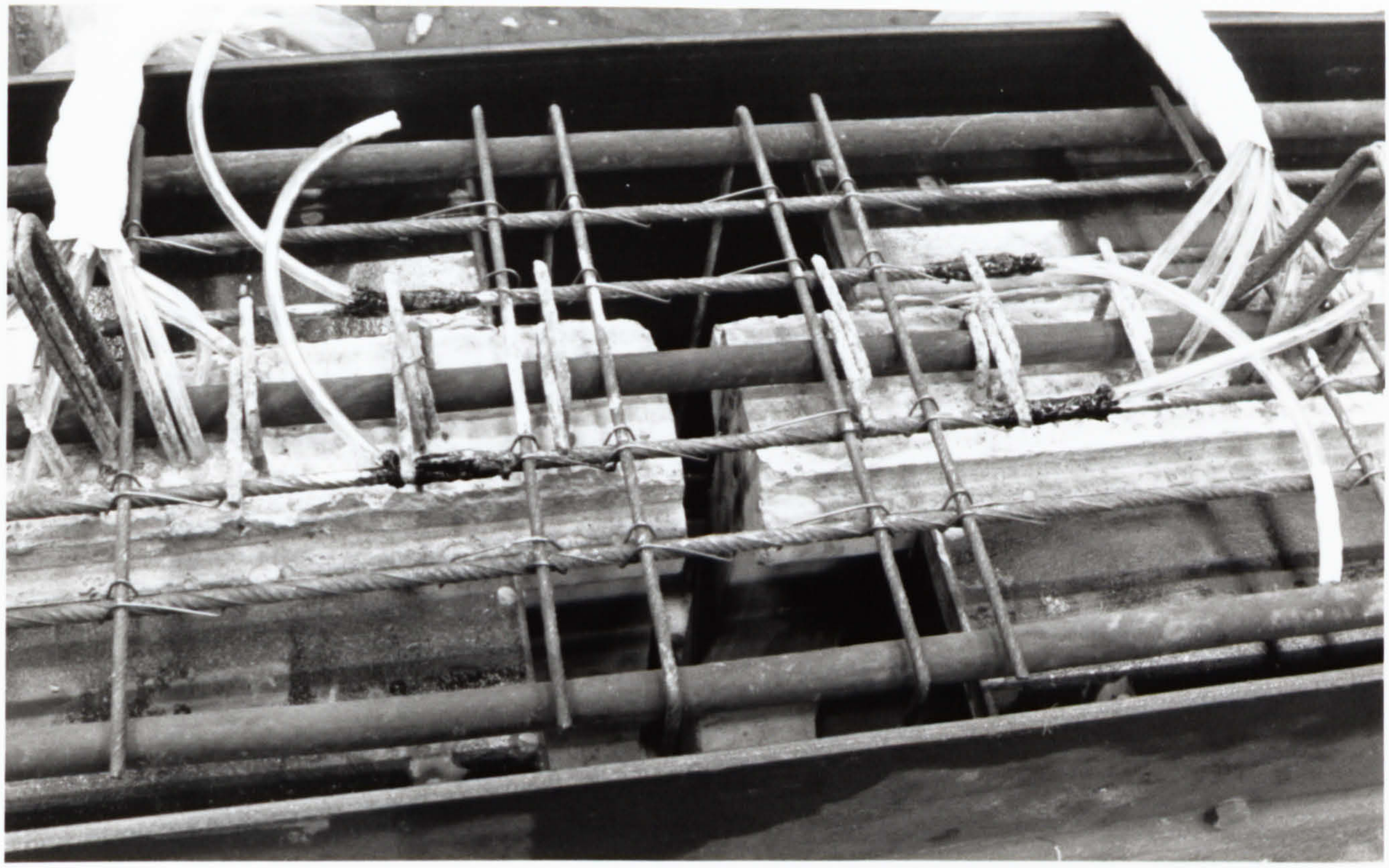

Plate 4.1 Details of the Joint Before Casting Top Slab

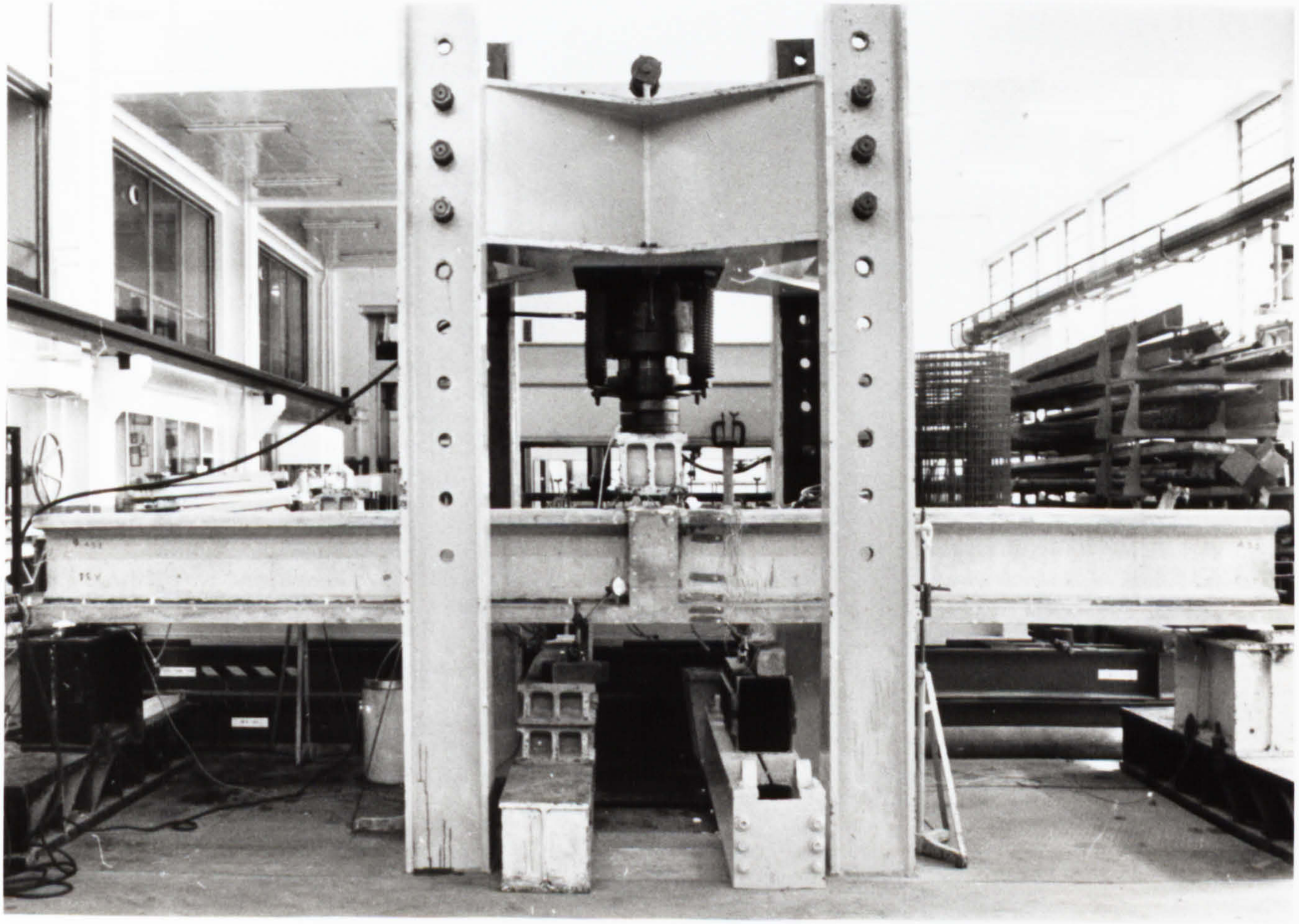

Plate 4.2 General view of the Test Rig in Series-A.

Table. 4.1 Designation of Beams for Series-A and Reinforcement Details of Top Slab

Beam	Details of Insitu Top Slab	
	Prestressing Steel	Non-Prestressed Steel
A-1	Nil	7 T 12
A-2	3 No. 9.6 mm ø Strands	4 T 8
A-3	5 No. 9.6 mm ø Strands	2 T 8

Table 4.2 Results of Control Specimen Tests of Series-A

Model Beam	Beam Component	Cube Strength at Transfer (N/mm ^{2})	At the Time of Testing			
			f_{cu} N/mm^2	f_{cf} N/mm^2	f_{ct} N/mm^2	E_c kN/mm^2
A-1	A-1-1	44.1	68.5	5.30	3.64	36.5
	A-1-2	43.5	66.1	5.70	3.75	36.8
	Top Slab	-	60.9	5.31	3.63	33.9
A-2	A-2-1	43.0	68.0	4.81	3.48	34.8
	A-2-2	44.2	67.3	4.74	3.58	34.6
	Top Slab	41.8	58.6	4.65	3.32	33.6
A-3	A-3-1	40.0	58.4	4.45	3.37	34.3
	A-3-2	41.2	60.9	3.98	3.68	34.0
	Top Slab	48.0	61.6	4.30	3.38	32.0

Note : f_{cu} = Cube Strength

f_{cf} = Flexural Tensile Strength of Prisms

f_{ct} = Splitting Tensile Strength of Cylinders

E_c = Static Modulus of Elasticity

Model Beam Designation	Top Slab		Shear Reinforcement		Shear Span	
	Type of Slab	Reinforcement	Size & Spacing	Percentage	Span (m)	Shear Span / Effective Depth
B-1	Reinforced	7 T 12	6mm @ 125mm	0.84 %	1.0	2.35
B-2	Partially Prestressed	4 T 8 and 3 No. 9.6mm strands	6mm @ 125mm	0.84 %	1.0	2.35
B-3	Fully Prestressed	2 T 8 and 5 No. 9.6 mm strands	6mm @ 125mm	0.84 %	1.0	2.35
B-4	Reinforced	7 T 12	6mm @ 200mm	0.53 %	1.0	2.35
B-5	Partially Prestressed	4 T 8 and 3 No. 9.6mm strands	6mm @ 200mm	0.53 %	1.0	2.35
B-6	Partially Prestressed	4 T 8 and 3 No 9.6mm strands	6mm @ 250mm	0.42 %	1.0	2.35
B-7	Partially Prestressed	4 T 8 and 3 No.9.6mm strands	6mm @ 200mm	0.53 %	1.5	3.50
B-8	Reinforced	7 T 12	6mm @ 200mm	0.53 %	1.5	3.50

Table 4.3 : Designation and Details of Model Beams in Series B.

Table 4.4 Results of Control Specimen Tests of Series-B

Beam	Beam Component	f_{ci}	At the Time of Testing			
			f_{cu}	f_{cf}	f_{ct}	E_c
B-1	Precast	43.1	60.2	4.86	3.67	34.4
	Top slab	-	50.4	4.23	3.54	33.2
B-2	Precast	44.0	60.4	5.44	3.41	33.9
	Top slab	45.3	52.0	5.31	3.33	33.3
B-3	Precast	45.0	59.7	5.62	3.46	33.8
	Top slab	42.0	53.8	5.38	3.33	33.3
B-4	Precast	43.8	59.6	5.14	3.60	33.2
	Top slab	-	53.0	4.80	3.18	32.2
B-5	Precast	41.5	54.0	5.00	3.36	32.0
	Top slab	41.3	54.2	5.01	3.36	32.3
B-6	Precast	43.0	57.8	4.95	3.28	33.1
	Top slab	40.5	48.8	4.36	3.08	31.9
B-7	Precast	40.8	53.5	4.15	3.27	31.4
	Top slab	42.2	51.5	3.90	3.19	32.6
B-8	Precast	43.7	53.6	4.00	3.15	33.4
	Top slab	-	51.2	4.05	3.18	32.6

Note : f_{ci} = Cube strength at transfer (N/mm^2)

f_{cu} = Cube strength (N/mm^2)

f_{cf} = Flexural tensile strength of prisms (N/mm^2)

f_{ct} = Splitting tensile strength of cylinders (N/mm^2)

E_c = Static modulus of elasticity of concrete (kN/mm^2)

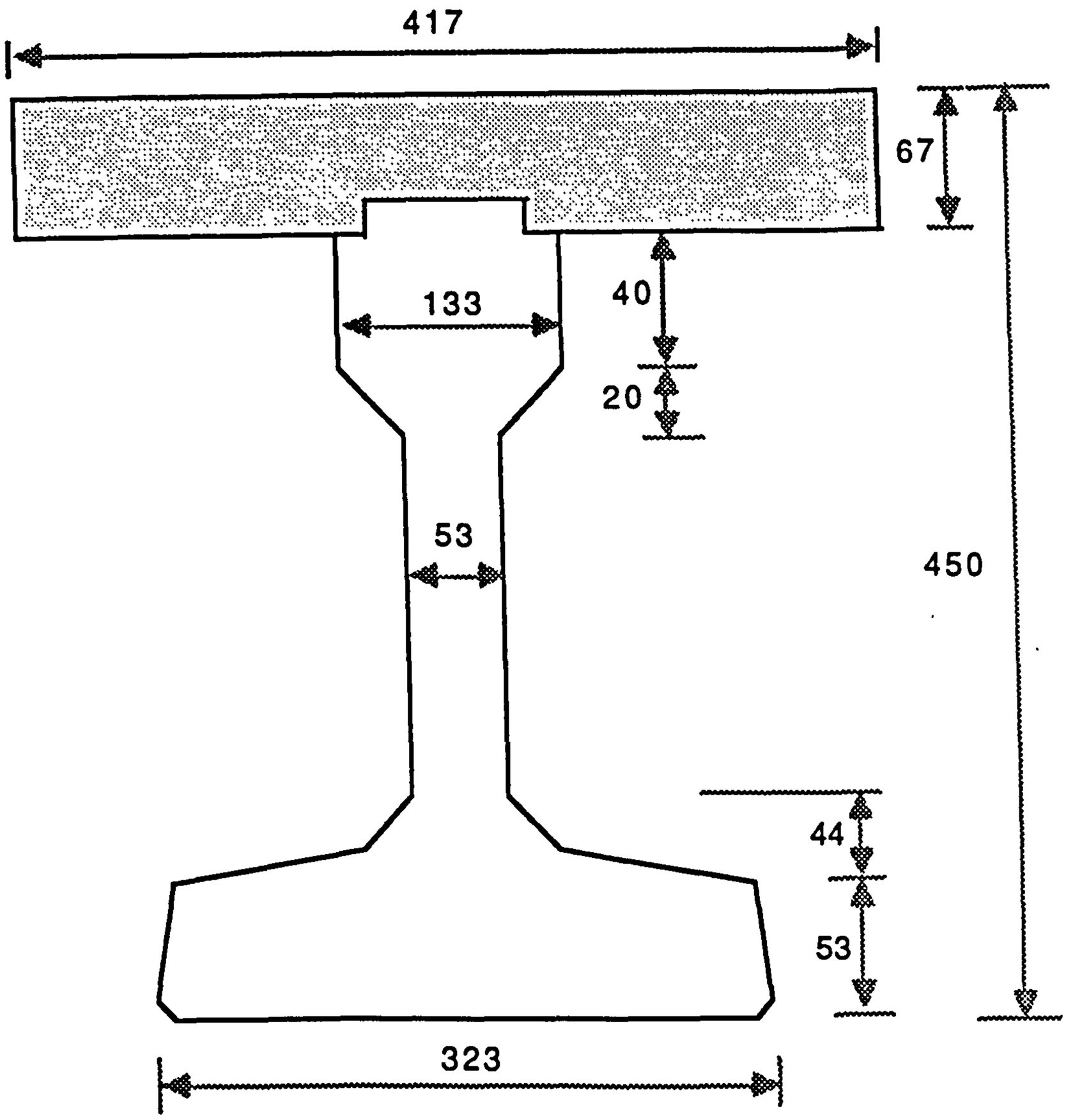

(Note : All Dimensions are in mm)

Fig. 4.1 : 1/3- Scale Model Beam of M-8 Section

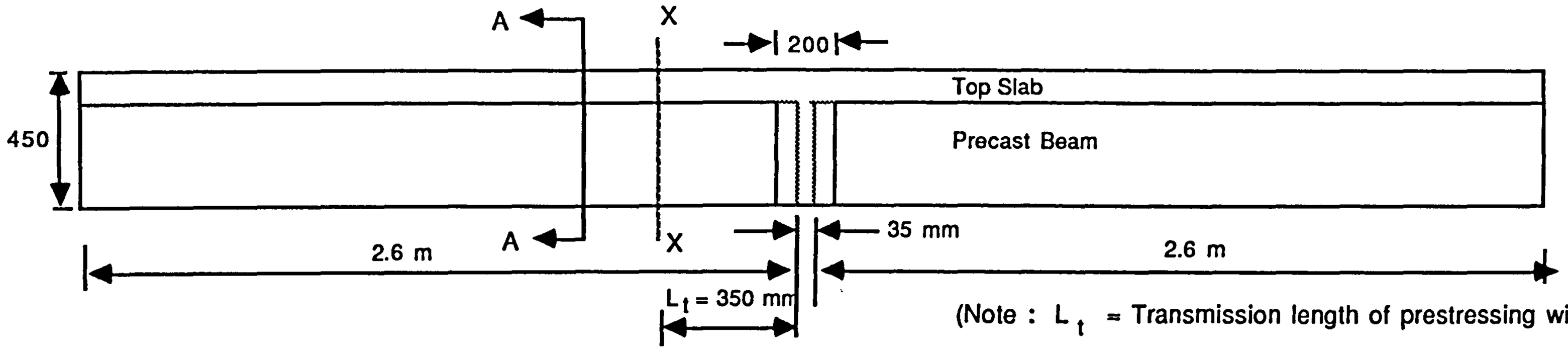

(Note : L_t = Transmission length of prestressing wires)

Longitudinal Section

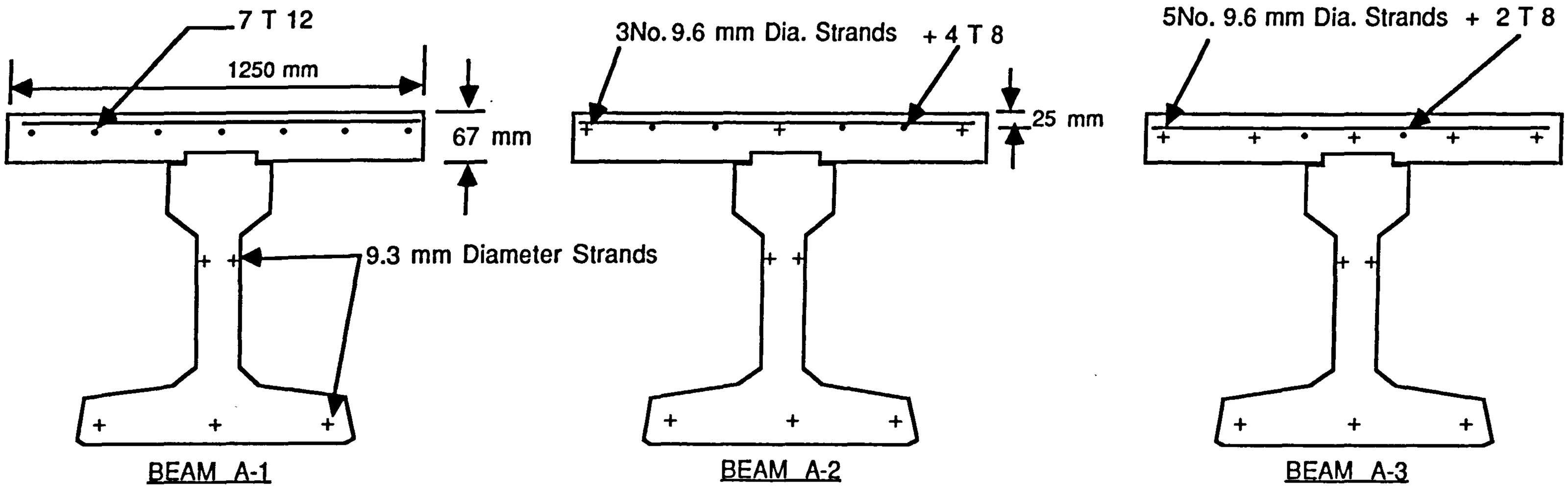

Section A-A

FIG. 4.2 Details of Model Beams in Series- A

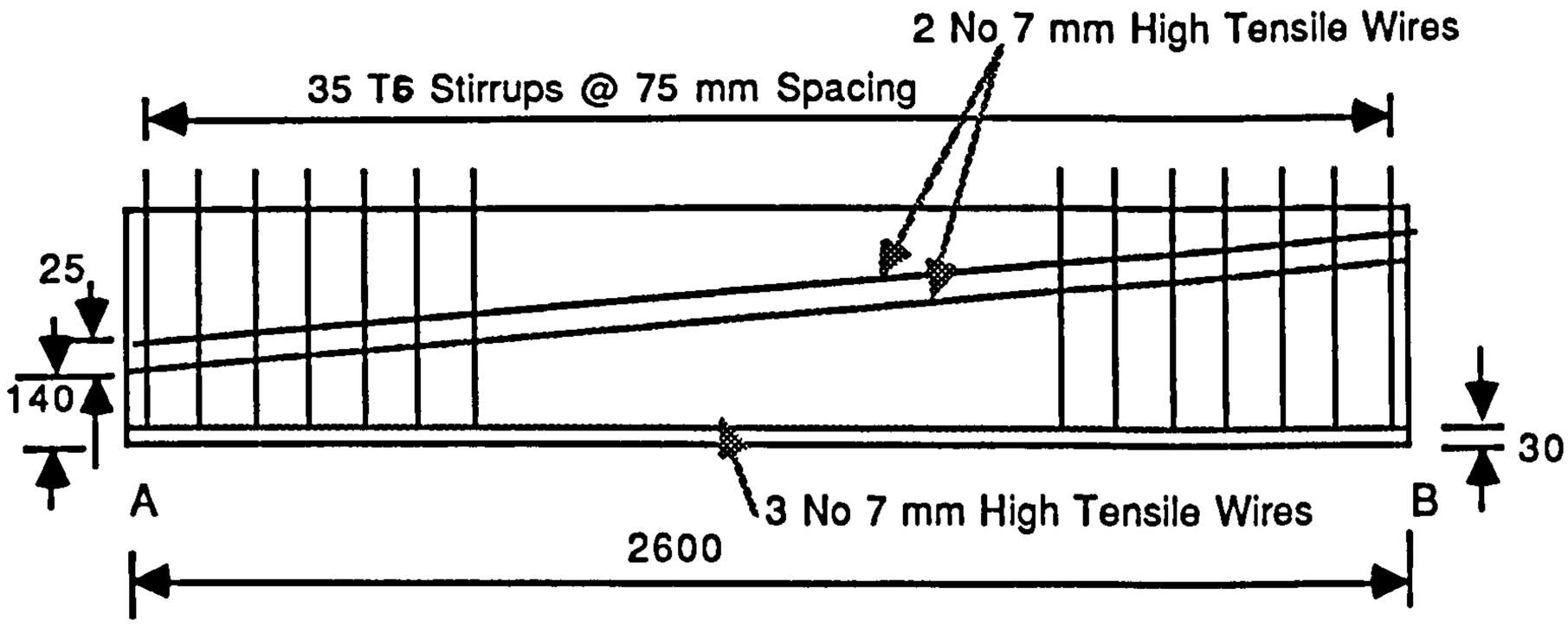

Fig. 4.3 Reinforcement Details of Pretensioned Beams in Series-A

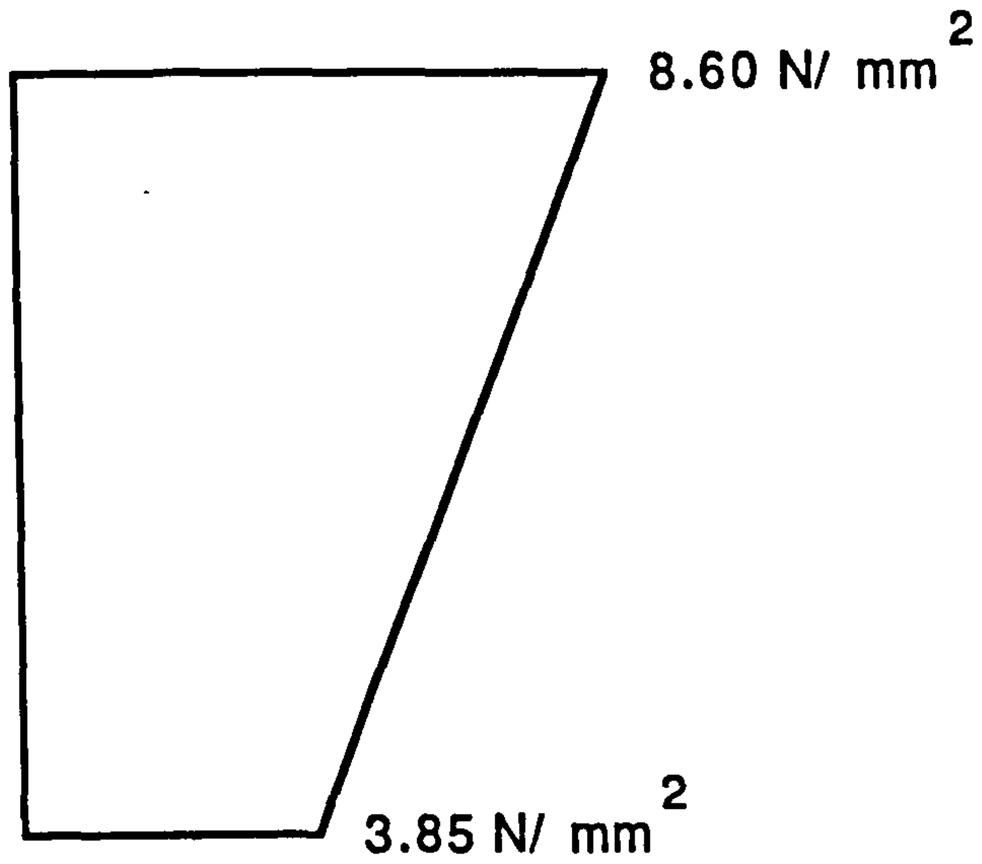

Fig. 4.4 Prestress in 1/3 Scale Precast M Beams at Section X-X (Fig. 4.2)

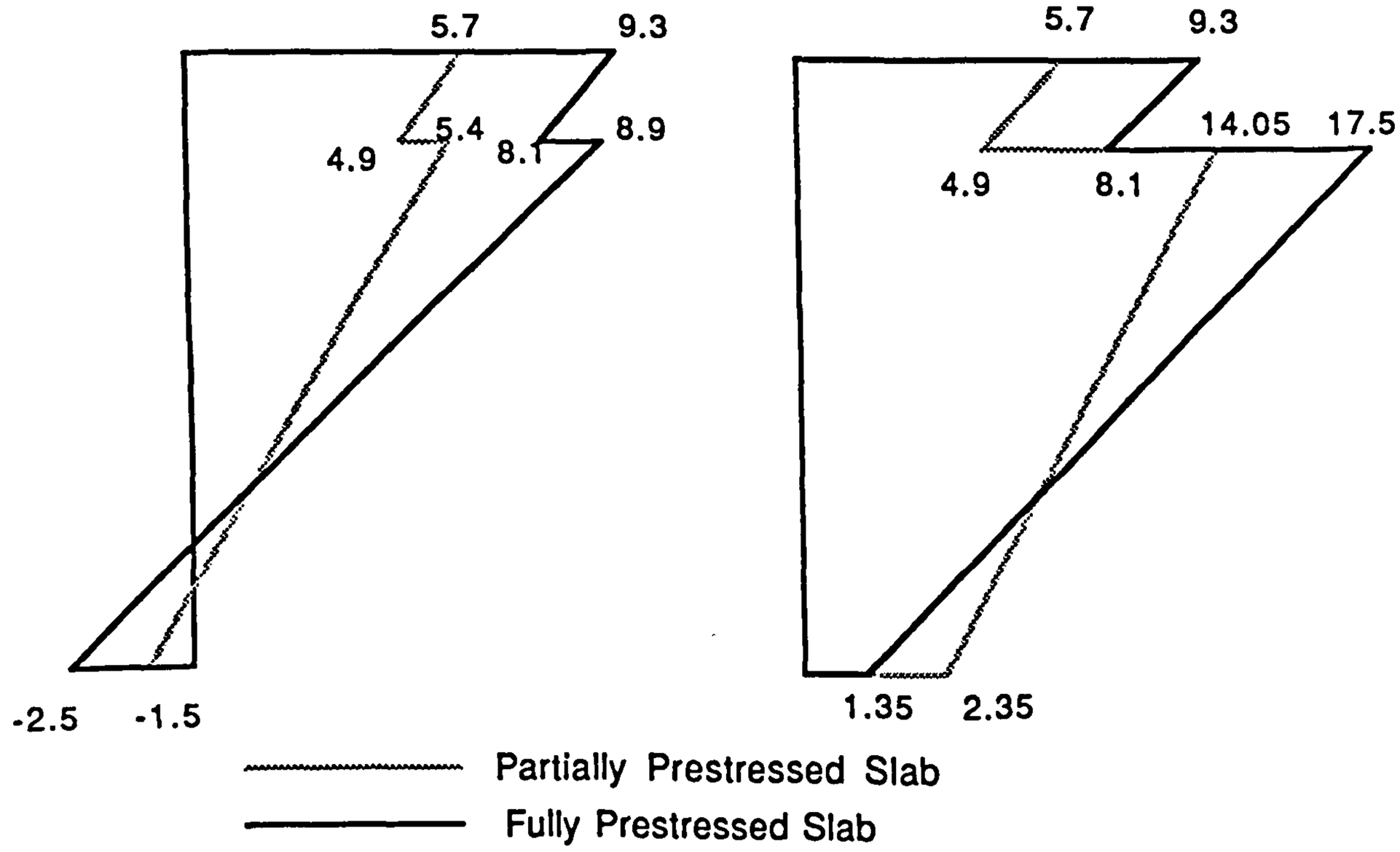

(a) Prestress Distribution due to Prestress in the Slab

(b) Resultant Prestress Distribution in the Composite Beam

Fig. 4.5. Prestress in the Composite Section at Section X-X (See Fig. 4.2)

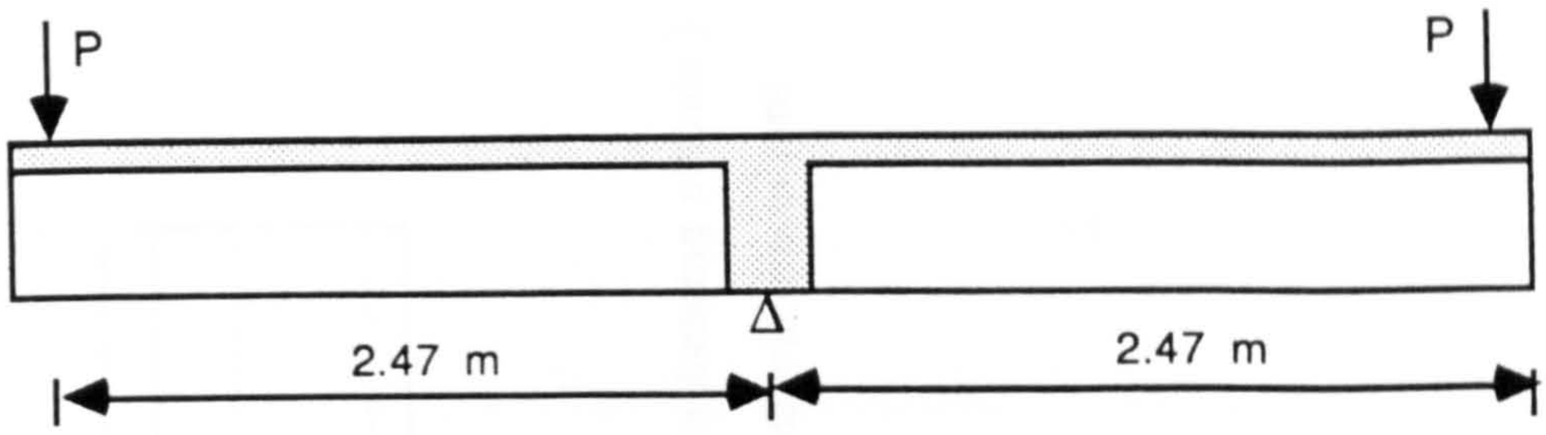

(a) Double Cantilever Loading

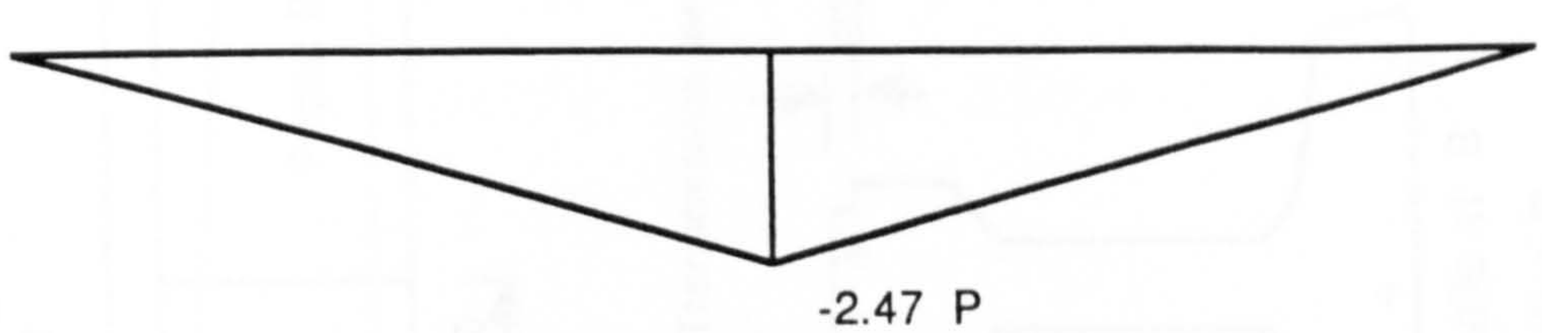

(b) Bending Moment diagram

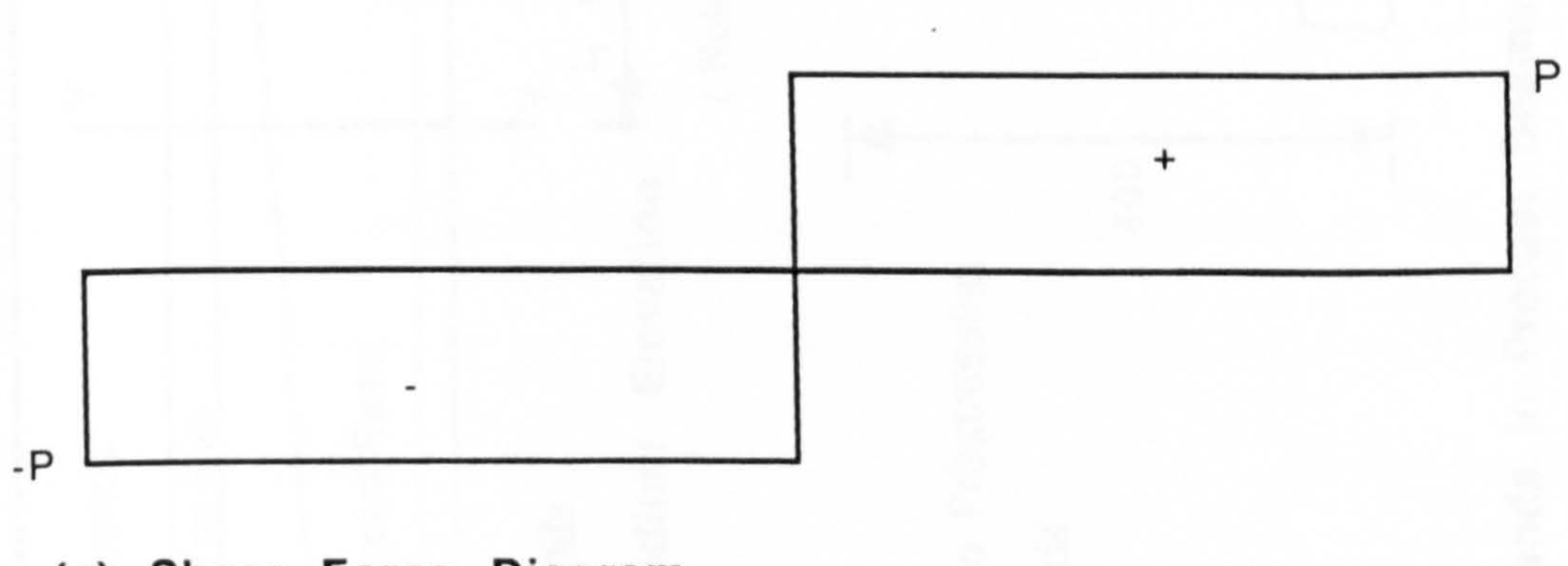

(c) Shear Force Diagram

Fig. 4.6 Double Cantilever Loading for Flexural Tests

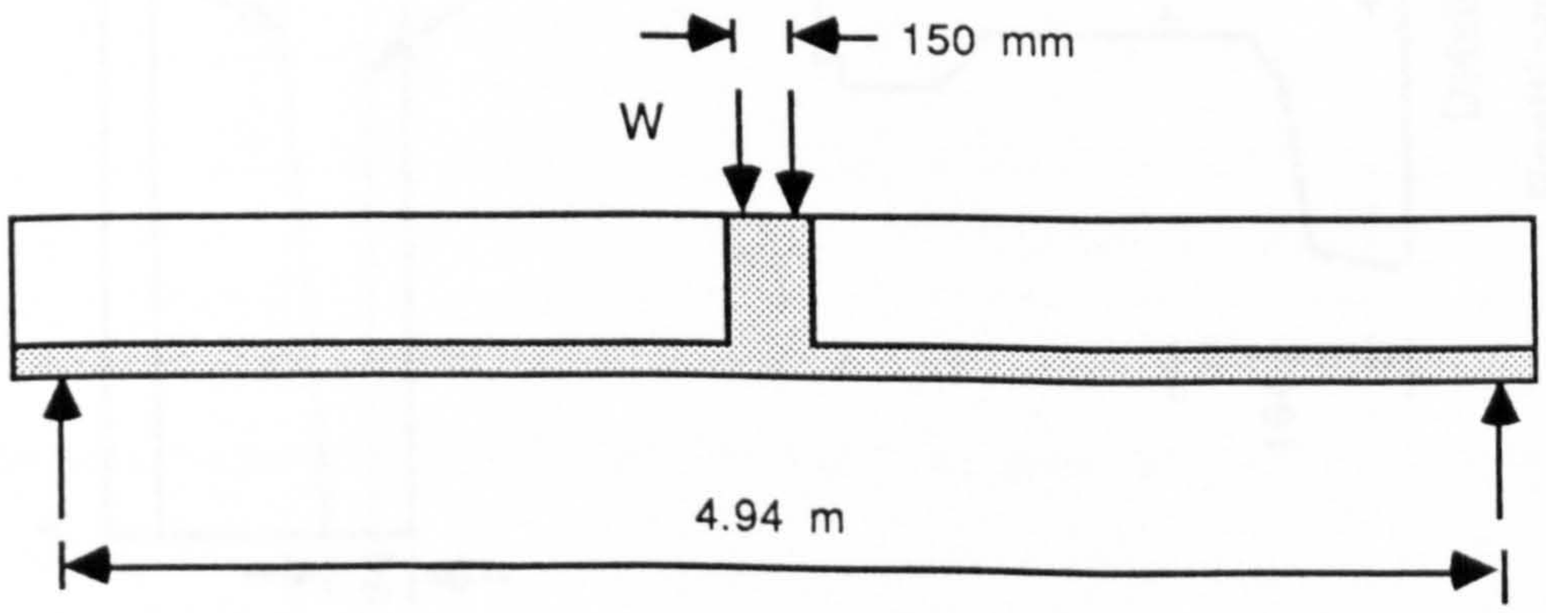

Fig. 4.7 Adopted Loading Arrangement for Series A

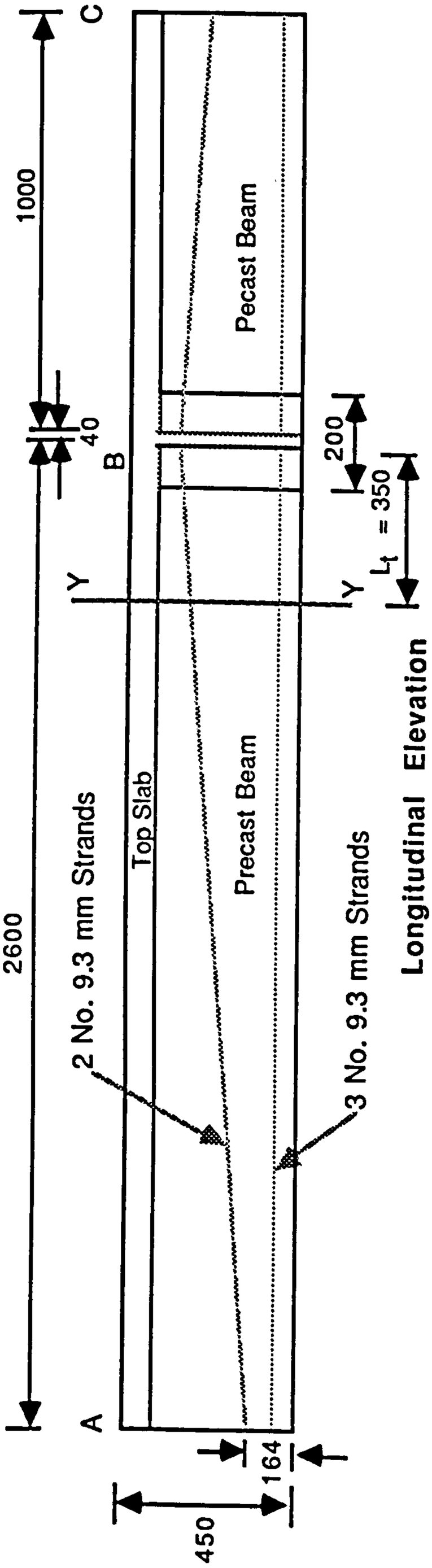

Positions of 9.3 mm Strands in Precast Beams of Series-B

Details of Model Beams in Series B

Fig. 4.8

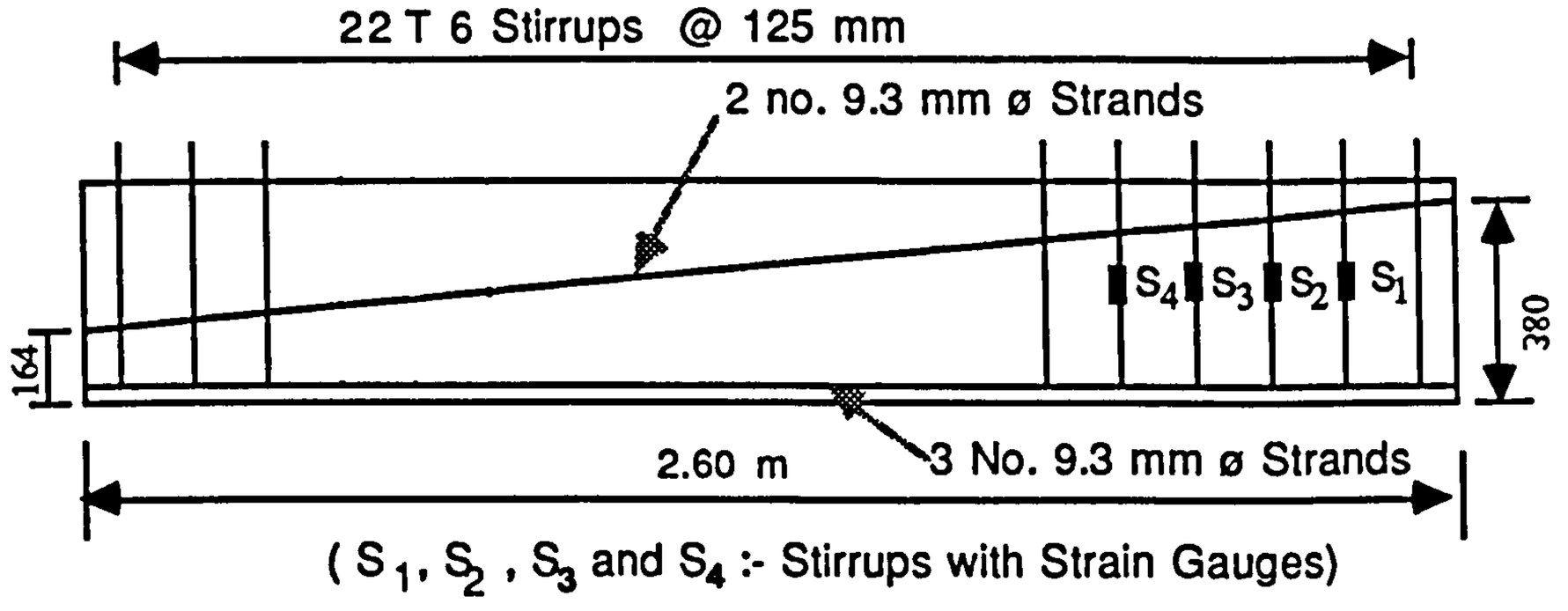

(a) Reinforcement Details for Precast Beams of Model Beams B-1, B-2 and B-3

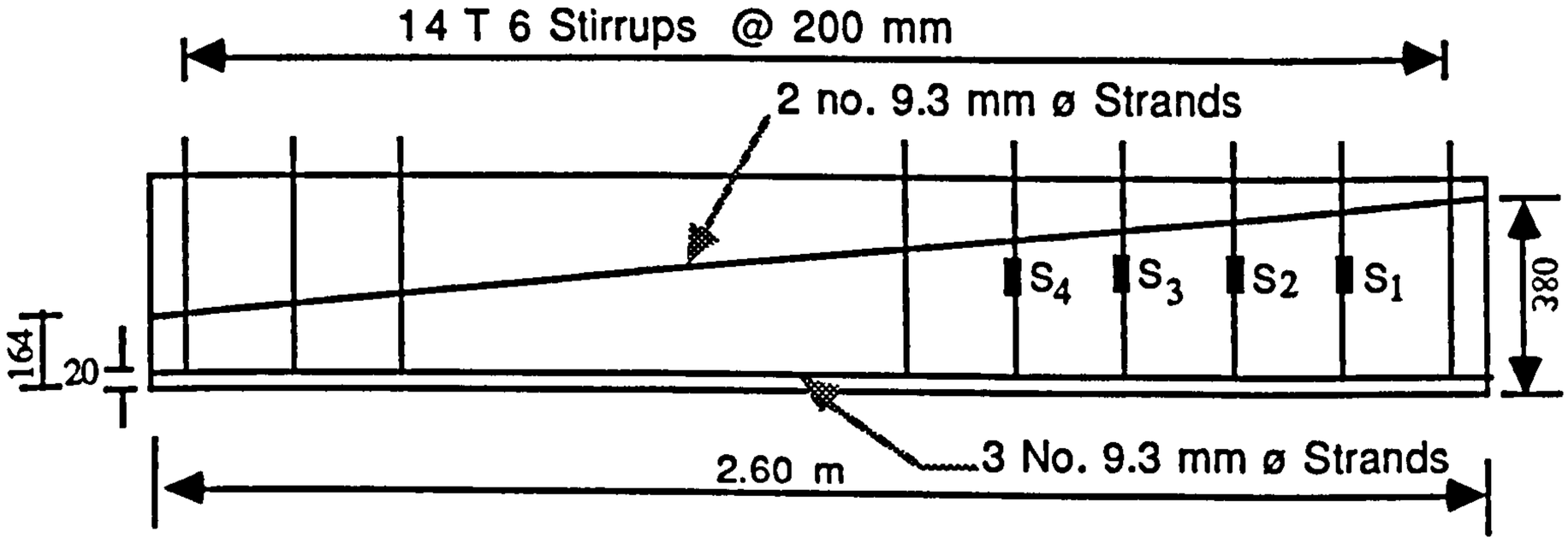

(b) Reinforcement Details for Precast Beams of Model Beams B-4, B-5, B-7 and B-8

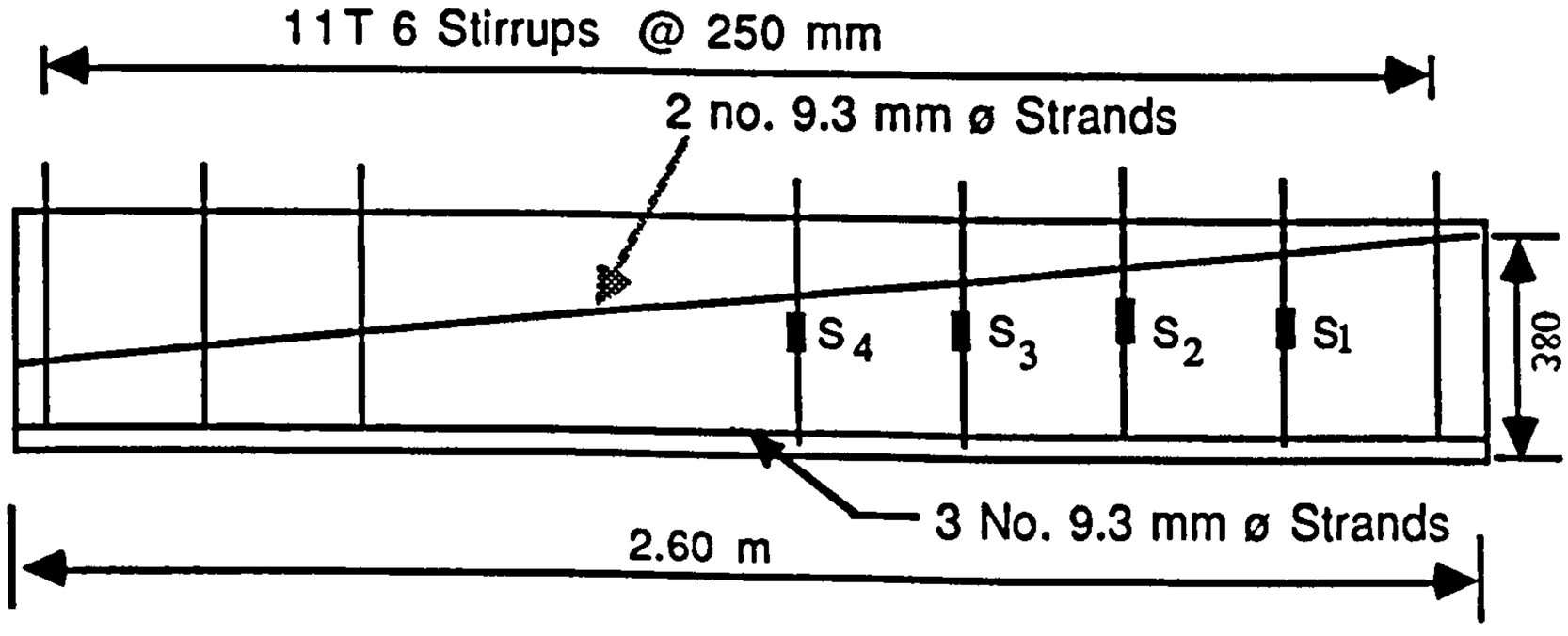

(c) Reinforcement Details for Precast Beams of Model Beam B-6

Fig. 4.9 Reinforcement Details of Precast Beams in Series-B

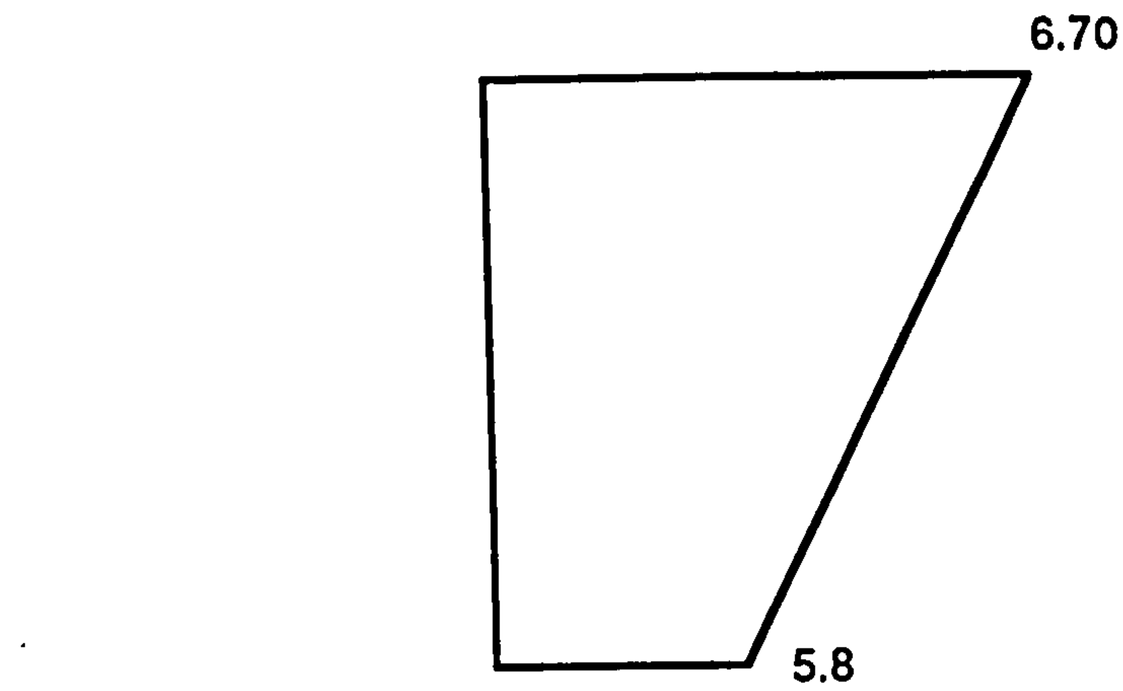

(a) Prestress Distribution in the Precast Beam alone at Section Y-Y (Fig. 4.8)

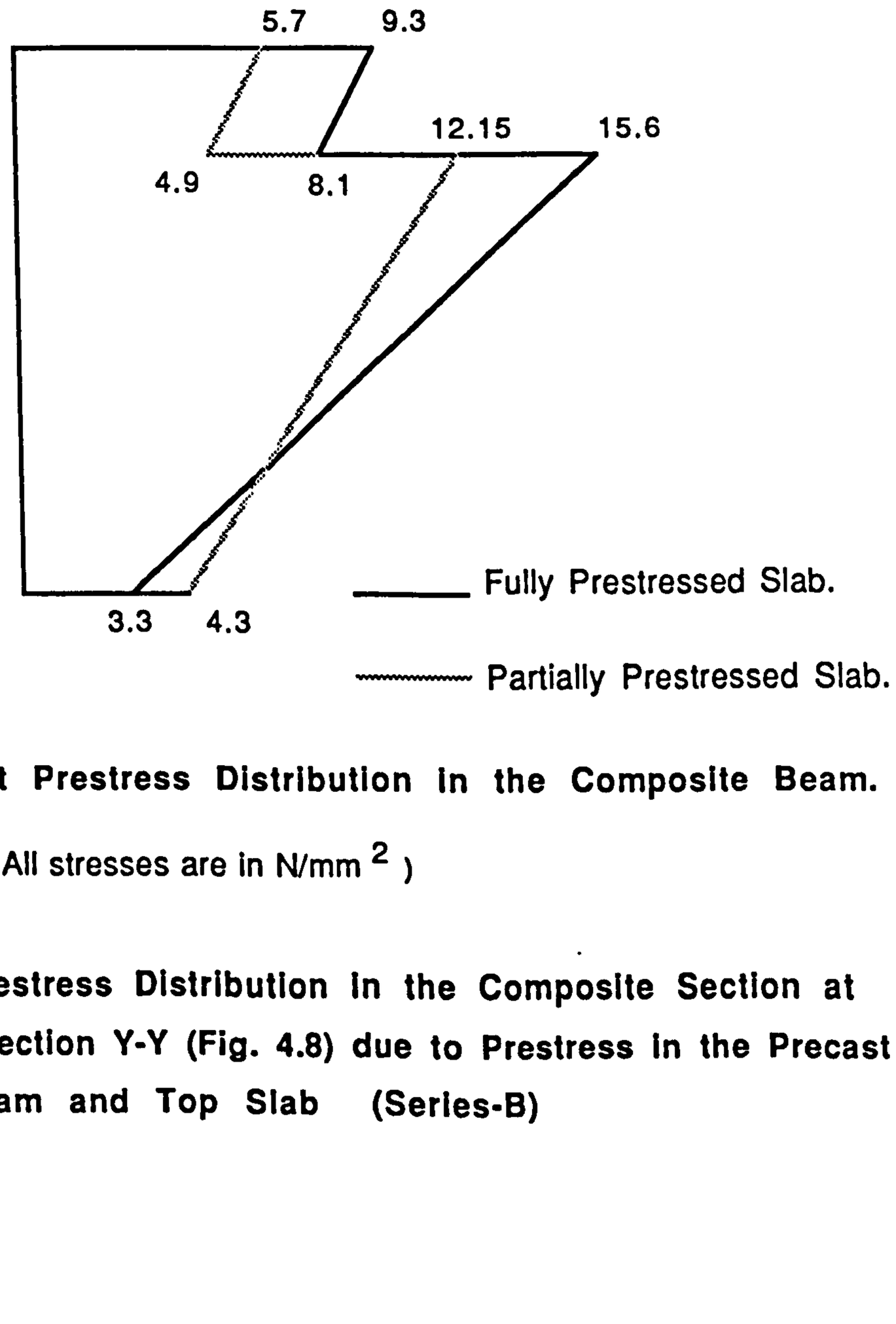

(b) Resultant Prestress Distribution in the Composite Beam.

(All stresses are in N/mm ^{2})

Fig 4.10: Prestress Distribution in the Composite Section at Section Y-Y (Fig. 4.8) due to Prestress in the Precast Beam and Top Slab (Series-B)

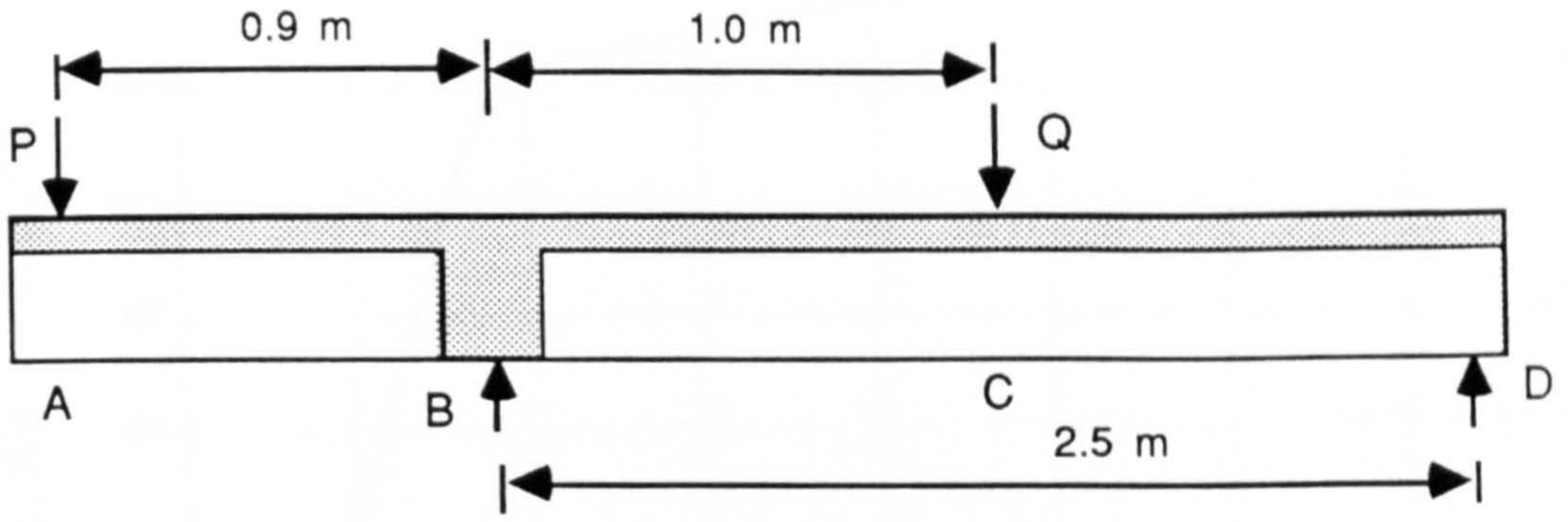

(a) Positions of Loads and Supports.

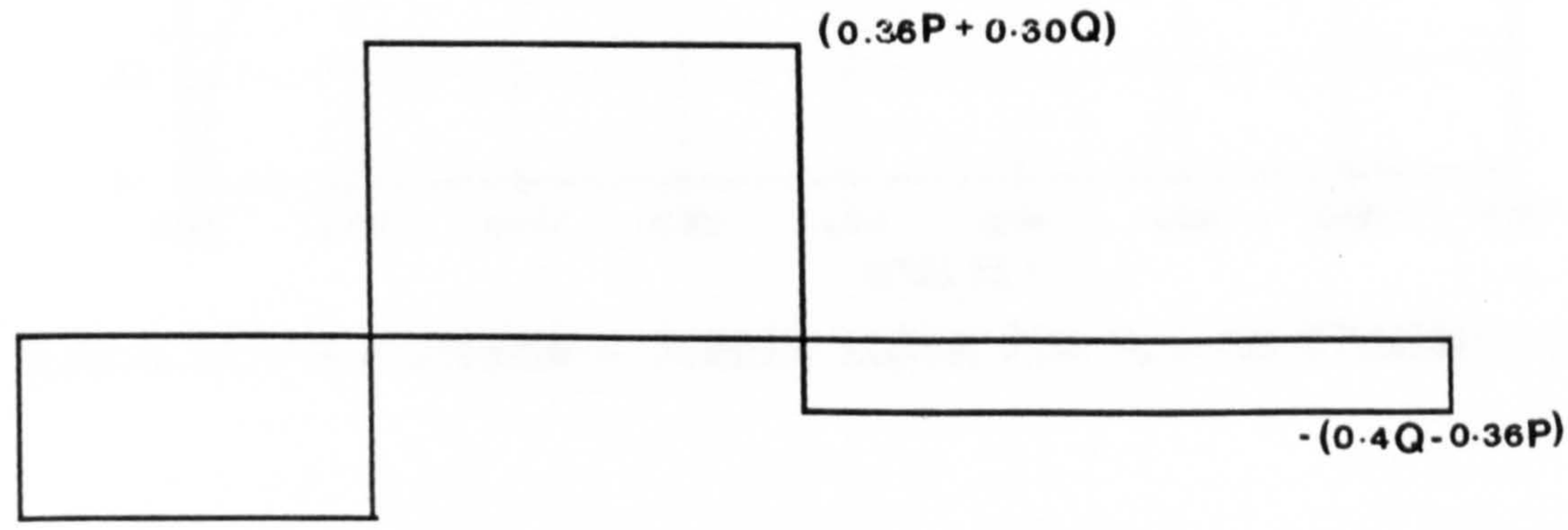

(b) Shear Force Diagram.

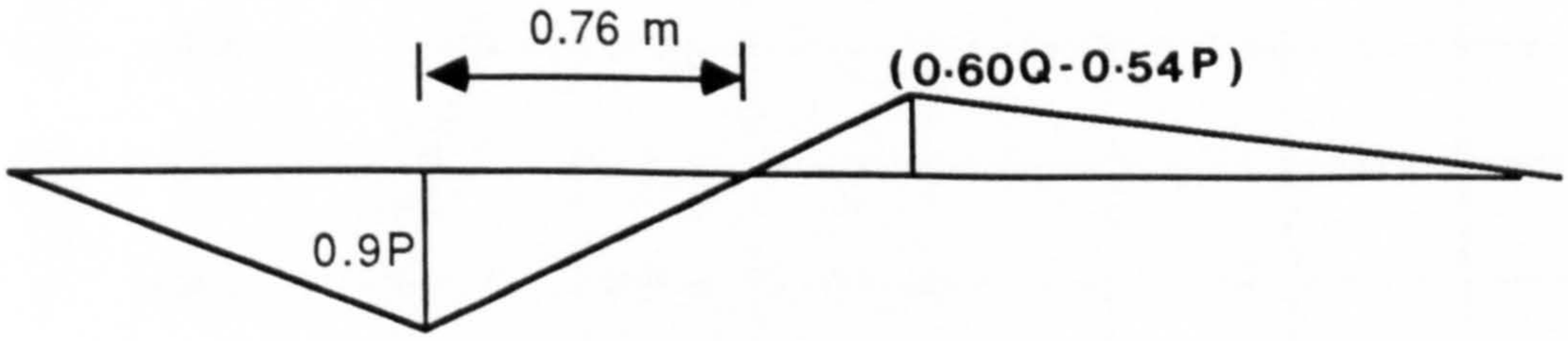

(c) Bending Moment Diagram.

Fig.4.11 Loading Arrangement for Shear Test Series.

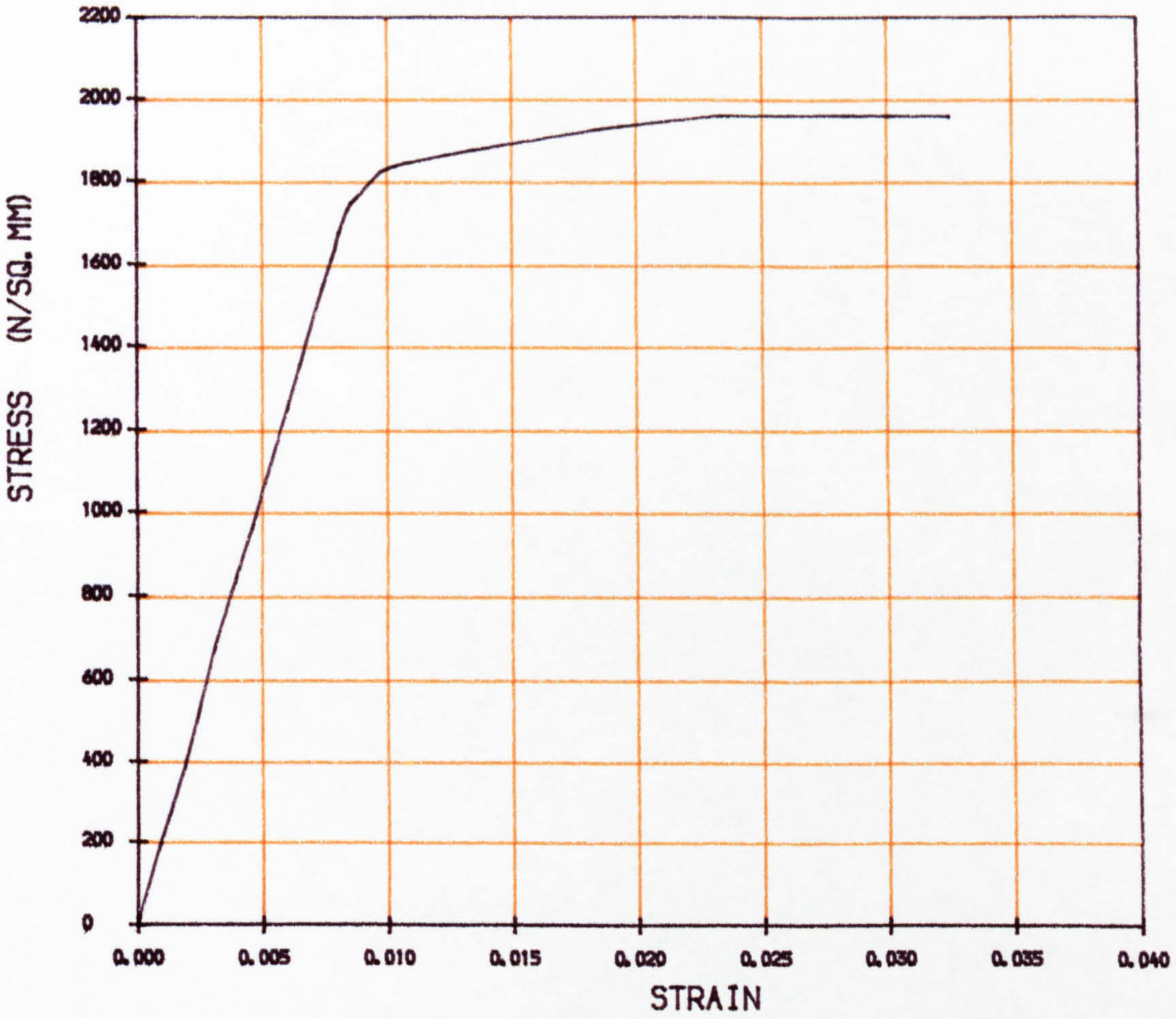

FIG. 4.12 (a) : STRESS - STRAIN CURVE FOR 9.3 MM STRAND

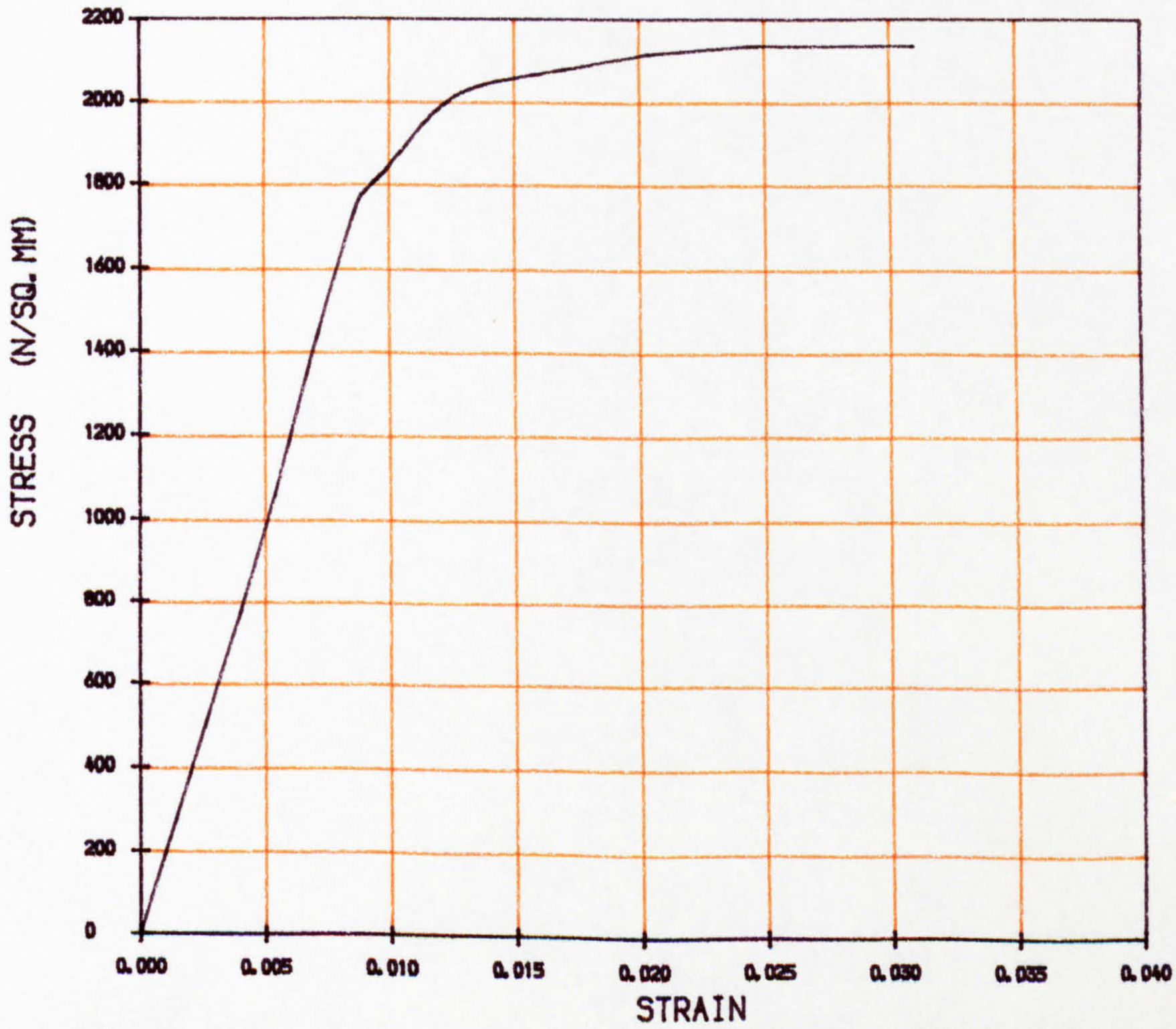

FIG. 4.12 (b) : STRESS - STRAIN CURVE FOR 9.6 MM STRAND

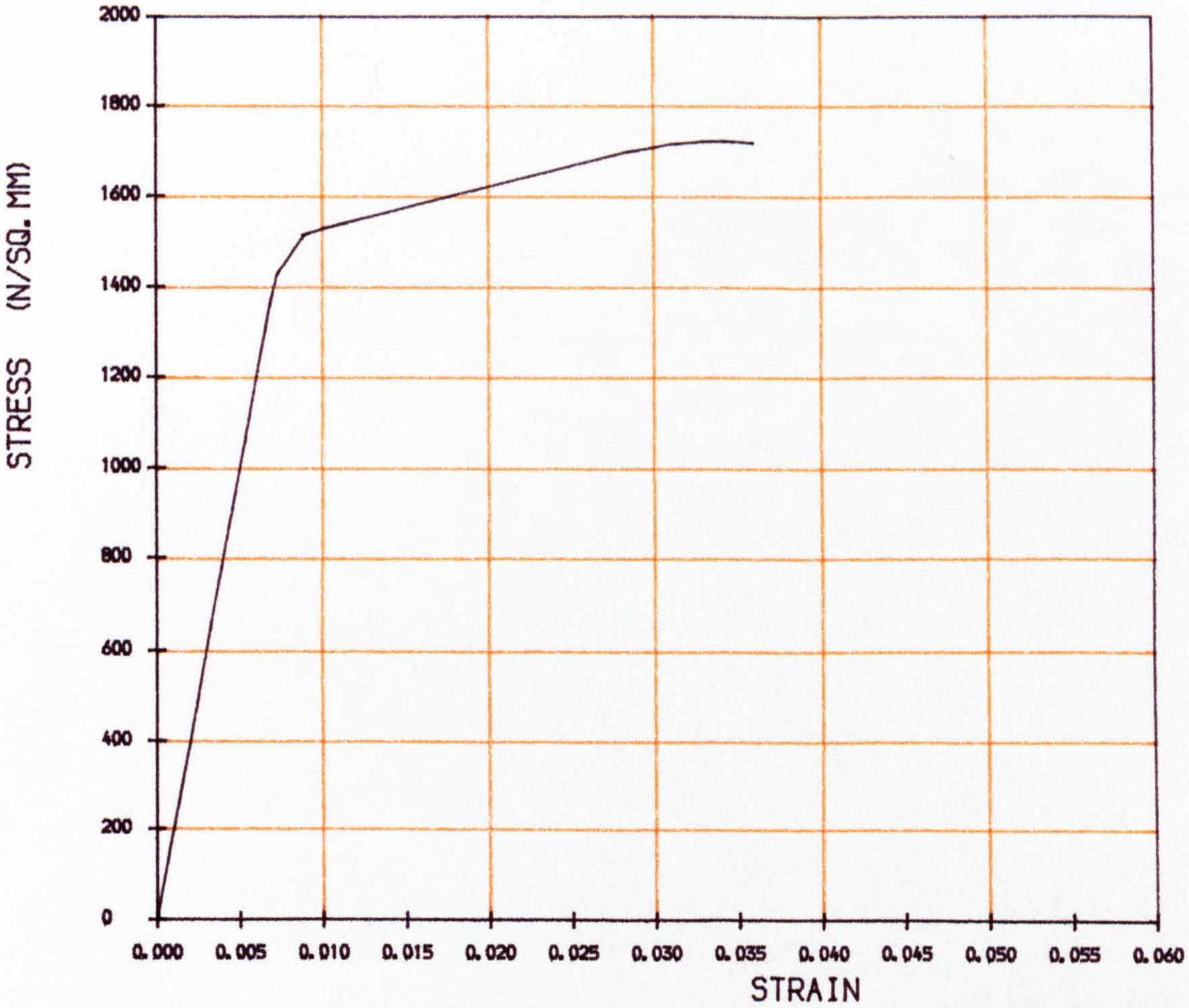

FIG. 4.12(c) STRESS - STRAIN CURVE FOR 7 MM HIGH TENSILE WIRE

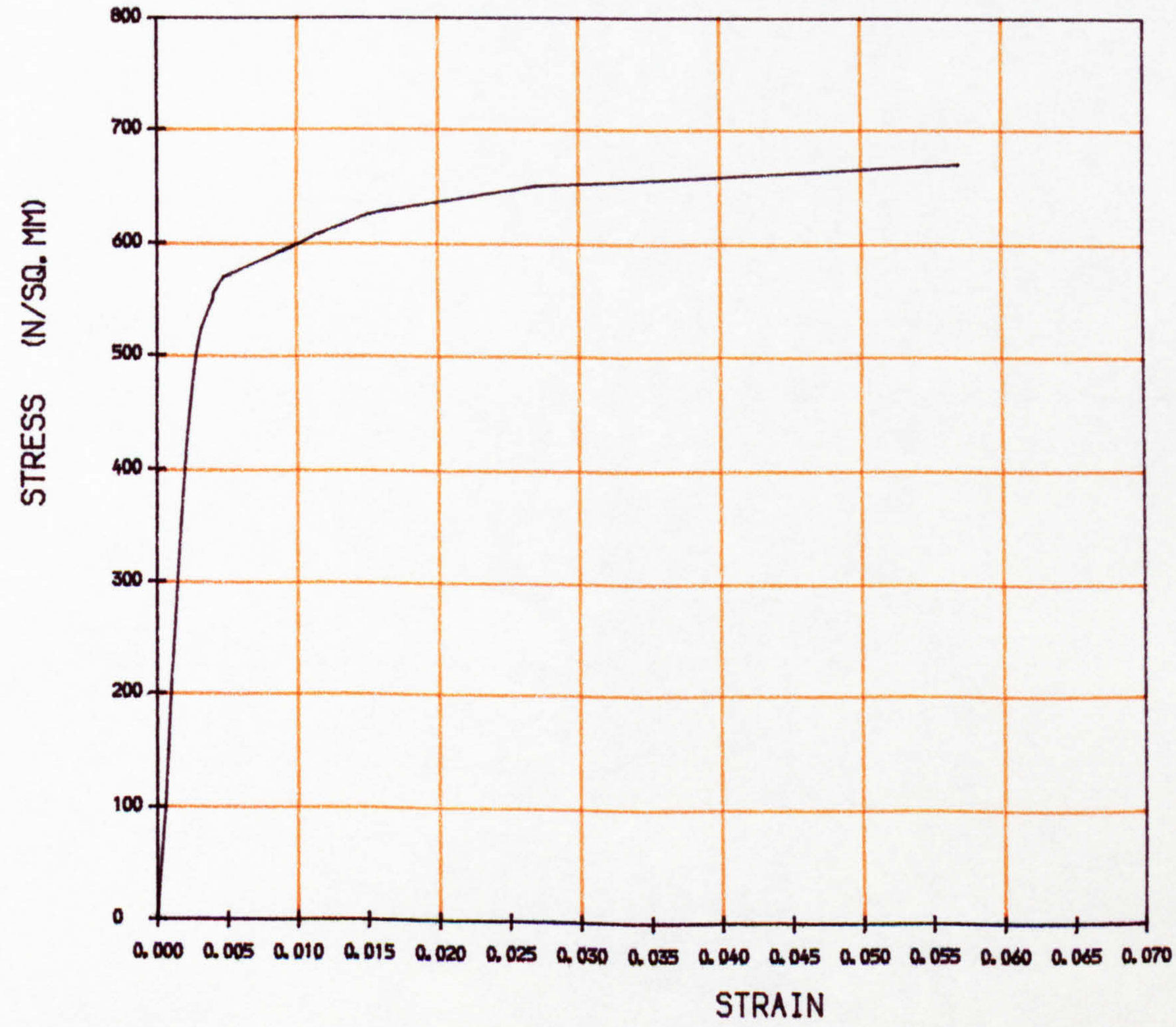

FIG. 4.12(d) . STRESS STRAIN CURVE FOR 6 MM HIGH YIELD BAR

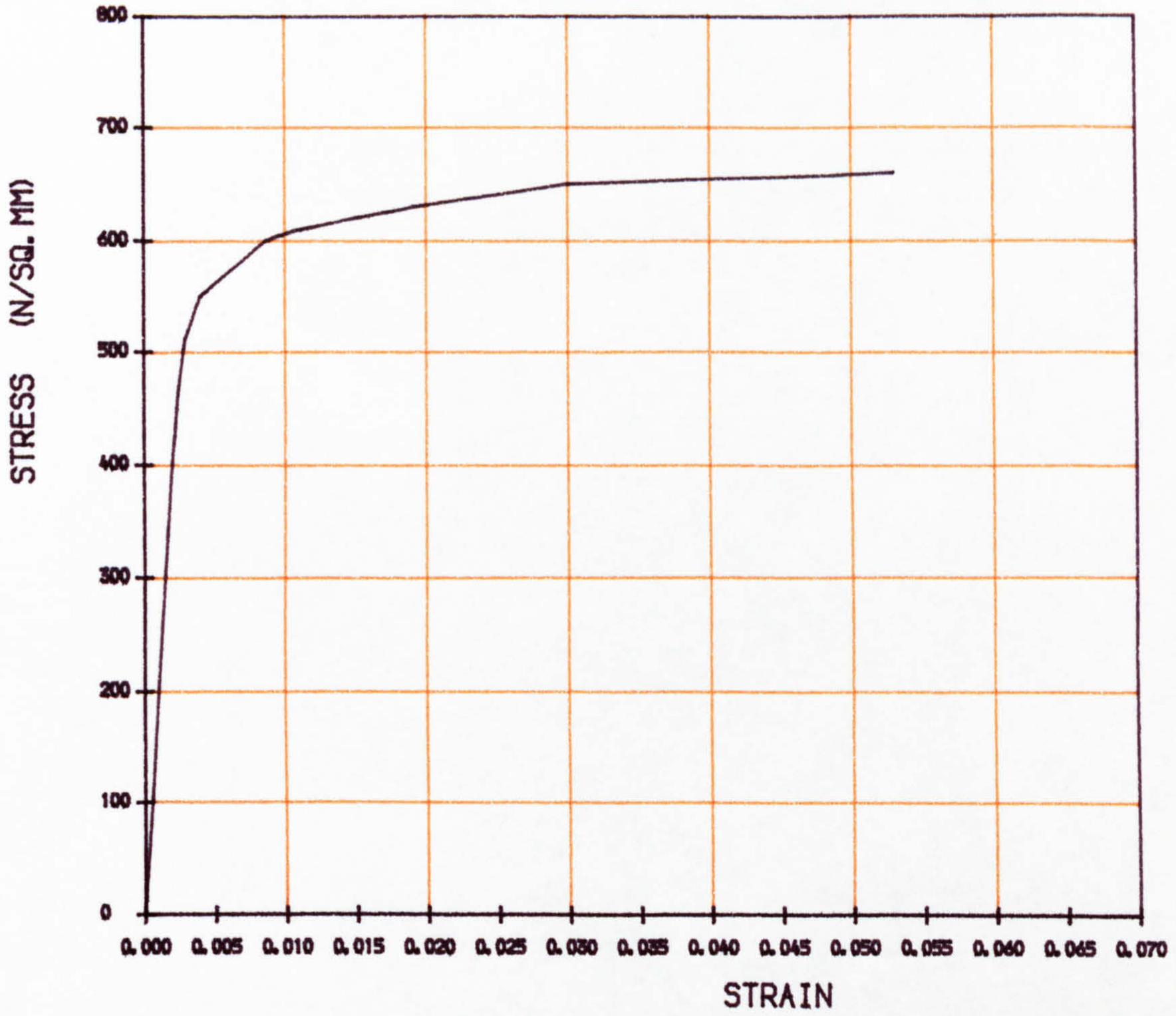

FIG. 4.12(e) : STRESS-STRAIN CURVE FOR 8 MM HIGH YIELD BAR

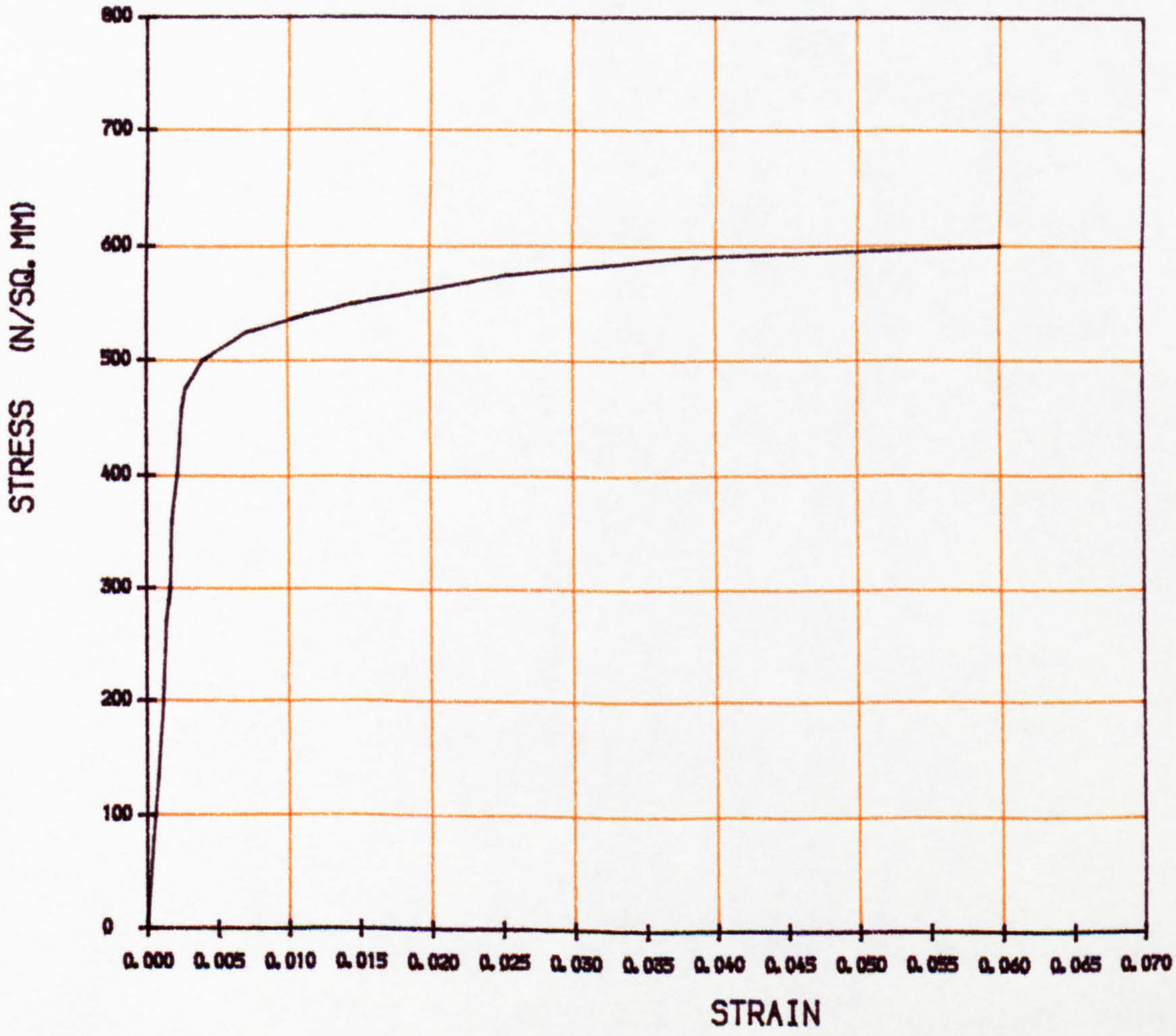

FIG. 4.12(f) : STRESS- STRAIN CURVE FOR 12 MM HIGH YIELD BAR

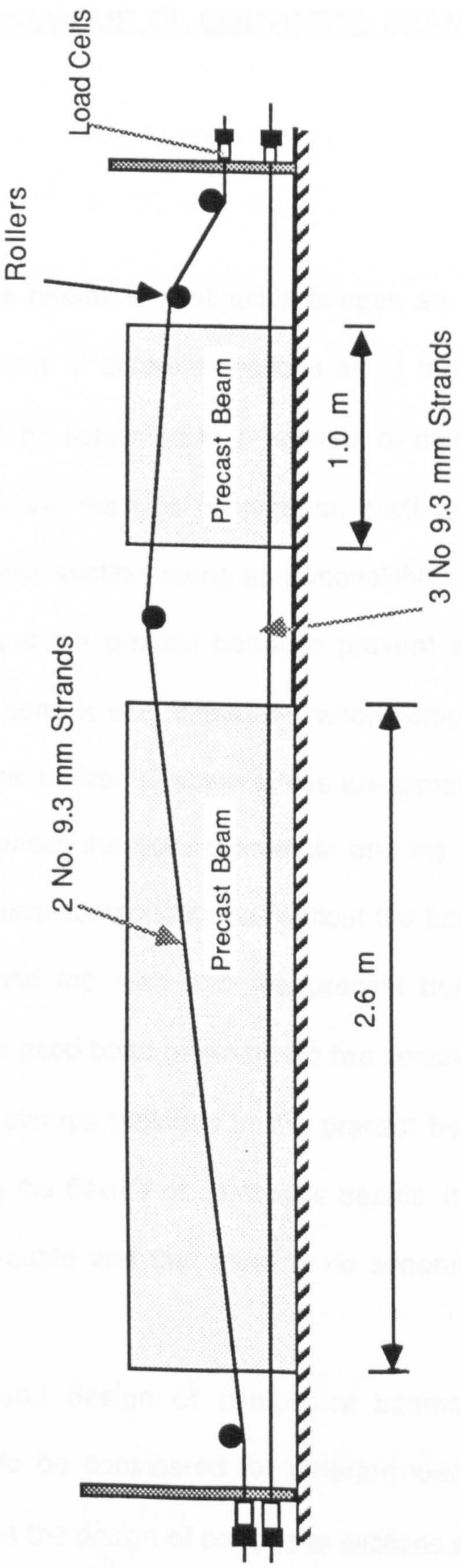

Fig. 4.13. Pretensioning Arrangement for Series-B Beams (Side Channels Omitted for Clarity)

CHAPTER 5

FLEXURAL BEHAVIOUR OF COMPOSITE BEAMS

5.1 General

Composite concrete beams in continuous bridges are subjected to positive or negative bending moments at different sections along the bridge. It is possible that the same section can be subjected to a reversal of moments under different loading conditions. Whichever the type of moment, it will be resisted by the two components of the composite section acting as a monolithic beam, if there is good bond between the slab and the precast beam to prevent any excessive slip or separation. This interface bond is very important when composite action develops under bending moments, as horizontal shear stress are generated at the interface. Composite behaviour increases the flexural strength and the stiffness compared to the member made of identical components but without the bond[42]. The horizontal shear transfer between the top slab and the precast beam can be achieved conveniently by ensuring a good bond between the two concrete elements and also by extending the vertical stirrups provided in the precast beam into the top slab. In this chapter concerning the flexure of composite beams, it will be assumed that the interface bond is adequate and that there is no separation between the two components.

In the analysis and design of composite beams under flexure, the appropriate section has to be considered for different loading and construction stages. Therefore it makes the design of composite sections more complicated than for monolithic beams. According to the major design codes[27,28,35,39], composite sections are mainly designed using the specifications for reinforced

concrete and prestressed concrete beams.

The internal support section of a composite beam, made continuous by the conventional method of providing reinforcing bars in the top slab, must be designed as a reinforced concrete section. However, when a prestressed slab is used in the the negative moment region to develop continuity, such sections can be designed as prestressed sections. The relevant specifications of codes of practice for designing composite beams at the interior supports which are subjected to negative moments, will be briefly discussed in the following sections. Those points which are useful for the analysis of results of flexural test series in which beams were tested as statically determinate structures to simulate negative moment regions, will be given the main attention.

5.2 Analysis of Composite Beams in Bending

For the analysis of reinforced and prestressed concrete beams up to failure, it is necessary to make certain assumptions and to know the complete stress-strain characteristics of concrete and steel. The following assumptions are those which are generally made for both reinforced and prestressed concrete sections.

(1) Plane sections remain plane during bending.

(2) Strain in steel is the same as the strain in surrounding concrete

The first assumption implies that the strain distribution is linear across the section, whereas the second assumes that there is no slip between concrete and steel. Depending on whether the section is uncracked or cracked, other assumptions are made to simplify the analysis.

5.2.1 Stress -Strain Curve for Steel

To simplify the analysis, idealised stress-strain curves can be used in place of the actual curve. The idealised curves given in codes of practice consist only of straight line portions making them much easier to use. In BS 5400 : Part 4 [27], the idealised curves for prestressing and reinforcing steel have three linear portions. In BS 8110[28] and CEB-FIP Model Code[40], only two linear portions represent the entire stress-strain curve of reinforcing bars while three linear segments are used for prestressing steel. According to these two codes, the stress-strain curve of reinforcing bars is taken to be same both in tension and compression but BS 5400 uses a lower strength for compression. The idealised curve for prestressing steel is given in Fig. 5.1 and that of reinforcing bars as recommended by BS 8110 and BS 5400: Part 4 are shown in Fig. 5.2.

5.2.2 Stress-Strain Curve of Concrete

The stress-strain characteristics of concrete are much less well defined than those of steel. They depend on many factors such as the method of testing, the rate of loading, size and shape of specimens etc.. The actual stress-strain curve in compression begins with a linear portion and becomes non-linear when the stress approaches the maximum value. Finally, it has a descending branch before failure in compression at a maximum strain between 0.003 and 0.004 [43,44].

In the analysis of concrete beams under service loads, it can be safely assumed that the stress-strain relationship of concrete is linear. However, for ultimate strength analysis, the non-linear, non-elastic portion of the curve has to be considered. For this, the design codes allow the use of idealised stress-strain curves for concrete in compression in which the descending branch of the actual

curve is ignored.

For more accurate and rigorous methods of analysis at ultimate limit state, a rectangular-parabolic stress-strain curve is considered in British codes BS 8110, BS 5400: Part 4 and CP 110 [45] which has now been withdrawn. The maximum compressive strain of concrete is limited to 0.0035 and the stress to $0.67f_{cu}/\gamma_m$. The CEB-FIP Model Code also recommends a rectangular parabolic curve. The American codes [35,39] do not specify a particular shape and allow any curve of appropriate shape which results in predicting the actual strength with the maximum compressive strain limited to 0.003. The idealised curve of BS 8110 is shown in Fig. 5.3(a).

As the parabolic-rectangular curve is not convenient for the use in normal design work, all major British design codes allow the use of a rectangular stress block. It considerably simplifies the design calculations without sacrificing much accuracy. Slight variations exist in the depth and magnitude of the compressive stress in the rectangular stress block adopted by different design codes. In BS 5400: Part 4 and CP 110, the stress block extends to the neutral axis with compressive stress being $0.6f_{cu}/\gamma_m$. In the new BS 8110, the depth has been changed to 0.9 times the neutral axis depth while the magnitude of compressive stress is $0.67f_{cu}/\gamma_m$. ACI Building Code(318-83), AASHTO Specifications and CEB-FIP Model Code also adopt similar stress blocks that do not extend to the neutral axis. Some of these stress blocks are shown in Fig. 5.3(b).

Beeby [46], after studying different types of stress blocks found that the BS 8110 type stress block yielded results close to those obtained from using the parabolic-rectangular stress block for most practical cases. It will thus be used for analysis of composite sections in this report.

5.3 Serviceability Requirements of Composite Beams

The serviceability requirements of reinforced concrete and prestressed concrete members are also applicable to composite beams consisting of precast prestressed beams and in-situ top slab. Additionally, the effects of differential shrinkage have to be considered under service conditions. At the interior supports, there are restraint moments due to differential shrinkage and due to creep of concrete under dead loads and prestress in the precast beams. These are long-term effects and therefore not applicable to the short-term tests.

When continuity is established between precast beams by providing reinforcing bars in the slab, the negative moment region of the beam is designed as a reinforced concrete section and therefore the design will be based mainly at ultimate limit state conditions. However, crack widths and deflections are checked at serviceability limit state and the methods of calculating these will be given later.

For prestressed concrete sections with a prestressed slab in the negative moment regions, the serviceability limit state is very important. The members are classified according to the extent in which tensile concrete stresses are allowed. The stresses in composite beams can be calculated at the service loads using elastic theory and giving consideration to the different stages of loading.

5.3.1 Limiting Tensile Stresses for Prestressed Concrete Beams

According to BS 5400: Part 4 and BS 8110, no tensile stresses are allowed in Class 1 prestressed beams. Class 2 beams are allowed to develop tensile stresses under service loads but they are not allowed to exceed the design flexural strength of concrete ($0.45\sqrt{f_{cu}}$ for pretensioned beams and $0.36\sqrt{f_{cu}}$ for post

tensioned beams). For Class 3 beams, cracking is allowed but control of crack widths is expected by limiting the fictitious tensile stress which would be developed in an uncracked beam [27,28]. An increase in the tensile stress is allowed when additional non-prestressed reinforcement is provided in the tension zone. As partially prestressed concrete beams are cracked under service loads, the cracked section must be used in the analysis if higher accuracy is required. The analysis of uncracked and cracked prestressed and reinforced concrete sections will be given later.

5.3.2 Limiting Compressive Stresses for Prestressed Concrete Beams

The compressive stress in the bottom flange of a continuous composite beam near the interior support can be significant under service loads due to the fact that compressive stresses due to service loads add to the already existing prestress in the girder. According to BS 8110, a maximum compressive stress up to 0.4 f_{cu} is allowed near the supports of continuous beams while ACI Code specifies a limit of $0.45f_c'$.

5.4 Analysis of Interior Support Section Under Negative Moments

5.4.1 Uncracked Section

The uncracked prestressed concrete beams can be analysed using the elastic theory with the linear elastic stress-strain characteristics of steel and concrete. It will also be applicable for reinforced concrete sections under small bending moments. The predicted behaviour of both prestressed and reinforced beams using such theory will be linear up to the cracking moment. For analysis, transformed

concrete sections which takes account of the area of prestressed and non-prestressed steel is used and sectional properties are determined accordingly.

In the analysis of continuity connections subjected to negative bending moments, the prestress in the ends of precast beams can be neglected. As far as the negative bending is concerned, the critical section is either the diaphragm or the adjacent composite section which is well within the transmission length of the prestressing steel.

5.4.2 Cracking Moment

In concrete beams, cracking is considered to occur when the tensile stress in the extreme fibres exceeds the modulus of rupture (f_r), which is the flexural tensile strength of concrete. Before the cracks which are visible to the naked eye occurs, very fine micro cracks develop at a tensile stress between 2 and 4 N/mm^2 which is about the direct tensile strength of concrete[37].

The modulus of rupture of concrete is generally obtained from flexural tests on concrete prisms. These small scale prisms tend to exhibit a greater strength than large scale beams due to the presence of steeper strain gradients in small beams[47,48]. Various design codes also give the values of modulus of rupture related to the square root of compressive strength of concrete. ACI Building Code[35] and AASHTO Standards [39] recommends a value of $7.5\sqrt{f_c'}$ psi ($0.627\sqrt{f_c'}$ N/mm^2) for f_r. Although, British codes do not directly specify a value for f_r, a design tensile strength of $0.45\sqrt{f_{cu}}$ is given for flexural cracking of pretensioned members[27,28]. When the partial safety factor is excluded, this implies a tensile strength of $0.58\sqrt{f_{cu}}$ which is very close to the value of $0.556\sqrt{f_{cu}}$ proposed by Beeby[49]. For post-tensioned beams with grouted

tendons, a slightly lower flexural tensile strength of 0.36 $\sqrt{f_{cu}}$ is specified by the codes. Leonhardt[50] has recommended that although the tensile strength of concrete is slightly higher in flexure than in axial tension, the values for direct tension should be used for flexural cracking. He also reported that concrete cracks when the tensile strain exceeds 0.010% to 0.012% regardless of the concrete strength.

The cracking moment of a prestressed member can be expressed in the general form by using the elastic theory and the transformed sectional properties of beam section as

$$M_{cr} = (P/A + P\ e\ y/I + f_r)\ I/y \qquad \text{.....Eqn. 5.1}$$

where y is the distance between the extreme fibres in tension and the centroid.

The flexural cracking results in a marked change in the behaviour of the beam. Cracking reduces the stiffness of the beam causing the deflection to increase at a higher rate with increase in load. A similar effect can be seen on moment-curvature relationship. A sudden increase in the stress of the tensile steel can also be expected when the cracking occurs as the tensile resistance of concrete is transferred to steel. These three phenomena are very useful additional checks to obtain the cracking load in experimental work.

5.4.3 Analysis of Cracked Section

5.4.3.1 Reinforced Concrete Section

Reinforced concrete beams develop flexural cracks at very early stages of loading and the behaviour of the cracked section is important under service loads. When cracking occurs, the tensile resistance of concrete in the tension zone is transferred to the reinforcement, causing a sudden increase in steel stress. Although at the cracks the tensile force is entirely carried by reinforcement, the

uncracked concrete between cracks continue to resist tensile stresses. This effect which reduces the average tensile stress in steel in the cracked zone is called tension stiffening. At loads well above the cracking load, the effects of tension stiffening tend to reduce due to closer spacing of cracks at such loads. According to British codes[27,28], a triangular stress distribution is considered below the neutral axis with a tensile stress of 1.0 N/mm^2 at the level of tension steel to take into account of tension stiffening in the calculation of curvature of cracked sections. Another alternative is to consider an effective area of concrete around the tension steel and this has been discussed by Clark and Speirs[51]. The latter has been adopted by CEB-FIP Code[40].

An analysis of a cracked reinforced concrete section is given herein. The stress and strain distributions in concrete are considered to be linear. The neutral axis depth is determined ignoring the tension stiffening. Then, the tensile stresses in concrete as specified in BS 8110 are considered and the stresses in concrete and steel are modified assuming that the position of the neutral axis remains unchanged. Allen[52] has shown that this approach can be used with out much error.

Consider the composite section shown in Fig. 5.4 with a reinforced concrete slab subjected to a negative moment M which is greater than the cracking moment. The stress and strain distributions (ignoring tension in concrete) are shown in Fig.5.4.

Considering the equilibrium of forces

$$A_s f_s = 0.5 f_c b x - (b-b_w) f_c (x-h_f)^2 / 2x \quad \text{.....Eqn. 5.2}$$

Equilibrium of moments gives

$$M = 0.5 f_c b x (d-x/3) - (b-b_w) f_c (x-h_f)^2 (d-h_f-(x-h_f)/3)/2x \quad \text{.....Eqn. 5.3}$$

Considering strain compatibility,

$$\frac{f_s}{E_s} = \frac{f_c}{E_c}\,\frac{(d-x)}{x} \qquad \text{.....Eqn. 5.4}$$

Therefore , $f_s = \alpha\, f_c\, (d-x)/x$ .....Eqn. 5.5

where $\alpha = E_s / E_c$

Solving Equations 5.2 and 5.5 gives

$$x\, b_w = -((b-b_w)h_f + \alpha\, A_s) + (((b-b_w)h_f + \alpha\, A_s)^2 + b_w((b-b_w)\, h_f^2 + 2\,\alpha\, A_s\, d)^{0.5} \qquad \text{.....Eqn. 5.6}$$

Substituting the values of x in Eqns. 5.2 and 5.5, f_c can be found and therefore f_s (from Eqn. 5.5). When the tension stiffening is considered, the value of f_s is modified to account for the contribution to the tensile force from tension carried by concrete.

This method can be used with reasonable accuracy if the compressive stress is less than half of the compressive strength of concrete and steel stress is below the yield stress[43]. Similar results can be obtained by using a cracked transformed section.

The equations can be modified for rectangular sections such as diaphragms by making b_w equal to b.

5.4.3.2 Partially Prestressed Concrete Section

Cracked partially prestressed concrete sections can be analysed assuming linear elastic behaviour. Partially prestressed beams are generally expected to be cracked under service loads.

Although both linear and non-linear methods are available for the analysis of partially prestressed sections, non-linear methods tend to be tedious for composite sections. Here, one of the linear methods of analysis given in the Concrete Society Technical Report 23-Partial Prestressing [37] is considered. The load at which the concrete stress in a partially prestressed beam at the level of steel becomes zero is considered as the reference load for the analysis of the cracked section. The moment at the section and the force in both the prestressed and non-prestressed steel at this load are denoted by M_o and F_o. A composite section subjected to hogging moment is given in Fig.5.5(a). It is assumed that the prestress in the girder at the interior support is negligible. The stress distribution due to prestress applied to the slab is shown in Fig.5.5(b). When moment is increased further, cracks will develop. Stress and strain distributions of the cracked section under a moment M are also shown in Fig.5.5.

Considering the equilibrium of forces,

$$F_o + (A_s + A_{ps})\, f_s = 0.5\, f_c\, b\, x - f_c (b-b_w)\, (x-h_f)^2 / 2x \qquad \text{..Eqn.5.7}$$

Similarly, the equilibrium of moments yields,

$$M = f_c\, b\, x\, (d-x/3)/2 - f_c\, (b-b_w)(x-h_f)^2\, (d-h_f-(x-h_f)/3)/2x$$

.....Eqn. 5.8

Assuming that strain in steel and concrete is same,

$$f_s = \alpha\, f_c\, (d-x)/x \qquad \text{.....Eqn. 5.9}$$

Substituting this in Equation 5.8

$$\frac{M}{F_o D} = \frac{b\, x^2\, (3d-x) - (b-b_w)\, (x-h_f)^2\, (3d-2h_f-x)}{3\, b\, x^2 - 3\, (x-h_f)^2\, (b-b_w) - 6\, \alpha\, (A_{ps}+A_s)(d-x)}$$

.....Eqn. 5.10

For a given M , this cubic equation can be solved to obtain the neutral axis depth x. Alternatively, the value of x can be obtained from the charts given

in the Concrete Society Technical Report[37]. Charts are also available to obtain the change in force in reinforcing steel. Otherwise, the lever arm z can be calculated from the following equation.

$$z = \frac{b\,x^2\,(\,3d-x\,) - (\,b-b_w\,)\,(\,x-h_f\,)^2\,(\,3d-2h_f-x\,)}{3\,b\,x^2 - 3\,(\,b-b_w)\,(\,x-h_f\,)^2} \qquad \text{...Eqn. 5.11}$$

and then the stress in the steel is given by

$$f_s = (\,M/z - F_o\,)\,(\,1/\,(\,A_{ps} + A_s\,) \qquad \text{....Eqn. 5.12}$$

and the compressive stress of concrete (f_c) can also be obtained by substituting the value of f_s in Eqn.5.9.

5.5 Deflection of Composite Beams

Deflection of concrete beams can be divided into two categories. These are the short-term deflection due to applied loads and the long term deflection due to permanent loads, creep, shrinkage etc. Only short term deflection of composite beams under negative bending is considered here. The methods which are generally used for reinforced and prestressed concrete beams are also applicable for composite beams, and the methods given in British and American codes will be discussed. Uncracked and cracked sections are considered separately.

5.5.1 Uncracked Section

Short term deflection of uncracked concrete members can be determined using the general deflection formula for beams.

$$\Delta = K\,M\,L^2 / E\,I \qquad \text{....Eqn. 5.13}$$

where K is a coefficient which depends on the position of the given section, load distribution and support conditions. It is assumed that the stress-strain relationship of concrete is linearly elastic. The second moment of area (I) can be based on the transformed section but the use of the gross section also gives results with sufficient accuracy [3]. This method can be used for Class1 and Class 2 prestressed members which remain uncracked under service loads. The above formula can also be expressed in terms of curvature.

5.5.2 Cracked Section

Cracking of reinforced and partially prestressed concrete beams under service loads not only reduces the stiffness but also creates a variation of the second moment of area along the beam. At a cracked section, the value of I depends on the depth of the tensile zone. In between two cracks a stiffer section exists, which makes the computation of deflection of cracked members more complicated than for an uncracked beam. The following are some of the methods given in the design codes.

5.5.2.1 British Codes method [27,28]

BS 8110 and BS 5400: Part 4 use the curvature in the deflection formula. The curvature of a cracked section is given by

$$\text{Curvature} = 1/r = \varepsilon_c/x = \varepsilon_s/(d-x) \qquad \text{....Eqn. 5.14}$$

where ε_c and ε_s are the concrete strain in extreme compression fibres and the steel strain respectively, and x is the neutral axis depth.

This method takes into account the tension stiffening effects to some extent

by allowing a tensile stress of 1 N/mm^2 at the level of steel. The tensile strain in steel is calculated by considering the contribution of concrete tensile zone. Deflection can be calculated from the curvature using the simplified equation.

$$\Delta = K L^2 \ (1/r_b) \qquad \text{.....Eqn. 5.15}$$

where K is the constant which depends on the shape of bending moment diagram and $1/r_b$ is the curvature at mid span section or at the support. The values of K are given in the codes [27,28].

5.5.2.2 ACI Code Method [35,36,39]

The ACI Building code and AASHTO adopt an effective second moment of inertia (I_e) to calculate deflection of cracked reinforced concrete beams. It is given by the equation

$$I_e = (M_{cr}/M_a)^3 I_g + (1-(M_{cr}/M_a)^3) I_{cr} \leq I_g \qquad \text{.....Eqn. 5.16}$$

where M_{cr} is the cracking moment and M_a is the maximum moment in the member at the stage deflection is computed. I_g and I_{cr} are the moments of inertia of gross concrete section and cracked section. If the M_a is less than M_{cr}, then I_g should be used in the deflection formula.

For prestressed concrete beams which are cracked under service loads, the calculation of deflections using uncracked section is conservative[36]. Therefore in such cases, the above method or any other method which considers the cracked section must be used. Branson who proposed the I_e concept has shown that it can be used for partially prestressed concrete beams and composite beams when moments are greater than the cracking moment [54,55,56].

The calculation of I_{cr} for prestressed concrete beams is not as

straightforward as for reinforced concrete beams due to the variation of the neutral axis of prestressed concrete beams with applied moment. The accurate determination of I_{cr} is tedious and there are several approximate methods which can give the value of I_{cr} with sufficient accuracy. The PCI Hand book[53] uses the following expression for fully prestressed beams.

$$I_{cr} = n_p A_{ps} d_p^2 (1 - \sqrt{\rho_p}) \quad \text{....Eqn. 5.17}$$

where n_p is the modular ratio for prestressing steel and ρ_p is the ratio of prestressed reinforcement (A_{ps}/bd_p).

This expression can be modified to include partially prestressed concrete beams with non-prestressed reinforcement.

$$I_{cr} = (n_p A_{ps} d_p^2 + n_s A_s d_s^2) (1 - \sqrt{\rho_p + \rho_s}) \quad \text{....Eqn. 5.18}$$

Alternatively, I_{cr} can be expressed in terms of the curvature of cracked section ($\emptyset_{cr}$).

$$I_{cr} = M / E_c \emptyset_{cr} \quad \text{.....Eqn. 5.19}$$

For a given variation of I_{cr}, the change in I_e is relatively small[3]. Therefore the use of these approximate methods would be adequate for the general computation of I_{cr}.

5.6 Crack Control in Composite Beams

5.6.1 General

Flexural cracking adversely affects the structural behaviour of concrete beams as mentioned in Section 5.4.2. In addition, cracking affects durability. This is of great importance in composite bridge decks in which the concrete top slab is

in hogging moment regions, as the top slab can be exposed to severe exposure conditions. Cracking is considered as a serviceability criterion in design of concrete beams.

In general, cracking is controlled under service conditions by limiting the tensile stress in Class 1 and Class 2 prestressed members or by limiting the maximum crack width to acceptable levels in members where cracking is expected. BS 5400: Part 4 allows a maximum crack width of 0.15 mm in very severe exposure conditions while CEB-FIP Code limits the crack width to 0.10mm. The crack width requirements can be satisfied by proper detailing of reinforcement or by calculating the crack width and checking it against the given limits.

The width of flexural cracks depends on several factors, of which, the amount of concrete cover, the distribution of tension steel and steel stress are the most important. Most design codes give approximate methods for calculation of crack widths. Only the method given in BS 8110 will be discussed here. Generally, crack width calculations are necessary only for reinforced concrete beams as tensile stress limits given for partially prestressed concrete beams are based on limiting the crack width to 0.1 mm and 0.2 mm under service loads.

5.6.2 Calculation of Crack Width According to BS 8110 [28]

The method given in BS 8110: Part 2 is similar to the BS 5400: Part 4 method. The surface crack width(w) can be calculated from the following equation.

$$w = \frac{3\, a_{cr}\, \varepsilon_m}{1 + 2((\, a_{cr} - c_{min}\,)/(\, h-x\,))} \quad \text{.....Eqn. 5.20}$$

where h = overall depth of beam

x = neutral axis depth

a_{cr} = distance from the point where crack width is calculated to the nearest longitudinal bar

c_{min} = minimum cover to tensile reinforcement

ε_m = average strain at the level where the cracking is considered

The average strain ε_m is calculated considering the tension stiffening effects of concrete as in the deflection calculations. ε_m can be calculated from the approximate formula given in BS 8110.

$$\varepsilon_m = \varepsilon_1 - \frac{b\,(h-x)(a'-x)}{3\,E_s\,A_s\,(d-x)} \qquad \text{....Eqn. 5.21}$$

where ε_m = the strain at the level considered calculated ignoring tension stiffening effects.

b_t = width of section at the centroid of tension steel

a' = distance from compression face to the point at which the crack width is calculated

It is not possible to calculate deflection and crack width with great accuracy as most of the parameters in the formulae cannot be determined precisely. However, the methods described are adequate for design calculations in practice.

5.7 Ultimate Flexural Strength of Composite Beams

5.7.1 General

Composite concrete beams, like monolithic beams exhibit non-linear behaviour at ultimate limit state. Either steel or concrete, or both, may undergo plastic deformations before the beam fails. Therefore, both elastic and plastic ranges of stress-strain curves of concrete and steel must be used to analyse the beam section for ultimate strength. The mode of failure of a composite beam in negative bending can be under-reinforced, balanced or over-reinforced, depending on the amount of prestressed and non-prestressed steel in the top slab and the amount of prestress in the precast beams. Kaar, Kriz and Hognested [8] found that when the slab reinforcement percentage was less than 1.5% and prestress in the precast beams was not greater than 0.32 f_{cu}, the failure of the interior support section of continuous composite beams were initiated by the yielding of steel in the slab. These conditions are met in most composite bridge decks. They also found that the effects of prestress in precast beams on ultimate strength of the beams were negligible under those conditions. These have been adopted by the British and American codes [27,35,39].

5.7.2 Methods of Calculation of Ultimate Strength of Composite Beams

The ultimate strength of a concrete beam can be theoretically determined from moment -curvature relationships. As this method is very tedious, design codes give two alternative methods to determine ultimate strength of concrete beams. They are the strain compatibility method in which the ultimate strength is determined by a trial and error approach and the use of design formulae given in

codes. The former can use the rectangular-parabolic curve or rectangular stress block for concrete in compression. The design formulae are based on the rectangular stress block.

Both methods will be briefly described considering the specifications given in BS 8110. Several assumptions including those mentioned in Section 5.2 are made. The maximum concrete strain is taken to be 0.0035 and idealised stress strain curves of steel are used.

At the ultimate limit state of flexure, both prestressed and reinforced concrete beams behave in a similar manner. For prestressed concrete beams, it is necessary to consider the strain in prestressed steel due to the prestressing force in them. When using the strain compatibility method, it is possible to include the tension and compression steel anywhere in the section in the calculations.

5.7.2.1 Strain Compatibility Method [29,38]

The approach used for non composite sections can also be used for composite sections. An M-beam composite section subjected to hogging moment is considered in Fig.5.6. The section is idealised into a section made of rectangles. The rectangular stress block given in BS 8110 is considered. The linear strain distribution at ultimate moment is also shown in Fig.5.6. The basic steps for the analysis of a prestressed composite beam are

(1) Assume a value for the neutral axis depth x and determine strain of steel in tension and compression zones by considering the strain distribution.

(2) Calculate stresses of steel from corresponding stress-strain curve and then determine the total tensile force (T).

(3) Calculate total compressive force (C) due to compression of concrete.

(4) Check whether T and C are equal. If not modify the value of neutral axis depth x and repeat the steps 1 to 3 until the equilibrium of forces is obtained.

(5) Finally, calculate the ultimate moment M_u taking moment of tensile forces in steel at different levels about the centroid of the concrete compression zone (or the moment of all forces about the neutral axis).

5.7.2.2 Design Formulae given in BS 8110 [27,28]

The use of the strain compatibility method for general design work is time consuming without the use of computers and therefore codes allow the use of design formulae to calculate the ultimate strength. Although the formulae have been primarily developed for beams with a rectangular compression zone, the equations can be modified for other cases. For prestressed sections it is assumed that all the prestressing steel is concentrated at one level in the tensile zone. When non-prestressed reinforcement is present in the tensile zone, it is included in the formula as an equivalent area of prestressing steel. For a given area of prestressing steel, the position of neutral axis and the stress in the prestressing steel can be obtained from the table given in the Code.

For the composite section given in Fig 5.6

$$M_u = 0.405\, f_{cu}\, b\, x\, (d - 0.45\, x) \qquad \text{If } h_f \geq 0.9\, x \qquad \text{.....Eqn. 5.22}$$

$$M_u = 0.45\, f_{cu}(b-b_w)\, h_f\, (d-h_f/2) + 0.405\, f_{cu}\, b_w\, x\, (d-0.45\, x)$$

$$\text{If } h_f < 0.9\, x \qquad \text{.....Eqn. 5.23}$$

For reinforced concrete sections, in which the ultimate moment determines the area of reinforcement required, equations are given in BS 8110 to

determine neutral axis depth and lever arm for a given rectangular section and moment. To avoid an over-reinforced design, Code limits the maximum neutral axis depth to 0.5d. The Code also gives an approximate formula for flanged beams in which the neutral axis is outside the flange assuming that the neutral axis depth is 0.5 d. This would be conservative for beams which are partially continuous at the interior supports.

5.7.2.3 ACI Building Code Equations [35,36]

For the design of prestressed concrete members, approximate equations are given in the Code to calculate the stress in prestressing steel (f_{ps}) at ultimate moment. The non-prestressed steel and compression steel can also be included in the equations. However, the code equation can be applied only if the effective prestress (f_{pe}) is not less than 0.5 f_{pu} . For reinforced concrete sections, the steel stress is taken to be equal to yield stress f_y in under reinforced beams. Once the steel stress is known, the depth of the compression zone is determined considering the equilibrium of forces. The rectangular stress block is used for concrete in compression. Finally, the nominal flexural resistance is obtained by taking moments of forces in steel about the centroid of the compression zone of concrete. At ultimate limit state of flexure, a strength reduction factor of 0.90 is applied to the nominal resistance to obtain the ultimate flexural resistance of the section.

5.7.3 Maximum and Minimum Steel Areas for Reinforced and Prestressed Concrete Beams

Concrete beams are designed to be under-reinforced so that failure is

initiated by the yielding of steel, and which normally ends with crushing of concrete, and this type of failure gives adequate warning before failure. Over-reinforced sections fail in compression before the steel yields which is not desired as it results in sudden, brittle failure. For prestressed concrete beams, there is no clear demarcation line between under-reinforced and over-reinforced designs. However, design codes give some guidance to avoid over-reinforced designs by specifying maximum limits to the area of steel.

ACI Building Code limits the reinforcing index w of a prestressed concrete beam with or without non-prestressed steel to $0.36\beta_1$ where β_1 is a factor depends on compressive strength of concrete. w is defined as

$$w = \frac{A_{ps}}{b\,d_p}\,\frac{f_{ps}}{f_c'} + \frac{A_s}{b\,d}\,\frac{f_y}{f_c'}\,\frac{d}{d_p} \qquad \text{....Eqn. 5.24}$$

For reinforced concrete sections, the maximum reinforcement ratio is limited to 0.75 times the balanced ratio (ρ_b). The derivations of ρ_b for rectangular and flanged sections are given in the Commentary on the ACI Code[36].

In British codes, over-reinforced designs are avoided by limiting the ratio of neutral axis depth to effective depth. For reinforced concrete sections, this limit is taken as 0.50 and for prestressed concrete beams, the maximum value of x/d depends on the ratio of prestress in strands to the ultimate strength and the type of beam [27,28].

Under-reinforced sections with a very low percentage of tension steel is also undesirable as they may fail by fracture of steel immediately after flexural cracking. To avoid this type of sudden failure and to ensure sufficient ductility of the beam, codes recommend minimum values for the amount of reinforcement. BS 5400: Part 4 specifies a minimum area of 0.15% of concrete area for reinforced concrete sections. In BS 8110, the minimum percentages of tensile

reinforcement are tabulated for rectangular and flanged beams, and the ACI code limit is $1.38/f_y$.

According to BS 8110, for prestressed concrete beams the area of prestressing steel provided must give an ultimate moment of resistance greater than the moment required to produce a tensile stress of $0.6\sqrt{f_{cu}}$ at the extreme tension fibres to prevent the failure of beam before cracking. The ACI code also follows a similar approach.

The above mentioned limits for maximum and minimum steel areas for prestressed and reinforced concrete beams can also be used in the design of composite concrete beams as the ultimate strength of the section is mainly governed by the strength of materials and the geometry of the section.

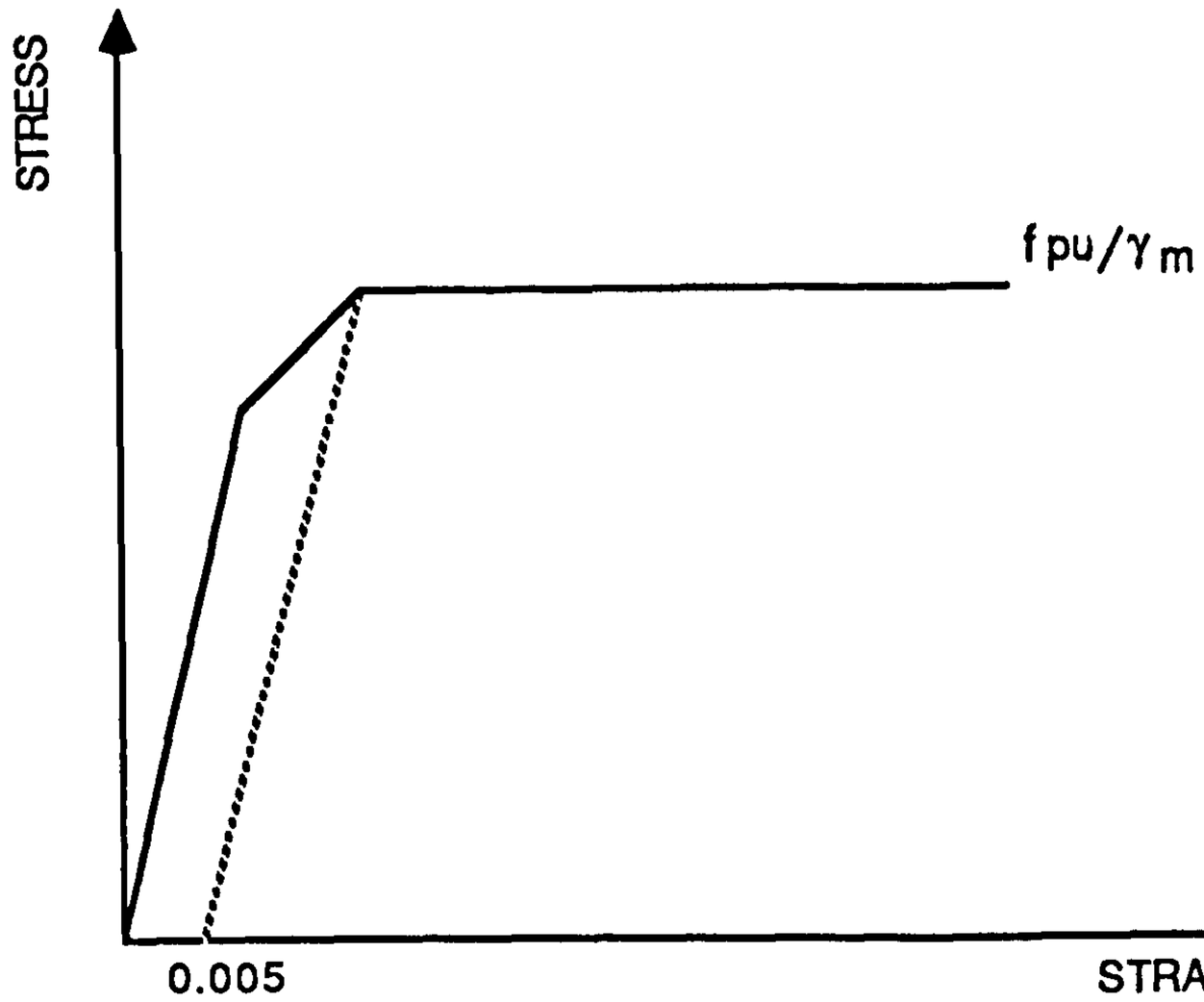

FIG. 5.1 : SHORT-TERM DESIGN STRESS-STRAIN CURVE FOR PRESTRESSING TENDONS (BS 8110 AND BS 5400)

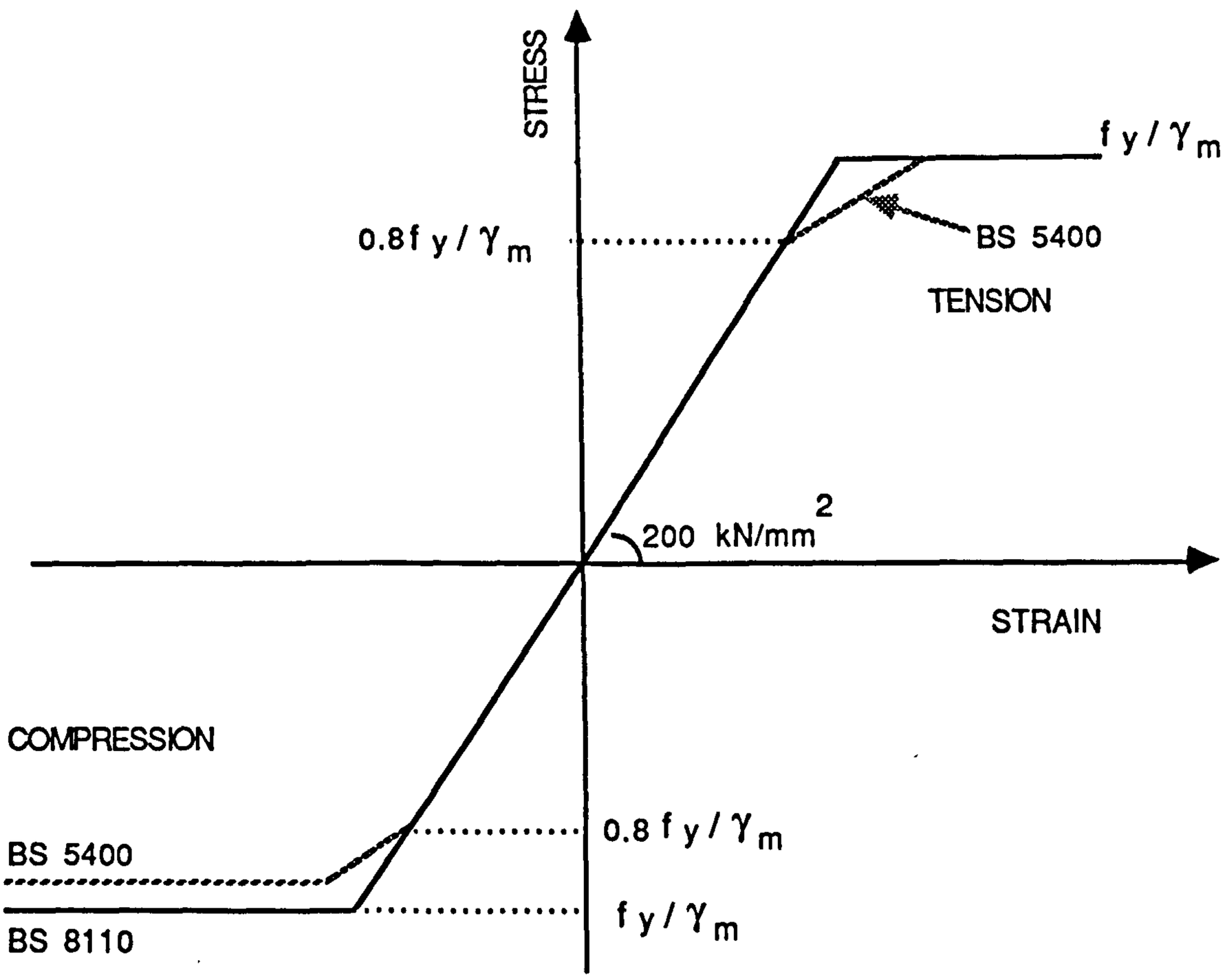

FIG. 5.2 : SHORT TERM DESIGN STRESS-STRAIN CURVE FOR REINFORCEMENT (BS 8110 AND BS 5400)

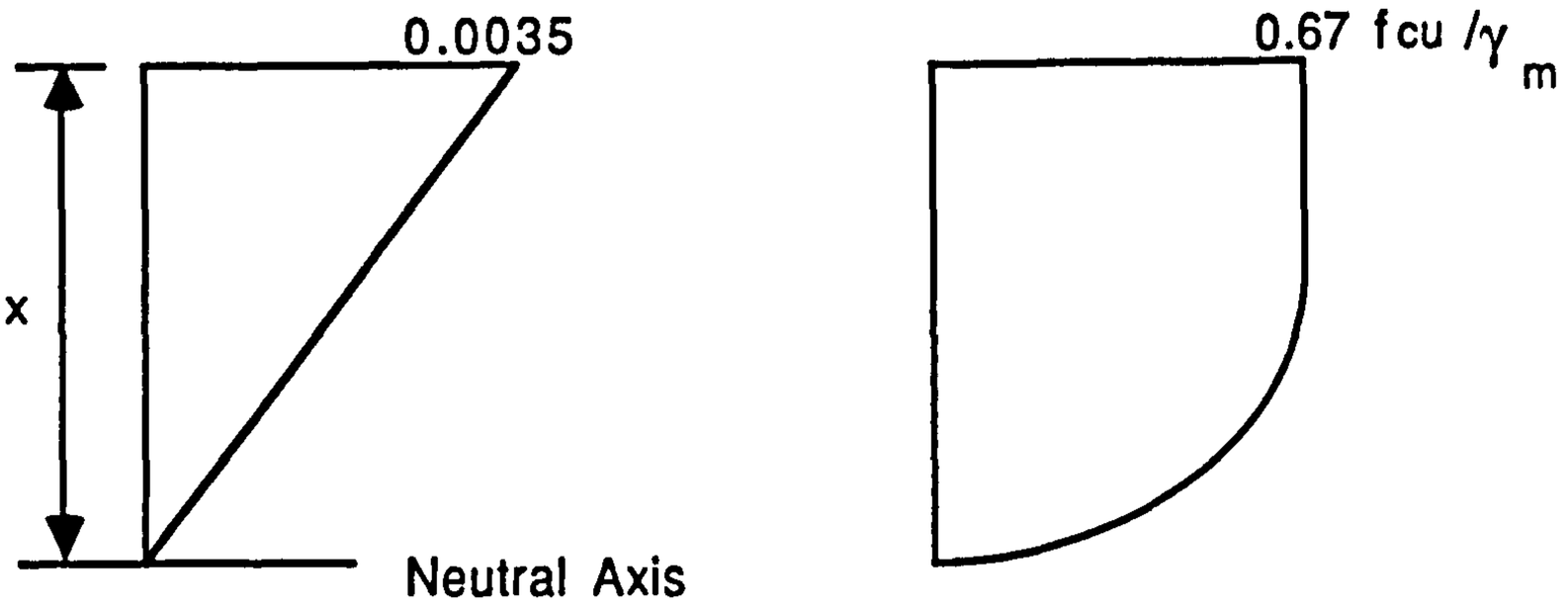

(1) Strain Distribution at Ultimate Moment

(2) Parabolic-Rectangular Stress Distribution

(a) Stress- Strain Curves of Concrete Given in British Codes

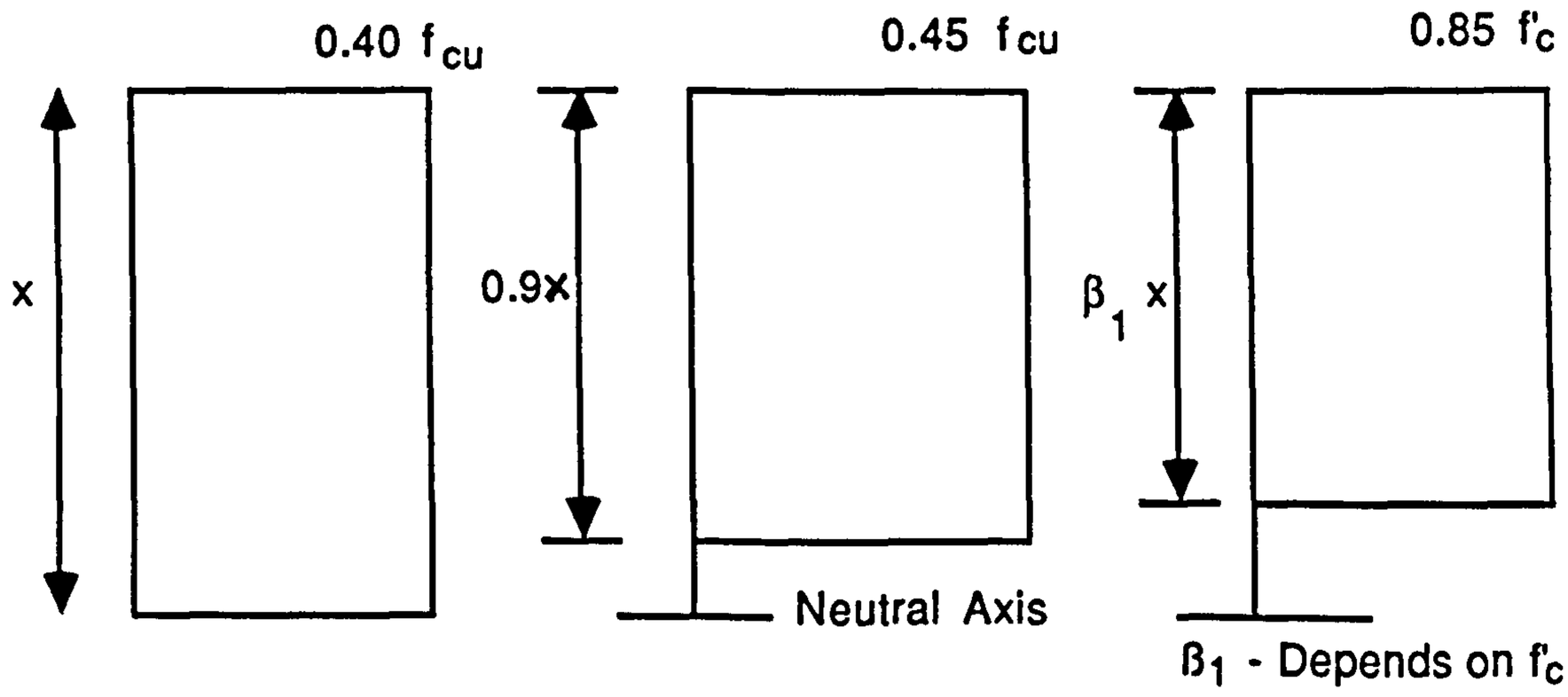

(1) BS 5400 : Part 4 (2) BS 8110 (3) ACI 318-83

(b) Simplified Stress Blocks for Concrete

Fig. 5.3 : Idealised Stress - Strain Curves for Concrete

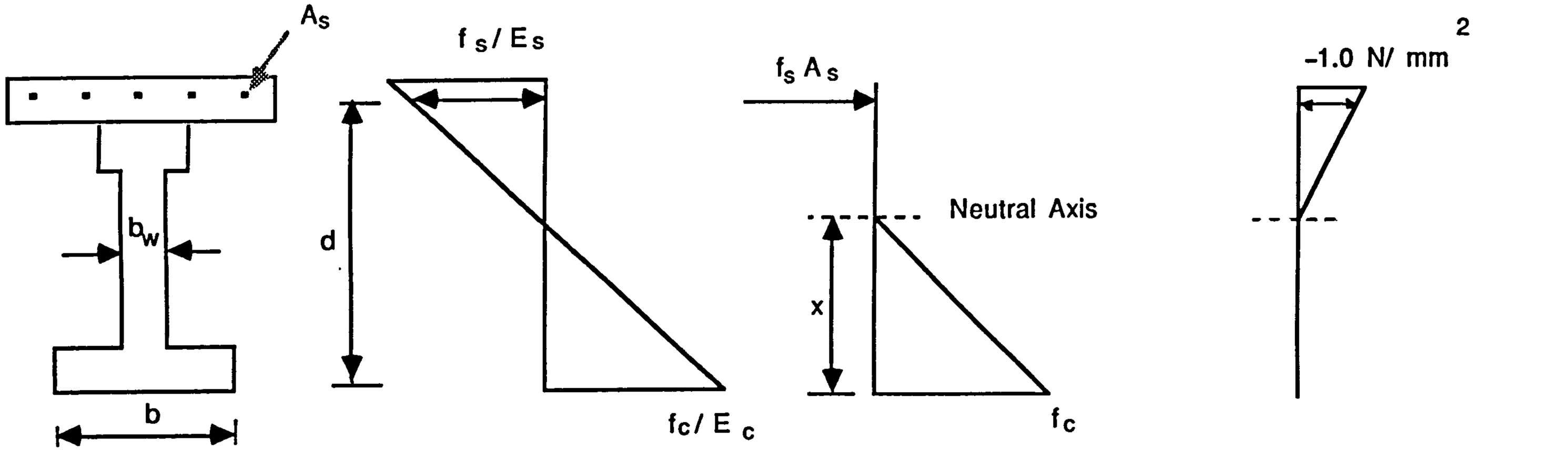

(a) Composite Beam Section (b) Strain Distribution (c) Stress Distribution under Service Conditions (d) Tensile Stress Distribution

Fig. 5.4 : Cracked Composite Section with Reinforced Concrete Top Slab (Subjected to a hogging moment)

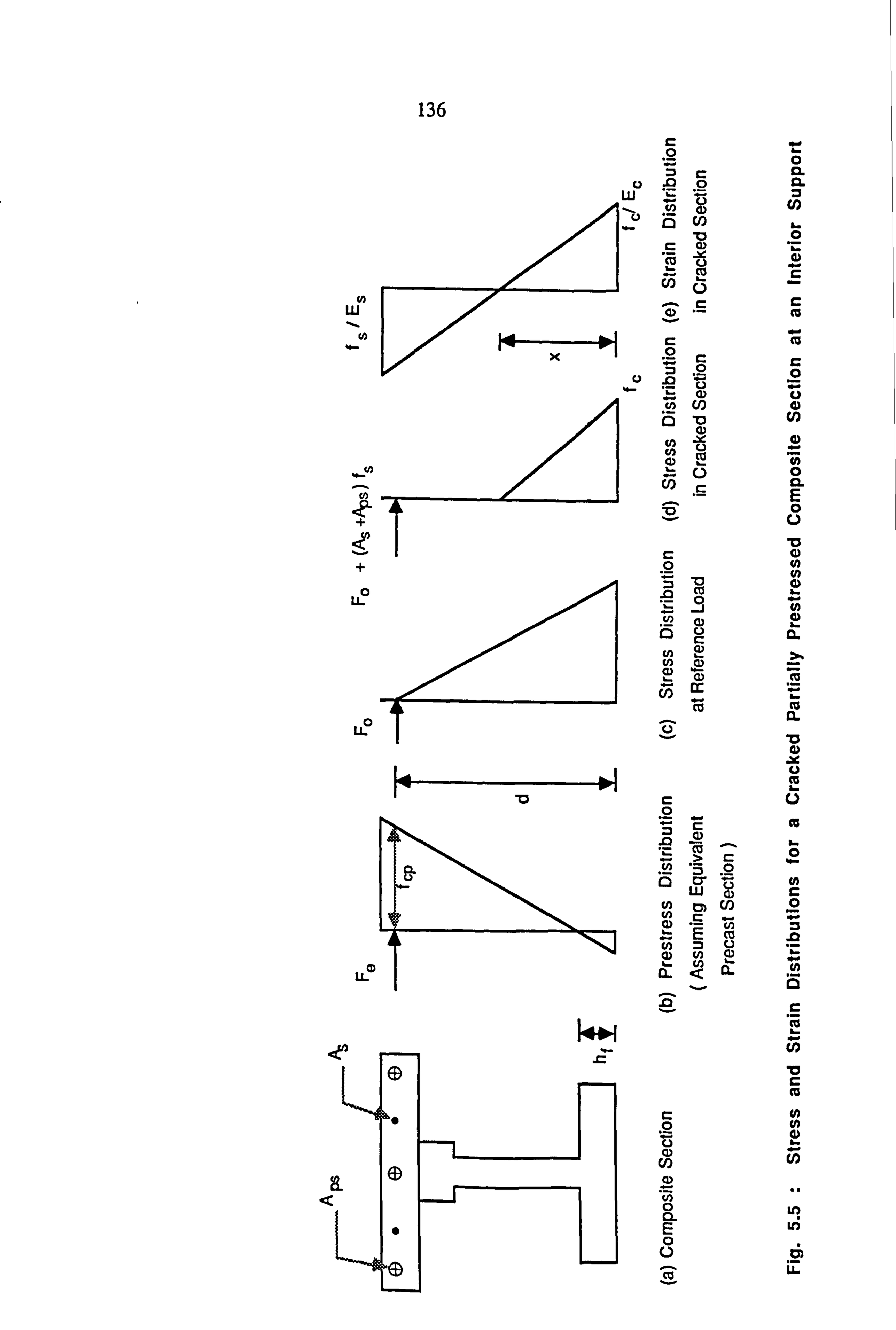

(a) Composite Section (b) Prestress Distribution (c) Stress Distribution (d) Stress Distribution (e) Strain Distribution
(Assuming Equivalent at Reference Load in Cracked Section in Cracked Section
Precast Section)

Fig. 5.5 : Stress and Strain Distributions for a Cracked Partially Prestressed Composite Section at an Interior Support

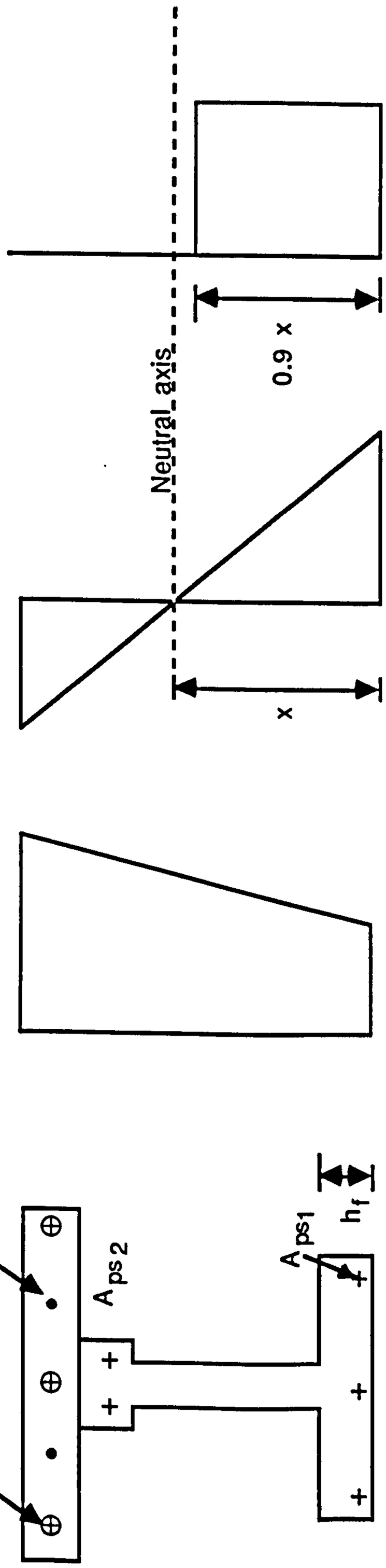

(a) Composite Section

(b) Strain Distribution due to Prestress in the Top Slab

(c) Strain Distribution at Ultimate Moment

(d) Stress Distribution at Ultimate Moment (BS 8110)

Fig. 5.6: Stress and Strain Distribution for a Composite Section with a Partially Prestressed Slab
(At an Interior Support)

CHAPTER 6

EXPERIMENTAL OBSERVATIONS AND ANALYSIS OF RESULTS OF FLEXURAL TEST SERIES

6.1 General

In this chapter, the results of the flexural test series are presented. The details of the three 1/3 scale composite beams and the test procedure have been previously described in Chapter 4. This test series was intended to study the flexural behaviour of the continuity connection between composite precast beams with insitu concrete prestressed top slabs. Three beams were tested as simple beams in an inverted position with two point loads spaced 150 mm acting on the diaphragm (These have been considered as a single load for convenience). The observed behaviour of beam A-1, which had a reinforced concrete slab, and beams A-2 and A-3, with prestressed slabs, up to failure will be presented, and also a comparison will be made between the properties of those beams obtained both experimentally and theoretically.

As previously mentioned in Chapter 4, beam A-1 was tested by applying continuous load increments up to failure whereas the two beams with prestressed slabs, A-2 and A-3, were first loaded to the cracking load, then unloaded and loaded again in the second stage up to failure. The main measurements taken during testing at different load levels were the deflection, surface strains of the beam at different sections, strains in steel in the slab and in the precast beams, and crack widths. The appearance and distribution of cracks in different parts of the composite section and the mode of failure were also observed. The positions of gauges to measure flexural strains in concrete and deflection are shown in Fig.6.1.

6.2. Flexural Cracking of Test Beams

6.2.1 Cracking Load

The flexural cracking loads of the three beams were obtained by visual inspection for the appearance of the first flexural crack during loading. In beam A-1, the first crack appeared at the joint between the diaphragm and the composite beam at a load of 25 kN. With increasing load, more cracks appeared propagating upwards. At 50 kN, cracks had extended into the web of the precast beams. The first flexural crack for beam A-2 developed at 75 kN at almost the same location as in A-1 whereas in beam A-3, the first crack appeared at 115 kN in the diaphragm. In the second stage of loading of A-2 and A-3 after unloading, cracks reopened at 45 kN and 70 kN respectively. At about 80 kN , cracks which had appeared in the insitu slab of composite section penetrated to the precast beam in A-2, and the same was observed in A-3 at about 150 kN. It is possible to estimate the prestress in the extreme tensile fibres from the load at which cracks reopened in the second stage. Theoretically, cracks must reopen when the tensile stress due to applied load exceeds the prestress (i.e. when the net stress at the crack is zero) as concrete no longer has the tensile strength at the cracks. However, friction in the concrete delays the reopening of crack to the stage where it is visible without special optical aids.

The measured cracking loads were compared against the theoretical values which were obtained using the elastic theory and transformed concrete section using the Equation 5.1 given in Chapter 5. The flexural tensile strength of concrete was obtained from the modulus of rupture test [58] for 100x100 mm prisms cast at the same time as the test beams. The ratio between experimental cracking load and theoretical cracking load for beams A-2 and A-3 was close to unity. The ratio for A-1 was 0.73. This may be due to the fact that any small errors in the measured or

calculated cracking load could affect the ratio considerably when the cracking load was small. These ratios and the ratio of measured cracking load to design service load are given in Table 6.1.

6.2.2 Propagation and Distribution of Cracks

At the cracking load of the beams tested, only one crack was visible and it was confined to the slab or diaphragm. When more cracks appeared in the beam with increasing load, the crack patterns of the two beams on either side of the diaphragm were nearly the same. The cracks which appeared first did not extend or widen compared to the cracks which appeared later. The appearance of the first flexural cracks in the diaphragm in all three beams was mainly due to the fact that the applied bending moment was greatest within the diaphragm. Even when prestress was applied to the top slab (A-2 and A-3), the first crack still appeared in the diaphragm. As the cross sectional area and the section modulii of the rectangular diaphragm were larger than that of the composite section, the extreme tensile fibres of the of the diaphragm had a smaller compressive stress from the prestressing force in the slab. It would not be economical to design the prestressing force to satisfy the requirements of the diaphragm which is relatively short. Also, the test results showed that the flexural cracks in the diaphragm did not widen or propagate as much as the other cracks in the composite section. Therefore, in the design of composite bridge decks with a prestressed slab in the hogging moment regions, the prestressing force should be chosen considering the composite section at the joint rather than the diaphragm.

The average spacing of cracks in A-1 and A-2 were about 100-125 mm while A-3 had a average crack spacing of about 200 mm. This means that when two beams with a prestressed slab were compared, a closer spacing of cracks was found in A-2 which had more non-prestressed reinforcement than A-3 at higher loads.

However, in any of the beams, the crack spacing was not uniform in the cracked zone.

When some of the flexural cracks extended into the web of the precast beams, they became inclined towards the loading point above the diaphragm. More details of these flexural shear cracks will be given later. The typical crack patterns observed in the flexural test series are shown in Plate 6.2.

6.2.3 Crack Width

Crack width is a very important serviceability criterion in reinforced and partially prestressed concrete beams. During the loading of the beams, the maximum crack width was measured using a hand microscope. The measured crack widths of the three beams are plotted against load in Fig. 6.2. The cracks in A-1 were about 0.10 mm wide when they first appeared, and at the service load, they were about 0.15 mm wide. In A-2 and A-3, crack widths were measured during the second stage of loading. In those two beams, crack widths were very small when they reopened. At the cracking load of A-2, cracks in A-1 were more than 0.2 mm wide. After reopening of the crack in the second loading stage, crack widths for A-2 increased gradually at nearly uniform gradient with load. In A-3, crack widths increased at very slow rate up to about 120 kN and then increased rapidly. The load vs crack width curves of A-1 and A-3 were nearly parallel. In A-3, which had fewer flexural cracks than A-2, crack width increased very rapidly from about half the failure load.

The maximum surface crack width of A-1 was calculated using the formula given in BS 8110 which was described in Section 5.6.2 and which takes into account tension stiffening of concrete. The method seemed to underestimate the crack width at higher loads whereas at smaller loads, the predicted crack width was close to that measured.

6.3. Load-Deflection Relationships

The load-deflection curve is a very important characteristic of a structural member when studying its overall behaviour under loading as it reflects the effects of cracking and is also a measure of ductility of the member. The deflection of the beam near the ultimate moment is also of interest as adequate warning in the form of large deflections is desired for structural members before failure.

6.3.1 Load-Deflection Curves for Flexural Test Series

The load vs deflection curves of the three beams A-1, A-2 and A-3 both at the mid-span (diaphragm) of the beam and also 800 mm from mid-span are given in Figs. 6.4 and 6.5. The load-deflection curves of all three beams were linear up to the cracking load, although this was not so predominant in A-1 which had a reinforced concrete slab and therefore a smaller cracking load. After cracking the curves deviated from linearity and deflection increased at a varying rate. In this second stage, steel stresses were still within the yield stress. In the final stage, deflection increased considerably almost at a constant rate. Crack widths also increased rapidly as the steel in the top slab became non-elastic. At this stage, the load-deflection curves for the three beams were parallel. All three beams underwent considerable deflection before failure and the beam with a fully prestressed slab had the greatest deflection. It can be seen from the curves that the ductility of the beams was not affected by prestressing the slab when compared to the reinforced concrete slab.

The residual deflection of beams A-2 and A-3, when unloaded after the first flexural cracking was very small, showing that the composite beams with prestressed slabs subjected to flexural cracking in the slab almost completely

recovered to the original uncracked state when the overload causing the cracking is removed. When A-2 and A-3 were loaded again, load-deflection relationship was very similar to that of the first cycle, confirming that the prestress in the top slab minimised any loss of stiffness due to cracking.

6.3.2 Comparison of Measured and Calculated Deflection.

The measured deflection at mid-span was compared to the deflection calculated using ACI method (I_e Method) [35] and BS 8110 [28]method and are shown in Figs. 6.6 to 6.8. Up to cracking , the moment of inertia of the transformed concrete section was used and the measured and calculated deflection showed very close agreement. After cracking, the ACI method seemed to predict the deflection better than the BS 8110 method. However, both methods slightly overestimated the deflection of cracked section. For the BS 8110 method, the cracked section for both prestressed and reinforced concrete beams was analysed using linear elastic theory considering the tension stiffening effect of cracked concrete. In the ACI method, I_{cr} for the cracked section was calculated using the formula given in PCI Handbook[53]. It can be concluded that both ACI and BS 8110 methods, which are mainly given for monolithic beams, can be adequately used to calculate short-term deflection of composite beams subjected to hogging moments.

6.4 Strains In Steel

6.4.1. Strains in the Non-prestressed Steel in the Slab

The strains in the non-prestressed steel in the slab of the composite beams were measured using electrical resistance gauges which were fixed to the reinforcing bars in line with the faces of the diaphragm. The variation in the

average strain in the top slab reinforcement with the applied load in the three beams A-1, A-2 and A-3 is shown in Fig. 6.9. All the reinforcing bars in the slab were at one level and therefore the strains recorded by the strain gauges on different bars were similar for a particular beam.

It can be seen from these curves that steel stresses, or strains, were very low in beams with prestressed slabs up to the cracking load, and the rate of increase in strain was small but constant. After cracking, the steel strains increased rapidly but the rate of increase was still fairly constant. In the final stage of loading before failure, the steel strains increased very rapidly until the reinforcing bars ruptured at the failure load. All three beams continued to carry more load after the load at which the strain readings indicated the commencement of yielding of steel.

The load-steel strain relationships of flexure test beams were similar to the load-deflection curves of the beams. However, the load-deflection curves represented the overall properties of the beams over the entire length while load vs steel strain curves were more affected by the position and distribution of cracks. When the strain gauges on the reinforcement were not located at the position where the first crack appeared, the rapid increase in the measured steel strain associated with cracking was delayed. This was especially noticed in beam A-3.

The stresses determined from measured strains in the reinforcing bars were compared with steel stresses calculated using the linear elastic theory. Fig. 6.10 shows the comparison between the measured and calculated stresses of slab reinforcement in A-1. The analysis was carried out using the method described in Section 5.4.3. When tensile stresses in concrete are considered, the triangular stress distribution with 1.0 N/mm^2 tensile stress at the level of tension steel given in BS 8110 was used. The calculated values seemed to give better agreement when such tension stiffening effects were considered.

The stress in the non-prestressed reinforcement in beams with a prestressed slab (A-2 and A-3) was calculated using the linear method of analysis

given in the Concrete Society Technical Report 23 [37]. In these two beams also, the stresses calculated allowing for tension in the concrete in the cracked zone were closer to the experimental stresses than when the tension in the concrete was ignored. The experimental and calculated steel stresses in beams A-2 and A-3 are shown Figs. 6.11 and 6.12 .

From Figs. 6.10 to 6.12, it can be observed that by using the above mentioned linear elastic methods, the steel stresses in the reinforcement in the top slab of composite beams can be calculated to be in good agreement with the experimental values. Also, the linear part of the load-steel stress curves of the three beams up to cracking load justifies the use of the linear stress-strain relationship of concrete up to cracking. The approximately linear part of the curve from cracking load to the load at which steel begins to yield also indicates that the use of linear methods of analysis is still valid in this steel stress range. In the three beams tested, yielding of steel took place well above the service loads. Therefore, it can be concluded that the linear methods given in Sections 5.4.3.1 and 5.4.3.2 can be used without significant error in place of more rigorous non-linear methods to analyse reinforced and prestressed continuous composite sections at interior supports under service loads and with small overloads. However, at high overloads, the actual stresses tend to deviate from the theoretical values obtained using above methods, and it can also be concluded that the consideration of tension in concrete in the cracked zone is important in such analysis as the area of concrete at the tensile face (insitu slab) is relatively large when composite beams are subjected to hogging moments.

6.4.2 Strains in Prestressing Steel

Electrical strain gauges were used to measure strains in the 7 mm diameter prestressing wires in the precast beams. The location of these gauges was about

275 mm from the end of the beam at the joint which was about half of the transmission length of the wires. Strain gauges were fixed to the wires in all three layers. (The positions of the prestressing wires in the precast section at the end have been given in Chapter 4.) Initially, these gauges were used to check the prestressing force in the wires during pretensioning, and when the strains were measured after transfer of prestress, they were found to be about 40% 0f the applied strain.

Figs. 6.13 and 6.14 show the average strains in the top layer (in the top flange) and the bottom layer of precast beams of A-1, A-2 and A-3 measured during testing. The strains were measured up to the failure load.The changes in the strains with increasing load were small and yield strain was not reached. The maximum change was about 1000 microstrain (for which the corresponding stress was about 200 $N/mm^{2)}$. The location of the gauges was about 175 mm away from the failure plane.

6.5 Surface Strains of Concrete

The surface strain distributions (longitudinal strain) at different sections were measured during the testing of beams. In beams with a prestressed slab, strain distribution due to prestress in the slab was also measured. Mechanical (Demec) gauges of gauge length 150 mm and 200 mm were used together with a few electrical resistance gauges(PL 60). 150 mm gauges were used on the diaphragm which was not wide enough for 200 mm gauge length and as the formwork for the I beams could not be removed before the transfer of prestress, surface strains due to prestress in these beams could not be measured.

6.5.1 Concrete Strain Distribution due to Prestress in the Slab

In beams A-2 and A-3 which had a post-tensioned slab, the strain distribution in the composite section adjacent to the diaphragm(250 mm from the centre of beam) both before and after post-tensioning of slab, was measured using 200 mm Demec gauges. Post-tensioning was undertaken in several stages as described in Chapter 4. The measured strain distributions in A-2 and A-3 due to prestress in the slab were linear over the depth of the composite section (which consisted of a precast beam and insitu top slab) as shown in Fig. 6.15 and Fig. 6.16. The strain distribution was similar to the calculated strain distribution obtained assuming elastic theory and full composite action between two concretes, and the difference in strength of the two concretes was considered in the calculation of sectional properties of the composite section. The two ends of the beam deflected upward during the stressing and therefore the calculated strain distributions were modified for strains due to the self weight of the beam segments. Although tensile stress at the bottom of the precast beams due to prestress in the slab exceeded 1.0 N/mm^2, the combined prestress including the prestress in the beams was compressive.

Figs. 6.15 and 6.16 also show the strain distribution at the same section in beam A-2 and A-3 at the time of testing. The increase in compressive strain was mainly due to creep and shrinkage. As can be expected, the increase in compressive strain was greater in the insitu top slab than in the precast beam due to the relatively young age of the concrete in the slab at the time of post-tensioning.

6.5.2 Concrete Strains during Loading

Before the beams were loaded, additional flexural strain gauges were fixed to both beams on either side of the diaphragm. The horizontal positions of these

gauges are shown in Fig. 6.1.

6.5.2.1 Strain Distribution in the Diaphragm

The measured surface strains in the rectangular diaphragm at different loading levels are shown in Figs. 6.17 to 6.19. It can be seen that in all three beams, for about two thirds of the depth of the beam from the top (considering the inverted position) the concrete strains remained very small throughout the loading. That part of the diaphragm was restrained from developing tensile strains or compressive strains as normally expected with increasing load. As a result of this restrained action, the flexural cracks which first developed in the diaphragm did not widen or propagate and the diaphragm remained relatively uncracked up to failure as seen in Plate 6.2. Failure also did not occur in the diaphragm but at the junction with the composite beams.

The increased strength of the the diaphragm observed in the tests can be attributed to the action of the two point loads (150 mm apart) on the diaphragm and to the lateral restraint offered by the precast beam ends embedded in the diaphragm. The two point loads induced compressive stresses which helped to restrain the penetration of cracks upwards and the rotation of the beam ends to cause separation from the diaphragm. Also the stress redistribution in the diaphragm after the first flexural cracks had appeared would have contributed to the smaller strains in the upper part of the diaphragm.

6.6.2.2 Concrete Strains of Composite Section in the Cracked Zone

Although concrete strain distributions at several sections along each half of the span were measured, only the results of those which were close to the critical section in flexure (the joint) will be discussed here.

Figs. 6.20 to 6.24 show the variation of the measured strain distribution with increasing load in the composite sections at 250 mm and 700 mm from the centre of the beam in the tests of A-1, A-2 and A-3. The strain distributions were approximately linear over the depth of the composite section and there were no discontinuities at the interface between the slab and the precast beam except where the strain gauges were crossed by cracks, which indicated that the composite action and continuity between the precast beams existed throughout the loading.

The measured compressive strains in the bottom flange of the I beams indicated that strains were about 0.001 to 0.0015 near the diaphragm, which were less than half of the ultimate concrete strain given in both codes [27,28,35] or reported on tests on prestressed beams [59,60]. However, the concrete strains could not be measured near the failure load nor at the failure plane which happened to be the plane where the composite beam and the diaphragm met. Also the plotted surface strains were due to the applied load only and the strain due to the prestress in the beams were not included.

6.6 Flexural Strength of Beams

Beams A-1 and A-2 were designed to have the same ultimate strength. Beam A-3, which was designed to have no tensile stresses under service moments, had a higher design strength, due to the greater area of prestressing steel in the slab, than in A-2. Both A-2 and A-3 had 8 mm diameter reinforcing bars in the top slab which are desired in actual bridge construction to carry any shrinkage stresses before the application of prestress in addition to their contribution to the ultimate strength.

6.6.1 Mode of Failure

All three beams were under-reinforced and therefore the failure was due to yielding of reinforcement in the slab. At failure, the prestressed and non-prestressed steel ruptured after undergoing yielding for some time. The position of the failure plane was identical in all three beams and occurred at the joint between the diaphragm and one of the precast beams. Although flexural cracks appeared in the diaphragm, they did not extend to cause failure in any of the beams. Similar observations were reported by Kaar et al [8] in PCA Pilot Tests. This was further confirmed by the concrete strain distributions in the diaphragm section of the three beams (Figs.6.17 to 6.20) in which concrete strains in the upper half of diaphragm did not show any significant change.

Before failure occurred, by rupture of steel in the slab, considerable deflection and very wide cracks were observed, giving ample warning of the impending failure. All three beams carried ultimate moments of more than twice the cracking moment. Therefore code requirements regarding the prevention of sudden failure after flexural cracking were satisfied. The area of steel in A-1, A-2 and A-3 was considerably greater than the minimum values specified by British and American codes. The location of the failure plane observed in the tests are shown in Plate 6.1 and 6.2 .

6.6.2 Comparison between Measured and Calculated Ultimate Strength of Beams

The failure loads of A-1, A-2 and A-3 were 140 kN, 190 kN and 265 kN respectively, and as the beams were tested in a simply supported manner, the ultimate moment could be easily calculated from these failure loads. The measured ultimate strengths were compared with the ultimate strength calculated using the

strain compatibility method, and also using code equations. For the strain compatibility method, the rectangular stress block given in BS 8110 was used. Kaar et al [8] had found that improvements gained by the use of curved stress-strain relationships were small. However, the actual stress-strain curves were used for the prestressing and reinforcing steel. The critical section was considered to be the joint between the composite section and diaphragm. In the strain compatibility method, two cases, one considering the prestress in the precast beams and the other ignoring such prestress were considered.

The measured and calculated ultimate strengths (using the different methods mentioned above) are presented in Table 6.2, where it can be seen that when prestress in the girder is neglected, the ultimate moment obtained by the strain compatibility method, BS 8110 equations and ACI 318-83 Building Code equations are very close. The measured strength of A-1 was slightly smaller than the calculated strength and both beams A-2 and A-3 had a higher measured strength than the calculated strength. The ratio between measured and calculated moment (strain compatibility method) were 0.92, 1.23 and 1.30 respectively. No partial safety factors were applied to the calculated flexural strengths given in the Table 6.2.

When the contribution of prestressing steel in the precast beam was considered, it was assumed that only 20% of the prestressing force was effective at the section considered. This factor was selected assuming a uniform build up of prestress within the transmission length of the wires. The same factor was considered when the change in the steel stress due to change in concrete strain was calculated at the ultimate moment. The calculated flexural strength after prestress in the beams was considered was 240.3 kNm, 241.0 kNm and 287.4 kNm for A-1, A-2 and A-3 respectively, giving a ratio of measured to calculated strength of 0.72, 0.96 and 1.12. For beam A-1, this overestimated the ultimate strength, whilst for

beams with prestressed slabs, consideration of prestress increased the ultimate strength bringing them closer to the experimentally obtained strength.

The above results indicate that beams A-2 and A-3 with a prestressed top slab had a higher flexural capacity than the theoretical strength calculated without considering the prestressing steel in the precast beams. This increase was greater in A-3 which had the largest area of prestressing steel in the slab. With both prestressed and non-prestressed steel in the slab of A-2 and A-3, the non-prestressed steel was placed closer to the tensile face than the prestressing steel, and therefore the strain in the reinforcing bars in the slab was higher than the strain in the prestressing strands. This resulted in the reinforcing bars yielding and becoming plastic before the prestressing steel. According to the stress-strain characteristics of the two types of steel, prestressing steel begins to yield at a much higher strain than non-prestressed steel. Although prestressing steel is already already under stress at the commencement of loading, the above factors would have caused the reinforcing bars to fail first. This in turn must have delayed the failure of beams with a prestressed slab. It was observed in tests that the failure of A-1 with only reinforcing bars in the slab was more sudden than the other two beams and also that in A-3 the critical crack at the diaphragm which caused the failure propagated across the diaphragm. The two point loads which were considerably larger in A-3 than in other two beams, must therefore have prevented the crack propagating vertically to the top.

Although the above factors may have contributed to the increased flexural capacity of the beams with a prestressed slab, the contribution of prestressing steel in the precast beam must have been more significant and the precast beams used in this series had four 7mm prestressing wires in the beam close to the tensile face. Although the failure plane was just within the development length of the wires, they must have carried some tensile force at ultimate load. When the effects of prestress in the precast beams were considered, it was assumed that only 20% of the

prestress was effective at the failure plane. The same percentage was considered for strains in the wires due to the applied load.

The percentage of effective prestress at the failure plane assumed in the calculations was an approximate value. In PCA Pilot Tests [8] the theoretical strength became closer to the measured strength when the prestress in the precast beams was considered assuming that full prestress was effective at the end of the beams. However, such an assumption is not correct as shown by the strain measurements of prestressing wires in this test series. The current design codes[27,35] recommend that the prestress in the precast beam is ignored in the calculation of ultimate capacity at the interior supports of continuous composite beams. For beams with prestressed slabs, the increased strength of the connection can be exploited by using a suitable percentage of prestress in the girders considering the transmission length of prestressing steel and the width of the diaphragm. Otherwise, it can be considered as an additional safety factor against failure or for moment redistribution. However, more experimental results of tests on continuous beams are required to develop design procedures. In most practical cases, ultimate flexural capacity will not normally be critical when prestressed slab are used to develop continuity.

6.7 Shear Stresses in Beams

6.7.1 Vertical Shear at the Continuity Connection

The three beams in the flexural test series were provided with sufficient shear reinforcement to avoid shear failure before the intended flexural failure. All three beams had 6 mm diameter high yield stirrups at 75 mm spacing.

When the beams were tested as simply supported with a point load at the mid span (the two closely spaced point loads are assumed to be equivalent to a point load), two equal shear forces were produced which were uniform throughout each

half of the span. The shear span was 2.395m and the ratio of shear span to effective depth was 5.6 for the three beams. As the magnitude of the shear force was half of the applied load, these shear forces at the failure were 70 kN, 95 kN and 132.5 kN for A-1, A-2 and A-3 respectively. The shear stresses were considered to be of concern near the diaphragm where both bending moment and shear force were high. In the three beams, inclined cracks appeared in the web of the precast beams with increased loading. The number of inclined cracks in A-1 and A-2 was small and these cracks initially appeared as vertical flexural cracks in the slab before becoming inclined towards the loading point as loading increased. In A-3 , there were some independent inclined cracks which appeared near the failure load. The main reason for A-3 having more flexural shear cracks and web shear cracks was that the shear force applied to the beam was considerably higher. However, in none of the beams, did these shear cracks develop in to a major inclined crack sufficient to cause failure. The inclination of the shear cracks was approximately 45^0 to the horizontal but those cracks which were closer to the diaphragm had a greater inclination.

The strains in the stirrups in the cracked zone near the joint were measured using electrical resistance gauges attached to the stirrups in the web. The variation of strains in the stirrups in the three beams located close to the diaphragm in the cracked zone is shown in Fig. 6.25. The measured stirrup strains indicated that the maximum increase in stress in stirrups was about 250 N/mm^2 which was about half of the yield stress of the steel used for the stirrups.

6.7.2 Horizontal Shear at the Interface

During the testing of beams to failure, the interface between the in-situ concrete slab and the precast beams was closely observed, and there were no signs of separation or interface failure to be seen in any of the beams. No surface roughening

was undertaken other than leaving the top surface of the precast beams in the 'as cast' condition before pouring the top slab. The bond between the two concretes together with the extended vertical legs of the 6 mm diameter stirrups of precast beams at the interface was quite sufficient in transferring the horizontal shear stresses, even in A-2 and A-3 which had additional horizontal stresses due to prestress in the slab and higher failure load. All three beams were therefore satisfactory in carrying both vertical and horizontal shear stresses up to the flexural failure of beams.

6.8 Conclusions and Design Implications

The theoretical and experimental work reported in the previous sections was carried out to study the effectiveness of a new method of developing continuity between precast beams by means of a prestressed slab in place of the more conventional method of providing reinforcing bars in the top slab, and to observe the effects of such a prestressed slab on flexural behaviour. The series of tests carried out was only intended to study the behaviour of the continuity connection under negative moments and to compare the beams made with either a reinforced slab or a prestressed slab. The following points are the important observations and the conclusions that can be drawn from them.

(1) One of the main advantages of prestressing the top slab in continuous bridge decks is the improved crack control in regions of hogging moment. The results clearly show that in beam A-1, which had a reinforced slab, cracks were wide at their first appearance and exceeded the limiting crack width of 0.15 mm specified in BS 5400 : Part 4 under service loads. In the two beams A-2 and A-3, with a prestressed slab, cracking did not occur below service load. The cracking loads for A-2 and A-3 were 3.0 and 4.6 times that of A-1. Even when beams with a prestressed slab were subjected to an overload to cause cracking, they returned to

the original uncracked state when the overload was removed. The width of reopened cracks remained less than 0.05 mm in A-2 under service loads while reopening did not take place in A-3 which had the slab with the highest level of prestress. In beams with a reinforced concrete slab, cracks are expected to reopen at very small loads. Therefore, the results showed that the complete elimination of cracks or even limiting the crack width to very small values can be achieved when this new method is used compared to the reinforced concrete slab. This is a great advantage as the top slab in bridge decks is subjected to very severe exposure condition. The advantage of a prestressed slab over the reinforced slab will be more predominant when live load greater than that which was used in this study is considered.

(2) In the design of continuous composite bridge decks with prestressed slabs, the magnitude of prestressing force in the slab must be based on the stresses in the top slab of composite section at the interior supports under service moments. The larger cross section of the diaphragm makes it uneconomical to consider the diaphragm even though it is subjected to the maximum moment and the results of A-2 and A-3 justified this. Although the first flexural cracking was observed in the diaphragm, and the width or penetration of those cracks did not become critical in the later stages of loading.

(3) The propagation of flexural cracks into the precast beam was delayed when prestress was applied to the slab, due mainly to the additional compression applied to the top of precast girder by prestress in the slab.

(4) Flexural stiffness of composite beams with a prestressed slab remained unaffected up to a higher load than in the beam with the reinforced slab under hogging moment. Up to cracking load, the flexural stiffness of all three beams was the same but beyond the cracking load, flexural stiffness reduced and therefore deflection increased. Beams A-2 and A-3 had a higher cracking load and therefore the deflection of those two beams was smaller than that of A-1. As the model beams were not loaded with the same sequence of loading as in actual bridge girders and

only part of the actual continuous bridge was simulated, the measured deflection did not represent the true deflection of the prototype composite beams continuous over two or more spans. Also, the deflection measurements were limited to short-term deflection only. However, the load- deflection relationships of the three beams tested represented the general properties of the continuity connection under negative moments and allowed an examination of the applicability of approximate deflection formula given in British and American codes for the calculation of deflection of composite beams. The use of BS 8110 method [28] and ACI Method (I_e Method) [35] to calculate deflection of test beams yielded values close to the measured deflections. Of the two methods, the ACI method gave closer agreement with the measured values. The results indicated that both methods are satisfactory for the calculation of short-term deflection of composite beams made of prestressed-reinforced or prestressed-prestressed elements when subjected to conditions similar to those in the tests, although they have been derived for monolithically cast beams.

(5) The linear methods used in the analysis of beams in place of the more rigorous non-linear methods, gave satisfactory results for all three beams. For beams with a prestressed top slab, the method given in the Concrete Society Technical Report 23 [37]was used to analyse the cracked section. Tension stiffening of the concrete was accounted for in the calculations by considering the triangular tensile stress distribution given in BS 8110. The approximate method proposed by Allen was used in the analysis to consider tension carried by concrete. and it was found to be satisfactory as shown in Figs. 6.10 to 6.12. Stress in the non-prestressed steel in A-2 and A-3 calculated using the linear method including tension stiffening effects, agreed very closely with the measured stress up to about 70% of the failure load. For A-1 also, the linear stress distribution assumed for the cracked section yielded similar results. This proportion of failure load represented

the stage when steel began to yield.

When tension carried by the concrete was completely ignored, the calculated steel stresses were considerably less than the measured values. This confirms the importance of considering the tension carried by the concrete in the cracked zone of composite beams under hogging moment. The area of concrete in the tensile face (i.e. top slab) was too large to be ignored in such cases. Also the test results showed that linear methods can be used to analyse cracked composite sections if the steel stresses are below the yield stress and the maximum compressive stress in concrete is not close to the compressive strength of concrete.

(6) The failure mode of all three beams was tension failure which resulted in the rupture of steel in the slab. The location of the failure plane was also the same and occurred at the junction between the diaphragm and the composite beam. The composite action and continuity between the two precast beams existed up to the failure which confirmed the structural soundness of the method of developing continuity using prestressed slab.

(7) The measured steel strains indicated that steel (non prestressed) began to yield at about 70% of the ultimate load. This shows that beams had a considerable amount of reserve moment capacity beyond the load at which steel began to yield. Also, the beams with a prestressed slab underwent large deflections before failure.These indicate that the ductility of beams was not affected by the prestress in the slab. The failure loads of the three beams were more than twice the cracking load which show that the code requirements to prevent immediate failure after cracking were satisfied.

(8) The measured concrete compressive strain near the diaphragm did not reach the ultimate compressive strain of 0.0035 specified in codes. However, concrete strain at the ultimate load was not measured at the failure plane. In most bridge decks also, the compressive stress in the bottom flange of precast beams will not be a critical factor in the design of the prestressing force to be applied to the top

slab.

(9) Although the diaphragm was made of concrete of lower strength than that of precast beam, it remained relatively undamaged up to the failure and the failure plane was outside the main part of the diaphragm. The increased strength of the diaphragm, which was rectangular, could be attributed to the two point loads applied on the diaphragm and ends of the precast beams in the diaphragm which restrained the propagation of cracks. In actual bridge decks, also, the two point loads on the compressive face of the diaphragm will be applied as the reaction from the bearings of the two precast beams in the adjoining spans which meet at the internal piers. This implies that in the design of continuous composite beams in the region of internal supports, the flexural capacity of the diaphragm is not as critical as that of the adjacent composite section.

(10) The ratio of measured ultimate strength to calculated ultimate strength increased from 0.92 to 1.30 when the slab type changed from reinforced to fully prestressed. The calculated strength for the above ratios was obtained by ignoring the prestress in the precast beams and the theoretical flexural capacity of the composite section calculated using British and American Code equations showed good agreement with the flexural strength calculated using a strain compatibility method with a rectangular stress block for the concrete. The increased ratio for the beams with a prestressed slab was considered to be due to the tension carried by the prestressing steel in the precast beams in the tensile zone , the presence of both prestressed and non-prestressed steel in the slab and the effects of the two point loads on the diaphragm.

(11) When the prestressing steel in the precast beams was included in the calculations, by considering 20% of prestress to be effective at the critical section, the calculated moment increased and became closer to the measured strength of A-2. The ratio of measured to theoretical strength for A-1 and A-3 were 0.72 and 1.12 respectively.

(12) The results of the three beam tests indicated that when the ultimate flexural capacity of continuous composite beams with reinforced slab is calculated at the interior support, it is safer to ignore the prestress in the precast beams. Similar recommendations have been made by Kaar et al [8] and current design codes [28,35]. In the design of composite beams with prestressed slabs, the increased strength of the beam can be utilised by considering the prestressing steel in the precast beam if a sufficient number of prestressing strands are located at the top of the beam and the prestress in the slab is high. An appropriate amount of the prestress at the critical section must be used considering the development length of prestressing steel in the precast beam and the width of the diaphragm.

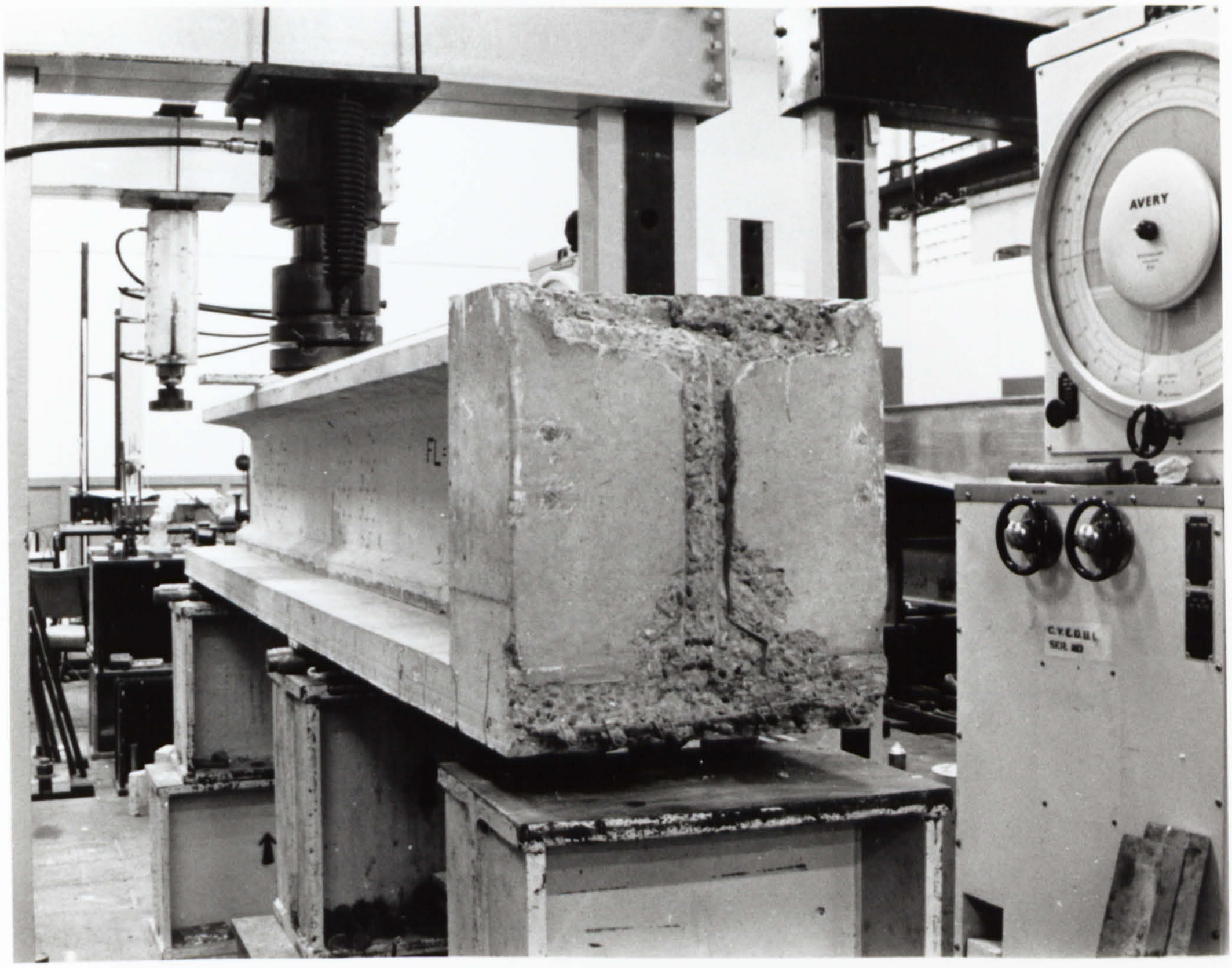

Plate 6.1 Failure Surface of Beam A-1.

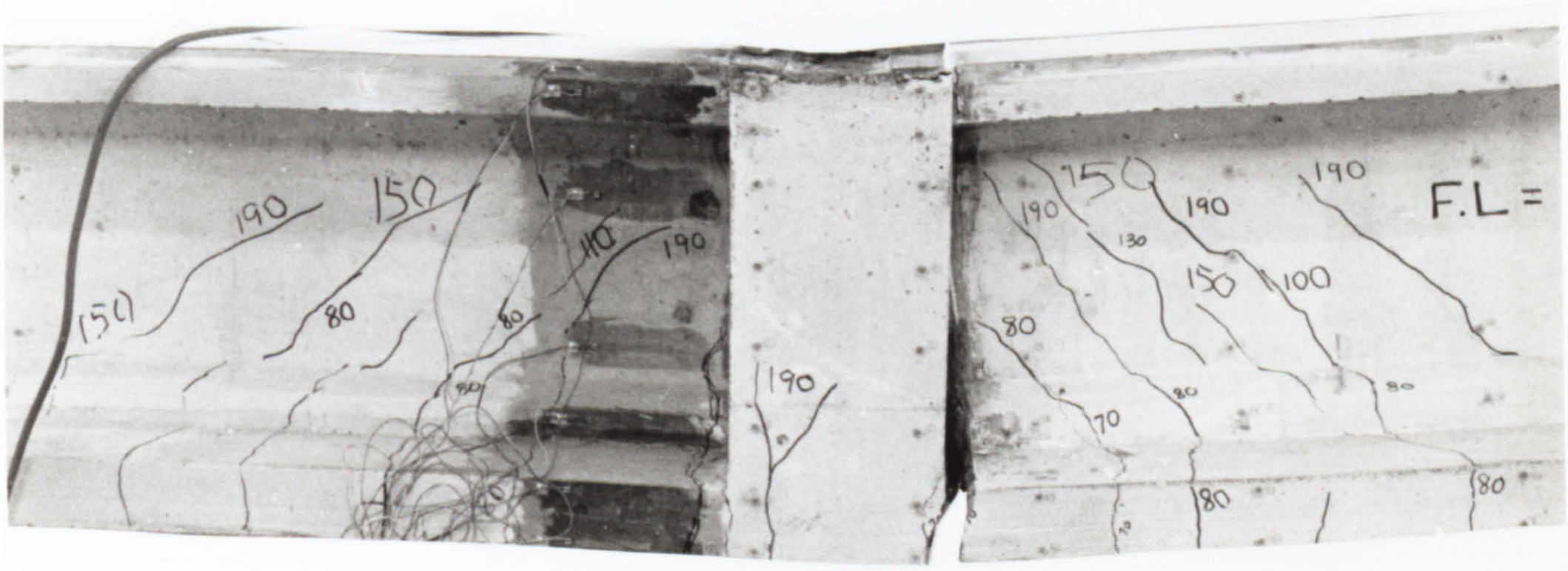

Plate 6.2 Typical Crack Patterns and Failure Plane of Flexural Test Series.

Table. 6.1 Flexural Cracking Load of Series-A Beams

Beam	Cracking Load		
	Experimental (kN)	Ratio of $\frac{\text{Experimental}}{\text{Theoretical}}$	Ratio of $\frac{\text{Experimental}}{\text{Service Load}}$
A-1	30.0	0.74	0.62
A-2	75.0	0.90	1.20
A-3	115.0	1.03	1.84

Table 6.2 Ultimate Flexural Capacity of Series-A Beams

Beam	Ultimate Flexural Strength (kNm)				Ratio of $\frac{\text{Experimental}}{\text{Calculated}}$	
	Measured	Calculated			Ignoring Prestress in Precast Beams (*)	Considering Prestress in Precast Beams (**)
		M_u*	M_u**	ACI Code Equation		
A-1	173.5	188.1	240.3	190.0	0.92	0.72
A-2	232.5	188.5	241.0	184.7	1.23	0.96
A-3	322.5	242.3	287.0	239.0	1.33	1.12

Note: * - Ignoring prestress in precast beams

** - Considering 20% prestress in precast beams at critical section

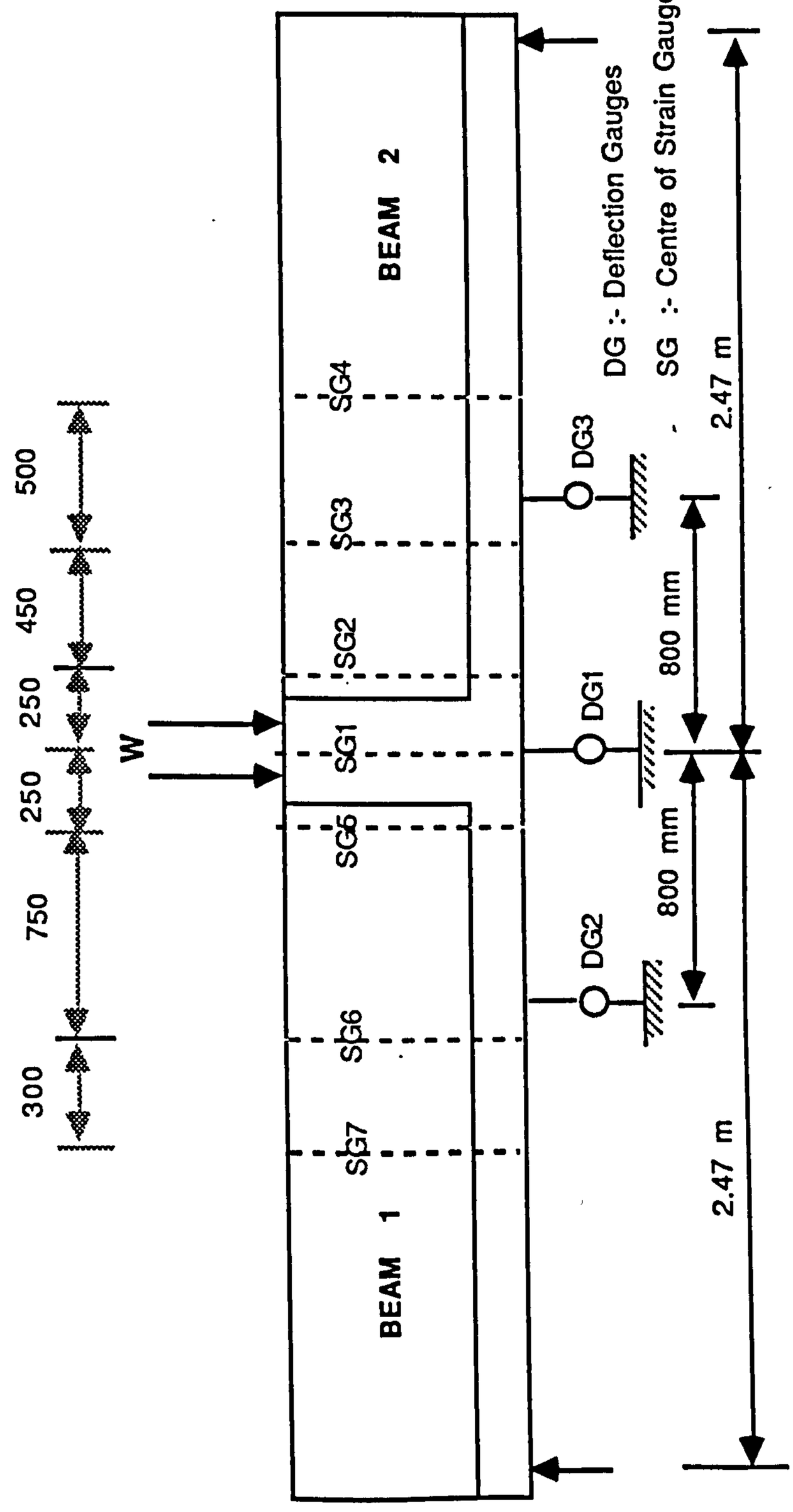

Fig. 6.1 : Positions of Deflection Gauges and Strain Gauges on Beams in Flexural Test Series

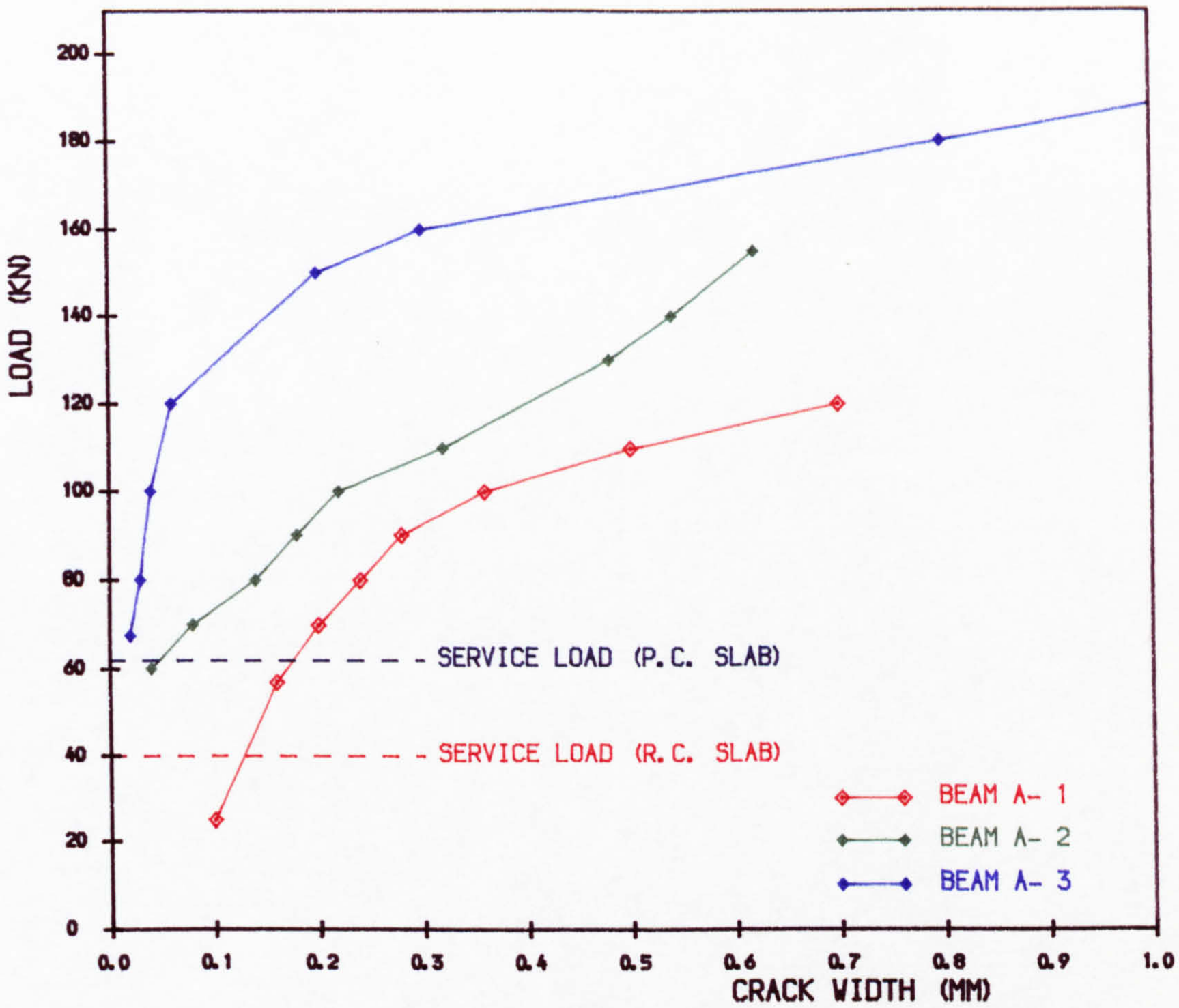

FIG. 6.2 : LOAD VS MAXIMUM CRACK WIDTH OF SERIES-A BEAMS

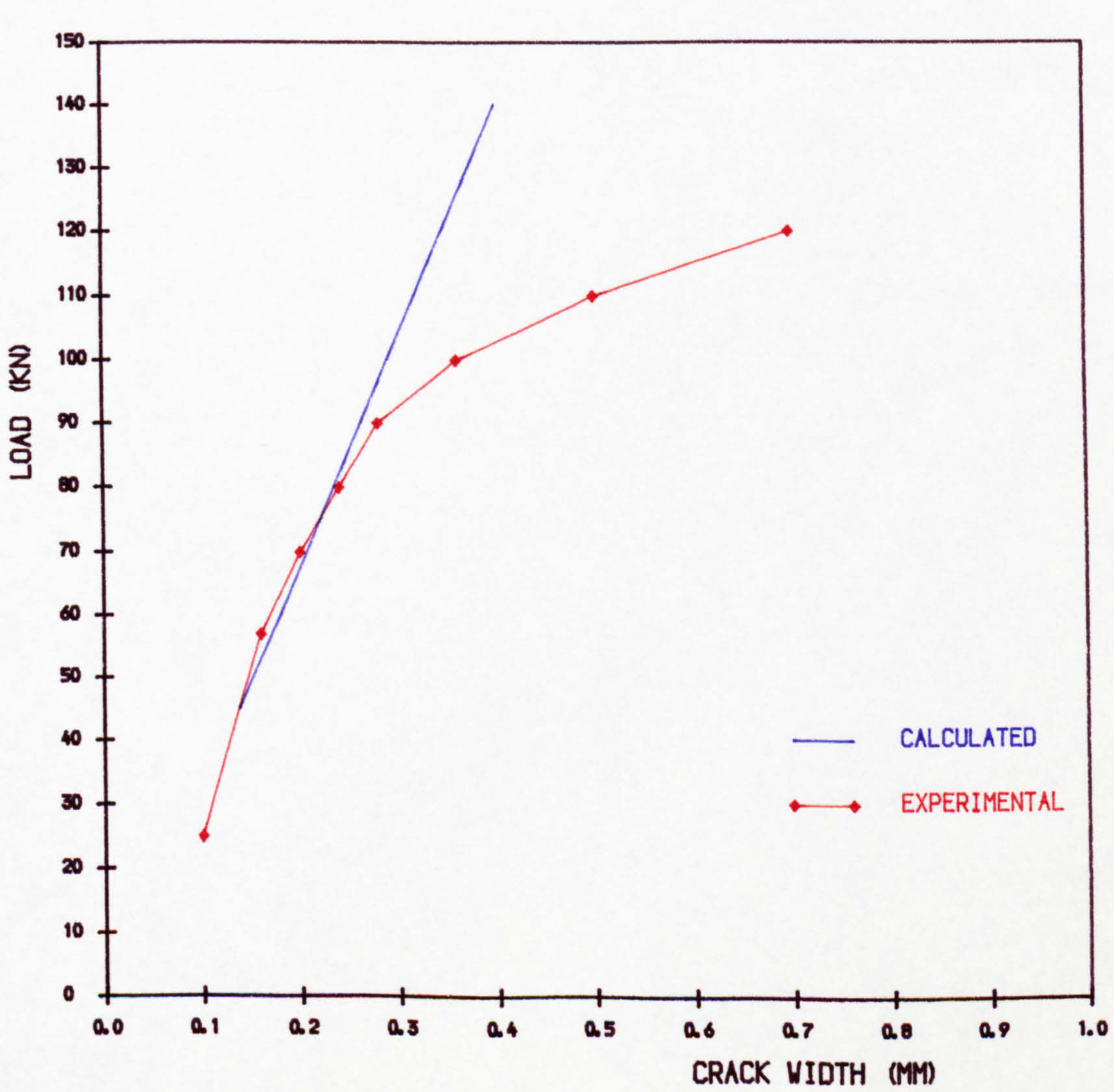

FIG. 6.3 : LOAD VS CRACK WIDTH OF BEAM A-1

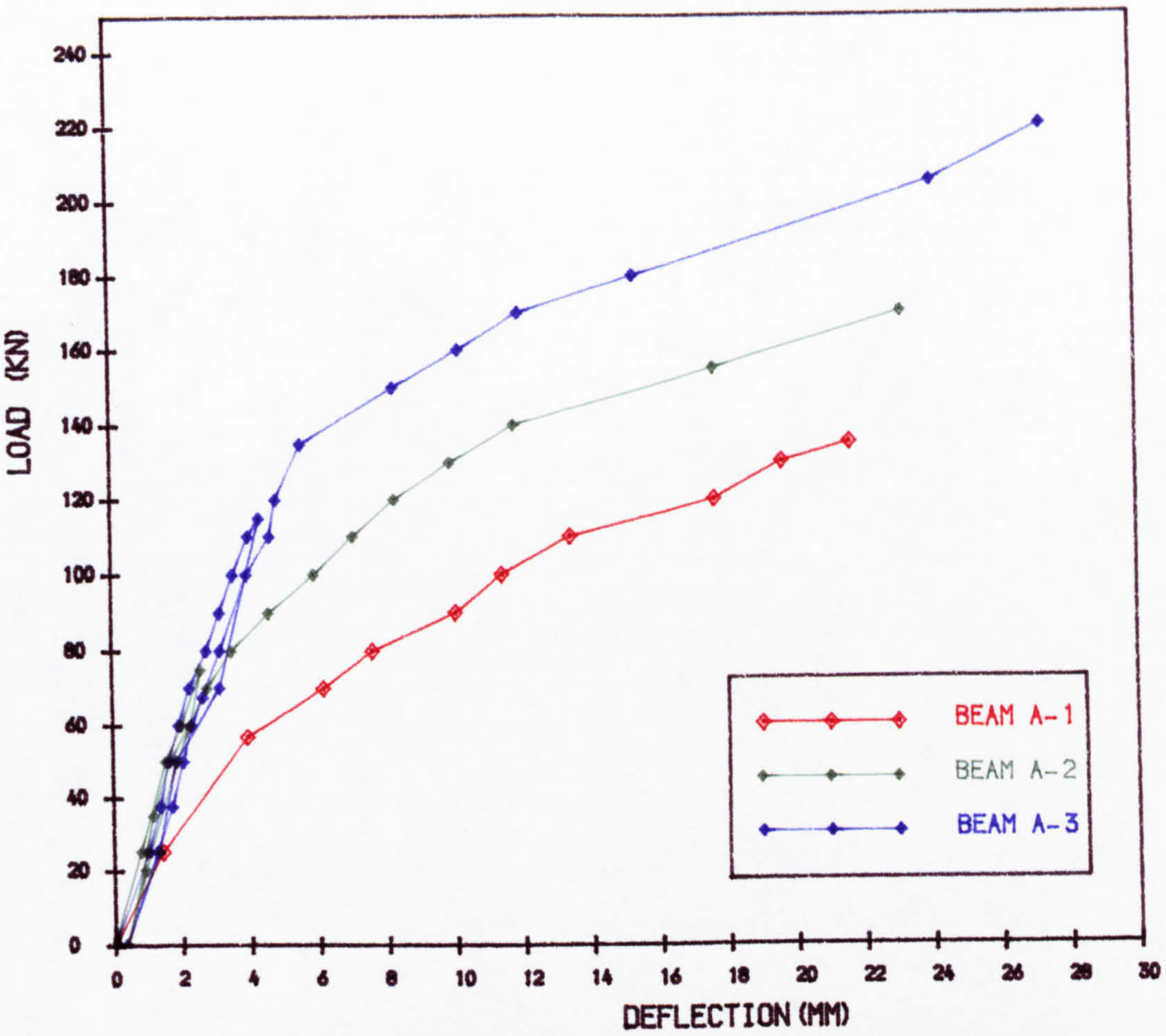

FIG. 6.4 : LOAD VS DEFLECTION CURVES OF FLEXURAL TESTS (CENTRE OF BEAM)

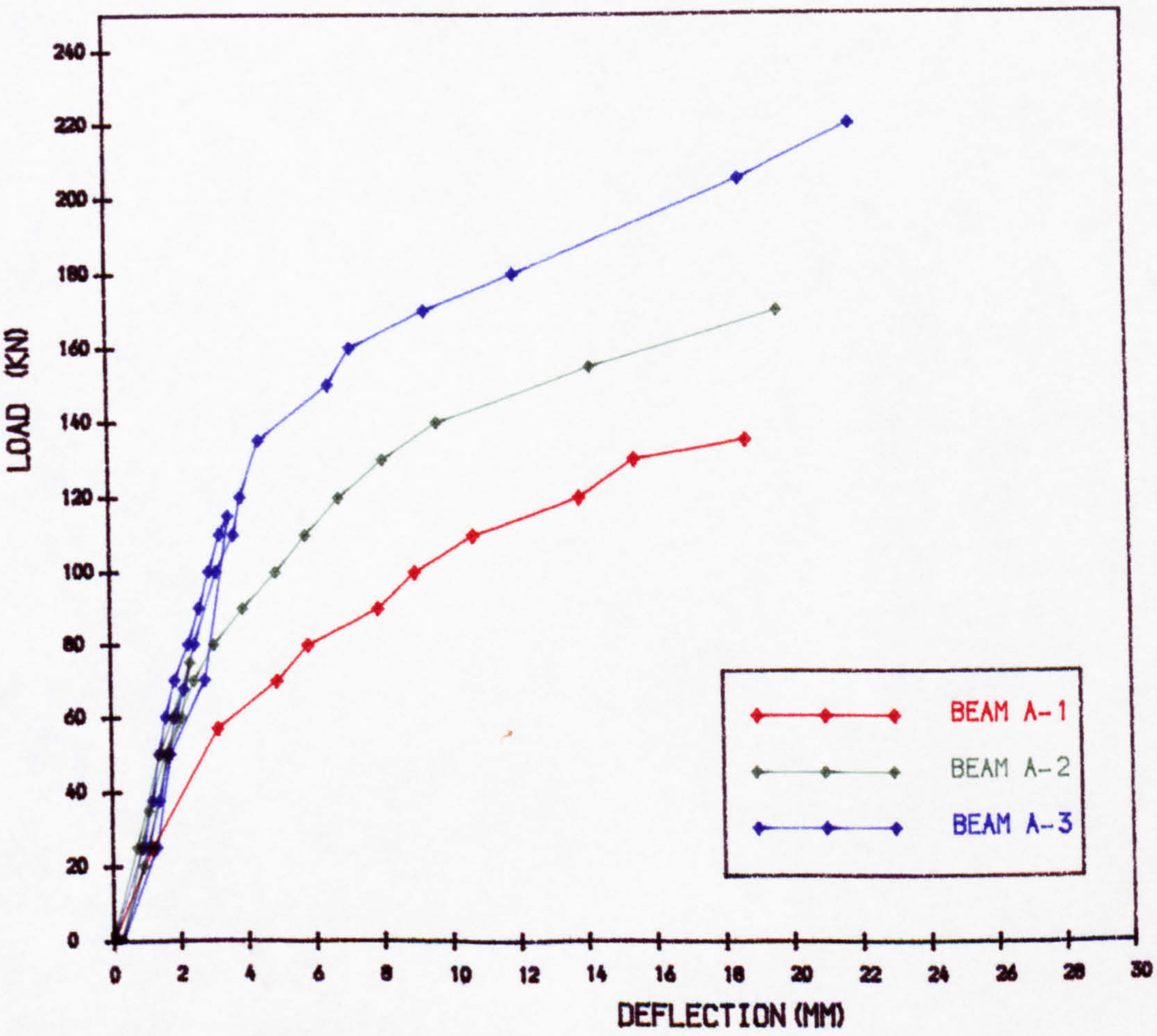

FIG. 6.5 : LOAD VS DEFLECTION CURVES OF FLEXURAL TESTS (800 MM FROM CENTRE)

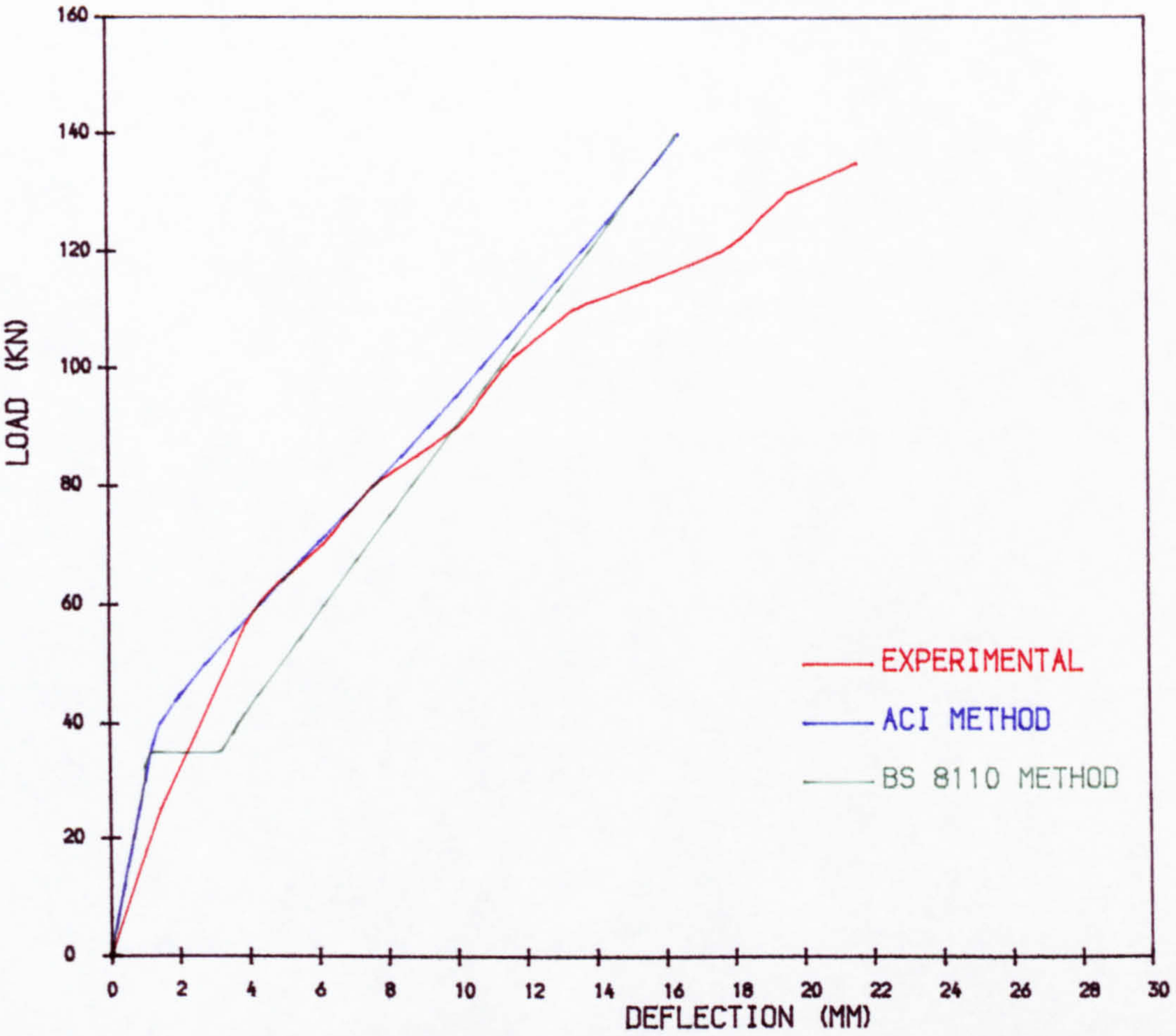

FIG. 6.6 : LOAD VS DEFLECTION CURVE OF BEAM A-1 (AT THE CENTRE)

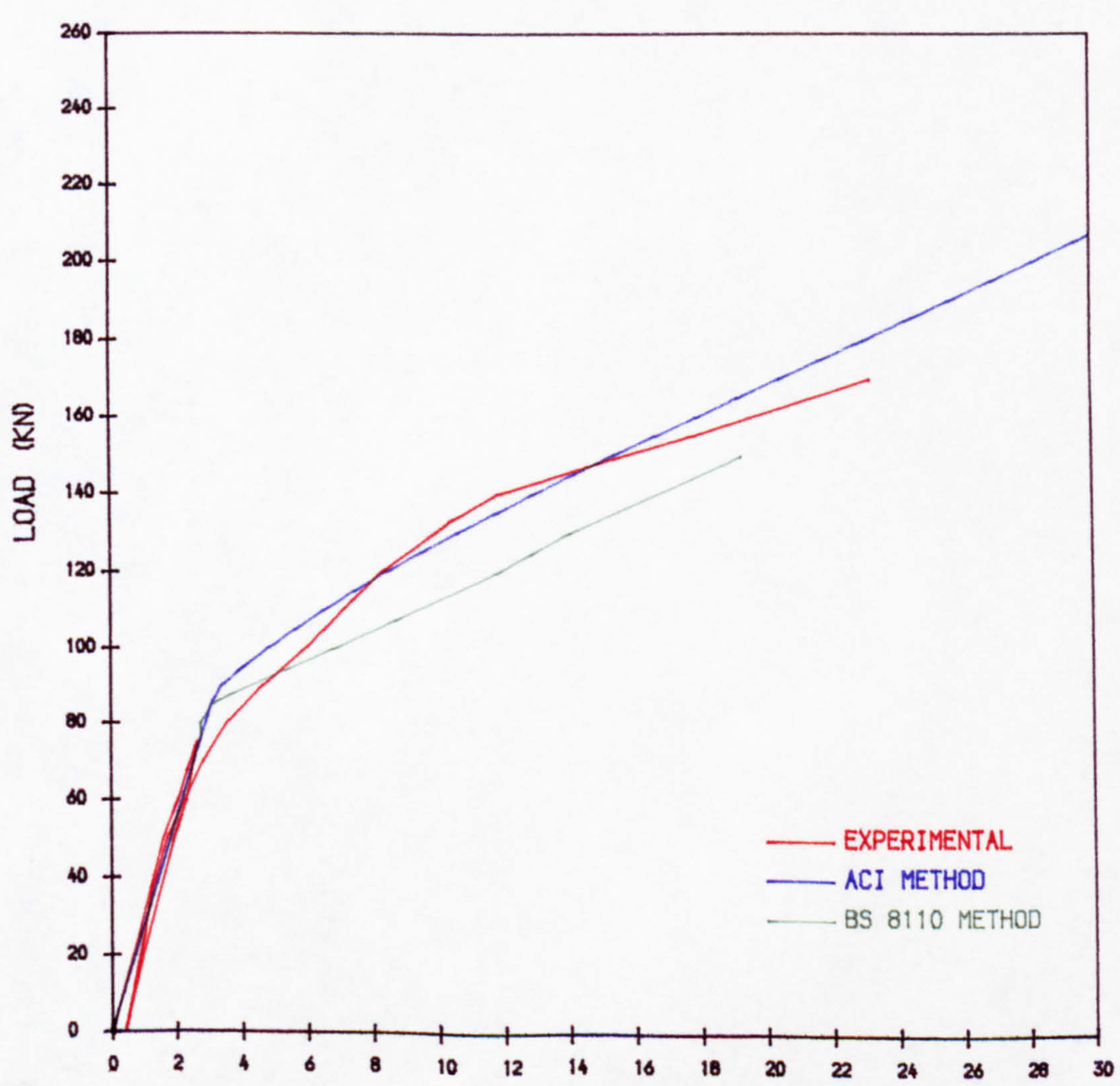

FIG. 6.7 : LOAD VS DEFLECTION CURVE OF BEAM A-2 (AT THE CENTRE)

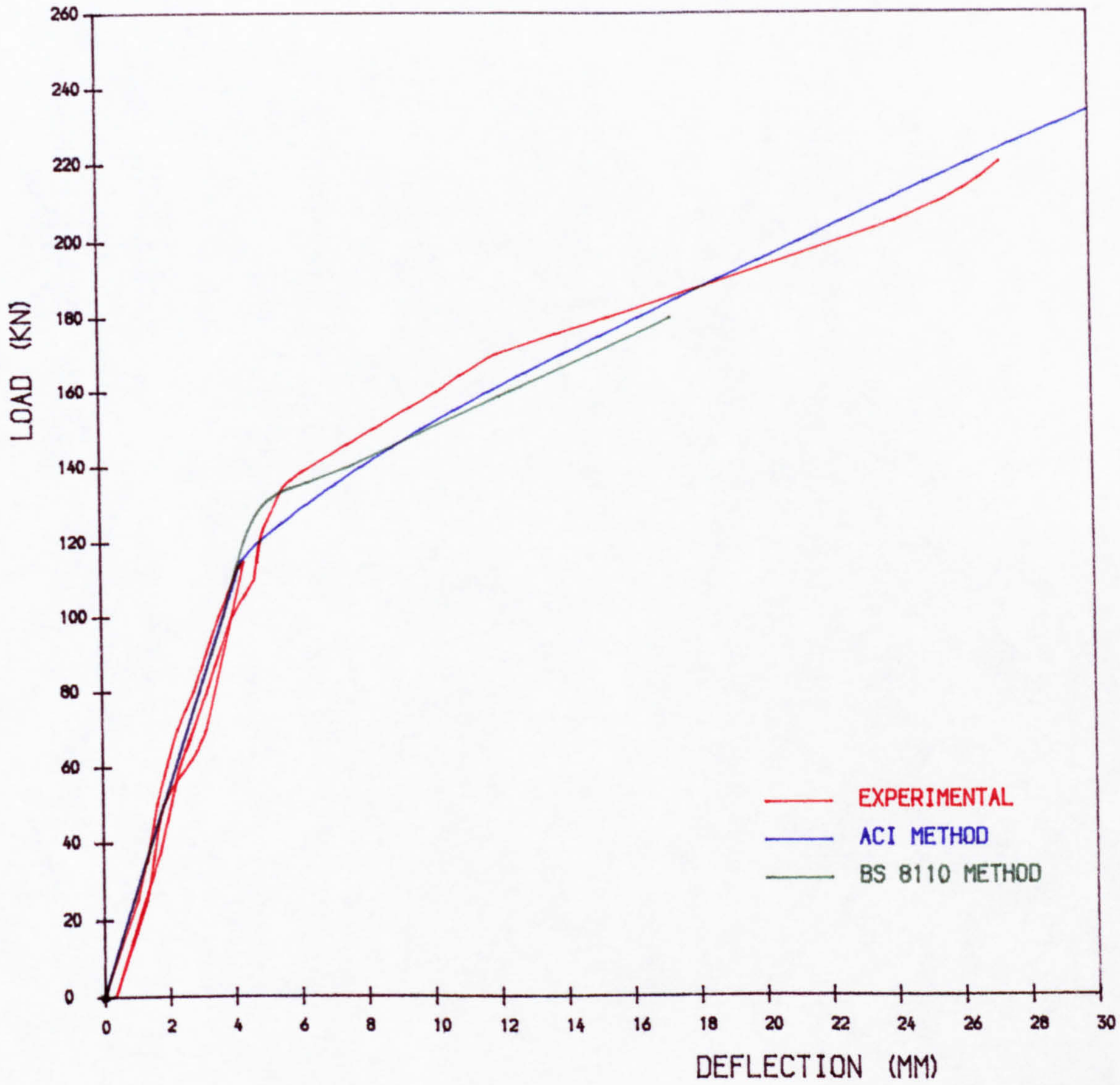

FIG. 6.8 : LOAD VS DEFLECTION CURVE OF BEAM A-3 (CENTRE)

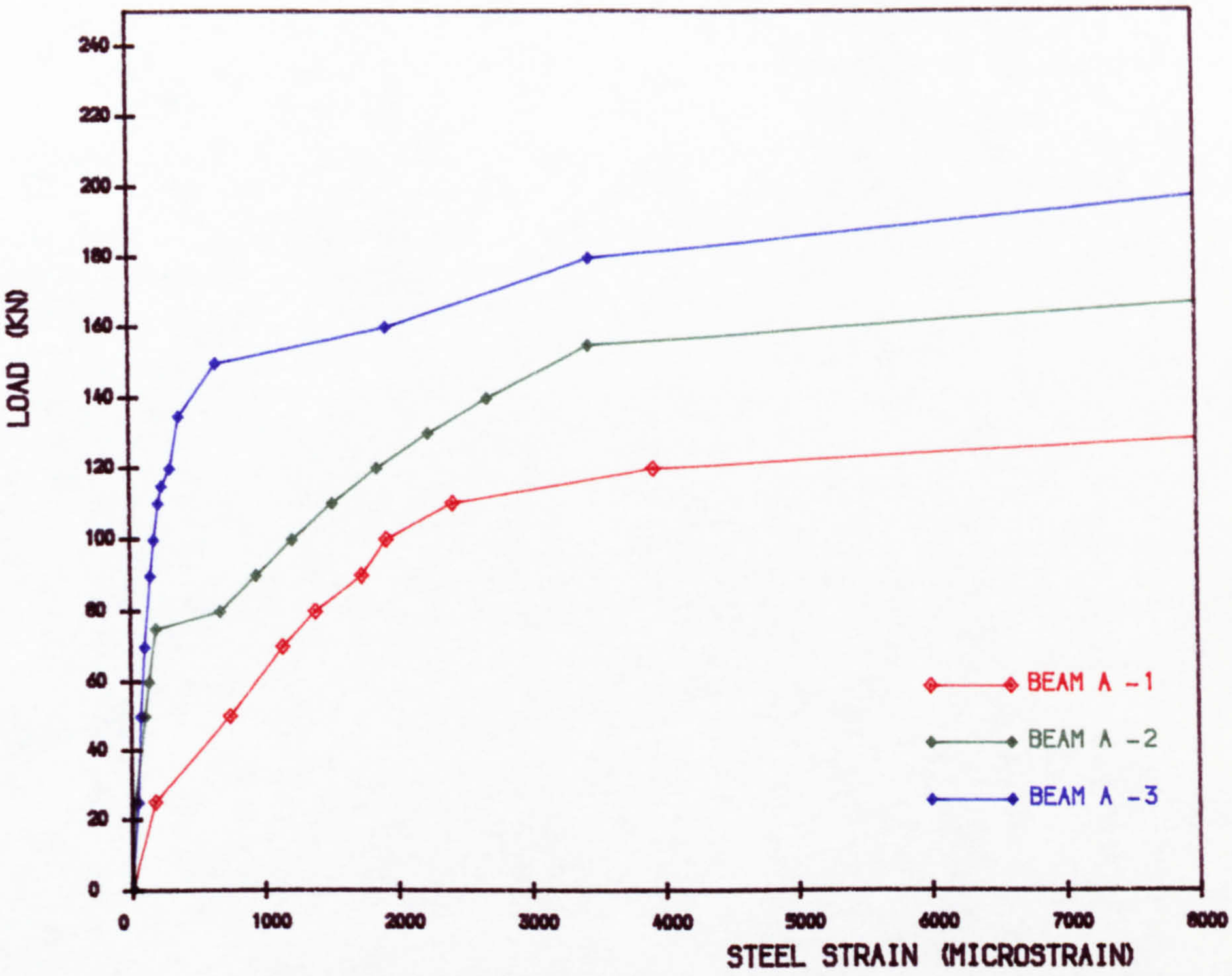

FIG. 6.9 : VARIATION OF STRAIN IN NON-PRESTRESSED STEEL WITH LOAD IN FLEXURAL TEST SERIES

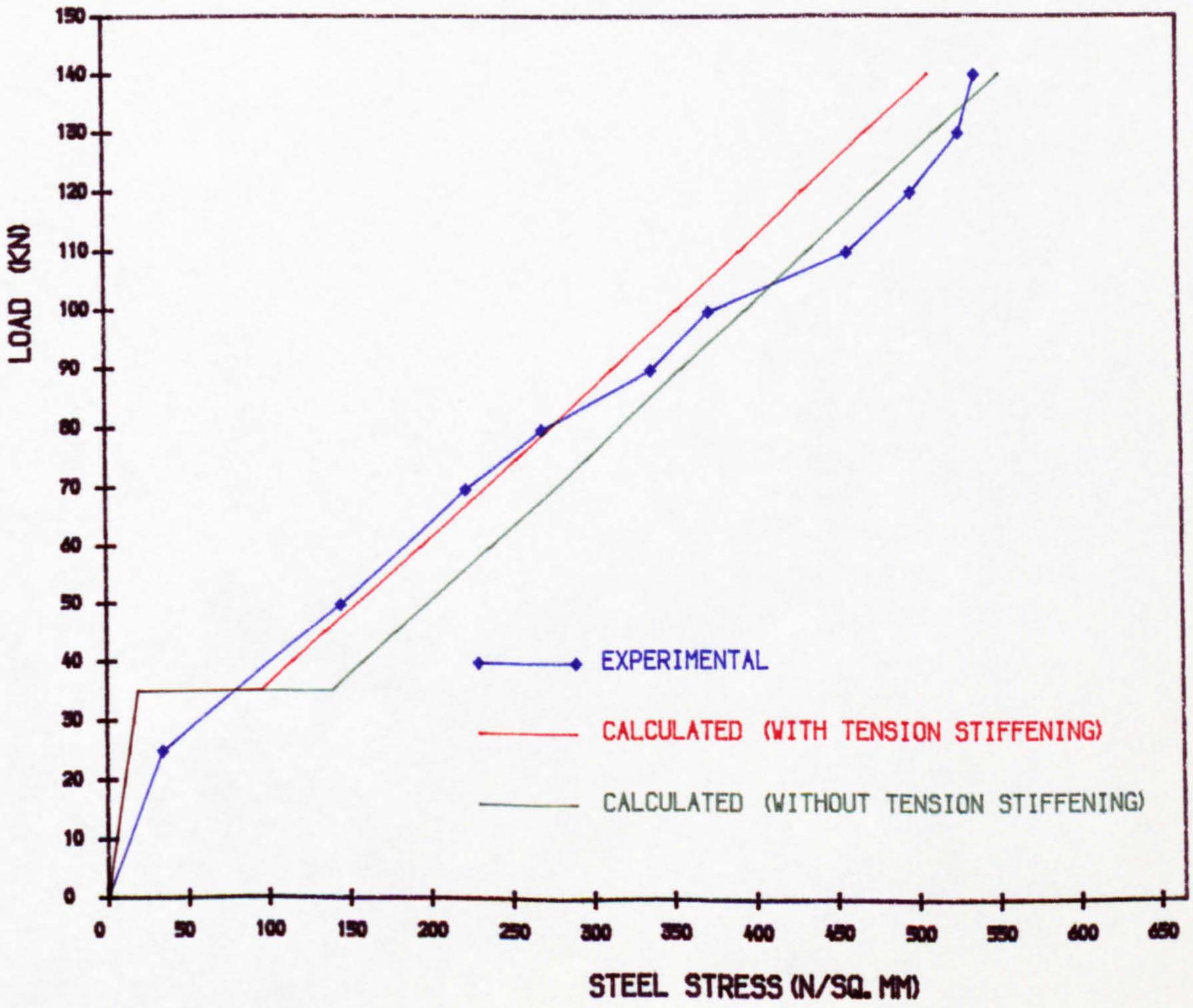

FIG. 6.10 : LOAD VS STRESS OF REINFORCEMENT (BEAM A-1)

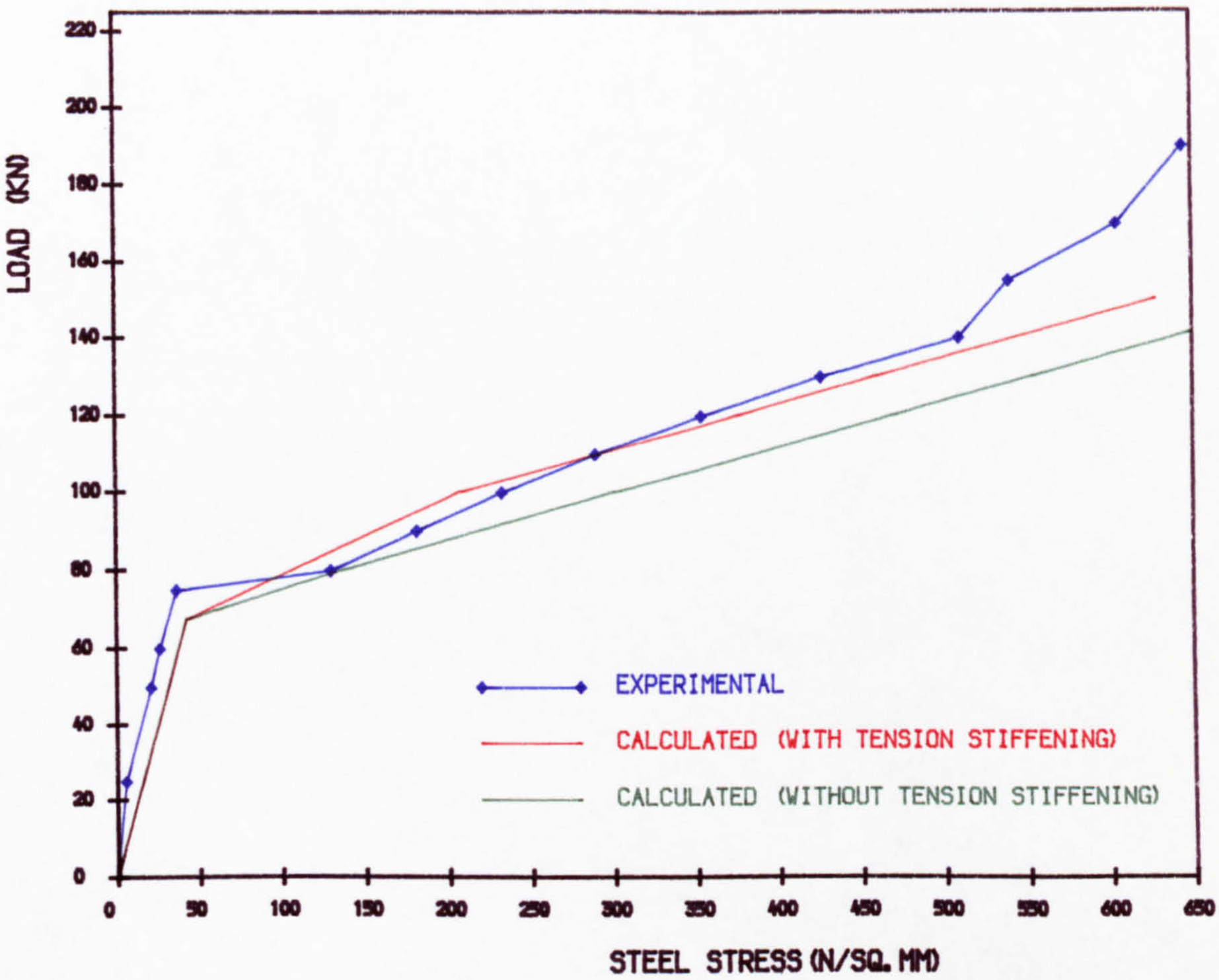

FIG. 6.11 : LOAD VS STRESS IN REINFORCEMENT (BEAM A-2)

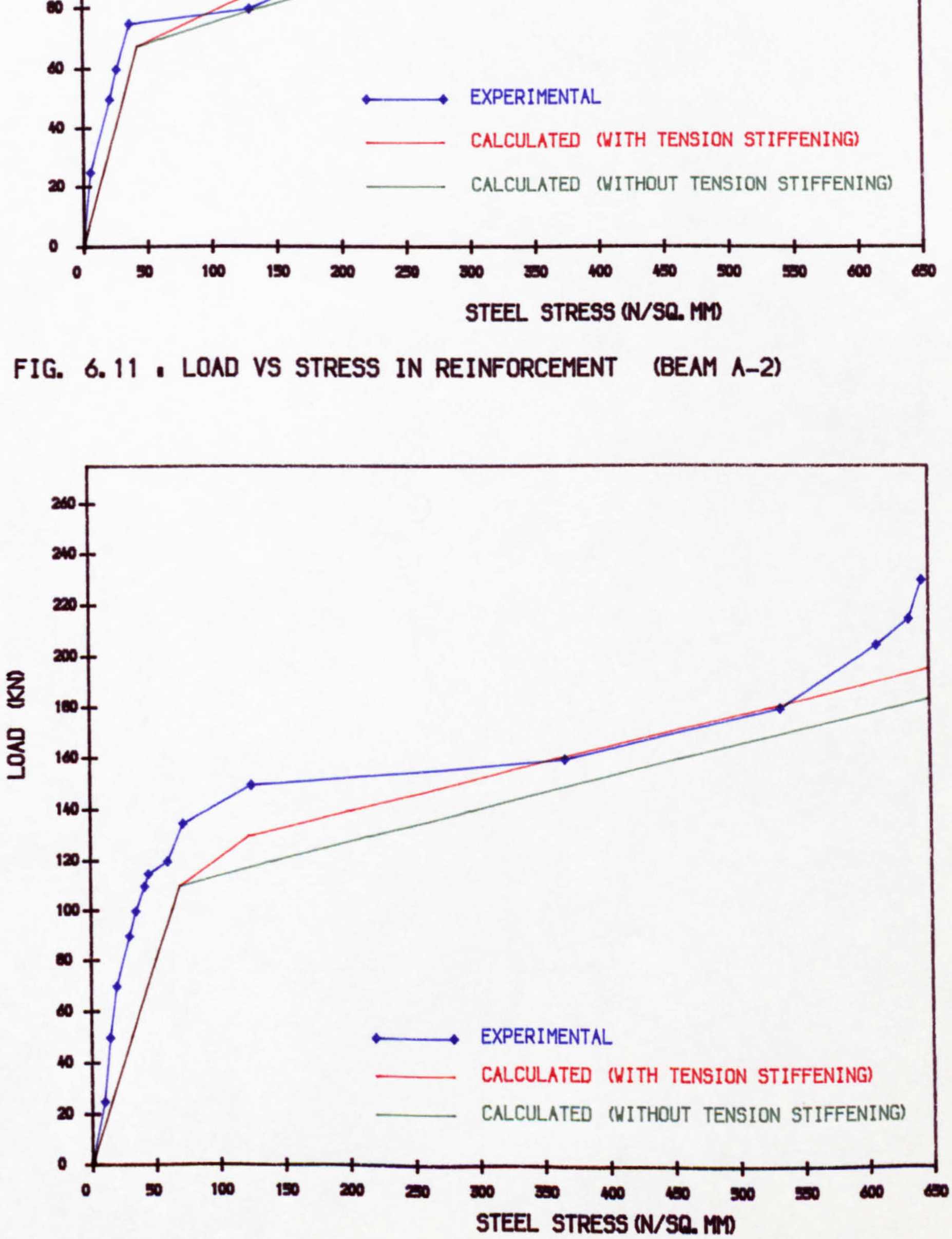

FIG. 6.12 : LOAD VS STRESS IN REINFORCEMENT (BEAM A-3)

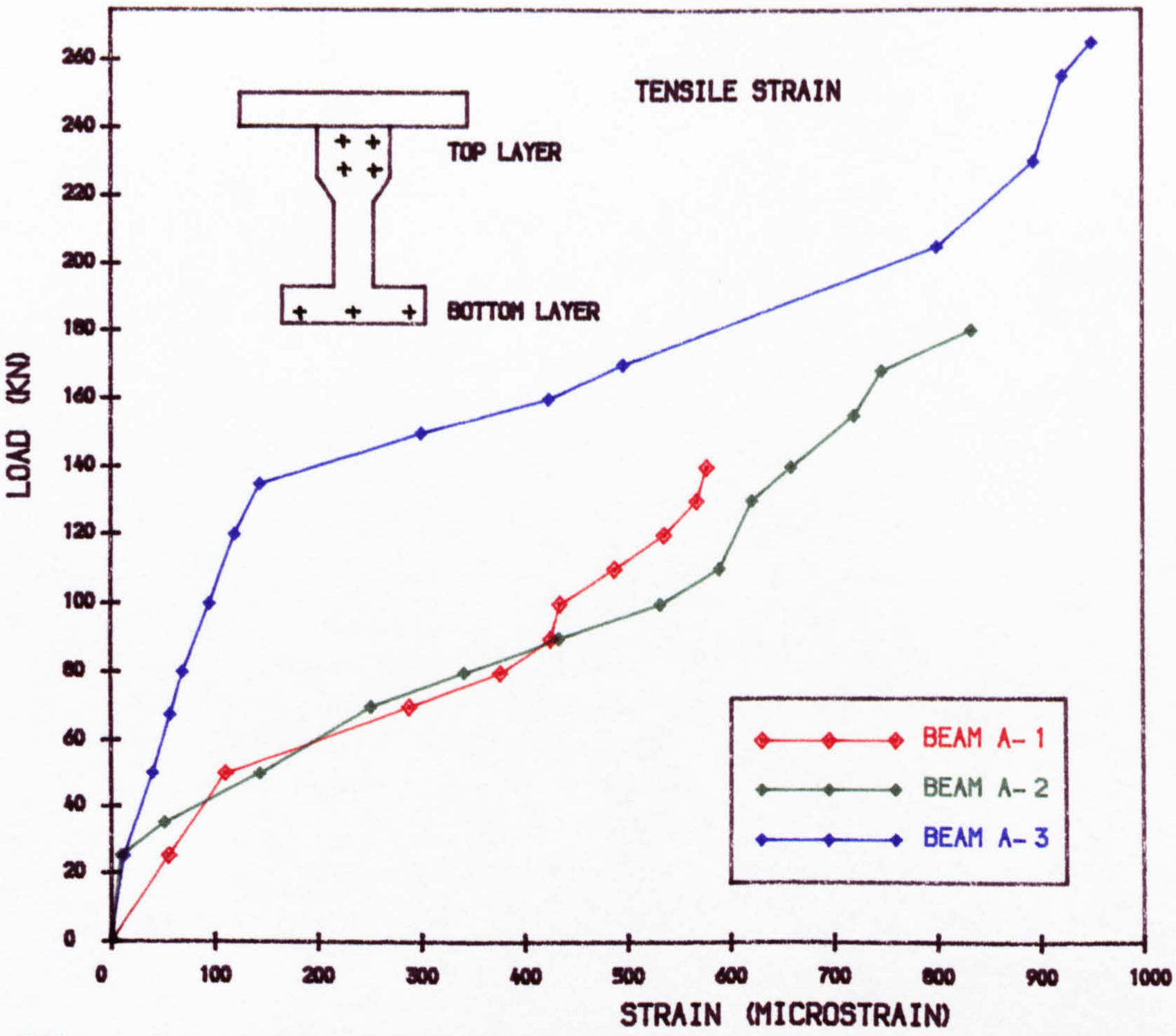

FIG. 6.13 : LOAD VS STRAIN IN PRESTRESSING WIRES (TOP LAYER)

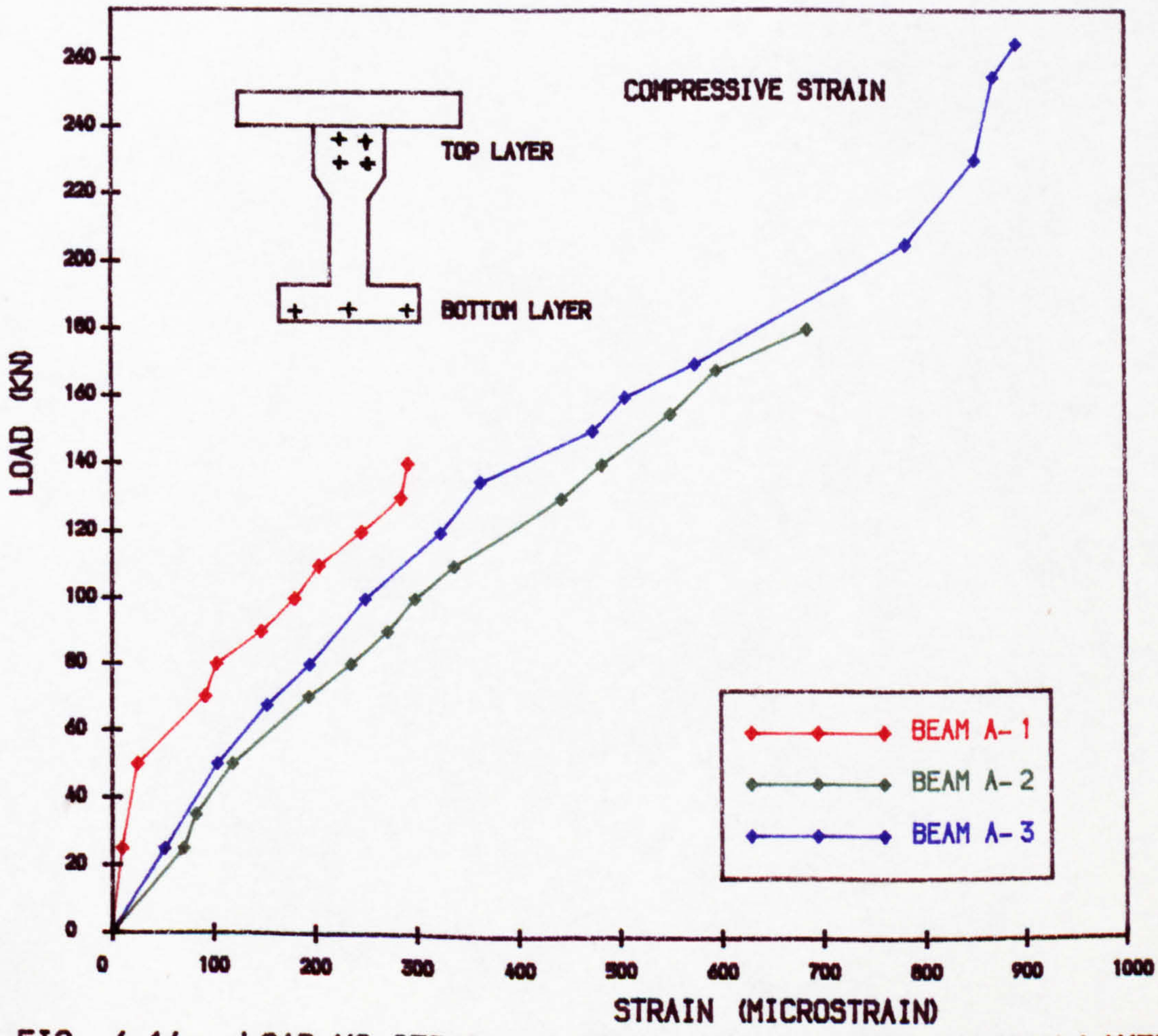

FIG. 6.14 : LOAD VS STRAIN IN PRESTRESSING WIRES (BOTTOM LAYER)

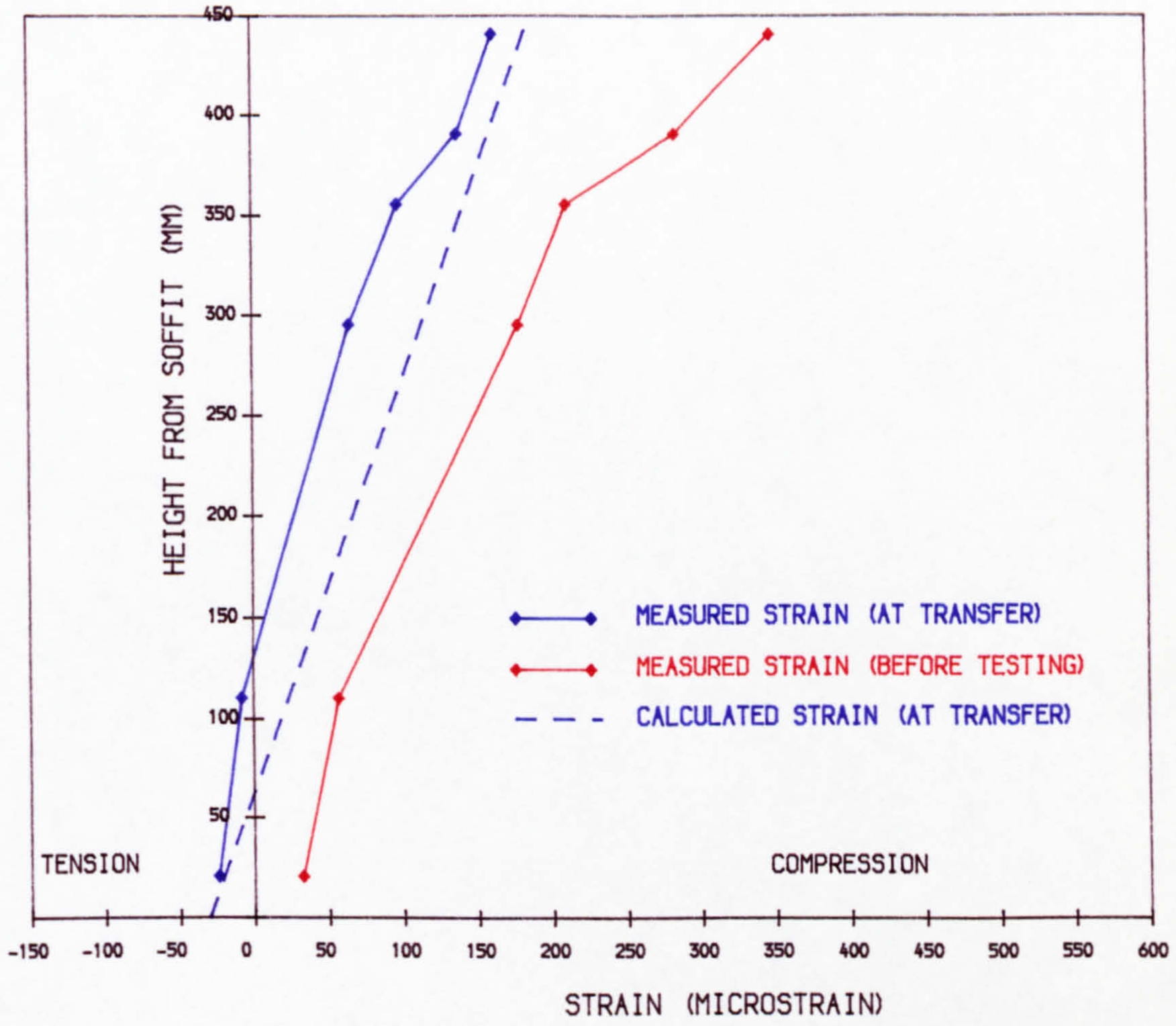

FIG. 6.15 : STRAIN DISTRIBUTION ACROSS CONCRETE SECTION DUE TO PRESTRESS IN THE SLAB (BEAM A-2)

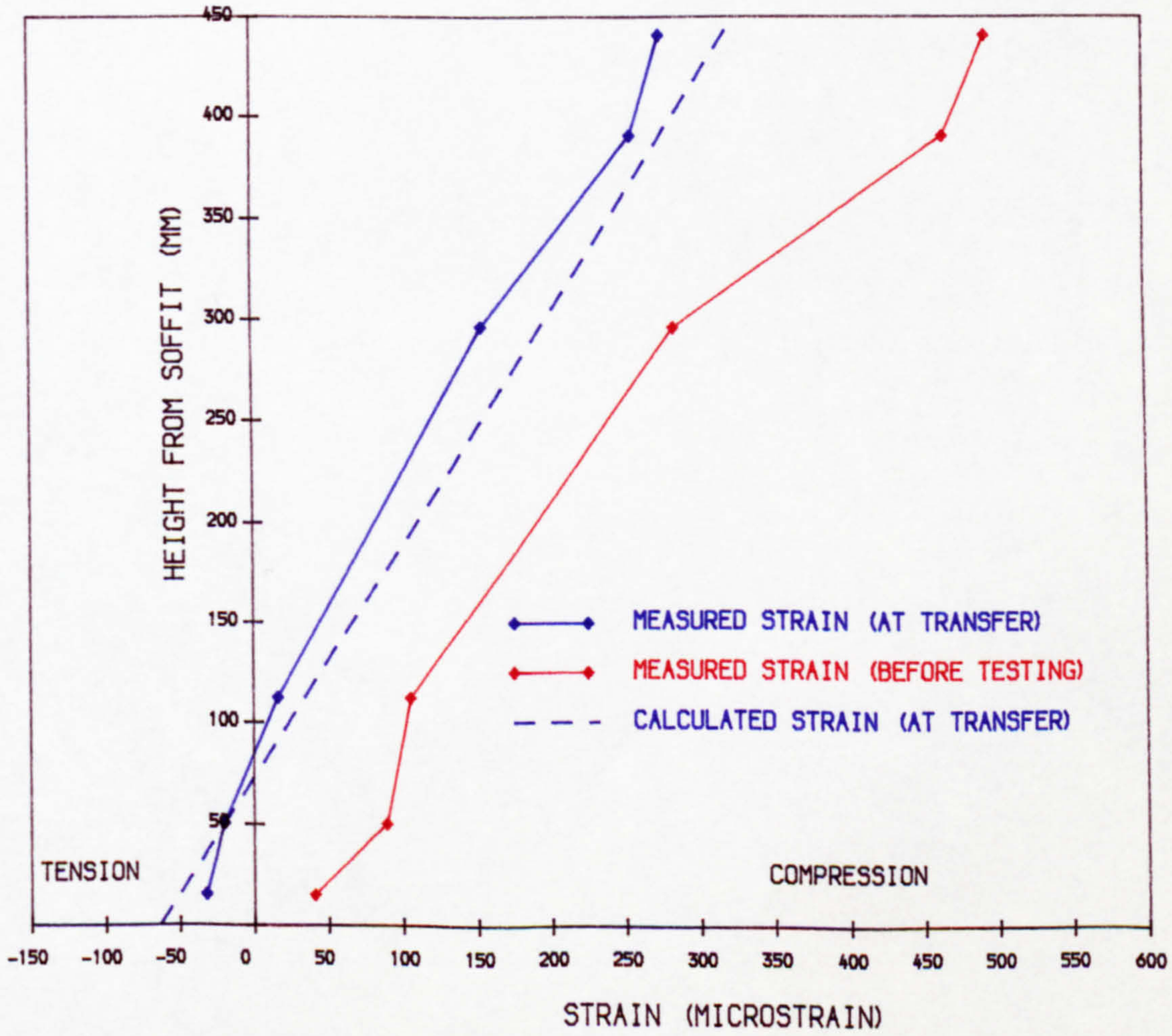

FIG. 6.16 : STRAIN DISTRIBUTION ACROSS CONCRETE SECTION DUE TO PRESTRESS IN THE SLAB (BEAM A-3)

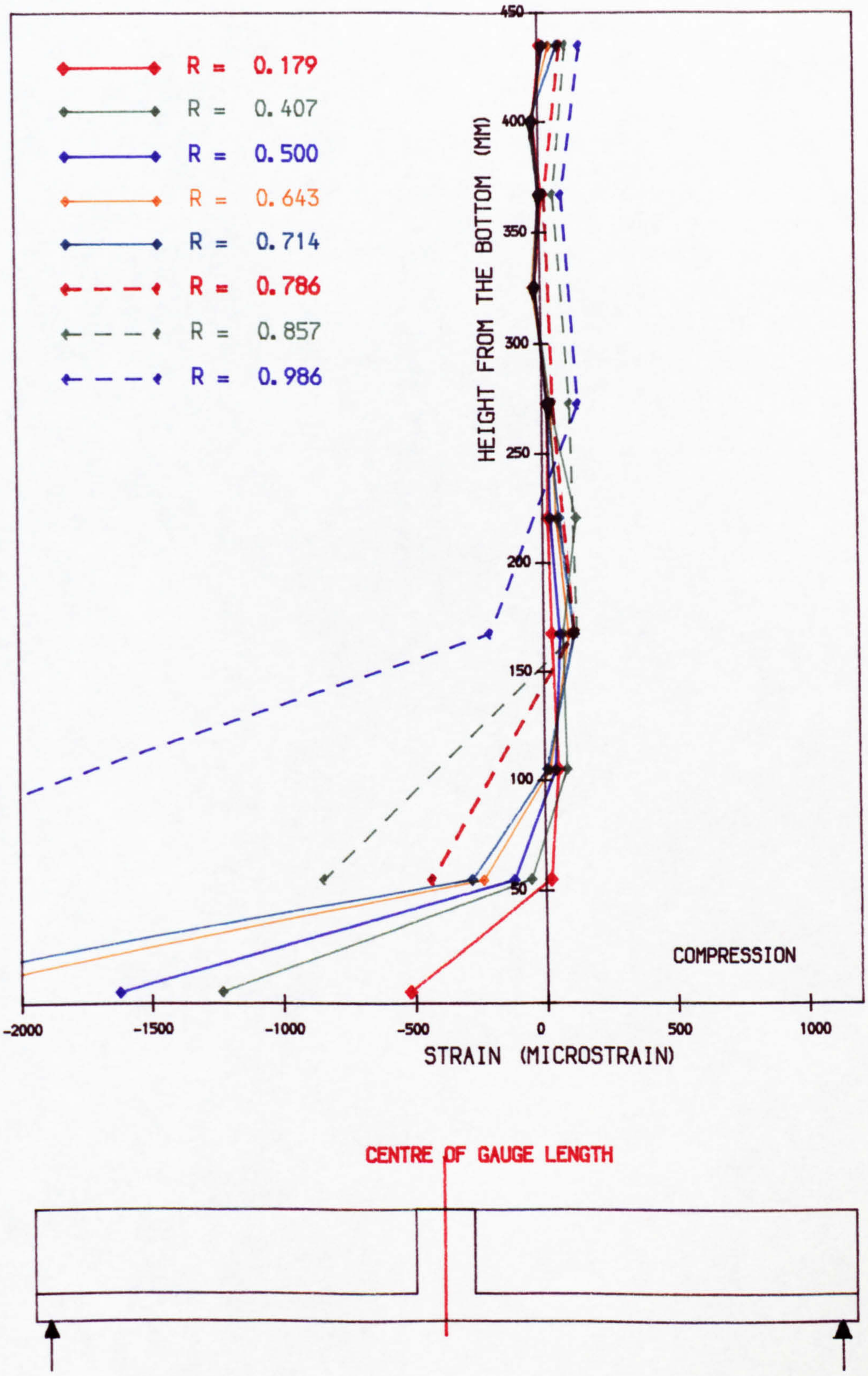

FIG. 6.17 : STRAIN DISTRIBUTION ACROSS CONCRETE SECTION

BEAM A-1 (DIAPHRAGM)

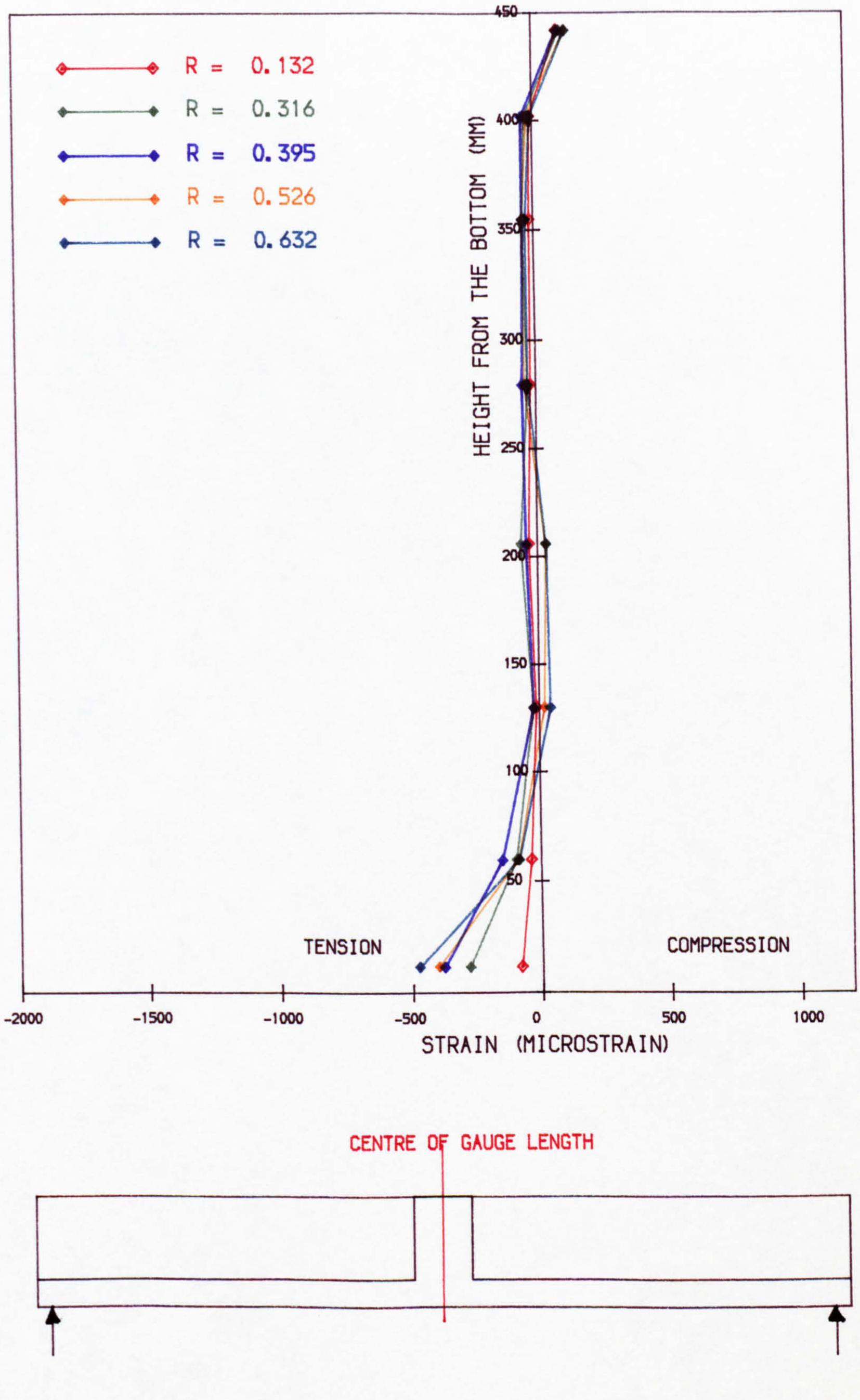

FIG. 6.18 : STRAIN DISTRIBUTION ACROSS CONCRETE SECTION

BEAM A-2 (DIAPHRAGM)

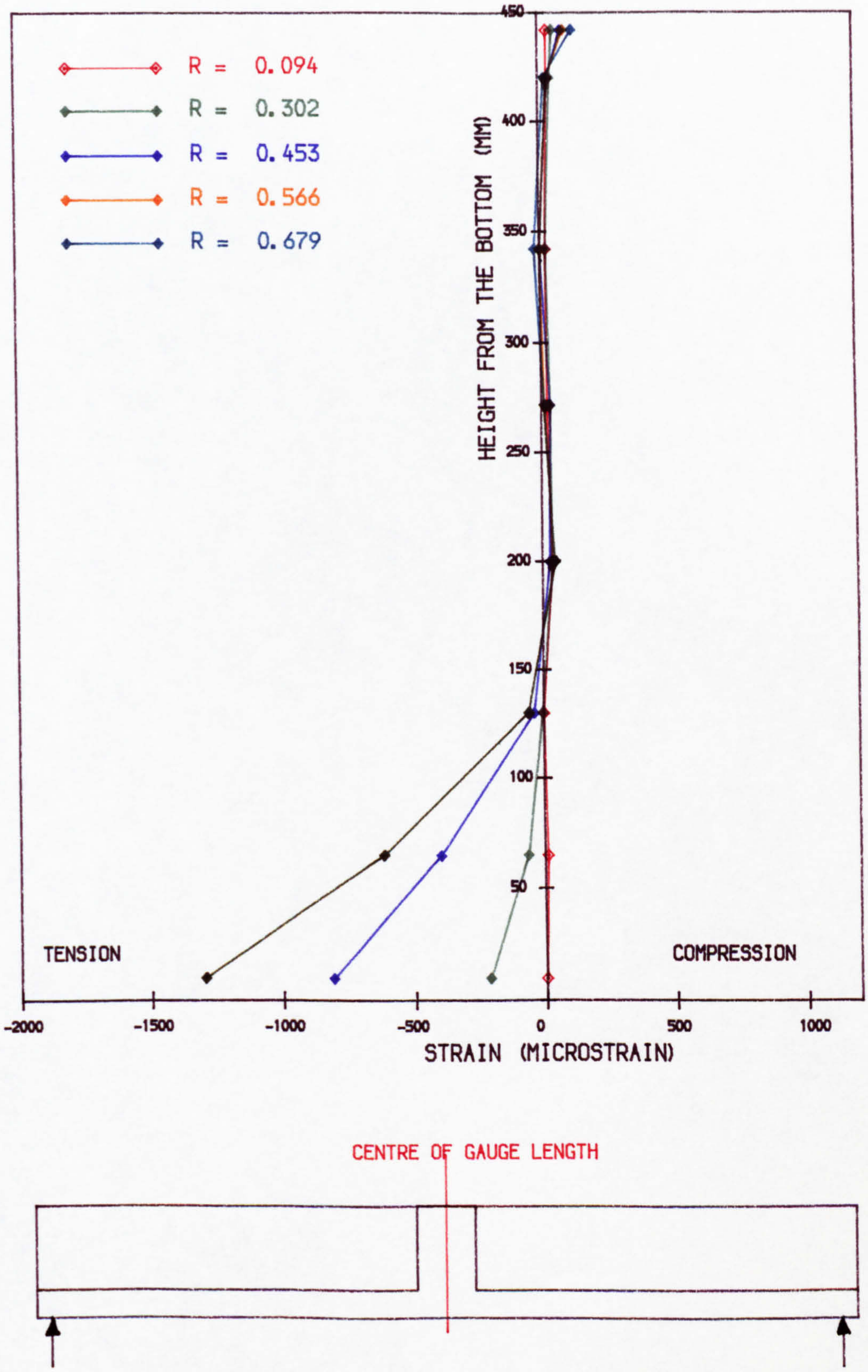

FIG. 6.19 : STRAIN DISTRIBUTION ACROSS CONCRETE SECTION

BEAM A-3 (DIAPHRAGM)

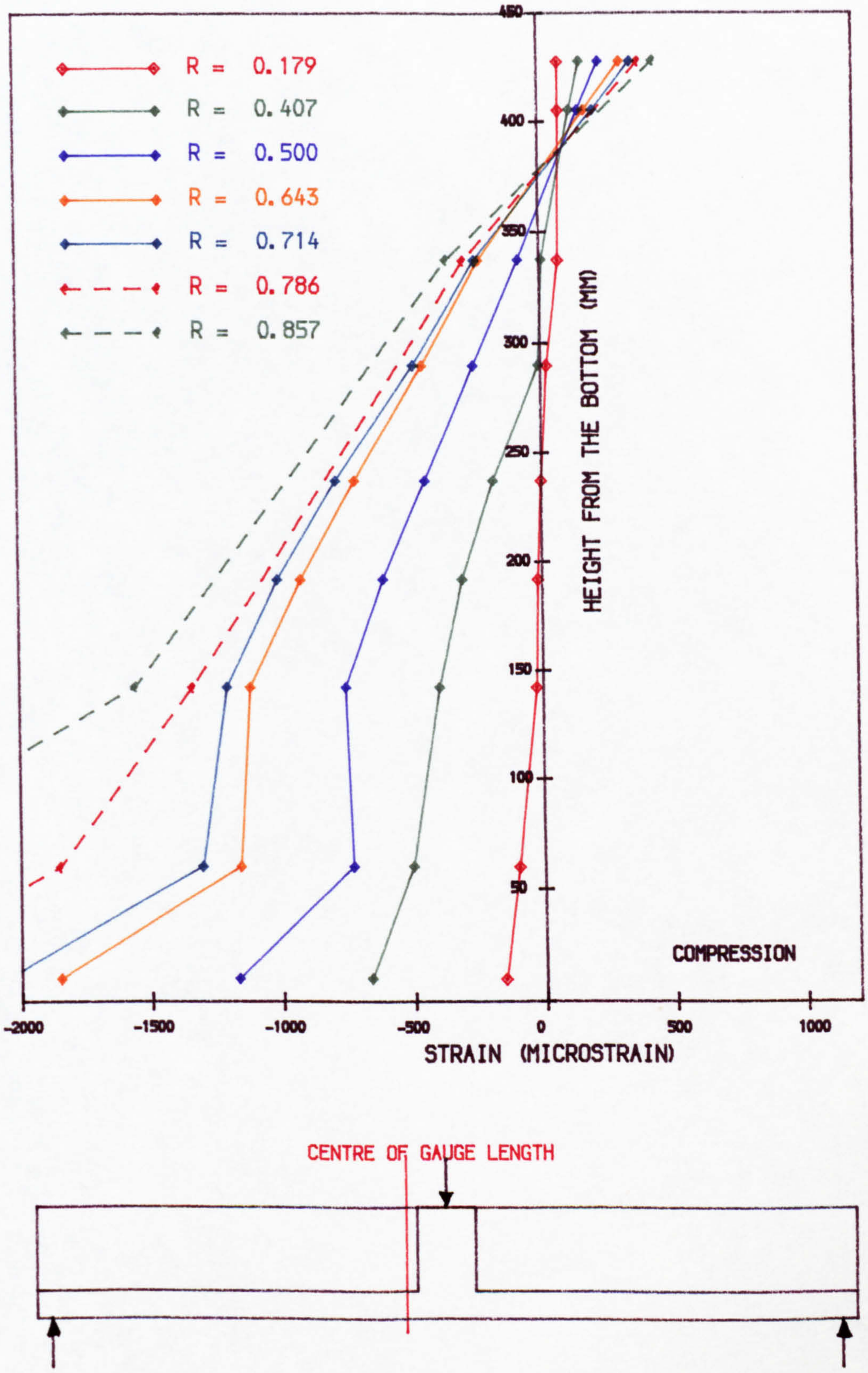

FIG. 6.20 : STRAIN DISTRIBUTION ACROSS CONCRETE SECTION

BEAM A-1 (250 MM FROM THE CENTRE) A-1-1

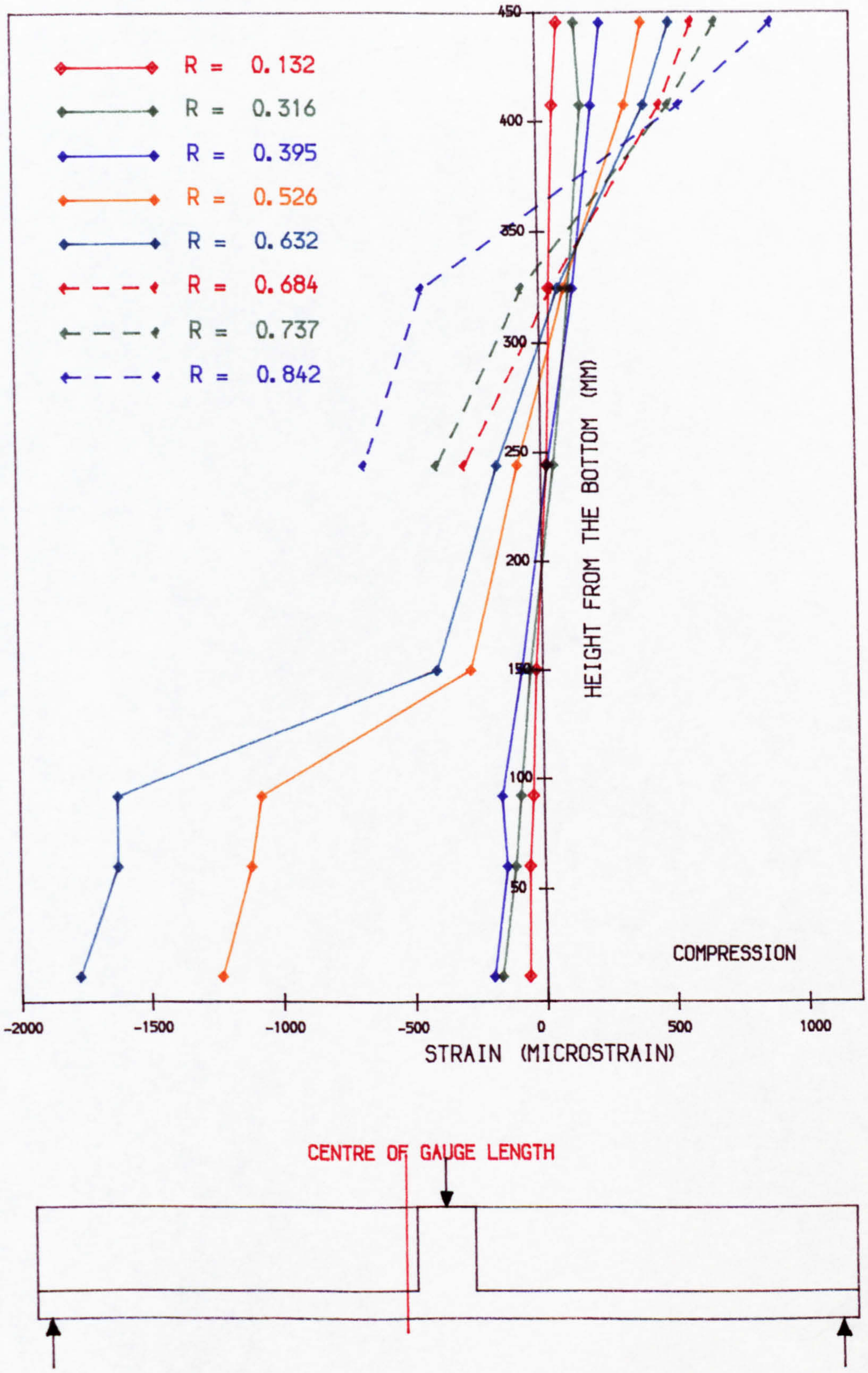

FIG. 6.21 : STRAIN DISTRIBUTION ACROSS CONCRETE SECTION

BEAM A-2 (250 MM FROM THE CENTRE) A-2-1

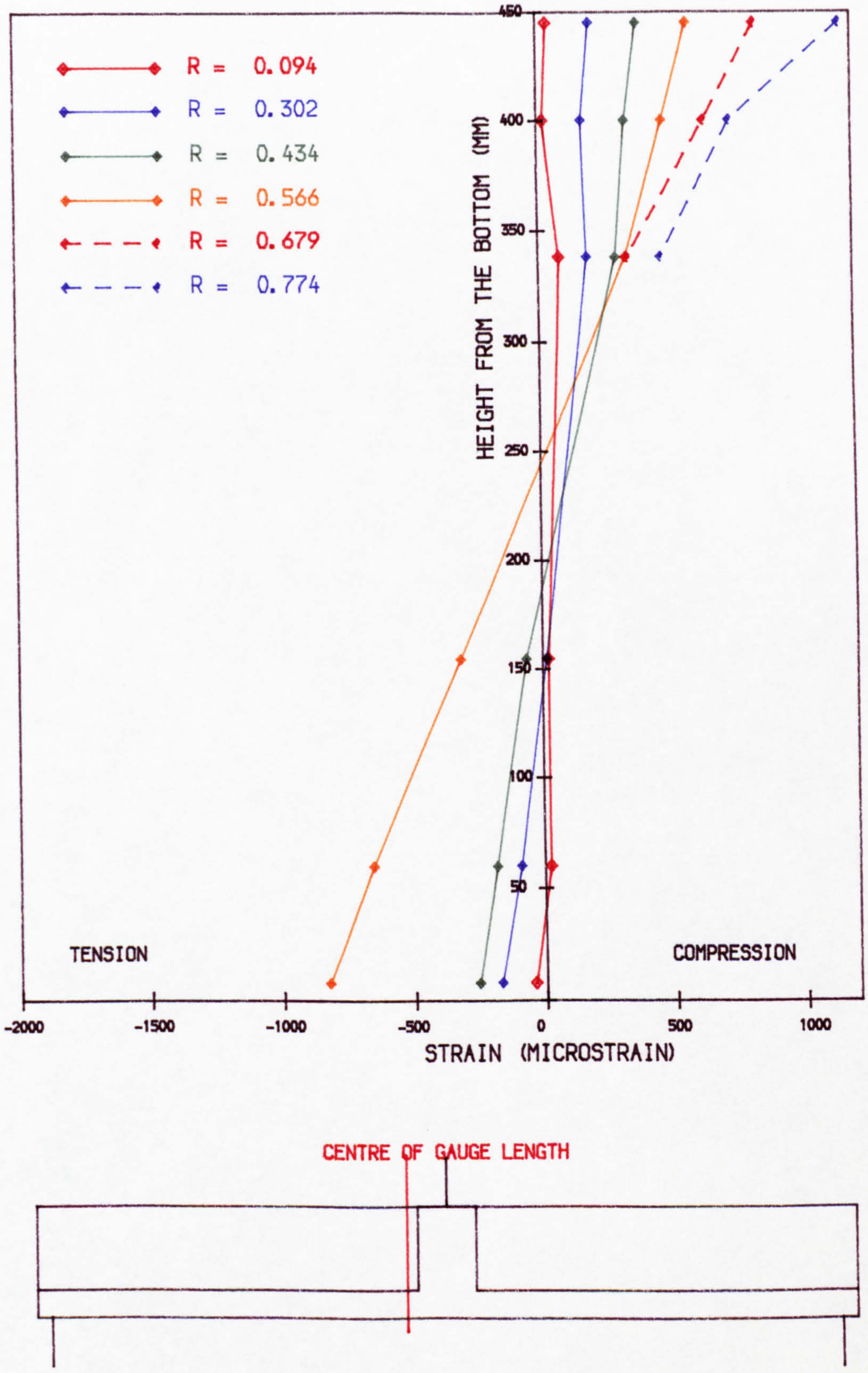

FIG. 6.22 : STRAIN DISTRIBUTION ACROSS CONCRETE SECTION

BEAM A-3 (250 MM FROM THE CENTRE) A-3-1

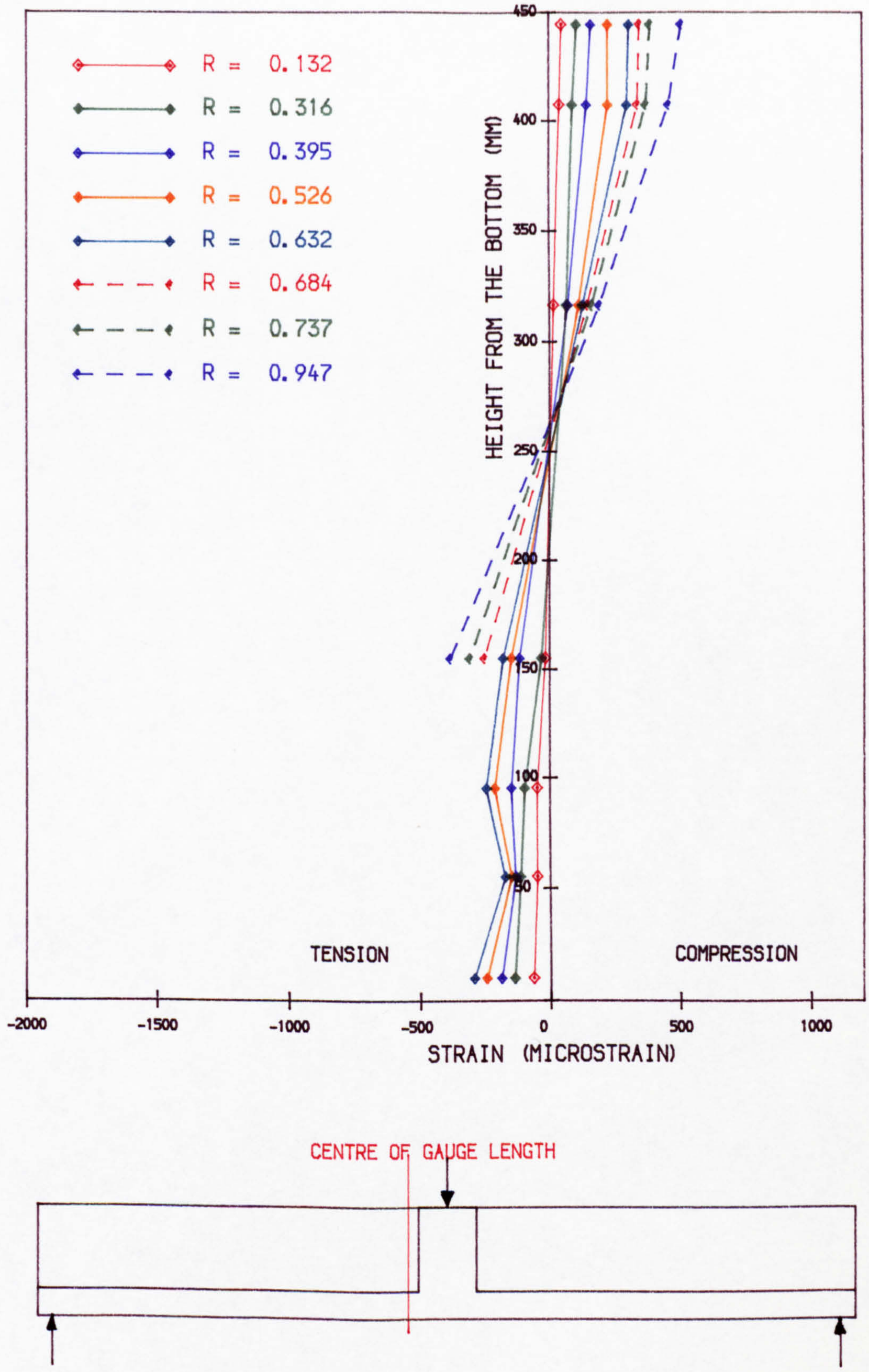

FIG. 6.23 : STRAIN DISTRIBUTION ACROSS CONCRETE SECTION

BEAM A-2 (700 MM FROM THE CENTRE) A-2-1

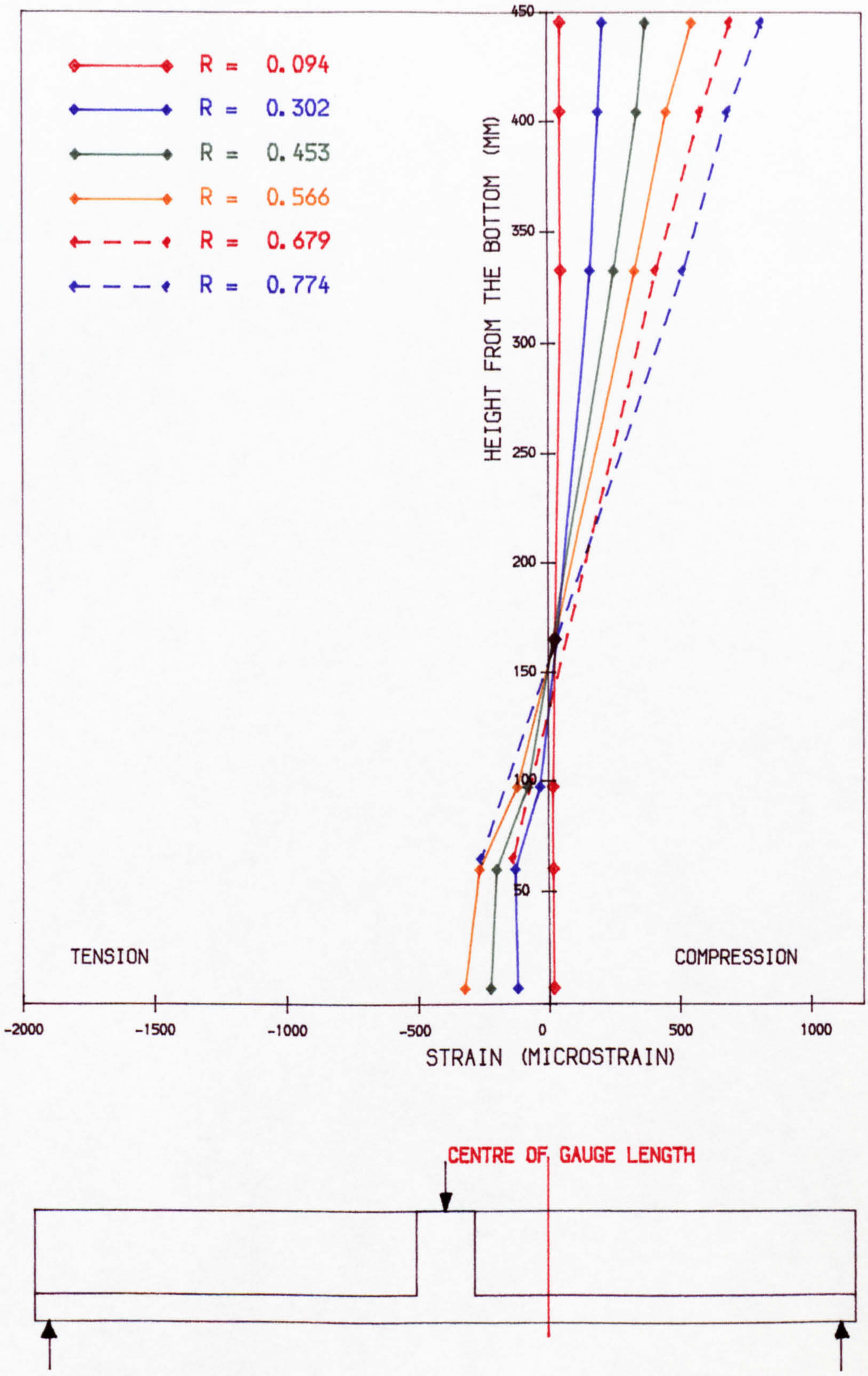

FIG. 6.24 : STRAIN DISTRIBUTION ACROSS CONCRETE SECTION

BEAM A-3 (700 MM FROM THE CENTRE) A-3-2

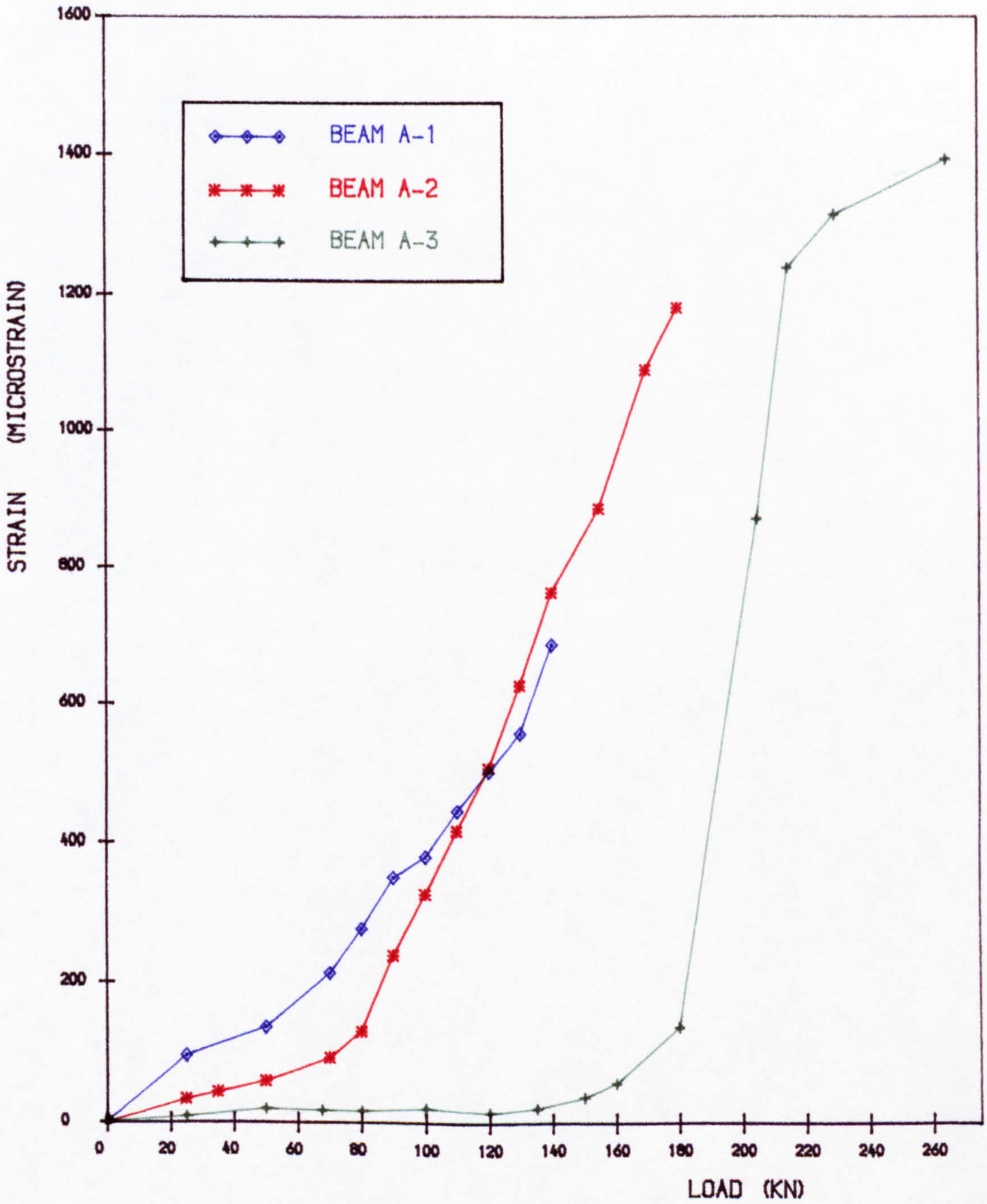

FIG. 6.25 : VARIATION OF STIRRUP STRAIN WITH LOAD IN BEAM A-1, A-2 AND A-3

CHAPTER 7

SHEAR STRENGTH OF COMPOSITE BEAMS

7.1 General

Shear strength of composite beams has received comparatively little attention from the research workers compared to monolithic reinforced and prestressed concrete beams. Due to this lack of experimental results on shear strength of composite beams, no clear design procedure has been developed for the design of composite beams for vertical shear. Also, the guidance given in codes of practice is inadequate. As shear failure is to be avoided due to its sudden and violent nature, insufficient design information on the shear strength causes great concern in the design of composite beams consisting of thin webbed precast beams with a top slab.

Although the horizontal shear strength at the interface between the top slab and the beam is equally as important as the vertical shear, it has received considerable attention in the past and the design clauses in the codes provide sufficient guidance to ensure that the bond between the two elements is adequate. Therefore more attention will be given to vertical shear in composite beams in this chapter, where the theoretical background for the analysis and understanding of the results of the shear test series (Series B) will be presented.

As most of the theories and analytical methods have been developed for monolithic beams, some of the most widely used theories and design procedures for monolithic prestressed beams will be discussed briefly as a useful reference for composite beams.

7.2 Shear Tests of Composite Beams

Of the very few experimental investigations reported on the shear

strength of composite beams [23,61-65], only Mattock and Kaar [23] have studied the shear strength of continuous composite beams in the hogging moment regions. (A review of this study was given in Chapter 2). In other tests, composite sections were mainly subjected to sagging moments.

Olesen et al [61] reported the results of shear tests of composite beams carried out at the University of Illinois as a part of an extensive experimental investigation on the shear strength of prestressed beams. Ten 1/3-scale composite beams were tested to fail in shear. Based on these results, they proposed an equation to determine the shear strength of sections uncracked in flexure in which the principal tensile stress criterion was examined. Also, an empirical equation to calculate the shear strength of sections cracked in flexure was proposed. In both expressions dead load effects were separated from the live load effects so that they could be easily applied to the composite beams.

In an experimental investigation carried out at the University of Leeds, Bennett[62,63] tested six composite beams in two series. The first series was intended to study the adequacy of design methods for the draft of CP 110: (1972) while in the second series, the effects of different stirrup shapes were investigated. The results for the beams in the first series, which contained shear reinforcement, showed that the methods given in the draft code were conservative in predicting the shear strength of composite beams. It was also found that the concept of considering the total shear strength of prestressed beams as the sum of the shear forces resisted by the concrete and the shear reinforcement was satisfactory.

Clarke and Evans [64] carried out a series of tests on composite beams to study the accuracy of CP 110 and BS 5400 in which the design clauses for monolithic prestressed beams are also recommended for composite beams. Two types of composite beams, one with rectangular precast beams and the other with I-section precast beams were tested. Tests indicated that both codes were

conservative in predicting the inclined cracking load. They also found that the beams tested had a considerable reserve capacity after inclined cracking although the codes treat the inclined cracking at the ultimate limit state.

In an another experimental investigation, Tay [65] carried out three test series on simply supported full size composite beams to study the shear behaviour under static loading, repeated loading and also for beams with deflected tendons. In the first series the level of prestress in the precast beams and the percentage of shear reinforcement were varied. The results of the tests were compared with the shear strengths calculated according to various codes of practice. Tay found that the superposition method (see Section 7.9.2) predicted the web shear cracking load with reasonable accuracy. For ultimate shear strength, the above method and CP 110 method were found to be conservative for beams with high prestress levels while they became slightly unsafe for beams with low levels of prestress. The superposition method gave the best agreement for the web crushing strength and the CEB-FIP method was found to be very conservative. The ultimate strength of beams was also compared with those calculated using plastic methods. Plastic methods gave reasonably good predictions only for beams with high percentages of shear reinforcement.

A more detailed review of the experimental studies mentioned above has been given by Tay [65].

7.3 Inclined Cracking In Concrete Beams

Shear failure of concrete beams is considered to occur after the development of inclined cracks in the beam. These inclined cracks are of two types, web shear cracks and flexure shear cracks.

Web shear cracks appear in the web or mid-depth of beams in regions which are not previously cracked in flexure [66,67], and are caused by the

development of high principal stresses in the web. Therefore these occur in the parts of the beam where shear stresses are high but flexural effects are small, and are more common in prestressed beams with thin webs and short shear spans[66,67,68].

Flexural shear cracks occur due to the combined effect of shear and flexure in regions where flexural effects are more significant than the principal tensile stresses in the web [66]. These cracks develop from vertical flexural cracks which then propagate as inclined cracks due to the shear stresses in the region. It is also possible for an inclined crack to merge with an already existing flexural crack. They are more common in reinforced concrete beams than in prestressed concrete beams as flexural cracks develop early in reinforced concrete beams, and are also more likely to occur in beams with a higher shear span to effective depth ratio (from about 3.0 to 6.0) and with thick webs.

It is possible that both types of inclined cracks can appear in the same beam in different regions[69]. Like flexural cracking, inclined cracking results in a significant change in the behaviour of the beam [70]. When shear reinforcement is provided, it causes the strains in the shear reinforcement to increase rapidly. Up to inclined cracking load, the stresses in the beam can be determined using elastic theory, but after inclined cracking, stress redistribution takes place in the beam making the post-cracking analysis very complicated. Various analogies and mechanisms have been suggested to explain the behaviour of beams after inclined cracking, and some of these will be discussed later in this chapter.

7.3.1 Analysis for Web Shear Cracking Load

Determination of the web-shear cracking load is generally based on the principal tensile stress concept [61,66,67]. Web shear cracks develop in a concrete beam when the maximum tensile stress in the beam exceeds the tensile

strength of concrete. Theoretically, to determine the web shear cracking load V_{co}, it is necessary to check principal tensile stresses at different levels to find the location of the maximum stress. As this is too tedious for general use, it can be assumed that the maximum principal tensile stress occurs at the centroid of the beam section.

The principal tensile stress equation is derived by considering an element in a monolithic beam subjected to bending and shear as shown in Fig. 7.1. f_x and f_y are the direct stresses acting on the element in horizontal and vertical directions while v is the shear stress. The stress conditions in any direction can be found by resolving forces in two directions or by Mohr's circle. The Mohr's circle for the stress system considered is also shown in Fig. 7.1. The principal tensile stress f_1 and principal compressive stress f_2 are given by

$$f_1, f_2 = 0.5(f_x+f_y) \pm 0.5 \sqrt{(f_x-f_y)^2 + 4 v^2} \qquad \text{.....Eqn. 7.1}$$

(Tensile stresses are considered positive)

The inclination (θ)of the plane of the principal tensile stress is given by,

$$\text{Tan } 2\theta = 2 v / (f_x - f_y) \qquad \text{.....Eqn. 7.2}$$

When Eqn. 7.1 is applied to a prestressed beam at the centroid, f_x and f_y become the horizontal and vertical prestress at the centroid. As prestressed beams generally have only a horizontal prestress f_{cp}, the principal tensile stress becomes,

$$f_1 = - 0.5 f_{cp} + 0.5 \sqrt{(f_{cp}^2 + 4 v^2)} \qquad \text{.....Eqn. 7.3}$$

As seen from the Mohr's circle (Fig. 7.1), it is possible to make both principal stresses compressive by applying a vertical prestress of appropriate magnitude [71,72]. However due to the practical problems associated with applying a vertical prestress, it is used only in special cases [71].

The Eqn. 7.3 can be rewritten as,

$$v = \sqrt{f_1^2 + f_1 f_{cp}} \qquad \text{.....Eqn. 7.4}$$

Inclined cracking is assumed to occur when f_1 reaches the tensile strength of concrete f_t. Therefore, the shear stress corresponding to the inclined cracking is obtained by substituting f_t for f_1.

The shear stress due to any applied shear force can be obtained from the basic elastic theory equation,

$$v = V (Ay) / I b \qquad \text{.....Eqn. 7.5}$$

where (Ay) is the first moment of area of concrete above the centroid.

Therefore the inclined cracking load V_{co} can be obtained by substituting for v in Eqn. 7.4.

$$V_{co} = (I\ b\ /(Ay))\ \sqrt{f_t^2 + f_t f_{cp}} \qquad \text{.....Eqn. 7.6}$$

For rectangular sections, $Ib/(Ay) = 0.67\ b\ h$

Therefore, $$V_{co} = 0.67\ b\ h\ \sqrt{f_t^2 + f_t f_{cp}} \qquad \text{.....Eqn. 7.7}$$

The above equation forms the basis for the British codes[27,28] to calculate V_{co} for both rectangular and non-rectangular beam sections. Ib/(Ay) for I sections is greater than 0.67 (about 0.80) and therefore the above expression tend to be conservative for such beams. However, the location of maximum principal stress moves towards the junction between the web and flange in I beams and thus these two effects tend to compensate each other [38,73]

In a reinforced concrete members, both f_x and f_y in Eqn. 7.1 are zero at the centroid. Therefore both principal tensile stresses, f_1 and f_2 are equal to the shear stress v, and the angle of inclination of the principal tensile stress is 45^0. In prestressed concrete beams this angle is less than 45^0 due to the added influence of prestress.

In the above derivation of V_{co}, the effects of point loads or reactions at the supports were neglected. The compressive stresses induced by these loads tend to reduce the principal tensile stress.

The value of f_t to be used in the calculation is speculative. Olesen [61] suggested that splitting tensile strength is a good representation of the tensile stress which cause the web shear cracking and recommended that f_t is taken as $0.415\ \sqrt{f_c'}$.

In British codes[27,28], f_t is taken as $0.36\sqrt{f_{cu}}$ (without safety factors) and American codes[35,39] recommend that the maximum principal tensile stress must be limited to $0.33\sqrt{f_c'}$. Tay [65] found that British codes value for f_t and the use of measured splitting tensile strength tended to slightly overestimate the web shear cracking load in composite beams.

7.3.2 Determination of Principal Stresses in Prestressed Concrete Beams

The actual location of the maximum principal tensile stress at a section of a prestressed concrete beam depends on the magnitude of shear force and bending moment, and also the prestress distribution at the section. Therefore its vertical position in a beam section can vary along the shear span [65,72,74]. If V_{co} is to be calculated accurately without using the code equations, it is necessary to find the maximum principal tensile stress at different sections.

7.3.2.1 Calculation of Principal Stresses in a Beam Section under Applied Loading

The principal stresses at a particular point in a prestressed concrete

beam under a particular load can be calculated using Eqn. 7.1 given for the stress system shown in Fig. 7.1. At a point away from the centroid, f_x is equal to the resultant stress due to prestress and the stress due to applied bending moment, and the shear stress v can be calculated from Eqn. 7.5.

7.3.2.2 Determination of Principal Stresses Using Strain Rosettes

As the principal stresses cannot be measured directly, the most convenient method of obtaining the principal strains in experimental work is to use strain rosettes to measure strains at a point in three directions. Normally, these three directions are chosen to be the horizontal, vertical and 45^0 inclined direction.

Considering a strain system similar to the stress system shown in Fig. 7.1, it is possible to express direct strain in any direction as

$$\varepsilon_1 , \varepsilon_2 = 0.5(\varepsilon_x + \varepsilon_y) \pm 0.5 \sqrt{(\varepsilon_x - \varepsilon_y)^2 + \gamma_{xy}^2} \quad \text{.....Eqn. 7.8}$$

The three strains ε_x, ε_y and γ_{xy} can be obtained from the three strain readings of the rosette. The strains in horizontal, vertical and 45^0 directions are denoted by ε_0, ε_{90} and ε_{45}. The procedure of determining the principal strain from strain rosette readings has been given in some detail in References 11, 65 and 74.

The principal tensile strain ε_1 and the principal compressive strain ε_2 are given by

$$\varepsilon_1 , \varepsilon_2 = 0.5(\varepsilon_0 + \varepsilon_{90}) \pm 0.5\sqrt{(\varepsilon_0 - \varepsilon_{90})^2 + (\varepsilon_0 + \varepsilon_{90} - 2\,\varepsilon_{45})^2} \quad \text{..Eqn.7.9}$$

The principal tensile stress f_1 and principal compressive stress f_2 can be

calculated from ε_1 and ε_2 using the basic elastic theory equations.

$$f_1 = (\varepsilon_1 + \nu\, \varepsilon_2)\, E_c / (1- \nu^2) \qquad \text{.....Eqn. 7.10}$$

and $$f_2 = (\varepsilon_2 + \nu\, \varepsilon_1)\, E_c / (1-\nu^2) \qquad \text{.....Eqn. 7.11}$$

In the above equations, the strain due to prestress and its Poisson's ratio effect must be included in the three strain readings.

7.3.3 Factors Affecting Principal Stresses in the Web

7.3.3.1 Effects of Reactions or Point Loads

The compressive stresses induced in the beam by the point loads or reactions at the supports reduce the principal stress in the vicinity of such loads and therefore increase the web shear cracking strength. Olesen et al [61] found that these effects were not significant beyond 0.75 times the overall depth from the point loads. Tay[65] also observed similar effects from the principal tensile strain measurements made on composite beams. The increased shear strength of the concrete beams due to the point loads close to the supports has been included in the design codes[27,40,41].

7.3.3.2 Shear Span / Effective Depth Ratio

The shear span to effective depth ratio (a_v /d) is considered to have a considerable influence on shear behaviour of concrete beams and failure modes. Its effects on prestressed concrete has been investigated by many researchers[23,74,76-79]

Arthur et al [76] found that web shear cracking strength increased with the reduction of av/d ratio when it is less than 3.0. Increase in web shear

cracking load with the reduction of a_v/d ratio has also been reported by Mattock and Kaar[23] an Elzanaty et al[79]. Balasooriya[74,75] found that web shear cracking load was not greatly affected by the shear span to effective depth ratio.

The shear span to effective depth ratio also influences the principal stress distribution in the shear span as it is an indicator of the relative magnitudes of flexural and shear effects. Tay [65] explained the influence of the shear span assuming that an imaginary inclined compressive force exists between the support and nearest point load along the line joining the two points. Its effect on principal stress distribution is greater when the shear span/effective depth ratio is small (less than 3.0).

7.3.4 Location of Critical Principal Tensile Stress in the Shear Span

From Eqn.7.1 it can be seen that the principal tensile stress will be maximum where the shear stress is high and the horizontal compressive stress is small. Mlingwa [72], after analysing the principal tensile stresses at different sections in the shear span of simply supported prestressed I beams, found that the location of the maximum principal tensile stress varied from the top of the web near the support to the base of the web near the loading point. He found that the principal tensile stress was maximum at the centroid in the region of the centre of the shear span. Tay[65] also observed similar variation in simply supported composite beams.

The reason for the occurrence of maximum principal tensile stress at the top of the web near the supports is that the flexural effects are small in this region and the prestress reduces at a greater rate than the shear stress when above the centroid. Therefore principal tensile stress becomes critical at the top of the web near the support at about 3/4 of the beam depth away from it (due to

the influence of bearing stresses). Near loading points, higher tensile stresses due to bending moment reduce the prestress at the base of web making it the critical point for principal tensile stress.

Continuous composite beams, at the interior supports, are subjected to both high shear forces and bending moments. As hogging moments reduce the prestress in the upper part of the web, the top of the web will have the maximum principal tensile stress near to the support. However the bearing stresses at the support will tend to reduce the principal stresses at sections very close to the support.

7.3.5 Analysis for Flexural Shear Cracking Load

Flexural cracking load is considered as the sum of the shear force required to cause flexural cracking and the additional shear force required to make any vertical cracks propagate as an inclined crack. It is difficult to determine the latter theoretically due to the complexity of stresses at the tip of the flexural crack under combined bending and shear. Therefore, empirical expressions are used to determine the flexural shear strength V_{cr}.

Tests on prestressed concrete beams have shown that the initiating flexural crack appears at a distance of approximately half the effective depth from the section under consideration. Therefore, flexural effects for the flexural shear strength calculation can be considered a distance of d/2 away from the section in the decreasing moment direction[61,80].

Sozen and Hawkins [82] reported that the following empirical equation would be a safe lower bound solution for V_{cr} after reviewing the recommendations of ACI-ASCE Committee 326 [70] and the existing test results.

$$V_{cr} = 0.6\, b\, d\, \sqrt{f_c'} + M_{cr} / (M/V - d/2) \qquad \text{.....Eqn. 7.12}$$

Olesen[61] proposed a similar expression in which dead load and live load

effects were separated and the first term was $bd\sqrt{f_c'}$.

The above equation has become the basis for expressions given in both British and American codes. By ignoring the d/2 term, replacing f_c' with $f_{cu,}$ and applying a partial safety factor of 1.5, the following expression given in CP 110[45] and BS 5400 [27] can be obtained[38].

$$V_{cr} = 0.037\ b\ d\ \sqrt{f_{cu}} + (M_{cr}/M)\ V \qquad \text{.....Eqn. 7.13}$$

The above formula has been derived from the results of tests on beams with a high prestress level (f_{pe} greater than $0.5f_{pu}$) and was thought to be not representative for all levels of prestress [73,83]. An alternative expression was thus developed to represent both reinforced and prestressed concrete beams. The flexural shear cracking load is considered as the sum of two terms A and B in which B is the shear force when flexural cracking occurs and A is the additional shear force required to develop a shear crack from the flexural crack. Assuming that shear behaviour of a prestressed beam after flexural cracking is similar to a reinforced concrete beam, term A is written as

$$A = (1 - n\ f_{pe} / f_{pu})\ v_c\ b\ d \qquad \text{.....Eqn. 7.14}$$

and the term B is taken as

$$B = M_o\ V / M \qquad \text{.....Eqn. 7.15}$$

where v_c = Shear strength of concrete given in the Code

M_o = Decompression moment related to the fibres at the level of centroid of steel

V and M are the design shear force and bending moment at the section under consideration.

By combining the two terms, V_{cr} can be written as

$$V_{cr} = (1-n\ f_{pe}/f_{pu})\ v_c\ b\ d + M_o\ V / M \qquad \text{.....Eqn. 7.16}$$

and this equation is considered to be applicable for all levels of prestress[38,73].

The above equation gives $V_{cr}=v_c bd$ for a reinforced concrete beam in which f_{pe} and M_o are zero. In order for this equation to agree with Eqn. 7.13 at higher levels of prestress($0.6f_{pu}$), the value of n is taken as 0.55. This equation with the above value of n, and M_o as the decompression moment of the extreme tension fibres is given in BS 8110 for all classes of prestressed beams.

7.4 Shear Strength of Monolithic Prestressed Concrete Beams

The approach of calculating the shear capacity of the concrete in prestressed concrete beams given in British and American codes [27,28,35,39] are similar except for the differences in the formulae used. Shear is considered at the ultimate limit state, and the shear strength of concrete uncracked in flexure (web shear cracking load) and shear strength of concrete cracked in flexure (flexural shear cracking load) are calculated separately for a given section, with the smaller value being taken as the shear capacity provided by the concrete.

The vertical component of the prestressing force of the beams having inclined tendons is added to the web shear cracking load in both British and American codes. In CEB-FIP Model Code[40], shear strength of concrete is calculated from one equation regardless of whether the section is cracked in flexure or not.

7.4.1 British Codes -BS 5400: Part 4[27] and BS 8110[28]

For prestressed concrete beams, the shear strength of a section uncracked in flexure V_{co} is calculated using the following equation which was based on the principal tensile stress equation (Eqn. 7.7).

$$V_{co} = 0.67\, b\, h\, (\, f_t^2 + 0.8\, f_{cp}\, f_t\,)^{0.5} + V_p \qquad \text{.....Eqn. 7.17}$$

The tensile strength of concrete f_t is taken as 0.24 $\sqrt{f_{cu}}$ which includes a safety factor. To have similar factors in both terms f_{cp} is multiplied by a factor of 0.8 (In the BS 5400 expression, this factor is taken as 0.87.) V_p is the vertical component of the prestressing force of inclined tendons.

The shear strength of prestressed concrete sections cracked in flexure, V_{cr}, is given in BS 8110 by Eqn. 7.16.

In BS 5400, Eqn 7.13 is given for Class 1 and Class 2 members while Eqn. 7.16 is to be used to calculate V_{cr} of Class 3 prestressed members.

V_{cr} calculated using Eqn. 7.13 or 7.16 is considered to be constant for a distance equal to half the effective depth measured in the direction of increasing moment.

The shear capacity of concrete is then taken as the lesser of V_{co} and V_{cr}.

7.4.2 American Codes - ACI 318-83[35] and AASHTO [39]

The expressions given in both codes for shear strength of prestressed concrete beams are the same. Web cracking load V_{cw} is based on limiting the principal tensile stress of concrete at the centroid to the tensile strength of concrete. The equation given in the Codes can be expressed in S.I. units as

$$V_{cw} = (0.29 \sqrt{f_c'} + 0.3 f_{cp}) b d + V_p \qquad \text{.....Eqn. 7.18}$$

Alternatively, V_{cw} can be obtained by limiting the principal stress at the centroid to 0.33 $\sqrt{f_c'}$.

A strength reduction factor(ø) of 0.85 is applied to the nominal shear strength obtained from the code equation. When ø is applied to 0.33$\sqrt{f_c'}$, it becomes equal to 0.28$\sqrt{f_c'}$ (or 0.25$\sqrt{f_{cu}}$).

The flexural cracking load, V_{ci}, of a prestressed beam is calculated from the following equation which is in S.I. units.

$$V_{ci} = 0.05 \sqrt{f_c'}\, b\, d + V_d + V_i\, M_{cr} / M_{max} \geq 0.14 \sqrt{f_c'}\, b\, d \quad \text{...Eqn.7.19}$$

where V_d = Shear force due to self weight

M_{cr} = Flexural cracking moment due to externally applied load

M_{max} = Maximum factored moment at the section due to externally applied load

V_i = Factored shear force due to applied load occurring simultaneously with M_{max}

The above equation resembles very closely the BS 5400 equation for Class 1 and Class 2 members.

7.4.3 CEB-FIP Model Code (40)

As previously mentioned, CEB-FIP Model Code does not consider web shear cracking and flexural shear cracking loads separately. Instead, the design shear strength of concrete V_{Rd1} is obtained using the following equation.

$$V_{Rd1} = \tau_{Rd}\, k\, (1 + 50\, \rho_l)\, b\, d\, \beta_1 \quad \text{.....Eqn. 7.20}$$

where τ_{Rd} = Shear strength of concrete given in the Code

$k = 1.6 - d\ (m) \geq 1.0\ m$

$\rho_l = A_s / b\, d \leq 0.02$

$\beta_1 = 1 + M_o / M_{sdu} \leq 2.0$

M_o = Decompression moment related to the extreme tensile fibres

M_{sdu}= Maximum design moment in the shear region under consideration

For checking design shear resistance of a beam with shear reinforcement, the CEB-FIP code specifies two methods, the Standard method and the Accurate method. The accurate method may be used for main girders of buildings and bridges, and also for beams subjected to combined bending and shear [84].

7.5. Behaviour of Beams After Internal Cracking

7.5.1 Shear Transfer Mechanisms of Cracked Beams

The large amount of research work on the shear strength of concrete beams has so far failed to produce an accurate rational theory or mechanism to analyse beams after inclined cracking. One of the main reason for this is that the beam is transformed into a complex indeterminate system after undergoing stress redistribution as a result of inclined cracking. However, the tests have shown that there are five main mechanisms which contribute to the shear transfer after shear cracking. These, which have been recognised by ACI-ASCE Committee 426[81], are as follows.

(a) Shear Stress in the Uncracked Concrete in the Compression Zone

(b) Aggregate Interlock

(c) Dowel Action

(d) Arch Action

(e) Shear Reinforcement

7.5.1.1 Shear Transfer by Uncracked Concrete Zone

After the development of inclined cracking, the uncracked concrete at the top of the crack continues to transfer a part of the applied shear force in addition

to carrying the flexural stresses. Its contribution depends on the depth of the uncracked zone. Investigations by Acharya and Kemp [85], Fenwick and Paulay[86] and Taylor [87] have revealed that the contribution of uncracked concrete zone could be between 20% and 40% of the total shear force.

7.5.1.2 Aggregate Interlock

It has been established by test results that shear is transferred across an inclined crack due to the friction of the crack surface which induces a tangential force. Tests on beams without shear reinforcement have shown that the contribution of aggregate interlock is between 30% and 50% [85,86,87]. As the magnitude of the shear force transmitted is influenced by the roughness of the surface, a smooth crack surface as that generally occur in high strength concrete may affect its contribution[80]. Also, its magnitude would decrease with the increase of the crack width[81].

7.5.1.3 Dowel Action

When shear cracks cross the main tensile reinforcement, a part of the shear force will be carried by the dowel action of the steel which resists the shear displacement. The shear force transferred by the dowel action is between 15% and 25% of the shear force [81,86,88]. Dowel action is limited by the tensile stresses developed in the concrete at the level of reinforcement. When these tensile stresses are high, splitting can occur along the steel [81].

7.5.1.4 Arch Action

After the development of inclined cracking, a simply supported beam can

be visualised as an arch which is tied at the bottom by the tension reinforcement. Any applied force is transferred as an inclined compressive force to the supports [81,86,89,90]. The appearance of tensile cracks at the top surface of the beam near the supports and the increase in the stresses in the longitudinal steel in excess of those predicted due to the flexural effects support the theory of arch action.

7.5.1.5 Web Reinforcement

Shear reinforcement is considered as the major factor which contributes to the shear capacity after inclined cracking. Results of a large number of tests have shown that shear reinforcement does not carry any significant force up to the inclined cracking load. Other than carrying the shear, web reinforcement contributes to the shear capacity of the beam by restraining the widening and propagation of inclined cracks and acting as anchors to the tension steel which carry shear by dowel action[70,81]. The determination of shear carried by the shear reinforcement will be discussed later in this chapter.

7.5.2 Shear Transfer Mechanisms of Prestressed Concrete Beams

Much of the experimental work to study the contributions of various mechanisms has been carried out on reinforced concrete beams. The contribution from aggregate interlock and dowel action to the shear transfer in prestressed beams is less than that in a reinforced concrete beam. As most prestressed beams have thin webs, the force transferred by aggregate interlock become smaller in these beams. Also the appearance of inclined cracks is delayed by the prestressing effect but these cracks widen more rapidly than in reinforced concrete beams, thereby reducing the force transmitted by aggregate interlock[81].

7.5.3 Modes of Failure of Beams in Shear

To study the shear strength of composite beams, a knowledge of failure modes of concrete beams in shear is very useful. The failure mode of beams in shear after inclined cracking depends on many factors such as shape of the member, amount of shear reinforcement, shear span/effective depth ratio, level of prestress in the beam etc. Only some of the more common types of failure will be discussed here.

7.5.3.1 Shear Compression

Shear compression failure occurs when inclined cracks propagate upwards into the compression zone of concrete and converge towards the loading point reducing the area to resist compressive stresses due to bending and shear. As a result, crushing of concrete occurs at the top [61,67,68,78,80,81]. This type of failure is more common in rectangular or thick webbed sections.

7.5.3.2 Diagonal Tension

In diagonal tension failure, which is normally associated with yielding of shear reinforcement, an inclined crack expands into both tension and compression faces of the beam causing failure. This occurs in thick webbed beams without reinforcement, or with a small amount of shear reinforcement, and with a shear span to effective depth ratio greater than 3.0 [81]. This type of failure is not desired as it is sudden and violent. It can occur immediately after the appearance of diagonal cracks if shear reinforcement is not provided [79,81].

7.5.3.3 Web Crushing

Thin webbed beams with smaller shear span/ effective depth ratios may fail due to high compressive stresses in the concrete between inclined cracks in the web [74,81]. This mode is related to prestressed concrete beams as they normally have thin webs. Web crushing failure is more gradual than diagonal tension. This mode of failure will be discussed in more detail with its design implications as the composite beams used in the experimental programme of this study had thin webbed precast beams.

7.5.4 Methods of Analysis of Beams after Inclined Cracking

Several analogies, such as arch analogy, truss analogy, frame analogy etc. have been used to explain the shear failure mechanisms of beams and to determine the ultimate shear strength. Of these, truss analogy is the most widely used as the geometry of the truss and its components can be defined more easily than the other analogies [67].

In arch analogy, as briefly mentioned in Section 7.5.1.4, a concrete beam is considered to be transformed into a system of tied arches as shown in Fig. 7.2. Kani [89] considered that the shear forces are transmitted by the external arch consisting of uncracked concrete and bounded by outermost inclined cracks, and also by the internal arches formed by the other inclined cracks. Due to the difficulty in defining the arch rib elements and in analysing the statically indeterminate tied arches, this analogy is not generally used to analyse beams for the ultimate strength[67].

Recently, considerable attention has been given to the use of plastic theory for the analysis of ultimate shear strength of reinforced concrete beams and good correlation between experimental and theoretical ultimate strengths has

been found[92,93,94]. Applying the theory of plasticity, it has to be assumed that concrete and steel are rigid, perfectly plastic materials.

Only the truss analogy which is used in codes of practice to determine the shear reinforcement requirements will be discussed here.

7.5.4.1 Classical Truss Analogy

The classical form of truss analogy which was developed by Ritter and Morsch more than 80 years ago idealised a concrete beam with inclined cracks into a statically determinate truss with parallel chords and web members at constant inclination[67,70,81]. The tension and compression chords of the truss are represented by the main tensile reinforcement and the concrete compression zone while the concrete in between inclined cracks formed the compression web members. The shear reinforcement is considered as the tension members of the web. A part of a cracked beam idealised as a truss is shown in Fig. 7.3.

In the classical truss analogy, the contribution to the shear from uncracked concrete zone, aggregate interlock and dowel action is ignored, and the total shear force is assumed to be carried by the shear reinforcement.

If it is assumed that the angle of inclination of inclined cracks is 45^0 to the horizontal, the shear force carried by vertical stirrups can be expressed as

$$V_s = (A_{sv} / s_v)\, f_v\, b\, d \qquad \text{.....Eqn. 7.21}$$

where f_v is the stress in the stirrup.

In prestressed concrete beams the angle of inclination of inclined cracks will be less than 45^0. Considering a general case in which cracks are inclined at an angle α and stirrups are inclined at angle θ to the horizontal, V_s can be expressed as,

$$V_s = (A_{sv}/s_v)\, f_v\, b\, d\, \mathrm{Sin}^2 \alpha\, (\mathrm{Cot}\,\theta + \mathrm{Cot}\,\alpha) \qquad \text{.....Eqn. 7.22}$$

7.5.4.2 Modified Truss Analogy

Experimental results have shown that the assumption in the classical truss analogy that the total shear force is carried by the shear reinforcement is not correct. Several modifications have been proposed to take into account of the shear carried by the concrete [95]. In the modified truss analogy which is used in design codes is considered as the sum of shear forces resisted by concrete and shear reinforcement [81].

$$V_u = V_c + V_s \qquad \text{.....Eqn. 7.23}$$

where Vc is the shear carried by concrete and Vs is the shear carried by shear reinforcement which is calculated using Eqn.7.21 or Eqn. 7.22.

7.6 Shear Resistance of Web Reinforcement According Current Design Codes

According to codes of practice [27,28,35,39,40] the total shear capacity of beams with shear reinforcement is considered to be the sum of shear force carried by the concrete V_c and the shear force carried by the shear reinforcement V_s. The latter is calculated using the truss analogy which was described in the previous section. In British and American codes, the shear carried by vertical stirrups is given by

$$V_s = A_{sv} f_{yv} d/ s \qquad \text{.....Eqn. 7.24}$$

where A_{sv} and f_{yv} are the area and yield stress of shear reinforcement and s is the spacing of stirrups.

When the Accurate method of CEB-FIP Model Code in which the angle of inclination of struts ø is allowed to vary between 31^0 and 59^0 is used, V_s is given

as

$$V_s = (0.9 A_{sv} f_{yv} d / s) (Cot \phi) \quad \text{.....Eqn. 7.25}$$

When the shear force due to design loads V_u is greater than V_c, shear reinforcement is designed to carry the difference. However, it is desired that at least a minimum amount of shear reinforcement is provided even when V_c is greater than V_u. Shear failure of beams without any web reinforcement is sudden and provision of even a small amount of shear reinforcement is considered to improve ductility and the shear capacity of the beam[73,80]. The minimum amount of shear reinforcement to be provided in cases when V_u is less than V_c is given in codes. Also codes specify maximum spacing of stirrups which is generally 0.75 times effective depth or overall depth. For high shear forces, this limit is reduced. The limit to the stirrup spacing is to ensure that any potential inclined crack will be crossed at least by one stirrup.

7.6.1 Minimum Area of Shear Reinforcement

According to BS 5400 and BS 8110, the minimum shear reinforcement to be provided in prestressed beams is

$$A_{sv} = 0.4 b s / 0.87 f_{yv} \quad \text{.....Eqn. 7.26}$$

ACI Building Code and AASHTO Standards specify that the minimum area of shear reinforcement in prestressed beams should be the smaller value of

$$A_{sv} = 0.35 b s / f_{yv} \quad \text{.....Eqn.7.27(a)}$$

and $$A_{sv} = (A_p/80) (f_{pu}/f_{yv}) (s/d) (d/b)^{0.5} \quad (\text{if } f_{pe}/f_{pu} \geq 0.40)$$

.....Eqn. 7.27(b)

The minimum area of shear reinforcement given in CEB-FIP Code is

$$A_{sv} = 0.0015 b s \quad \text{.....Eqn. 7.28}$$

7.7 Web Compression Failure and Maximum Allowable Shear Stresses in Beams

Web compression failure in which concrete between the inclined cracks in the web fails in compression is one of the common failure modes in shear of prestressed concrete beams with thin webs and high percentage of shear reinforcement. It could occur in composite beams which normally consist of two stiff top and bottom flanges and thin web such as those used in the laboratory investigation of this study.

Web crushing is considered as the upper limit to the shear capacity of beams beyond which the increase of shear reinforcement is not effective. In design codes, the maximum shear stress for prestressed beams limited by the web crushing is given as a function of the concrete strength. A brief review of the the web crushing failure of prestressed beams would be appropriate here to understand the behaviour of composite beams tested to fail in shear in this study.

Very little direct research has been done to investigate web crushing failure. However, web crushing has often been reported by investigators who carried out shear tests of reinforced, prestressed and composite beams[11,23,65,74]. Clarke and Taylor[96] carried out a detailed review of the published test results of beams failing in this mode. They reported that the percentage of tensile reinforcement and shear span/effective depth ratio had some influence on web crushing strength while the level of prestress did not show any significant influence. The tensile steel percentage tended to increase the web crushing load. For small shear spans, the web crushing strength showed an increase when the shear span/effective depth ratio was reduced. However they found that the test data available was not sufficient to derive any definite relationship. Balasooriya [74] carried out a series of tests on thin webbed

prestressed beams and found that the compressive stress in the web at web crushing was about $0.74f_{cu}$ [75].

Two factors which were found to have considerable influence on the web crushing stress are the inclination of shear reinforcement and the presence of ducts in the web of post-tensioned beams. Leonhardt and Walther [97] found that a beam with inclined stirrups failed in web crushing at a higher load than a beam with vertical stirrups. This has been adopted by CEB-FIP Code in specifying the maximum limit for the contribution of stirrups to the shear strength of beams. Leonhardt also recommended that an effective width of the web allowing for the diameter of ducts must be used to calculate the web crushing load. He suggested that the diameter of ducts if ungrouted or two third of diameter of ducts if grouted must be deducted from the actual width of the web. Clarke and Taylor[96] supported these recommendations after after an experimental investigation.

7.7.1 Provisions for Maximum Shear Stresses in Concrete Beams in Current Design Codes

The maximum shear stresses based on the web crushing stress are given in various design codes as the maximum allowable overall shear stress applied to the beam or the maximum allowable contribution from shear reinforcement to shear capacity.

7.7.1.1 British Codes [27,28]

According to BS 5400: Part 4[27] and CP 110[45]which has now been withdrawn, the maximum allowable shear stress in the beam v_{max} is given as

$$v_{max} = 0.75\sqrt{f_{cu}} \leq 5.8 \ N/mm^2 \qquad \text{.....Eqn. 7.29}$$

In BS 8110, a slightly different value is specified.

$$v_{max} = 0.8\sqrt{f_{cu}} \leq 5.0 \ N/mm^2 \qquad \text{.....Eqn. 7.30}$$

From the value of v_{max} , the maximum shear force V_{max} is calculated.

$$V_{max} = v_{max}\, b\, d \qquad \text{.....Eqn. 7.31}$$

where b and d are web width and effective depth respectively. Although any modification to web width for the presence of ducts in the web has not been specifically stated in BS 8110, it is recommended in BS 5400 and the Handbook to BS 8110 [29] that the diameter of ungrouted ducts and two third of diameter of grouted ducts must be deducted from the actual web width in the calculations using Eqn.7.31. This is in agreement with the recommendations of Clarke and Taylor[96].

7.7.1.2 American Codes [35,39]

Both ACI Building Code [35] and AASHTO [39] specifications for maximum shear carried by shear reinforcement V_s are the same. Maximum V_s is limited to

$$V_s = 8\sqrt{f_c'} \ \text{(psi)} = 0.664\sqrt{f_c'} \ \text{(S.I. units)} \qquad \text{.....Eqn. 7.32}$$

No reduction in web width for post tensioning ducts is mentioned. The maximum shear force that can be carried by a prestressed beam section is therefore given as

$$V_{max} = V_c + 0.66\sqrt{f_c'}\ b\, d \qquad \text{(S.I. units)} \qquad \text{.....Eqn. 7.33}$$

where V_c is the shear carried by concrete.

7.7.1.3 CEB-FIP Model Code [40]

In the Standard and Accurate methods given in the Model Code, the following values for maximum shear force (V_{Rd2}) are given .

$$V_{Rd2} = 0.30\, f_c'\, b\, d \qquad \text{(Standard Method)} \qquad \text{.....Eqn. 7.34}$$

and $$V_{Rd2} = 0.30\, f_c'\, b\, d \sin 2\theta \qquad \text{(Accurate Method)} \qquad \text{.....Eqn. 7.35}$$

where $3/5 \leq \cot\theta \leq 5/3$

The Code requires that the width of the web must be modified to $(b_w - 0.5\Sigma\phi)$ when the diameter of bars or tendons (ϕ) exceeds $b_w/8$.

7.8 Effect of Inclined Tendons on Shear Strength

In current codes of practice[27,28,35,39], it is considered that the vertical component of the prestressing force of inclined tendons contributes to the shear strength of prestressed beams. However, this increase is limited to the web shear cracking strength only. The vertical component of the inclined prestressing force is added to V_{co}. Flexural shear cracking load is considered to be adversely affected by inclined tendons and therefore no increase is allowed.

There have been several investigations into the effects of inclined tendons on the shear strength [65,66,98]. Test results reported by MacGregor et al[66] indicated that web shear cracking load increased when the tendons were inclined and the increase attributed to the inclined tendons was equal to the vertical component of the prestressing force. In beams that developed flexural shear cracks, the inclined cracking strength decreased with the increase in the inclination of tendons. It was observed that the initiating flexural crack developed at a smaller load and splitting occurred along the reinforcement. And also, the beams with inclined tendons tended to fail more in flexural shear than in web shear. These findings seemed to be the basis behind the treatment of inclined prestressing force in design codes. From a recent experimental investigation, Tay[65] concluded that the current design procedure of adding vertical component of the inclined prestressing force is satisfactory and the inclusion of it in flexural

shear may lead to unsafe predictions.

7.9 Shear Strength of Composite Beams

7.9.1 Monolithic Section Method

The most commonly used approach to design of composite sections in vertical shear is to treat them as monolithic sections and use the design clauses given for monolithic beams. This method is recommended by most major design codes where it is assumed that the total shear force is carried by the monolithic section.

A problem arises as to which section - precast section or composite section, should be considered as the appropriate monolithic section. It can be argued that the precast section should be considered as the shear is mainly resisted by the precast beam. Also in composite beams with a reinforced slab subjected to hogging moments, the slab may be ineffective in resisting forces due to cracking, and it has thus been suggested that only the precast section should be considered.

The arguments in favour of considering the entire composite section in carrying the shear forces is that both precast beam and the top slab behave compositely if the bond between the two elements is adequate. Also when the slab is cracked, it still contributes to the shear resistance by dowel action and aggregate interlock at the cracks. Therefore it is thought to be too conservative to consider only the precast section.

7.9.2 Method of Superposition

This method given in the Department of Transport Technical Memorandum BE 2/73[99] considers the two stage loading to which the actual composite bridge

beams are subjected. In the first stage, the precast section carries the self weight of the precast beam and the top slab. In the second stage, after the development of composite action, the overall section carries the loads applied subsequently such as superimposed dead loads, live loads etc. The effects of shear in either stage is determined by using the monolithic section approach to the particular section effective at the time. The overall shear capacity is then determined by superimposing the effects of these two stages as with bending moments.

The shear capacity of concrete in a composite section uncracked in flexure can be expressed as

$$V_{co} = V_1 + V_2 + V_p \qquad \text{..... Eqn. 7.36}$$

Where V_1 is the shear force carried by the precast section alone before the development of composite action and V_2 is the shear force due to loads applied in the second stage. The magnitude of V_2 is determined by limiting the resultant principal tensile stress at the composite centroid to the tensile strength of concrete f_t. The vertical component of the prestressing force of inclined tendons is also added to V_{co}.

To determine V_2, the shear stress at the composite centroid due to shear force applied to the precast section V_1 is calculated using elastic theory.

$$v_1 = V_1 (Ay)_p / I_p b_p \qquad \text{.....Eqn. 7.37}$$

where $(Ay)_p$ = first moment of area of that part of the precast beam above the level of centroid of composite section.

I_p = second moment of area of precast section

b_p = width of the web of precast section

The additional shear stress v_2 in the composite section, at its centroid,

due to loads in the second stage, is limited by the principal tensile stress not exceeding f_t, given by the equation

$$f_t = f_{cp}/2 + \sqrt{(f_{cp}/2) + (v_1 + v_2)^2} \quad \text{.....Eqn. 7.38}$$

where f_{cp} is the longitudinal stress at the composite centroid due to prestress and the stress due to bending moment M_1 which is associated with V_1.

Therefore, v_2 can be expressed as

$$v_2 = \sqrt{f_t + f_{cp}\, f_t} - v_1 \quad \text{.....Eqn.7.39}$$

The shear force V_2 corresponding to the shear stress v_2 is calculated using the sectional properties of the composite section which are denoted by the subscript c.

$$V_2 = (I_c\, b/ (Ay)_c)\, v_2 \quad \text{.....Eqn. 7.40}$$

The above method was similar to the approach suggested by Reynolds, Clarke and Taylor [73] for composite beams.

f_t is assumed to be $0.24\sqrt{f_{cu}}$ and a factor of safety of 0.8 is applied to prestress effects when they contribute to the shear strength.

In the D.Tp Technical Memorandum[99], the empirical equation used for the determination of shear resistance of monolithic beams cracked in flexure V_{cr} has been modified to include the effects of two stage loading associated with composite beams.

The Eqn 7.13 can be expressed in following form .

$$V_{cr} = 0.037\, b\, d\, \sqrt{f_{cu}} + V_1 - ((V-V_1)/(M-M_1))\, M_2 \quad \text{.....Eqn. 7.41}$$

M_2 is the additional moment required above M_1 to cause flexural cracking in extreme tensile fibres. Taking flexural tensile strength to be equal to $0.37\sqrt{f_{cu}}$, M_2 can be obtained by

$$M_2 = (0.37\sqrt{f_{cu}} + 0.8\, f_{pt} - M_1\, y_p / I_p)\, (I_c/y_c) \quad \text{.....Eqn. 7.42}$$

where f_{pt} is the prestress at the extreme tensile fibres.

The above approach seems more logical than simply assuming either a precast section or a composite section carrying the total shear force. However, its application becomes doubtful for composite beams subjected to hogging moments.

7.9.3 Recommendations in Current Codes of Practice for Design of Vertical Shear in Composite Beams

Both BS 5400 [27] and BS 8110[28] recommend that vertical shear in composite beams must be checked at the ultimate limit state using the monolithic section approach. It is therefore assumed that design principal tensile stress in the composite section is limited to $0.24\sqrt{f_{cu}}$ in determining V_{co}. The code does not make it clear which section, precast or composite, is to be considered. According to BS 5400, either section could be considered as carrying the total shear force due to ultimate loads.

ACI Building Code[35] also recommends that the composite section should be treated as a monolithic section. It states that the entire composite section can be assumed to carry the total vertical shear force. In AASHTO Standards [39], no special requirements for vertical shear are mentioned and therefore same clauses given in ACI Building Code are to be assumed. The monolithic approach is also recommended by CEB-FIP Model Code[40], provided that the shear force per unit length is within the values specified in the code.

It appears that the recommendations of all major design code regarding the vertical shear of composite beams are the same except for D.Tp Technical Memorandum[99] in which the superposition method described in the previous section is specified. The codes do not give any specific recommendations for composite beams subjected to hogging moments.

7.9.4 Shear Strength of Composite Beams Subjected to Hogging Moments

The codes of practice, as described in Section 7.9.3, do not recommend any specific methods for composite sections subjected to hogging moments. Therefore designers have to use either the monolithic section method or the superposition method for these cases also. Unlike sagging moment under which the in-situ slab remains in compression, hogging moments induce tension in the slab which may cause cracking if the slab is a reinforced concrete slab. As cracking can reduce the composite action and the effectiveness of the slab in carrying loads, the use of the entire composite section to determine the shear strength of such sections is subjected to uncertainty.

The experimental data available on the shear strength of composite beams subjected to hogging moments is very limited. Shear tests carried out by Mattock and Kaar [23] at PCA Laboratories provides the only experimental investigation that has so far been reported in this area. The influence of flexural cracks in the slab at the interior supports upon the shear capacity was studied. They reported that the flexural cracks did not adversely affect the shear strength at the interior supports.

Clark [38] suggested that the overall section could be used to calculate V_{co} but V_{cr} should be calculated following a conservative approach by ignoring the top slab. However the results of PCA Shear tests and the fact that the dowel action and the aggregate interlock carry a part of the shear force in the cracked state seem to indicate that it is unreasonable to ignore the top slab completely in the calculation of V_{cr}. More experimental data is required in this area. The shear tests of the present investigation will be very useful in clearing some of the above uncertainties in the design of such sections.

When continuity is developed by prestressing the slab, it is possible to

apply the design clauses for prestressed concrete beams for the entire composite section. In the calculation of V_{co}, the additional prestress induced in the precast beam due to the prestress in the top slab must be considered.

7.10 Horizontal Shear Transfer at the Interface

As the composite behaviour of a beam consisting of a precast beam and in-situ top slab depends entirely on its ability to transfer horizontal shear stresses at the interface, it is very important to ensure that the bond between the two elements is strong and that no separation takes place under loading. Several investigations have been carried out to study the horizontal shear resistance of composite beams[21,100,101]. After carrying out a series of push off tests and girder tests, Hanson[21] found that the composite action fails at a slip of about 0.125 mm.

It has been established that the bond between the two concretes can be improved by roughening the top surface of precast beams and providing shear connectors at the interface. In beam and slab bridge girders, the vertical stirrups provided in the precast beams can be extended to the top slab. Based on experimental results, codes of practice provide horizontal shear resistance for composite beams with different levels of surface roughness and different amounts of stirrups.

In the past the horizontal shear was checked under service conditions[45]. However, in current codes [27,28,35], it is considered at the ultimate limit state. Although BS 5400 recommends the use of elastic methods to calculate the shear stresses, it is not accurate due to the influence of cracking. Alternatively, horizontal shear stresses can be calculated by considering either the total tensile force or compressive force in the slab transferred across the interface at the ultimate limit state [3,38,43]. This approach has been recommended by BS 8110.

and ACI Building Code. When this approach is followed, the prestressing force in a prestressed slab will not affect the horizontal shear stresses at the interface as at the ultimate limit state its behaviour would be basically similar to a reinforced concrete slab.

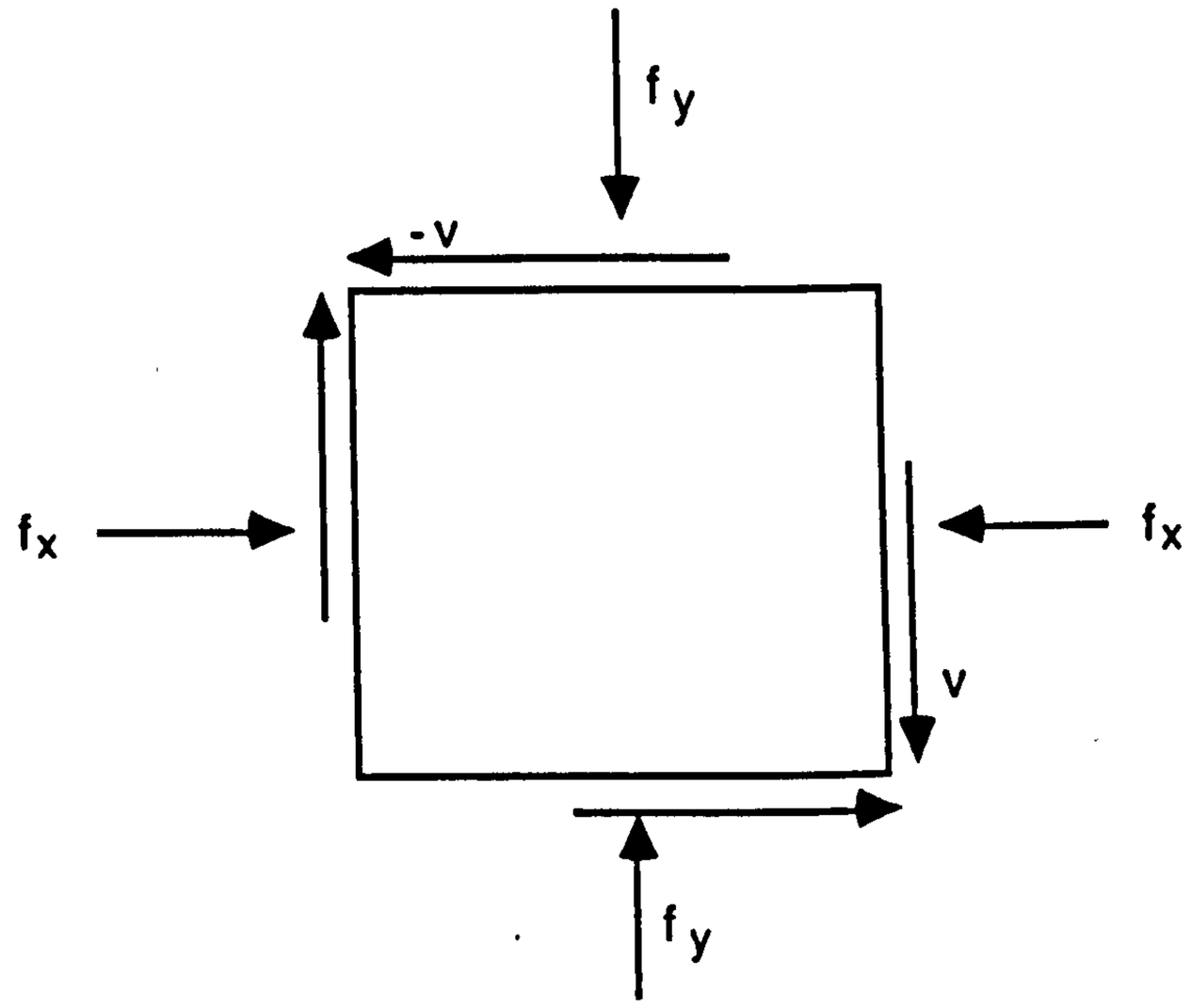

(a) Stresses Acting on the Element

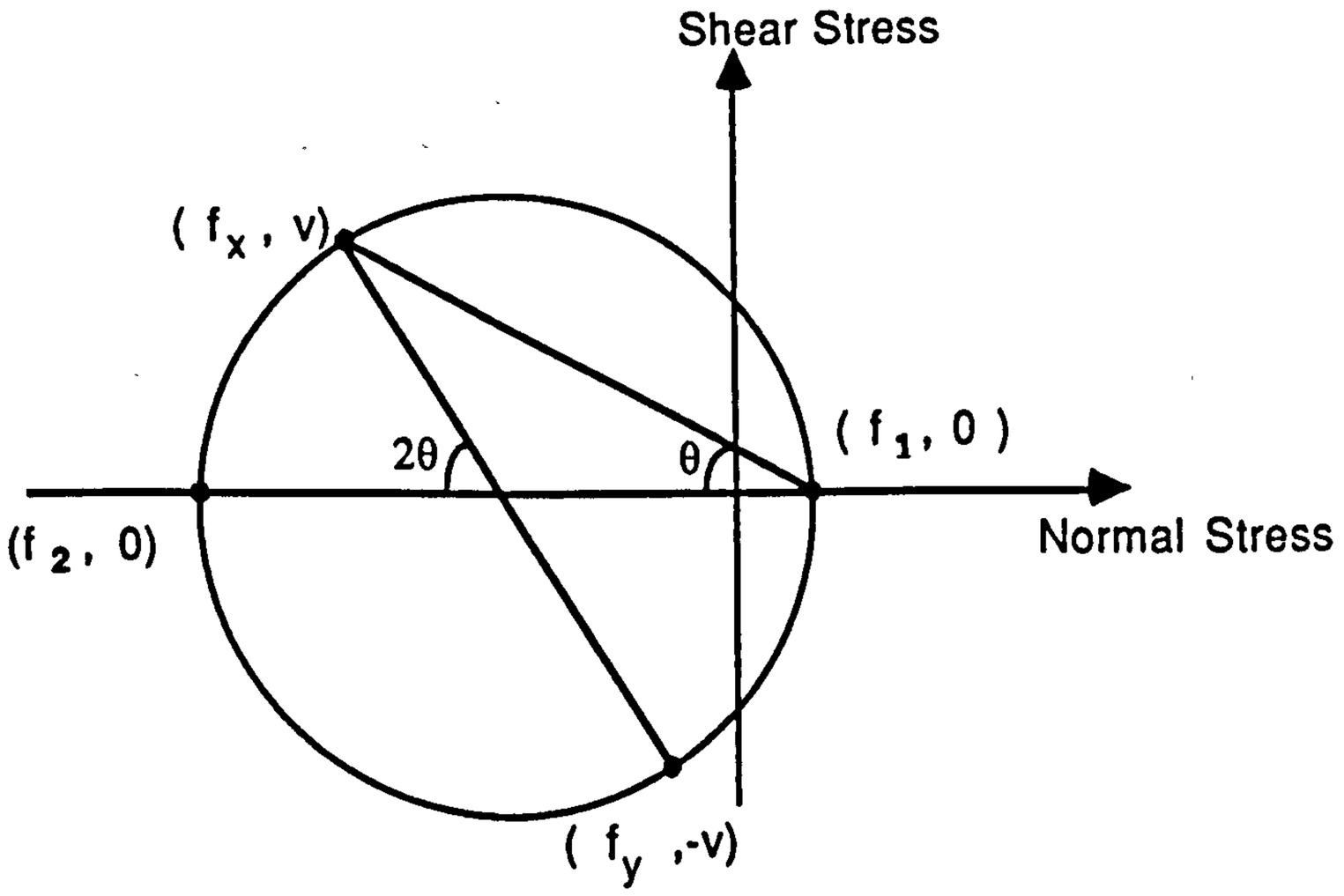

(b) Mohr's Circle for the Stress System

Fig. 7.1 Stresses Acting on an Element in a Prestressed Concrete Beam Subjected to Bending and Shear

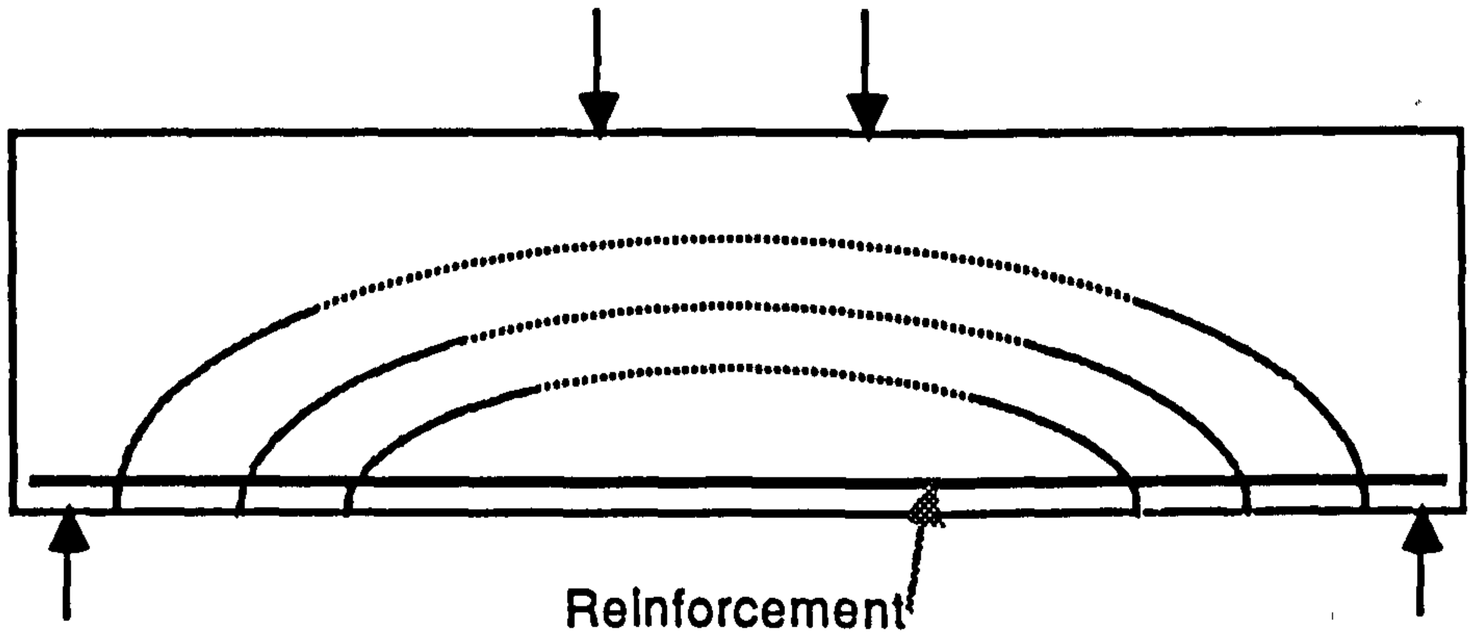

Fig. 7.2 Arch Analogy of a Beam with Inclined Cracks

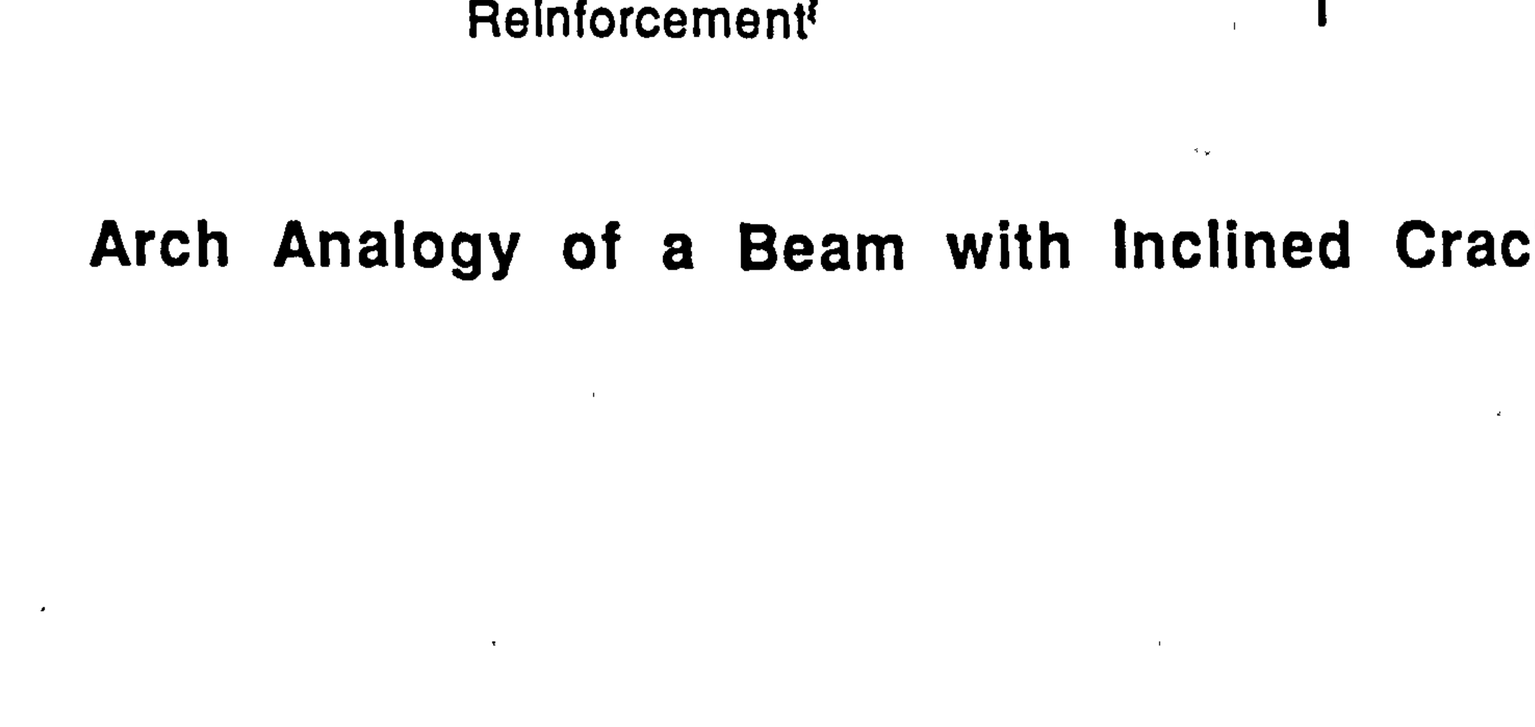

Fig. 7.3 Classical Truss Analogy of a Concrete Beam with Shear Reinforcement after Inclined Cracking

CHAPTER 8

OBSERVATIONS AND RESULTS OF SHEAR TEST SERIES

8.1 General

The experimental programme for the shear test series was designed to study the influence of prestressed slabs in continuous composite beams on shear strength. The additional prestress induced in the web by the prestressing force in the slab can be expected to improve the inclined cracking strength of the composite beams. The three types of slabs used in the composite model beams for the flexural tests were also used for the shear tests with similar steel arrangements in the slab so that a comparison could be made between the shear behaviour of beams made continuous by a reinforced concrete slab (conventional method) and beams made continuous by a prestressed slab (proposed new method). As vertical shear can be critical and could precede flexural failure at the interior supports of continuous composite beams, and bearing in mind that experimental data and code guidance on shear strength of continuous composite beams are extremely limited, the results of this test series should be of great importance in the design of this type of continuity connection.

8.1.1 Details of Test Beams

The details of the eight composite beams in the shear test series and the test procedure were given in Chapter 4. The first six beams (B1 to B6) were tested as shown in Fig. 4.11 with two point loads P and Q at a distance of 0.9 m and 1.0 m from the support at the joint. The loading was increased continuously up to

the failure with the ratio of P to Q being 0.84. As seen from the bending moment diagram (Fig. 4.11(b)), a point of contraflexure occurred at a distance of 0.76 m from support B in the span BC. However, the distance between B and C can be considered as the shear span [81] and therefore the distance between the support and the location where the hogging moment was zero for span BC was slightly less than that of span AB (0.9 m). For the last two beams, B-7 and B-8, the shear span BC was increased to 1.5m to study the influence of increase in the shear span to effective depth ratio. The design serviceability shear force for the model beams of the shear test series was 77.0 kN while the design ultimate shear force was 107.0 kN.

The measured strains in the shear reinforcement, surface strain rosettes, crack width, deflections etc. were monitored and will be discussed later. The location of strain rosettes and deflection gauges are shown in Fig. 8.1.

8.1.2 Prestress in Test Beams

The stress distributions due to prestress in the precast beam and in the slab were given in Chapter 4 (Fig. 4.10). The prestress distribution due to pretensioning strands in the precast beams was nearly uniform over the depth of the beam within the two shear spans AB and BC considered. At the end of the transmission length, the prestress at the top and the bottom of the precast beam near the joint was 6.70 and 5.80 N/mm^2 respectively.

8.2 Behaviour of Beams Prior to Inclined Cracking

The stresses in the web of the composite beams were analysed using elastic theory equations, but it is considered that this is only valid up to the point of inclined cracking. Analysis of theoretical and measured principal stresses are

described below.

8.2.1 Theoretical Principal Tensile Stresses in the Web

The principal stresses were calculated using Eqn. 7.1 for a grid of points in the web of the model beams in the shear spans AB and BC and for different loading levels. The bending stresses were calculated using the basic bending equation (f=M/Z) while the shear stresses were calculated using Eqn.7.5. The resultant longitudinal stress was obtained by combining the total horizontal prestress (due to prestress in both the beam and the slab) at the point under consideration. From the results of this analysis, the location of maximum principal tensile stress at different sections along the shear spans could be determined. The results are illustrated in Fig. 8.2 for a load near the inclined cracking load observed in the tests. In this analysis, the development of prestress within the transmission length was assumed to be linear.

It can be seen from Fig. 8.2 that for the given loading arrangement, the maximum principal tensile stress near the support B of the beams with either type of continuity connection occurred at the top of the web. The reason for this was that the prestress in the beam was smaller in this region due to transmission length while the flexural tensile stresses at the upper part of the beam were high due to greater bending moment at the support. In the composite beams with a reinforced concrete slab, the critical point remain at this level up to a distance of about 600 mm from the support B in both spans. Beyond that, the critical point moves downwards. In the beams with a prestressed slab, the additional prestress induced in the upper part of the precast beam made the top of web less critical when flexural tensile stresses began to diminish. The gradual downward movement of the location of the maximum principal tensile stress reached the bottom of the web at sections closer to the point load Q.

In Fig. 8.3, 8.4 and 8.5, the variation of the calculated principal tensile stress at the top of the web, at the centroid of the composite section and at the base of web along the shear spans AB and BC are shown for B-1, B-2 and B-3. It can be seen that in B-1 which had a reinforced concrete slab, the principal tensile stress at the the top of web is considerably greater than the stress at the centroid near the support. Beyond about 350 mm from the support, the difference in the tensile stress at the top of the web and the centroid became smaller and the magnitude of maximum principal tensile stress remains almost constant along the shear span .

In B-2 and B-3 which had a partially prestressed slab and a fully prestressed slab respectively, the difference between the principal tensile stress, at the three levels considered, and also the magnitude of maximum stress, decreased with the increase of prestressing force in the slab. Except at sections close to the support, the variation of the magnitude of the maximum tensile stress was small in all three beams.

The results of this theoretical analysis suggests that the principal tensile stress may be checked at the centroid of the composite beam at sections outside the transmission zone. However, in practical cases where prestress at the top of web is considerably smaller than that at the bottom, the top of the web will remain critical outside the transmission zone in beams with a reinforced concrete slab.

8.2.2 Principal Stresses Determined from Strain Rosettes

From the strain measurements of the rosettes shown in Fig. 8.1, the principal stresses were calculated following the procedure described in Section 7.3.2.2. In the calculations, the prestrain in the horizontal direction at the location of the rosettes was added to the strain measured during the loading. The Poisson's ratio effect of horizontal prestrain in the vertical and 45^0 inclined direction were also considered for the respective gauges. Poisson's ratio obtained

from the prism tests was found to have an average value of 0.15 for the beams tested in the shear test series.

8.2.2.1 Principal Tensile Stress

Due to the Poisson's ratio effect for the horizontal prestress, a principal tensile strain and principal compressive strain existed before the application of load. However, when principal stresses were calculated from Eqn.7.10 and Eqn.7.11, Poisson's ratio effects cancelled out and the magnitude of the principal tensile stress was zero while the principal compressive stress was equal to the horizontal prestress at that point.

The variation of principal tensile stress for rosettes 1 and 5 in span BC and 7 and 8 in span AB in several beams with increasing shear force are shown from Figs. 8.6 to 8.8. The theoretically calculated principal tensile stresses are also shown for comparison. It can be seen that the experimental stresses were greater than the calculated values specially at high shear forces. The experimental principal stress increased at approximately uniform rate with the load up to the cracking load.

8.2.2.2 Principal Compressive Stresses

The variation in the experimental and calculated principal compressive stress for Rosette 1 in span BC and Rosette 7 in span AB with the applied shear force are plotted in Fig. 8.10 and 8.11. The increase in the principal compressive stress with load was uniform up to the inclined cracking load, and the experimental principal compressive stress also tended to be greater than the calculated values.

8.3 Inclined Cracking in the Beams

8.3.1 Type of Cracking

In all eight beams tested, the type of inclined cracks which developed were essentially web shear cracks due to the high principal stresses in the web. This was due to the thin webbed section with a prestressed slab and shear span to effective depth ratio less than 3.0. Even when the this ratio was increased to 3.5 in the last two tests, flexural shear cracking did not develop.

Although flexural cracks appeared in B-1, B-4 and B-8, which had a reinforced concrete slab, well before the shear cracks appeared they did not develop into shear cracks. These flexural cracks appeared either in the diaphragm or in the composite section very close to the diaphragm. Similar observations have been reported by Mattock and Kaar[23] in the tests of continuous composite beams with reinforced slabs. As discussed in Section 7.3.5, the initiating flexural crack of a flexural shear crack generally develop at a distance of about d/2 to d from the section where shear is critical. The flexural cracks observed in the initial stages of cracking were limited to a zone of about 300mm on either side of the support B.

8.3.2 Measured Inclined Cracking Load

The loading arrangement used in the testing of all beams produced a slightly smaller shear force in the cantilevered span (span AB) than in the shear span of the main beam (span BC). However in the majority of beams, the first web shear crack appeared in the cantilever span, but in B-4 and B-6, which had a reinforced concrete slab, the shear span of the long beam(BC) developed the first crack.

One possible reason for the occurrence of initial inclined cracks in the cantilever span is that it underwent greater deformation due to applied loading

than the long beam. The load at the end of the cantilever restrained the deformation of the long beam while span AB was free to undergo any deformation. The greater deformations in the span AB would have increased the diagonal tensile strains, and this was shown by the 45^0 inclined strain gauges in the cantilever span recording a greater strain than the identical gauges in the long span. The slightly greater distance between the support and the point of zero moment in span AB may also have contributed to the reduced inclined strength of span AB.

The measured web shear cracking loads for the span AB and BC are given in Table 8.1.

The web shear cracks appeared suddenly without any warning and extended over the depth of the web instantly, and therefore it was not possible to find the exact location of the origin of the first web shear crack. The location of the centre of the first inclined crack of different beams is also shown in Table 8.1.

In the flexural test series which was carried out prior to the shear test series, flexural shear cracks were observed. The shear span to effective depth ratio for these three beams was 6.5. The flexural shear cracking load of the composite model beams with reinforced concrete slab(A-1), partially prestressed slab(A-2) and fully prestressed slab(A-3) were 35 kN, 45 kN and 75 kN respectively.

8.3.3 Experimental Principal Stresses at Inclined Cracking

The principal stresses determined from strain rosettes located in the region where inclined cracks appeared in the shear span of long beam are given in Table 8.2. The values of experimental principal tensile stresses were found to be in the range of 2.98 to 4.88 N/mm^2 with a mean value of 3.96 N/mm^2 for the series. The values of calculated principal tensile stress from elastic theory and the tensile strength values obtained from the splitting cylinder tests and the

British codes ($f_t=0.36\sqrt{f_{cu}}$) are also given for comparison. The experimental principal tensile stress values tended to be greater than the tensile strength values obtained from both sources.

The principal compressive stresses determined from the rosettes were in the range of 10.28 to 18.15 N/mm^2 and the mean value of this stress range was equal to $0.23f_{cu}$. Therefore any adverse influence of compressive stress on the tensile strength was small.

8.3.4 Propagation of Inclined Cracks

The first web shear crack appearing in the beams of the shear test series was about 0.06 mm to 0.08 mm wide. With increase in load, the crack width increased rapidly and this increase in the maximum inclined crack width of the beams of the shear test series are shown in Fig. 8.12 to 8.14. It can be seen that the rate of increase in crack width was approximately uniform. Near the failure, the cracks became very wide (greater than 2 mm).

When the web shear cracks appeared in the other span at a higher load, they were approximately 0.15 mm wide. Therefore, it appears that crack width is greater at the first appearance when the inclined cracking strength is higher. The crack widths in beams with a smaller percentage of shear reinforcement were observed to increase at a faster rate than those in beams with higher percentages of shear link reinforcement.

As the vertical shear strength of composite beams is considered at the ultimate limit state, the width of shear cracks are not given the same attention in design as is the flexural cracking under service conditions. However, in severe environments such as those to which the bridge beams are subjected, the width of the inclined cracks is also important. In the present test series, beams B-1 and

B-7, which were composed of a reinforced concrete top slab, developed shear cracks below the serviceability shear force, which was taken to be 76 kN. The inclined cracks were about 0.20 mm wide at this serviceability shear force. All the beams with a prestressed slab were free of any inclined cracks under the serviceability conditions.

The increase in width of flexural cracks in beams with the three types of slabs used in the series is shown in Fig. 8.15. Observed flexural cracks were comparatively narrower and the rate of increase of width was slower than for the shear cracks.

8.3.5 Inclination of Cracks

The inclination to the horizontal of the first web shear cracks observed in the shear test series varied from 30^0 to 45^0, but when further cracks subsequently developed, these were less steeply inclined. The first crack in the beams with a reinforced concrete slab had a greater inclination than that in beams with a prestressed slab.

The average inclination of the cracks in beams with a reinforced concrete slab was 32^0 to 35^0. In the beams with a partially prestressed concrete slab, this average inclination was 30^0 to 33^0, while the inclination of cracks in the beam with the fully prestressed slab was 29^0 to 32^0. The slight reduction in the angle of inclination of cracks from the beam with reinforced concrete slab to the beam with the fully prestressed slab is mainly due to the additional compressive stress induced in the web by the prestress in the slab.

The calculated angle of inclination of the maximum principal compressive stress obtained from the rosette readings near the cracking load is given in Table 8.3 together with the inclination of the first web shear crack and the average inclination of cracks in the two shear spans of each beam.

8.3.6 Influence of Prestress in the Top Slab on Inclined Cracking Load

The results shown in Table 8.1 of the first three beams, B-1(with a reinforced concrete slab), B-2 (with a partially prestressed slab) and B-3 (with a fully prestressed slab) clearly show the positive influence of prestress in the slab on the inclined cracking strength. The prestress in the top slab was the only variable in this group of beams. The additional prestress at the top of the web and at the centroid of the composite section due to the prestressing force in the slab of B-2 were 4.0 N/mm^2 and 2.95 N/mm^2 respectively while the additional prestress at the same two levels of B-3 were 6.54 N/mm^2 and 4.75 N/mm^2 .

The increase in the web shear cracking load of the two spans with the increasing prestressing force in the slab is shown in Fig. 8.16. The increase in web shear cracking load of both spans increased considerably in B-2 and B-3 compared with B-1. The ratio of inclined cracking load in the short beam of B-2 and B-3 to that of B-1 were 1.25 and 1.48 respectively while the respective ratios for the shear span of the long beam were 1.10 and 1.14 .

It is also possible to observe a similar trend in two other groups of beams in the series where the slab type was changed. In one group, B-5 and B-6 had a partially prestressed slab while the slab of B-4 was a reinforced concrete slab. The shear span of the long beam of B-5 and B-6 developed web shear cracks at a load of 1.32 times that of B-4 while in the other group, which consisted of B-7 and B-8, the corresponding ratio was 1.55.

Similar observations were made in the flexural test series in which flexural shear cracks developed. The ratio of inclined cracking load for beams with the partially prestressed slab and the fully prestressed slab to that of the beam with the reinforced concrete slab were 1.28 and 2.14 respectively.

8.3.7 Influence of Shear Reinforcement Percentage on Inclined Cracking Load

No definite trend was observed in the web shear cracking load when the shear reinforcement percentage was varied in the beams with the partially prestressed slabs and the beams with reinforced concrete slabs. The relationship between the measured web shear cracking load and the shear reinforcement percentage can be seen in Fig.8.17 for the beams with these two types of slabs. It indicates that the web shear cracking strength is not greatly influenced by the web reinforcement percentage. Similar observations were made in the tests on composite beams by Mattock and Kaar[23] and Tay[65].

8.3.8 Effect of Shear Span/Effective Depth Ratio on Web Shear Cracking

In the test series, the shear span to effective depth ratio of the main beam was varied for two beams with a prestressed slab(B-5 and B-7) and for two beams with a reinforced concrete slab(B-4 and B-8) while the remaining parameters remained constant. When the ratio changed from 2.35 for B-4 and B-5 to 3.53 for B-7 and B-8, a small reduction in the web shear cracking load was observed. The results of these four beams are plotted in Fig. 8.18. However, a much larger change was observed when the web shear cracking loads of B-1 and B-2, which had the same shear span to effective depth ratio as B-4 and B-5 but a higher web reinforcement percentage, were compared with the inclined cracking loads of B-7 and B-8.

8.4 Comparison Between Measured Web Cracking Strength and Code Predictions

The measured web shear cracking load of the two spans AB and BC were compared with the web cracking load calculated according to British, American and CEB-FIP codes. It was assumed that the entire composite section was effective in resisting the applied shear forces in all test beams. The calculated values were the same for both spans as the prestress in the two precast beams was identical. (All safety factors were excluded in these calculations.)

Design codes recommend that the vertical component of the prestressing force (V_p) of inclined tendons may be added to the shear strength. The comparison of the measured web cracking load with the predicted strength both by considering and ignoring V_p will be presented later.

For comparison, the web shear cracking loads were also calculated by applying the principal tensile stress equation at the centroid of the composite section and also at the top of the web, where the principal stress was found to be critical in the theoretical analysis (Section 8.2.1), while using the actual section properties of the composite section as the code equations have actually been developed for rectangular sections. Also, web shear cracking loads of composite beams were calculated assuming that total shear force is resisted by the precast section only. (The centroid of the precast beam was considered in this calculation.)

The values obtained from different methods are presented in Table 8.4 for comparison with measured values.

8.4.1 British Codes

Eqn. 7.17 is given in BS 8110 for the determination of web shear cracking load of prestressed concrete beams. The tensile strength of concrete f_t is taken to be equal to $0.36\sqrt{f_{cu}}$ when the partial safety factor of 1.5 is removed. In BS 8110, it is implied that the critical section for the web shear cracking strength near the supports is taken at a distance from the edge of the bearing for a distance equal to the height of the centroid of the section above the soffit. The validity of this, which is mainly given for simply supported beams, was examined by calculating the web shear strength of the composite beams tested at this section, which was found to be within the transmission length of the prestressing strands calculated according to the code equation,

$$l_t = K_t \times (\text{diameter})/\sqrt{f_{ci}} \qquad \text{..... Eqn. 8.1}$$

For the strands used, K_t was taken as 240 and the prestress at the required section was calculated using the equation given in BS 8110.

The comparison of the measured web shear cracking load for the two shear spans with the value calculated according to the British codes is given in Tables 8.4, 8.5 and 8.6. It can be seen that the code prediction of the web shear cracking strength for span BC of the main beam was safe and conservative even when V_p was added to V_{co}. The mean ratio of the measured cracking load to the calculated cracking load was 1.30. Smaller ratios were obtained for the two of the three beams which had a reinforced concrete slab.

For the cantilever span, the ratio between measured web cracking load and that predicted by the Codes was close to unity (1.03). However, when V_p was added to V_{co}, the mean ratio became less than 1.0. This indicated that it is safer to ignore the vertical component of prestressing force in the calculation of V_{co} of

cantilevered spans such as those tested in this series. However, such conditions do not generally exist in the actual bridge decks. The hogging moment region of the prototype continuous composite beams is represented by the span BC of the main beam.

The above results suggest that the British code equation for V_{co} can be safely applied to continuous composite beams by considering the entire composite section even though the top slab is cracked in flexure as observed in the beams with reinforced concrete slabs. The location of the critical section at a distance from the support equal to the height of centroid was found to be satisfactory for the shear span of the main beam and the concept of adding V_p to the web shear cracking load was found to be safe.

8.4.2 American Codes

The procedure adopted by the American codes, ACI Building Code [35] and AASHTO Specifications[39] is similar to that of the British codes except for slight variations in the equations. The code equation for the web shear cracking load was given in Chapter 7 (Eqn. 7.18) and the critical section was taken at a distance of half the overall depth from the support. A transfer length of 50 times diameter is recommended by the Codes and thus the critical section was within the transfer length and the prestress at the critical section was calculated assuming a uniform build up of prestress. The American codes specify an overall safety factor of 0.85 for the calculated shear strength.

The calculated values of the web shear cracking load using ACI equation are also given in Table 8.4. The ratios between measured and calculated strengths with and without considering V_p are given in Table 8.5 and 8.6 for the beams. It can be seen that the results are similar to those obtained using the British code equation.

8.4.3 CEB-FIP Model Code

The shear resistance of the concrete calculated according to the Eqn.7.20 are given in Table 8.4. The transmission length was taken as 50 times diameter of strands. The code recommends that shear need not be checked within a distance of d from the support. The partial safety factor of 1.5 for the concrete was excluded in the equation. The ratios of measured to calculated web shear cracking load are given in Tables 8.5 and 8.6. The code prediction for the main beam was found to be very conservative. The mean ratios for the two spans when V_p was included in the calculated web shear cracking load were 1.40 for the short beam and 1.92 for the main beam.

8.4.4 Other Methods

When the web shear cracking load was calculated by using the actual sectional properties and applying the principal stress equation to the top of the web, the values of V_{co} were close to the values calculated using the British code equation. This confirmed that the code equation, developed for the centroid of rectangular sections, is also valid for composite beams in which the critical principal tensile stress occurs at the intersection between the flange and the web. The values of V_{co} obtained at the centroid of the composite section were higher than the values obtained from the British code due to the geometry of the section. The mean ratio of measured V_{co} of the long beam to the calculated V_{co} at top of the web was 1.24 while the mean value of the ratio at the centroid was 1.09.

The consideration of only the precast section being effective in resisting shear forces applied to the composite section was found to be very conservative,

with a mean value of 1.56 for the ratio of observed to calculated web cracking load. However, this method gave good agreement for cantilevered span of beams with reinforced concrete slab.

8.4.5 Comments on the Prediction of Web Cracking Load by Different Codes

Comparison of the measured and calculated web shear cracking load according to different codes, ignoring safety factors, indicated that the British and American code equations for monolithic prestressed concrete beams gave a conservative prediction for beams tested in this series. It can be concluded that it is safer to use the entire composite section to determine the web shear cracking strength even when flexural cracks exists in the slab. The location of the critical section implied by the codes for simply supported beams, and the concept of adding the vertical component of prestressing force of inclined tendons was found to be satisfactory for the shear span section of the main beam. However, the above conclusions were based on the results of the tests in which the precast beams were not subjected to any shear force due to the self weight of beams prior to the development of composite section.

The same procedures were found to be slightly unsafe for short beam when V_p was included. For such beams, also, a safer prediction can be obtained by ignoring the contribution of V_p.

CEB-FIP model code equation for the shear resistance of concrete was found to be very conservative for the span BC of the main beam. It was also conservative for the cantilever span of the beams with the reinforced concrete slab.

Of the other methods considered, the application of the principal stress equation at the centroid of the composite section using actual section properties gave the best agreement with the measured web cracking load for the main shear span of the beams with a prestressed slab.

8.5 Flexural Shear Cracking Load of Series-A Beams

The flexural shear cracking loads, V_{cr}, measured in the flexural test series were compared with the values of V_{cr} calculated according to British and American codes. A section at half the effective depth from the diaphragm was considered to be the critical section. This fell within the transmission length of prestressing wires. The equations of BS 8110 and ACI Building Code were given in Chapter 7 (Eqns. 7.16 and 7.19).

The decompression moment M_o and the cracking moment M_{cr} required in the equations were calculated by considering the stress at the top of the insitu slab. The measured and calculated flexural shear cracking loads are presented in Table 8.7.

The flexural shear cracking loads for the three beams were also calculated using BS 8110 equation by considering the prestress at the top of precast beams for M_o, to examine whether cracking of the insitu slab can be completely ignored by considering only the precast section for V_{cr} of the composite beams under hogging moments. However, the sectional properties of the composite section were considered in evaluating M_o. The percentage of tensile reinforcement in the precast beam was considered to be zero in obtaining v_c from the Code table and the height of the precast beam was used in the equation in place of d. The values of V_{cr} calculated using this approach are also given in Table 8.7. The ratio of measured to

calculated flexural shear cracking load is given in Table 8.8.

It can be seen from Tables 8.7 and 8.8 that the BS 8110 equation gave the best agreement with the measured values and the ACI equation tended to be unsafe for the two beams with prestressed slabs. The consideration of the stress at the top of the precast beams using BS 8110 equation was also found to be unsafe for beams with prestressed slabs.

Although the number of tests were limited, it can be concluded that flexural shear cracking load can be safely predicted by using the BS 8110 equation, given for all classes of prestressed members, by considering the entire composite section at the level of the top of the insitu slab at a distance of d/2 from the support to determine M_o for beams with reinforced concrete or prestressed slabs.

8.6 Load-Deflection Relationship

The load-deflection curves of the eight beams measured at the end of cantilever and under the point load Q in the long beam are shown in Fig. 8.19 to 8.24. Up to the appearance of either flexural cracks or inclined cracks, a linear load-deflection relationship was observed in all beams. It was nearly identical in all beams with different types of slabs used in the investigation.

As with flexural cracking, inclined cracking also affected the stiffness of the member resulting in deflection increase with load at a higher rate. However, the effect of web shear cracking was not as significant as the flexural cracking. The change of gradient of the curve after web shear cracking was relatively small. However, the cantilever span showed a greater change in the slope after cracking, especially in beams with reinforced concrete slabs due to effects of both flexural and shear cracking.

As mentioned earlier, the measured deflection at the cantilever end was found to be greater than the deflection measured at the point load Q in the main beam.

8.7 Strain in the Longitudinal Reinforcement in the Slab

Strains in the non-prestressed reinforcement provided in the slab were measured at the support using electrical resistance gauges which mainly recorded the strains due to flexural effects. The measured strain in the steel is plotted against the applied load in Figs. 8.25 and 8.26.

Stresses in the non-prestressed steel remained below the yield stress up to the shear failure except in B-1 which had a reinforced concrete slab (and a high percentage of web reinforcement) yielded near the failure in shear. In all three beams with a reinforced concrete slab, strain in the longitudinal steel increased at a uniform rate after the flexural cracking. Strains measured in beams with prestressed slabs also showed smaller but nearly uniform rate of increase. The shear cracking in the web seemed to have no effect in the steel strain at the support. It should be noted that the highest failure load in this series produced a bending moment of 165.0 kNm which was slightly less than the flexural capacity of the beam with a reinforced concrete slab in Series A.

8.8 Ultimate strength of Beams

8.8.1 Failure Mode

All eight beams in the shear test series failed due to web crushing. As with inclined cracking, failure occurred in the majority of beams in the short beam. In B-1 and B-4 which had a reinforced slab, the span BC of the long beam also failed. In B-7, the failure occurred in the remote shear span from the joint of the long

beam (span CD). Although the relative magnitude of the shear force in this span increased after the distance between the point load Q and the support B was increased from 1.0m to 1.5m for the testing of B-7 and B-8, the main cause to the failure of this span was a horizontal crack which developed during transfer at the end of the beam at the level of prestressing strands. This crack propagated upwards at later stages of the loading.

The failure was observed to be gradual. In most beams, crushing occurred at the top of the web or in the upper half of the web. This was contrary to the observations of Mattock and Kaar[23] who reported that web crushing took place near the base of the web in continuous composite beams. Crack patterns and the failure zones of the beams tested in this series are shown in Plates 8.1, 8.2 and 8.3.

8.8.2 Comparison of Observed Web Crushing Strength with Design Code Predictions

The observed web crushing load was compared with the web crushing strength predicted by the British, American and CEB-FIP codes. (The recommendations of these codes were discussed in Chapter 7.) The measured and predicted web crushing loads are given in Table 8.9 while the ratios of observed to predicted strengths are presented in Table 8.10. The safety factors were incorporated in the calculated values.

Except for Beam B-7, the ratios of observed web crushing load to the strength predicted by BS 8110 were in the range of 1.35 to 1.92 with a mean value of 1.54, which was higher than the partial safety factor of 1.25 included in the specified maximum shear stress. This indicates that BS 8110 tends to underestimate the web crushing strength. The mean ratio of the prediction of BS 5400 was 1.35. The smaller ratio for the BS 5400 prediction was due to the

higher upper limit for the maximum shear stress given in BS 5400 for concrete strengths over 60 N/mm^2. The predicted web crushing loads by ACI Building Code were closer to the experimental results which gave a mean ratio of observed to measured of 1.12 which was sufficiently close to the safety factor adopted in the Code.

The above comparisons were made mainly with the web crushing load of the short beam. As the shear force applied to the shear span of the long beam was greater than the that on short beam, it had a higher strength against web crushing and therefore would have a higher margin of safety over the predictions of American and British codes.

Both Standard and Accurate methods of CEB-FIP Code gave unsafe predictions. In the Accurate method, the angle of inclined struts was taken as 33^0 (the measured inclination of shear cracks).

8.8.3 Influence of Shear Span/Effective Depth Ratio on Ultimate Strength

The shear span to effective depth ratio of span BC was increased from 2.35 to 3.5 for B-7 and B-8. As failure of B-7 occurred in the other shear span of the main beam, it was not possible to make a proper comparison of the influence of the ratio of the ultimate strength of beams with a partially prestressed slab. Also in B-4 and B-8 which had a reinforced slab, the failure occurred in different spans. When the shear force of span BC of B-8 which failed in the short beam, was calculated at the failure load, it was found to be 198.0 kN compared to Beam B-4 in which the failure occurred at 190.0 kN.

8.8.4 Influence of Prestress in the Slab on Ultimate Strength

In B-1, B-2 and B-3 the slab type changed from a reinforced concrete slab to a fully prestressed slab while other parameters remained constant. Although the failure of B-2 and B-3 occurred in the short beam, while B-1 failed in the main beam, comparison of shear carried by the shear span of the long beam indicated that beams with a prestressed slab had a slightly higher strength than beams with a reinforced concrete slab (230 kN of B-3 compared to 215 kN of B-1). Also when two beams with prestressed slabs B-2 and B-3 were compared, the beam with higher prestress in the slab showed a slightly increased strength. The same observations can be made from the results of B-4 and B-5 which had a identical but smaller percentage of shear reinforcement than the previously mentioned beams. The shear span of the main beam of B-5 (with a partially prestressed slab) was able to resist a shear force of 198.0 kN compared to the ultimate strength of the same span of B-4 (190.0 kN). However, as all beams failed in web crushing, the observed increase in the ultimate strength was not significant.

8.8.5 Influence of Shear reinforcement Percentage

Three percentages of shear reinforcement (0.84%, 0.53% and 0.42%) were used in the three beams with a partially prestressed slab while only the first two of the above percentages were used in two beams with a reinforced concrete slab to study the influence of percentage of shear reinforcement on the ultimate strength.

In the first group comprising B-2, B-5 and B-6, the ultimate shear strength increased with the shear reinforcement percentage even though failure of all three beams was caused by web crushing, which is considered as the upper

limit to the shear capacity of beams. The increase in ultimate strength of the beams with a partially prestressed slab and the beams with a reinforced slab is illustrated in Fig.8.27. The contribution of the web reinforcement to the ultimate strength will be discussed in more details in the next section.

8.8.6 Shear Reinforcement Behaviour

The spacing of the shear reinforcement, which consisted of two legged 6 mm diameter high yield stirrups, was uniform throughout the spans of each continuous beam in the test series. Electrical gauges were fixed to the stirrups near the connection at mid depth to monitor the stirrup behaviour under loading. The variation of the stirrup strain with load in the eight beams is shown in Figs.8.28 to 8.35.

As can be seen from the load-strain curves, the stirrup strains remained small up to the inclined cracking load. After a sudden increase when inclined cracks cross the stirrup, stirrup strains increased rapidly with further increase in the shear force. Yielding of stirrup steel took place in all eight beams and the additional shear force carried up to yielding from the inclined cracking load increased with the stirrup percentage and also with the increase in the prestress in the slab.

Except in B-7 and B-8 in which the distance between support B and the point load Q was greater than in other tests, the strains measured in the stirrups near the support were close and formed a narrow band in the load-strain graphs, specially at higher loads. Although the recorded strains from S-5 which was closest to the support in the short beams were smaller than those recorded by S-6, the next stirrup, in beams B-1, B-4 and B-8, the enhanced shear strength predicted in the codes was not observed in the shear span of the long beam for the majority of the beams tested.

8.8.6.1 Contribution of Web Reinforcement

In current design codes, shear forces applied after inclined cracking are considered to be resisted by both the concrete and the shear reinforcement as assumed in the modified truss analogy. When the two contributions are denoted by V_c and V_s, the applied shear force is equal to,

$$V = V_c + V_s \qquad \text{.....Eqn. 8.2}$$

The contribution of concrete is considered to be equal to the inclined cracking load in the British and American codes.

The shear force resisted by shear reinforcement can be expressed according to the truss analogy as,

$$V_s = r f_v b d \ \text{Cot}\,\theta \qquad \text{.....Eqn. 8.3}$$

where $r = A_{sv} / b s$

f_v = Stress in the shear reinforcement

θ = Angle of inclined struts

In Fig. 8.37 to 8.40, the comparison of the measured stress in a stirrup located in the failure zone for four beams with different slab types and shear reinforcement percentages, and with the stress calculated according the truss analogy and modified truss analogy, are shown. The angle θ was taken to be 45^0 and V_c was taken as the measured inclined cracking load.

It can be seen that while the truss analogy was very conservative for all the beams, the modified truss analogy tended to underestimate the stirrup stress for B-1 and B-3 which had the highest stirrup percentage. For the other two beams B-5 and B-6 which had smaller stirrup percentage, the measured values were sufficiently close to the modified truss analogy prediction. This indicated that

the modified truss analogy is less satisfactory for beams with a high amount of shear reinforcement which fail in web crushing. In the graphs, calculated stirrup stress using only 80% of inclined cracking load are also shown. This gave a good agreement with the experimental stresses of B-1 and B-3 with the highest stirrup percentage. In the other two beams, the experimental stress curve fit between the two analytical curves. The other beams in the series gave similar results. Therefore, for the beams failing in web crushing, modified truss analogy can still be used by considering a reduced contribution from concrete.

8.8.6.2 Contribution of Web Shear Reinforcement to the Ultimate Strength

The Eqn. 8.2 can be written for the ultimate limit state as,

$$V_u = V_c + V_s \qquad \text{.....Eqn. 8.4}$$

This equation is used by most major design codes for the ultimate shear strength. The contribution of V_s to the ultimate strength is calculated assuming that shear reinforcement yields before failure while contribution of concrete at ultimate limit state is considered to be equal to the inclined cracking load in British and American codes. The validity of the use of this modified truss analogy equation for the results of the tests beams which failed in web crushing was checked. The difference between ultimate shear strength V_u and the shear carried by stirrup V_s was checked against the measured inclined cracking load V_c and the results are given in Table 8.11.

It can be observed that for smaller shear reinforcement percentages (0.42% and 0.53%), the modified truss analogy used in codes gave values greater than unity for the ratio of $(V_u-V_s)/V_c$ while for beams which had the highest

shear reinforcement percentage (0.84%), the ratio was less than unity. For those three beams, the average ratio was 0.83, indicating that the contribution of concrete is less than that assumed in the codes. For beams with such high percentages of shear reinforcement in thin webbed composite sections, the truss analogy equation can be written as,

$$V_u = 0.8\,V_c + V_s \qquad \text{.....Eqn. 8.5}$$

The above factor for V_c was confirmed by the graphs of load vs experimental stress in stirrups in failure zone (Fig. 8.36 to 8.39)

Although in all beams tested stirrups in the failure zone yielded, the amount of strain in the stirrups at failure reduced when the shear reinforcement percentage was increased to 0.84%. This can be seen in stirrup strains of B-2 and B-3 (Figs. 8.29 and 8.30). Increase in the shear strength with any further increase in shear reinforcement percentage would be limited due to web crushing before the yielding of steel. The results indicate that 0.84% is near the upper limit of web reinforcement for the composite beam section used. However, more experimental data is needed to establish the limit.

8.9 Horizontal Shear Strength

During testing of beams, the interface between the top slab and the precast beam in both shear spans was closely observed for any sign of horizontal shear failure. None of the beams failed due to horizontal shear failure. A displacement type transducer was positioned at the interface in the shear span of the main beam at a distance of 300 mm from the diaphragm to detect any relative displacement between top slab and precast beam. The displacement measured throughout the loading of most beams were very small, with the maximum movement recorded being 0.115 mm, which occurred in B-4. Hanson[21] found

that interface failure occurs when the slip exceeds 0.125 mm. Therefore, the horizontal shear strength of all eight beams were satisfactory in transferring the stresses developed due to applied loads. Even though application of prestress introduced additional forces across the interface, the results show that it had no effect at the ultimate load.

The horizontal shear stress at the interface at the failure load was calculated for eight beams using the ACI Building Code equation,

$$v_h = V_u / b_v d \qquad \text{.....Eqn. 8.6}$$

where b_v = width of the interface plane

v_h = horizontal shear stress

These values were compared with the horizontal shear strength values given in ACI Code, BS 5400 and BS 8110 for 'as-cast' surface with links. The measured and the code values are given in Table 8.12. It can be seen that the horizontal shear strength given by all three codes was very conservative with ACI Code being the most conservative.

(a) Beam B-1

(b) Beam B-2

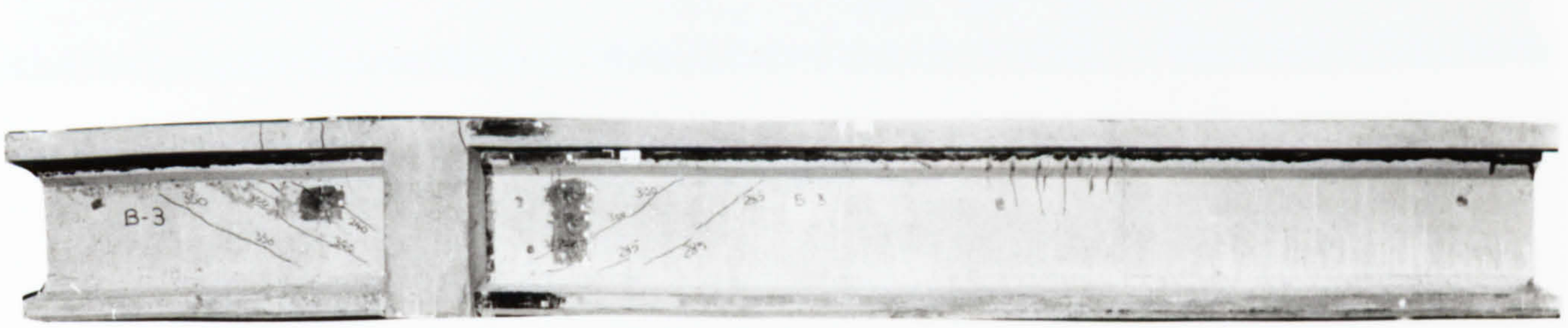

(c) Beam B-3

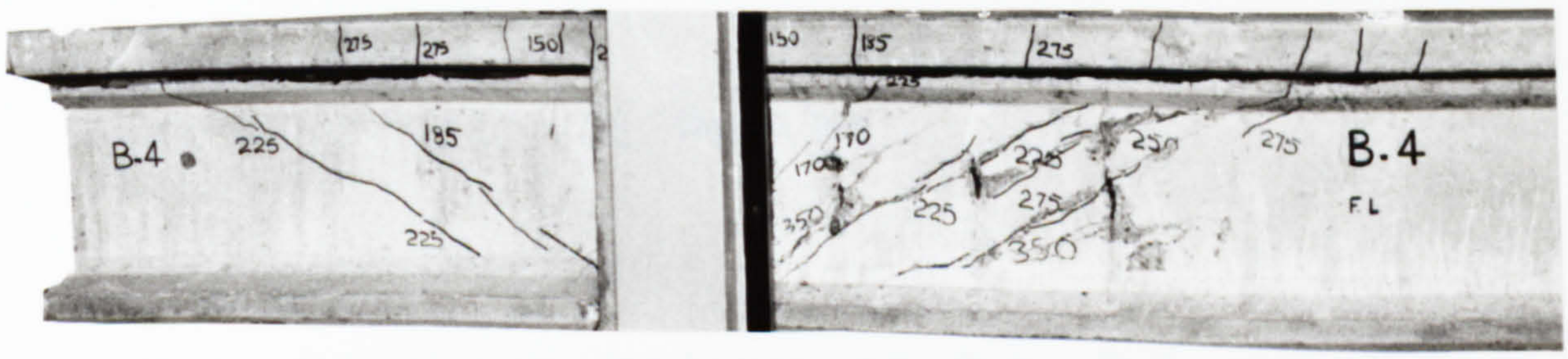

(d) Beam B-4

Plate 8.1 Crack Patterns of B-1, B-2, B-3 and B-4 at Failure.

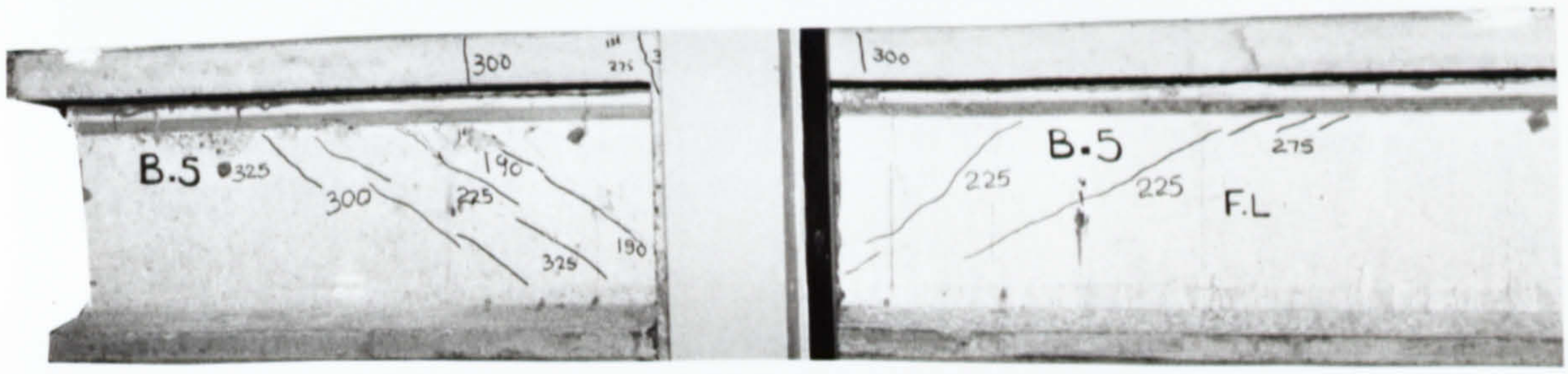

(a) Beam B-5

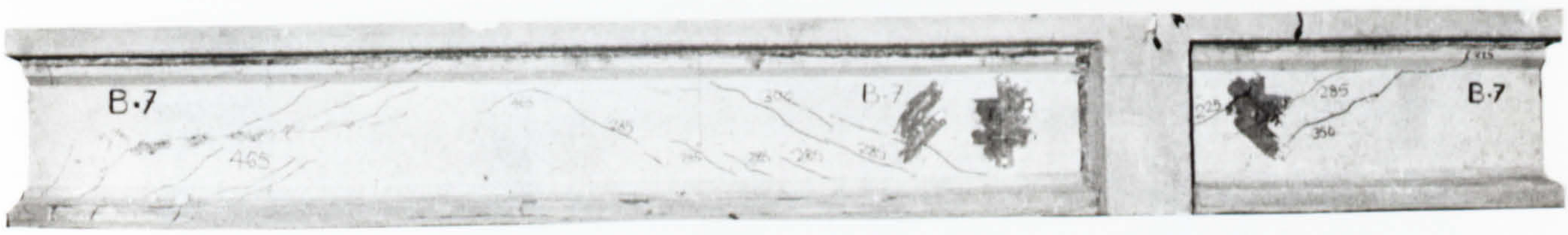

(b) Beam B-7

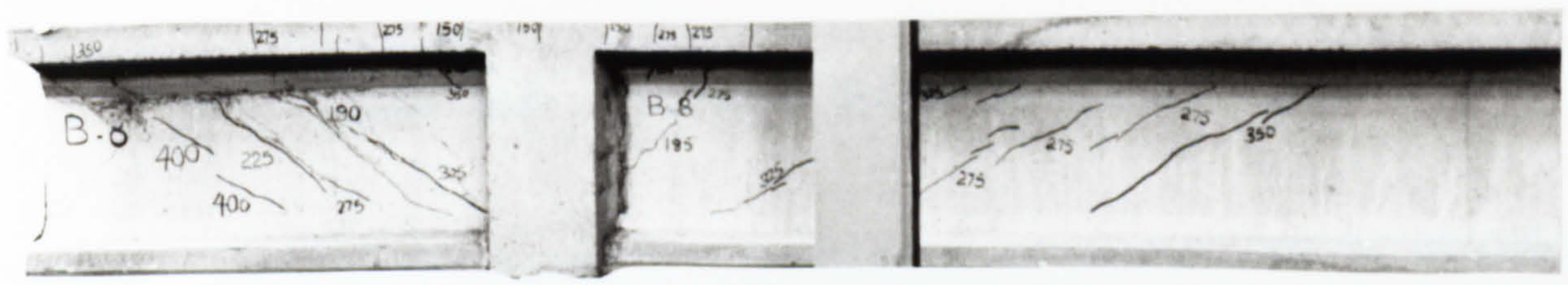

(c) Beam B-8

Plate 8.2 Crack Patterns of B-5, B-7 and B-8 at Failure

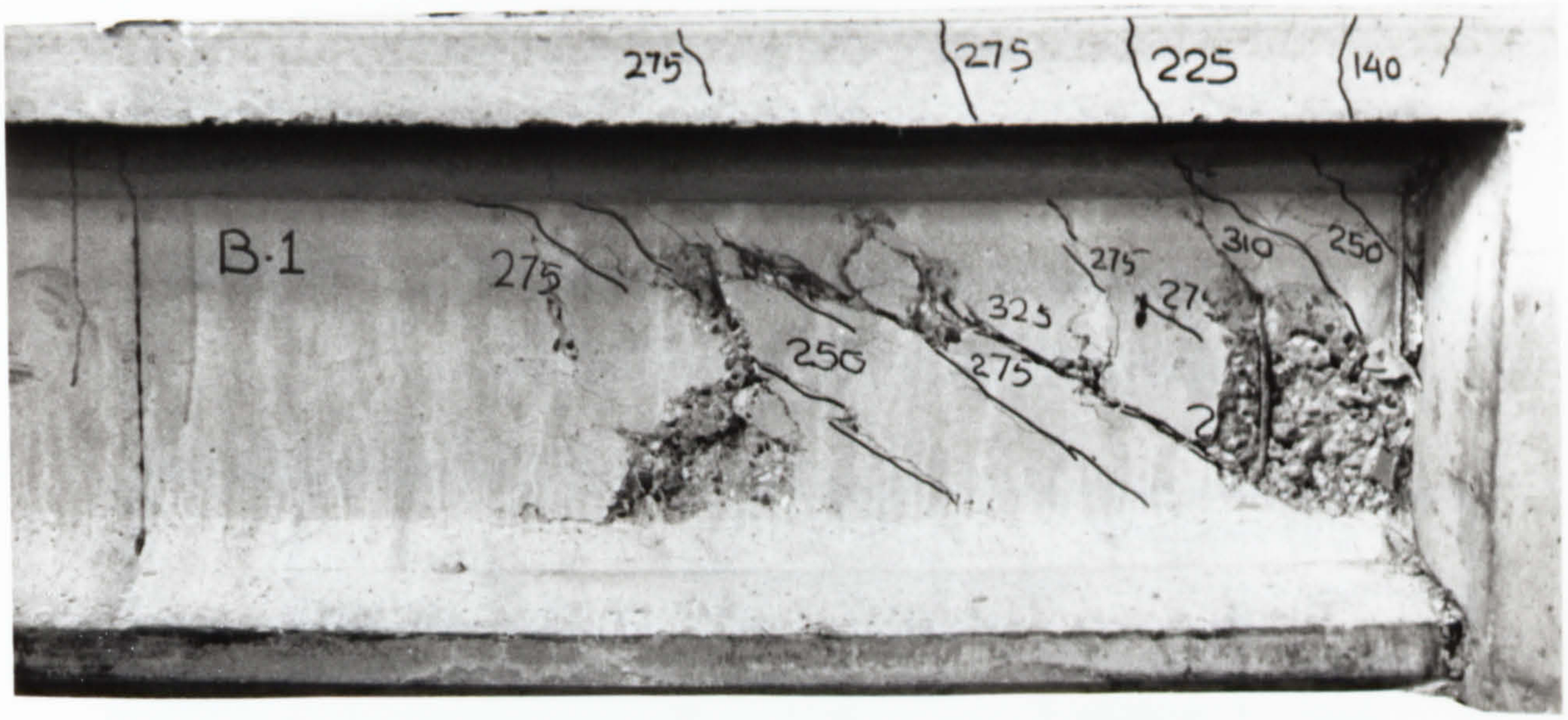

Plate 8.3 Failure Zone of Beam B-1

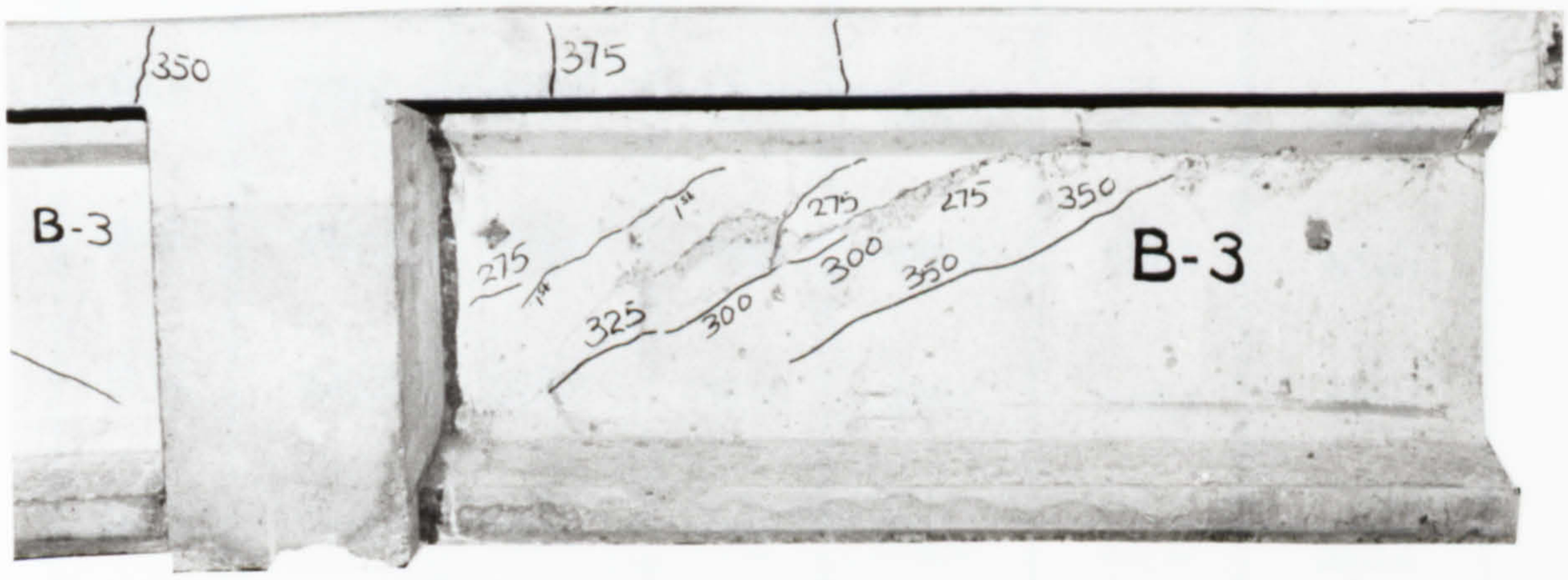

Plate 8.4 Failure Zone of Beam B-3

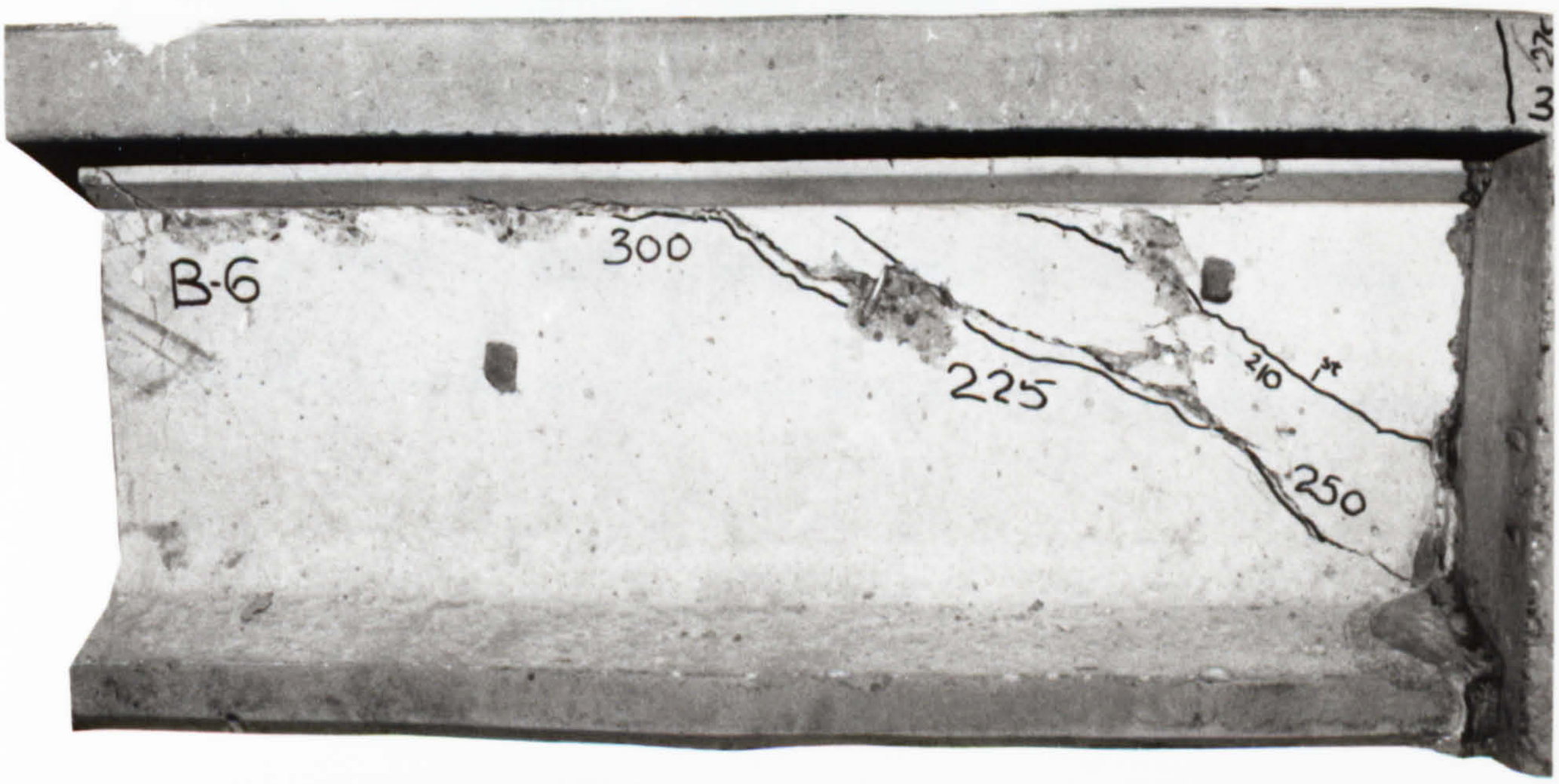

Plate 8.5 Failure Zone of Beam B-6

Table 8.1 : Measured Web Shear Cracking Load and Location of the Inclined Cracks

Beam No.	Total load at thefirst web crack (KN)	Total load at the first flexural crack (KN)	Short Beam (AB)		Main Beam (BC)	
			Web shear cracking load (KN)	Distance from support to the first crack (mm)	Web shear cracking load (KN)	Distance from support to the first crack (mm)
B -1	160.0	125.0	69.5	325.0	127.0	150.0
B -2	200.0	265.0	86.2	400.0	139.5	230.0
B -3	240.0	350.0	103.0	240.0	144.5	345.0
B - 4	170.0	90.0	77.5	175.0	87. 0	350.0
B - 5	190.0	275.0	82.0	260.0	114.5	220.0
B - 6	210.0	250.0	91.0	235.0	114.5	210.0
B - 7	225.0	325.0	80.5	210.0	110.0	750.0
B - 8	180.0	150.0	66.5	375.0	71.5	170.0

Table 8.2 Experimental Principal Tensile Stress near the Inclined Cracking Load

Beam	Principal Stress		Splitting Cylinder Tensile Strength	British Codes $0.36\sqrt{f_{cu}}$	Expeimental Principal Compressive Stress
	Experimental	Calculated			
	N/mm^2	N/mm^2	N/mm^2	N/mm^2	N/mm^2
B-1	4.52	3.50	3.67	2.79	-15.23
B-2	4.72	3.37	3.41	2.80	-13.84
B-3	4.88	3.54	3.46	2.78	-18.15
B-4	2.80	2.63	3.60	2.80	-10.28
B-5	2.98	2.18	3.36	2.64	-13.74
B-6	4.35	2.82	3.28	2.73	-14.70
B-7	4.12	3.66	3.27	2.63	-12.00
B-8	3.35	3.60	3.15	2.64	-10.30
Mean	3.96	3.16	3.40	2.73	-13.53

Table 8.3 Angle of Inclination of Web Shear Cracks

Beam	Slab Type	Measured Angle of Inclination (Deg.)			Calculated Angle of Inclination (Deg)
		First Web Shear Crack	Average		
			Short Beam	Main Beam	
B-1	RC	35	32	31	33
B-2	PPC	32	30	30	29
B-3	FPC	30	28	30	25
B-4	RC	35	35	35	29
B-5	PPC	33	34	35	28
B-6	PPC	38	30	30	26
B-7	PPC	32	30	30	26
B-8	RC	45	35	34	28

Note:

RC - Reinforced Concrete Slab

PPC - Partially Prestressed Slab

FPC - Fully Prestressed Slab

Beam	f_{cu} (N/mm^2)	Total Prestress at Centroid (N/mm^2)	Measured Web Shear Cracking Load (kN)		Calculated Web Shear Cracking Load (kN)					
			Short Beam	Main Beam	BS 5400 BS 8100	ACI Code	CEB-FIP Code	Using Principal Stress Equation (Eqn. 7.6) At Centroid	Using Principal Stress Equation (Eqn. 7.6) At Top of Web	Precast Beam Section
B-1	60.2	4.55	69.5	127.0	79.3	72.1	42.3	93.9	83.0	70.3
B-2	60.4	7.30	86.2	139.5	92.0	90.4	78.2	109.2	98.1	75.0
B-3	59.7	9.05	103.0	144.5	98.5	102.0	77.6	117.1	106.5	77.7
B-4	59.6	4.55	77.5	87.0	79.0	71.9	41.0	93.1	82.5	70.1
B-5	54.0	7.30	82.0	114.5	88.8	88.1	70.6	105.4	95.1	72.5
B-6	57.8	7.30	82.0	114.5	90.6	89.1	76.0	107.5	97.0	74.0
B-7	53.5	7.30	80.5	110.0	88.8	87.9	70.5	105.2	95.0	72.3
B-8	53.6	4.55	66.5	71.5	76.5	69.6	37.6	90.5	80.1	67.8

Table 8.4 Measured and Calculated Web Shear Cracking Load for Shear Test Series

(Partial safety factors were excluded)

Table 8.5 : Ratio of Measured Web Cracking Load to Calculated Web Cracking Load for Main Beam (Span BC)

Beam No.	Ratio $\frac{\text{Measured Web Shear Cracking Load}}{\text{Calculated Web Shear Cracking Load}}$					
	British Codes.	ACI Building Code	CEB - FIP Code	Using sectional properties		Precast section only (at centroid)
				At centroid	At top of Web	
B - 1	1.60	1.76	3.0	1.35	1.53	1.80
B -2	1.51	1.54	1.78	1.28	1.42	1.86
B -3	1.46	1.42	1.86	1.23	1.35	1.85
B -4	1.10	1.21	2.12	0,93	1.05	1.24
B -5	1.29	1.30	1.62	1.08	1.20	1.58
B- 6	1.26	1.28	1.50	1.065	1.18	1.55
B -7	1.23	1.25	1.56	1.045	1.16	1.52
B- 8	0.93	1.03	1.90	0.79	0.89	1.05
Mean	1.30	1.35	1.92	1.096	1.12	1.56

(Note : All partial safety factors were excluded)

Beam	Ratio of $\frac{\text{Measured } V_{co}}{\text{Calculated } V_{co}}$								
	Including V_p in V_{co}					Excluding V_p in V_{co}			
	BS 8110 BS 5400	ACI Code	CEB-FIP Code	Equation 7.6 at Top of Web	Precast Section	BS 8110 BS 5400	ACI Building Code	CEB-FIP Model Code	Precast Section
B-1	0.87	0.96	1.64	0.87	0.99	0.96	1.03	2.05	1.09
B-2	0.94	0.95	1.10	0.91	1.15	1.01	1.00	1.23	1.26
B-3	1.04	1.01	1.33	1.01	1.32	1.12	1.06	1.49	1.45
B-4	0.98	1.08	1.84	0.98	1.10	1.08	1.15	2.38	1.38
B-5	0.92	0.93	1.16	0.90	1.13	1.00	0.98	1.32	1.22
B-6	1.00	1.08	1.19	0.98	1.23	1.09	1.14	1.35	1.35
B-7	0.91	1.92	1.14	0.88	1.11	0.98	0.97	1.29	1.23
B-8	0.87	0.96	1.73	0.87	0.98	0.96	1.03	2.28	1.09
Mean	0.95	0.98	1.40	0.92	1.12	1.03	1.04	1.67	1.26

Table 8.6 Ratio of Measured Web Shear Cracking Load to Calculated Web Shear Cracking Load for Short Beam (AB)

(Partial Safety Factors were Excluded)

Table 8.7 : Measured and Calculated Flexural Shear Cracking Load for Flexural Test Series Beams

Beam No.	f_{cu} (N/mm)	Measured V_{cr} (kN)	Calculated V_{cr} (kN)		
			BS 8110	ACI	BS 8110* (Precast)
A-1	66.1	35.0	25.5	29.7	32.7
A-2	67.3	45.0	42.8	61.2	64.0
A-3	60.9	75.0	59.5	83.2	87.0

Note : * - Considering stress at the top of precast beam for M_o

Table 8.8 Ratio of Measured to Calculated Flexural Shear Cracking Load for Flexural Test Series Beams

Beam No.	Ratio of $\frac{\text{Measured } V_{cr}}{\text{Calculated } V_{cr}}$		
	BS 8110	ACI Code	BS 8110* (Precast Section)
A-1	1.37	1.18	1.07
A-2	1.05	0.73	0.70
A-3	1.26	0.90	0.86
Mean	1.22	0.94	0.87

Note :- * - Considering stress at the top of precast beam for M_o

Table 8.9 Observed and Predicted Web Crushing Load

Beam	Measured Web Crushing Load (kN)	Predicted Web Crushing Strength (kN)				
		BS 8110	BS 5400	ACI Code	CEB-FIP Code	
					Standard	Accurate
B-1	215.0	112.0	130.5	148.5	215.0	196.4
B-2	189.0	112.0	130.5	164.2	189.0	172.6
B-3	193.0	112.0	130.0	173.5	193.0	176.3
B-4	190.0	112.0	130.0	148.0	190.0	173.5
B-5	166.0	112.0	124.1	157.5	116.0	151.6
B-6	153.0	112.0	128.4	161.2	153.0	140.0
B-7	124.0	112.0	123.5	156.9	124.0	113.3
B-8	152.0	112.0	123.7	141.5	183.0	167.2

Table 8.10 : Ratio of Observed Web Crushing Load to Predicted Web Crushing Load.

Beam	Ratio = Observed Web Crushing Load / Predicted Web Crushing Load				
	BS 8110	BS 5400	ACI Building Code	CEB - FIP Standard	CEB - FIP Accurate
B - 1	1.92	1.65	1.45	1.00	1.09
B - 2	1.69	1.45	1.15	0.87	0.95
B - 3	1.72	1.48	1.11	0.91	0.99
B - 4	1.69	1.45	1.28	0.89	0.97
B - 5	1.48	1.27	1.05	0.86	0.94
B - 6	1.36	1.17	0.95	0.74	0.81
B - 7	1.11	0.95	0.79	0.65	0.71
B - 8	1.35	1.23	1.08	0.83	0.91
Mean	1.54	1.33	1.12	0.85	0.9

Table 8.11 Comparison of Shear Force Carried by Concrete According to Truss Analogy and Inclined Cracking Load

Beam	$r = \frac{A_{sv}}{b\,s}$	V_s (kN)	V_u (kN)	$V_u - V_s$ (kN)	$\frac{(V_u - V_s)}{V_c}$
B-1	0.0084	111.3	215.0	103.7	0.82
B-2	0.0084	111.3	189.0	77.7	0.90
B-3	0.0084	111.3	193.0	81.7	0.79
B-4	0.0053	69.6	190.0	120.4	1.38
B-5	0.0053	69.6	166.0	96.4	1.17
B-6	0.0042	55.6	153.0	97.4	1.07
B-8	0.0053	69.6	152.0	82.4	1.23
				Mean	1.05

Table 8.12. Experimental Horizontal Shear Stress and Horizontal Shear Strength Given In Codes

Beam	V_u (kN)	$v_h = \frac{V_u}{b_v d}$ N/mm^2	Horizontal shear strength given in codes N/mm^2		
			BS 5400	BS 8110	ACI Code
B-1	215.0	3.84	1.88	2.00	0.55
B-2	225.0	4.03	1.88	2.00	0.55
B-3	230.0	4.11	1.88	2.00	0.55
B-4	190.0	3.40	1.80	2.00	0.55
B-5	198.0	3.50	1.80	2.00	0.55
B-6	183.0	3.27	1.88	2.00	0.55
B-7	181.0	3.24	1.80	2.00	0.55
B-8	168.0	3.00	1.80	2.00	0.55

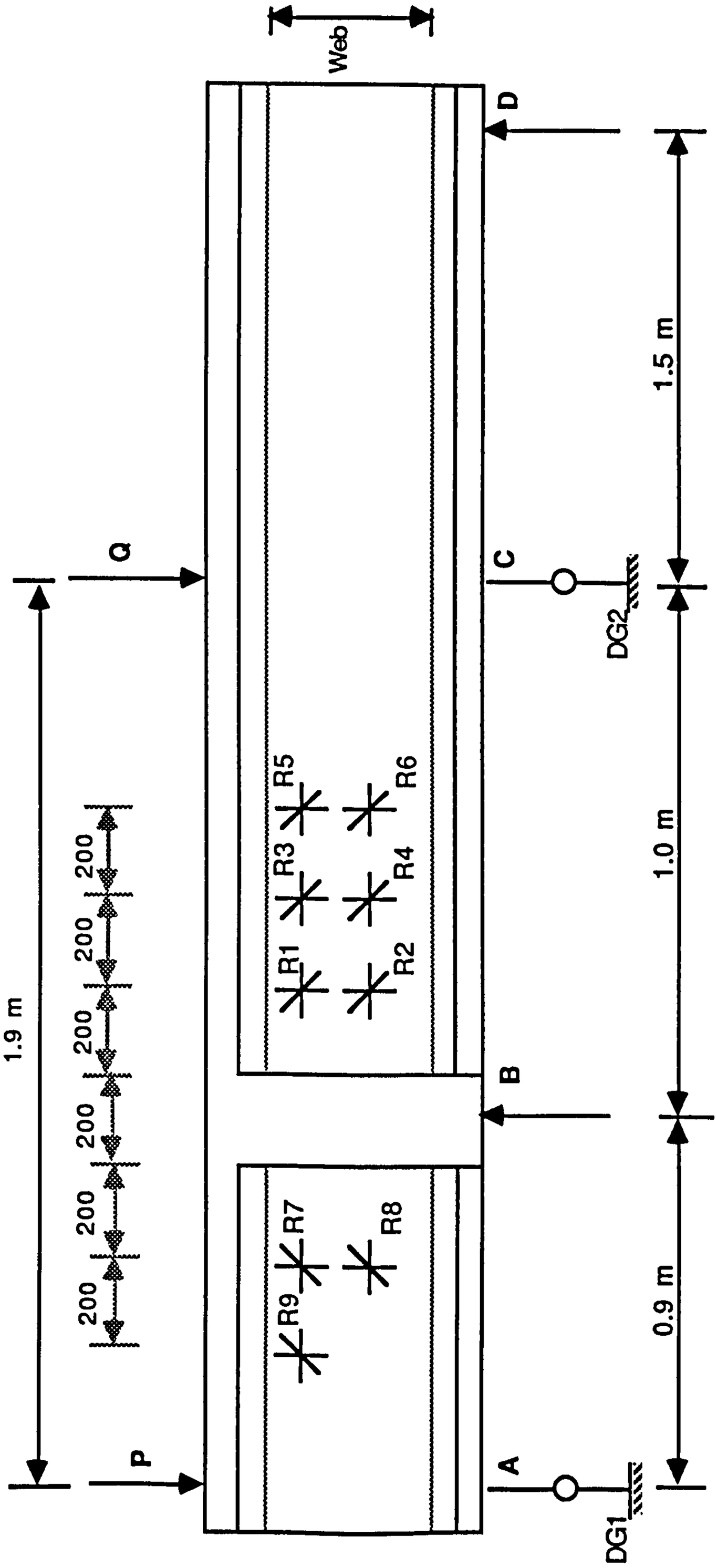

Fig. 8.1 : Location of Strain Rosettes and Deflection Gauges for Shear Test Series Beams

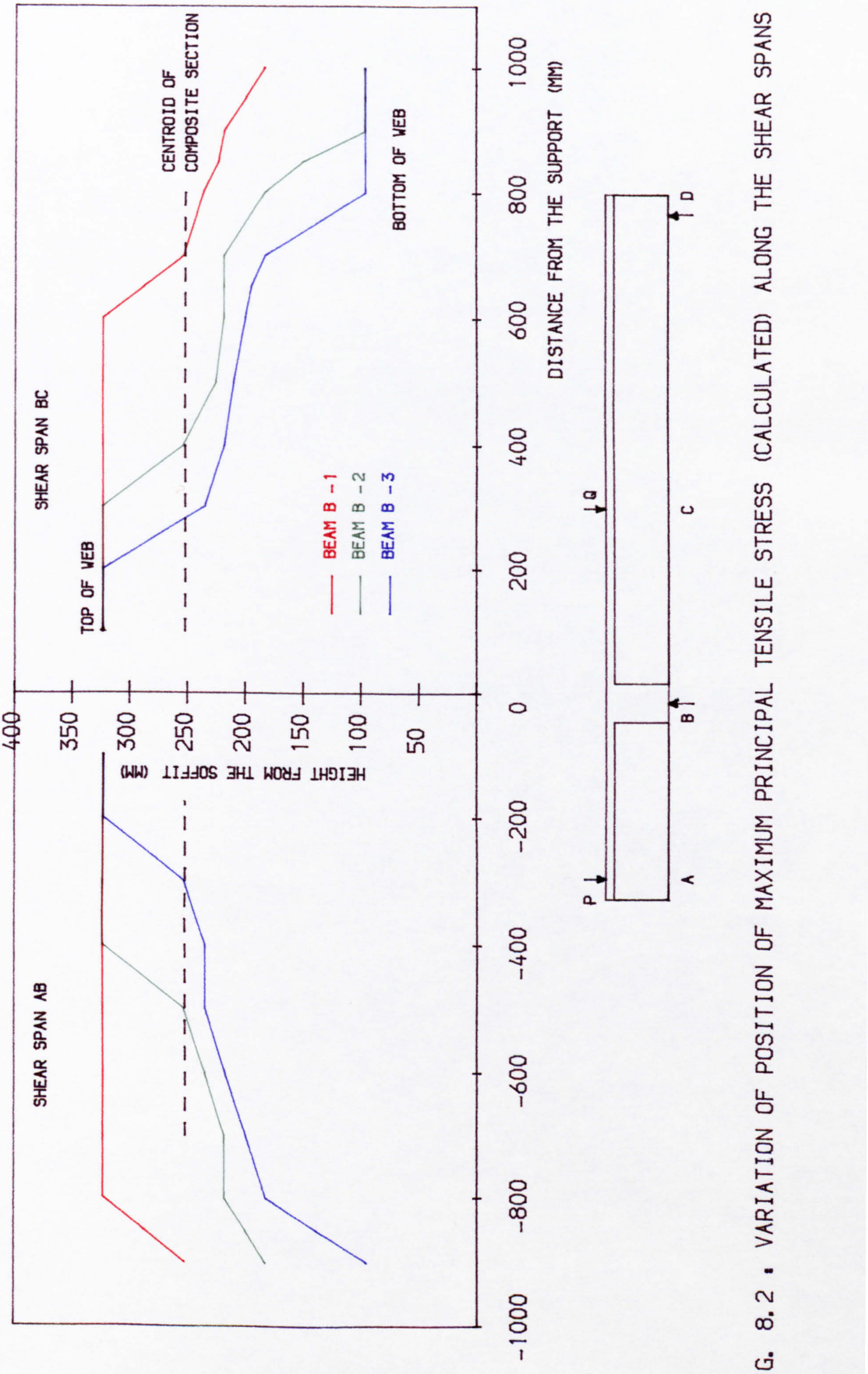

FIG. 8.2 : VARIATION OF POSITION OF MAXIMUM PRINCIPAL TENSILE STRESS (CALCULATED) ALONG THE SHEAR SPANS

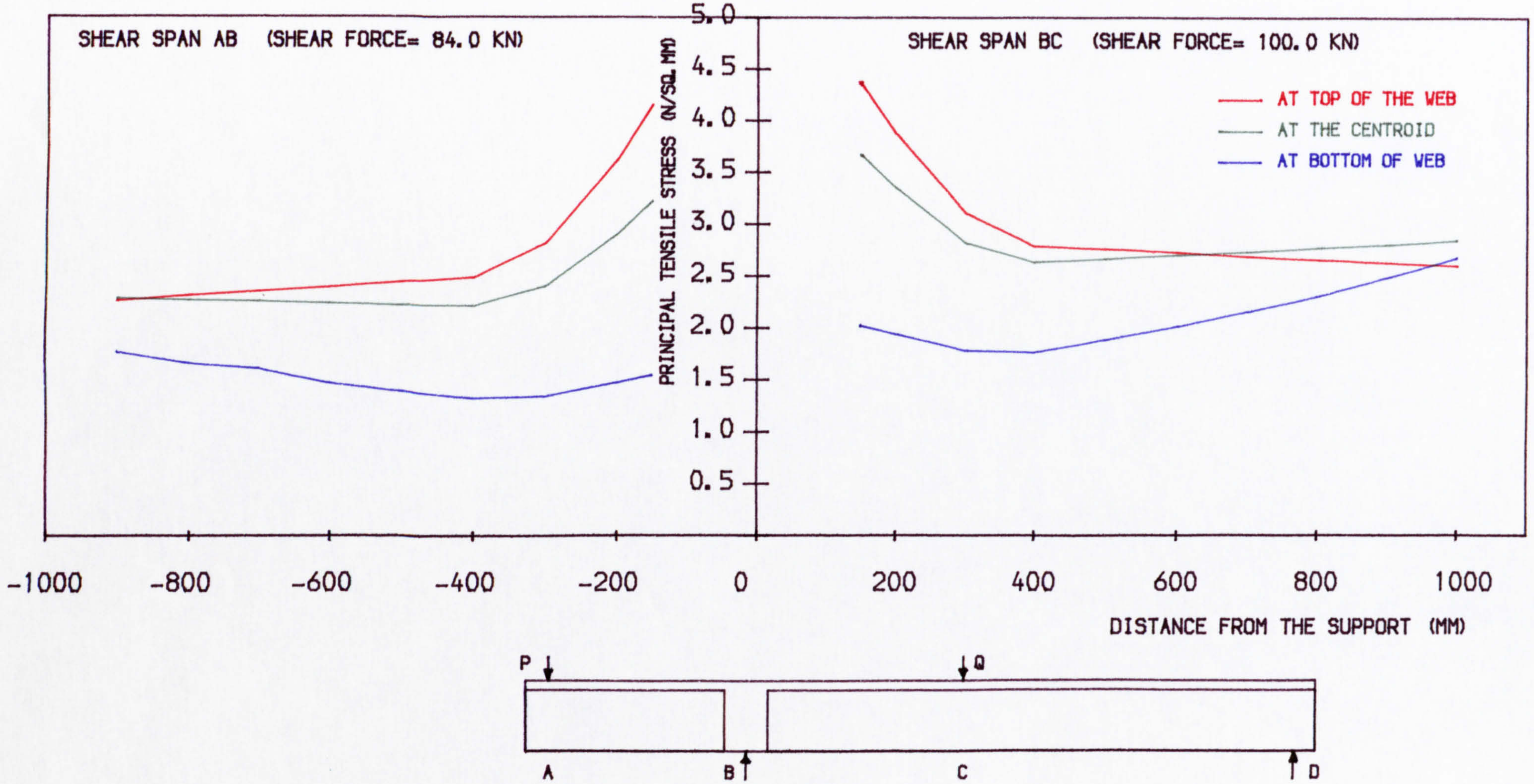

FIG. 8.3. VARIATION OF PRINCIPAL TENSILE STRESS (CALCULATED) ALONG THE SHEAR SPANS (BEAM B-1)

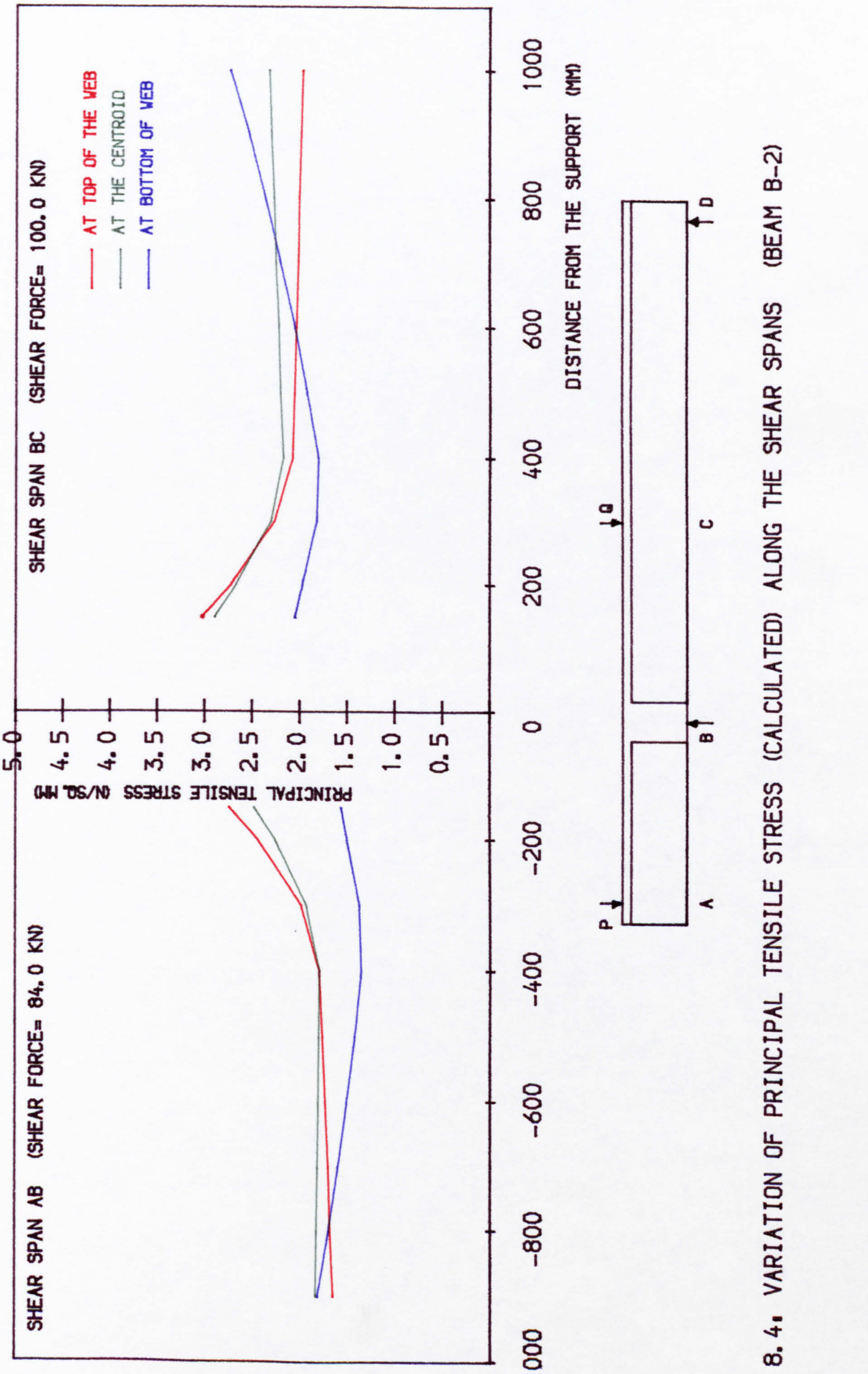

FIG. 8.4: VARIATION OF PRINCIPAL TENSILE STRESS (CALCULATED) ALONG THE SHEAR SPANS (BEAM B-2)

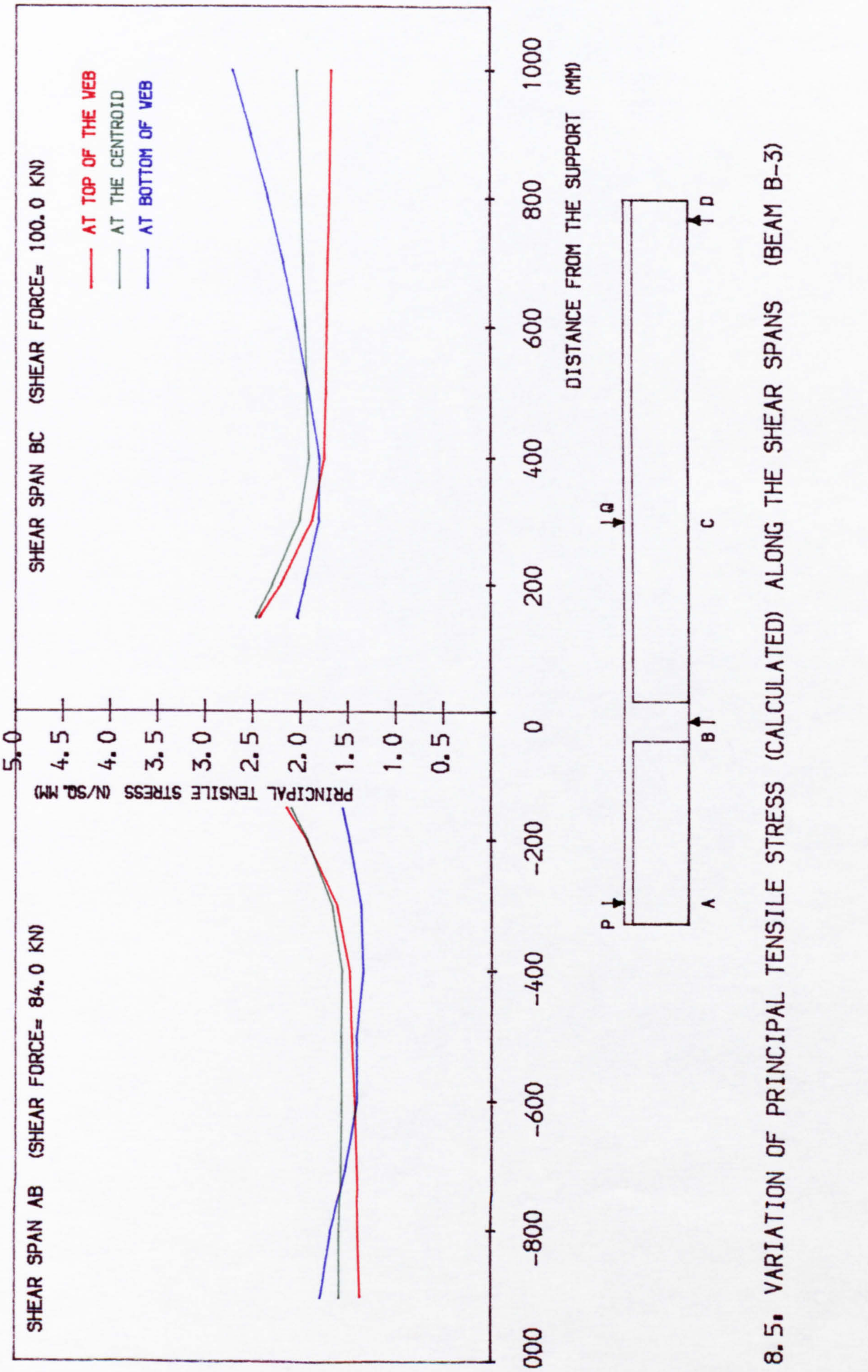

FIG. 8.5. VARIATION OF PRINCIPAL TENSILE STRESS (CALCULATED) ALONG THE SHEAR SPANS (BEAM B-3)

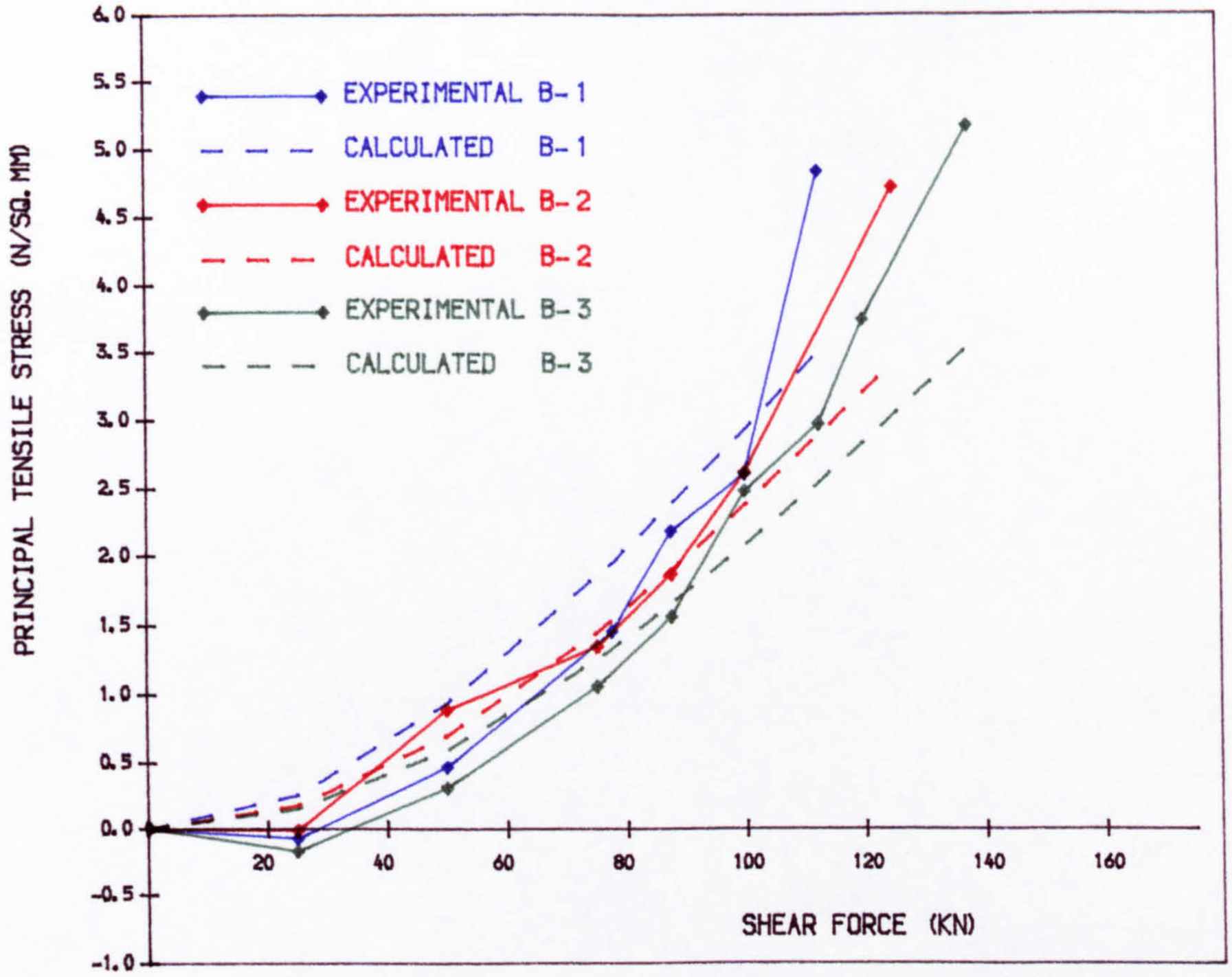

FIG. 8.6 : VARIATION OF PRINCIPAL TENSILE STRESS DETERMINED FROM ROSETTE 1 WITH SHEAR FORCE IN BEAM B-1, B-2 AND B-3

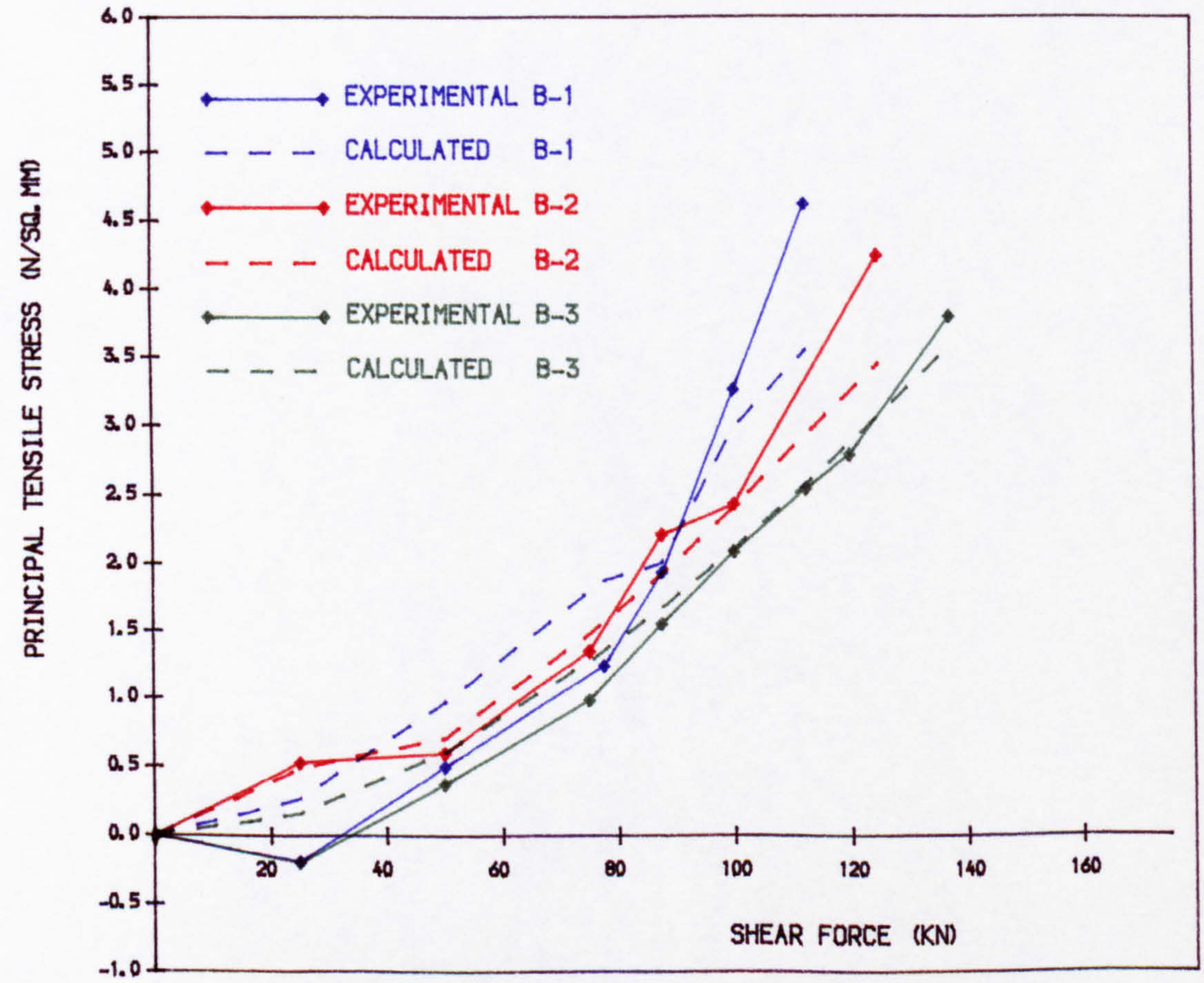

FIG. 8.7 : VARIATION OF PRINCIPAL TENSILE STRESS DETERMINED FROM ROSETTE 5 WITH SHEAR FORCE IN BEAM B-1, B-2 AND B-3

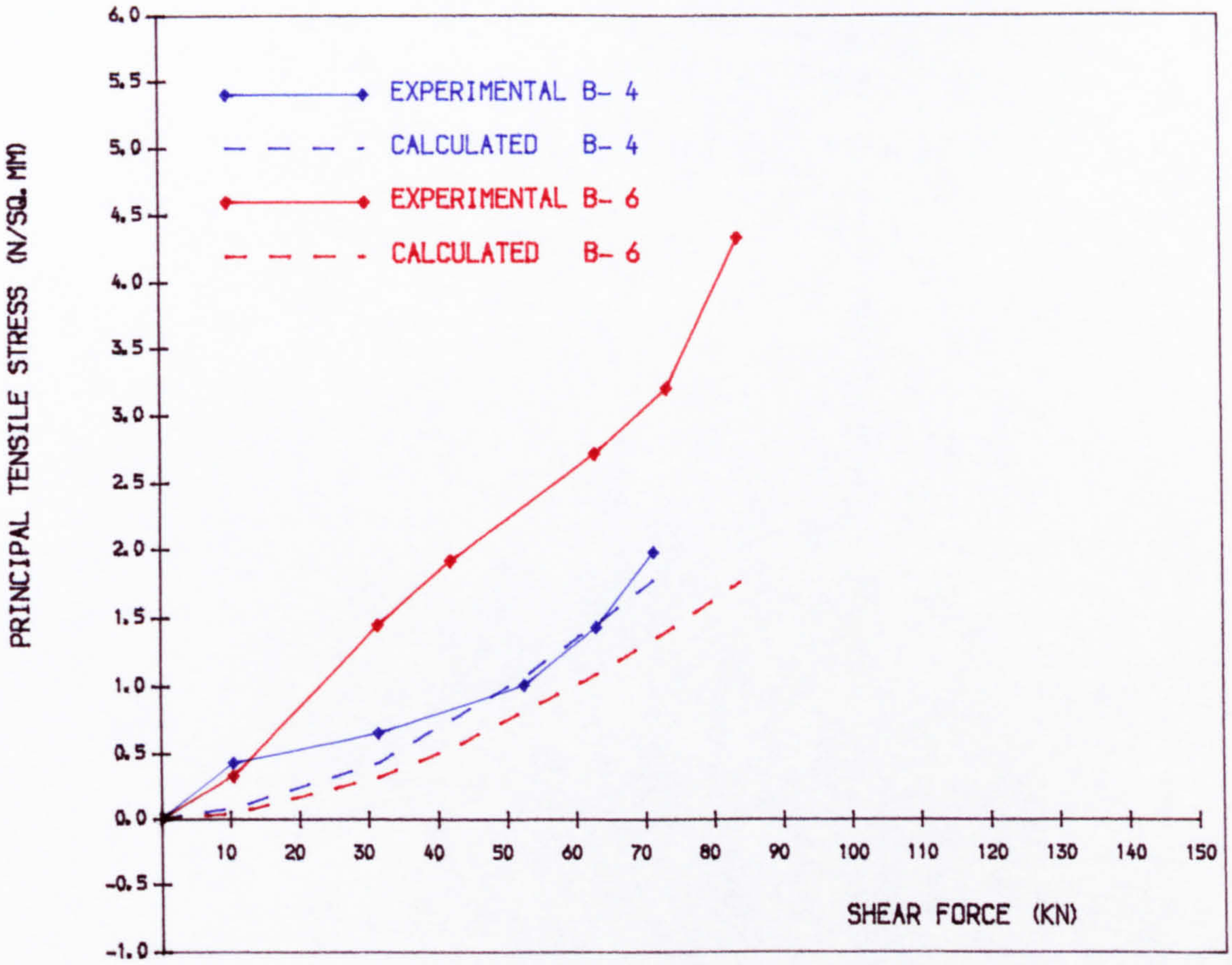

FIG. 8.8 . VARIATION OF PRINCIPAL TENSILE STRESS DETERMINED FROM ROSETTE 7

WITH SHEAR FORCE IN BEAM B-4 AND B-6

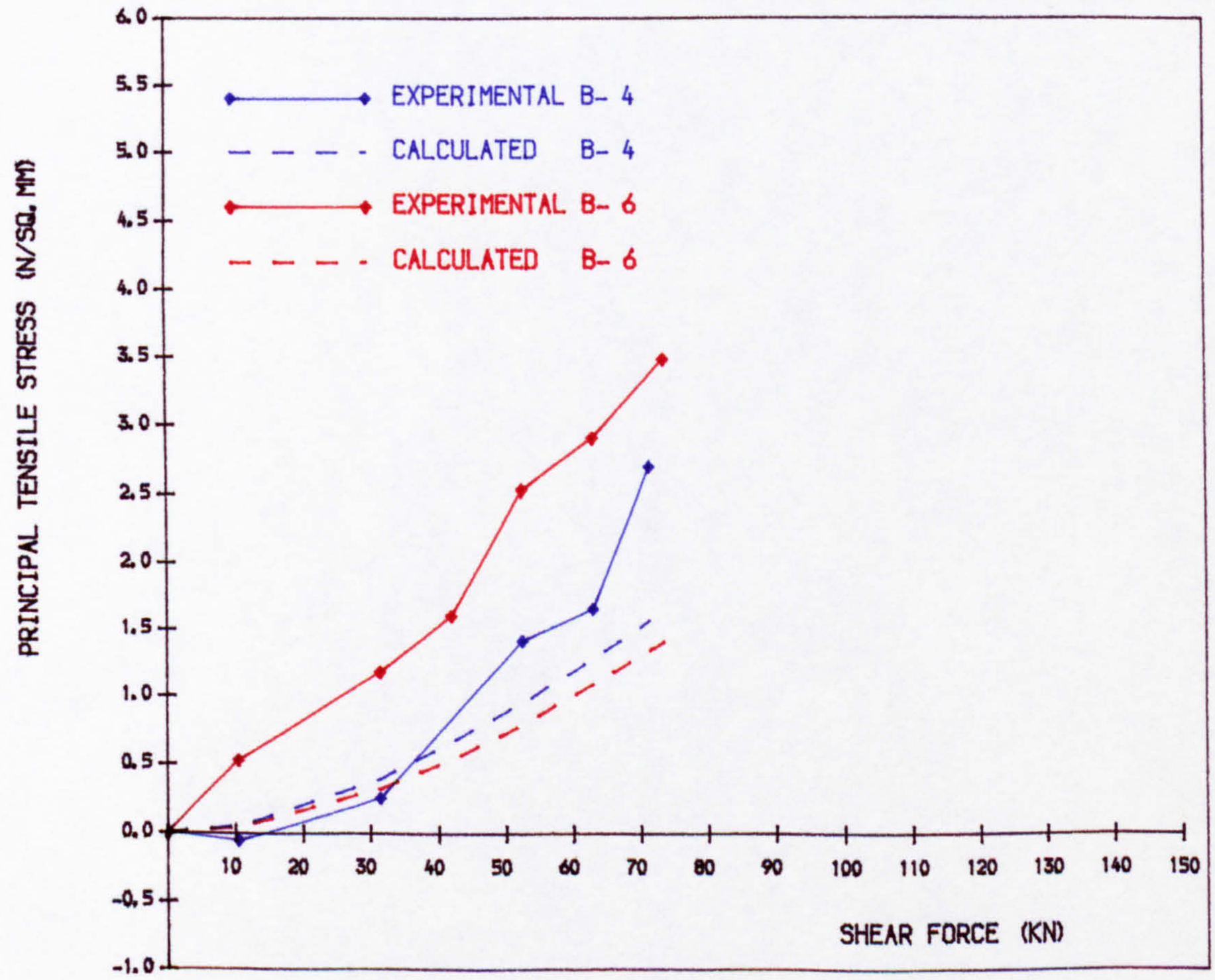

FIG. 8.9 . VARIATION OF PRINCIPAL TENSILE STRESS DETERMINED FROM ROSETTE 8

WITH SHEAR FORCE IN BEAM B-4 AND B-6

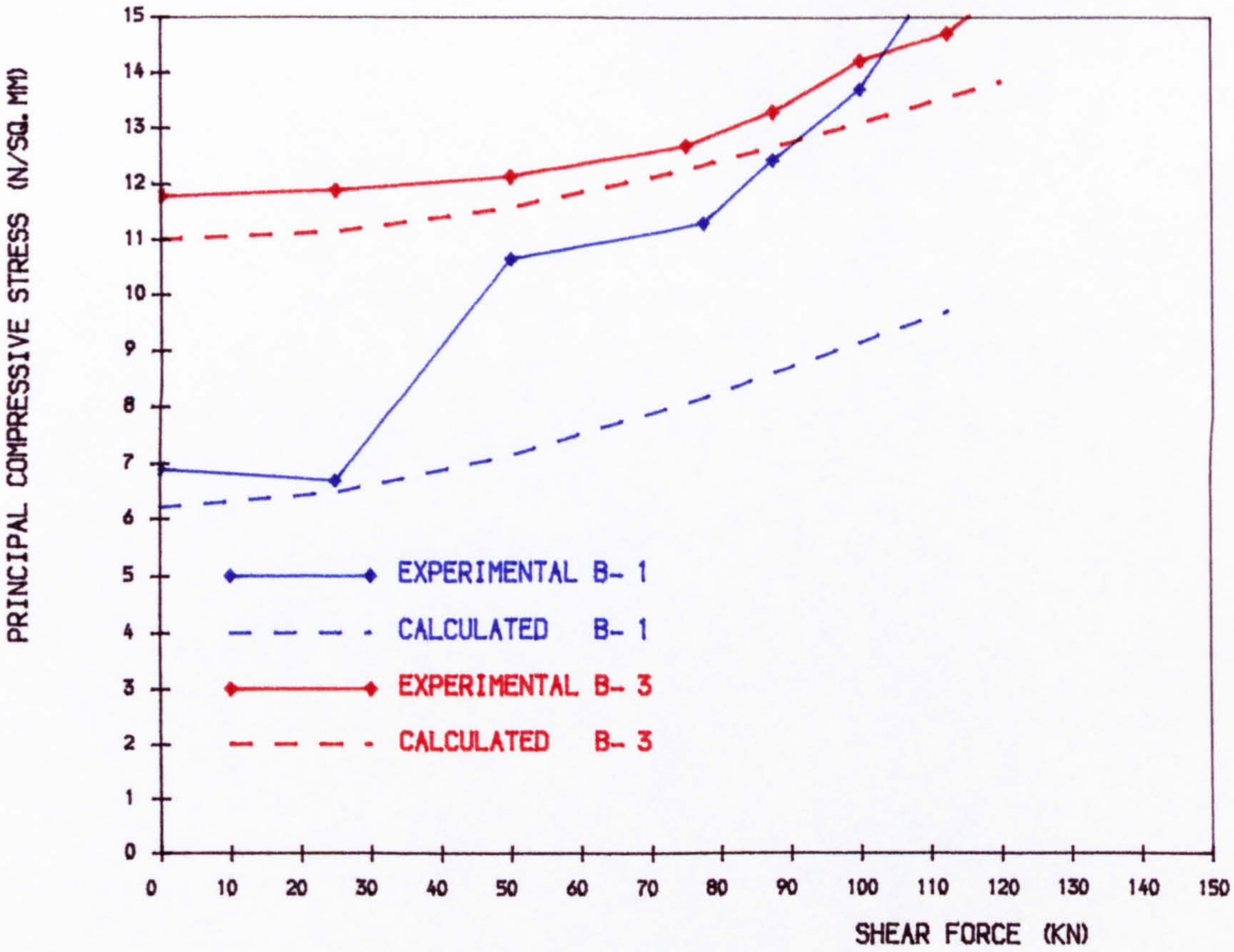

FIG. 8.10 : VARIATION OF PRINCIPAL COMPRESSIVE STRESS DETERMINED FROM ROSETTE 1 WITH SHEAR FORCE IN BEAM B-1 AND B-3

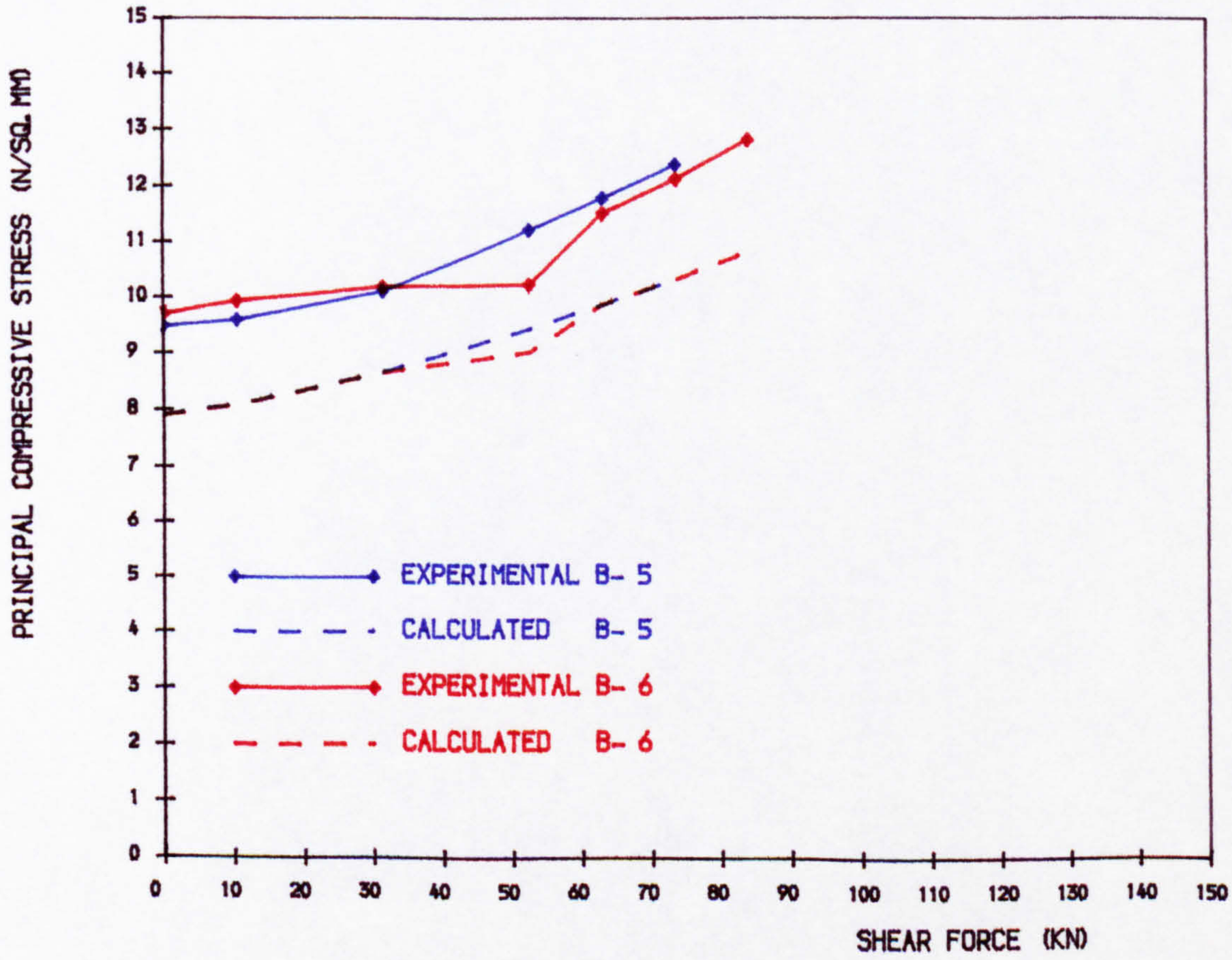

FIG. 8.11 : VARIATION OF PRINCIPAL COMPRESSIVE STRESS DETERMINED FROM ROSETTE 7 WITH SHEAR FORCE IN BEAM B-5 ANDB-6

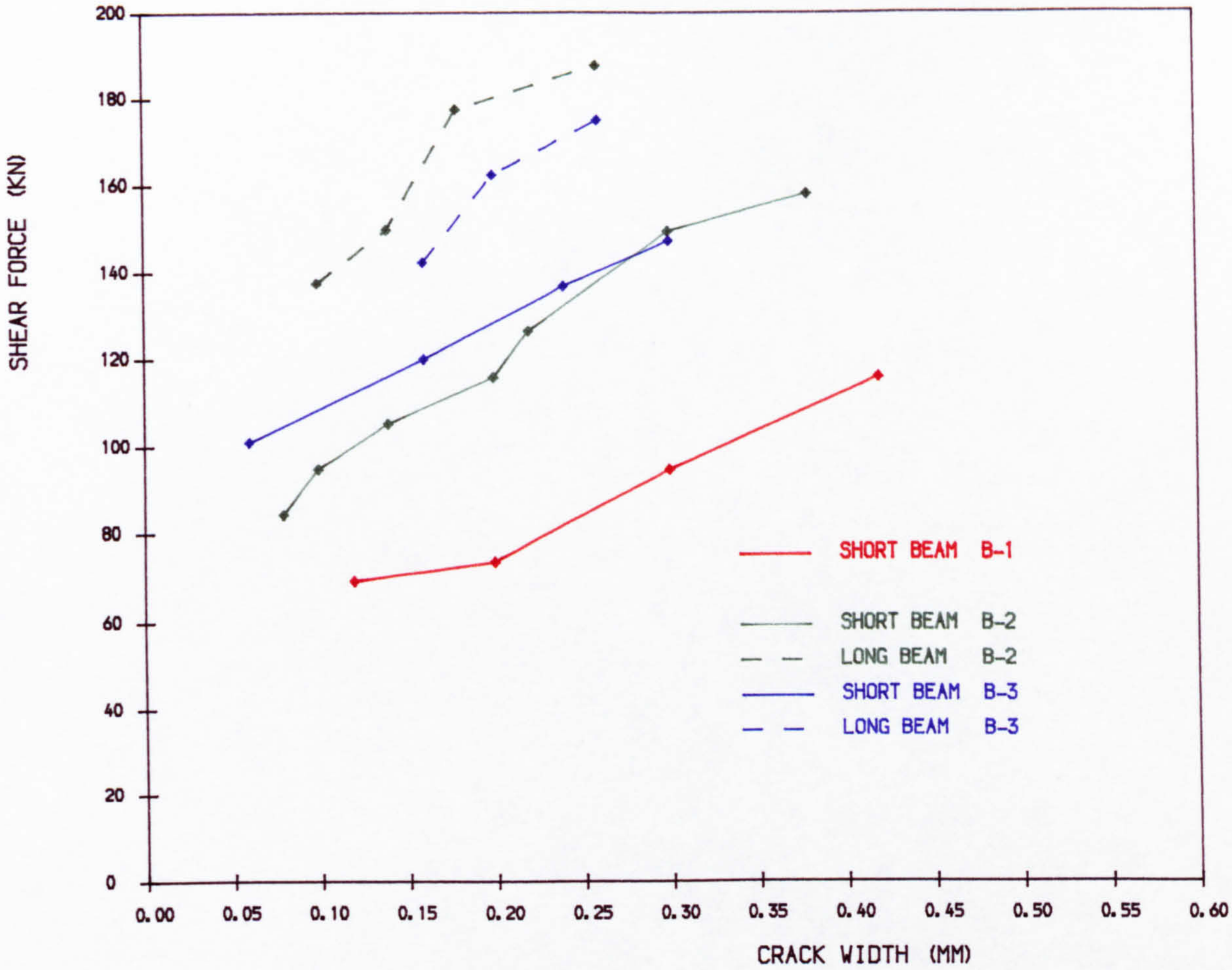

FIG. 8.12 : LOAD VS MAXIMUM CRACK WIDTH FOR BEAMS B-1, B-2 AND B-3

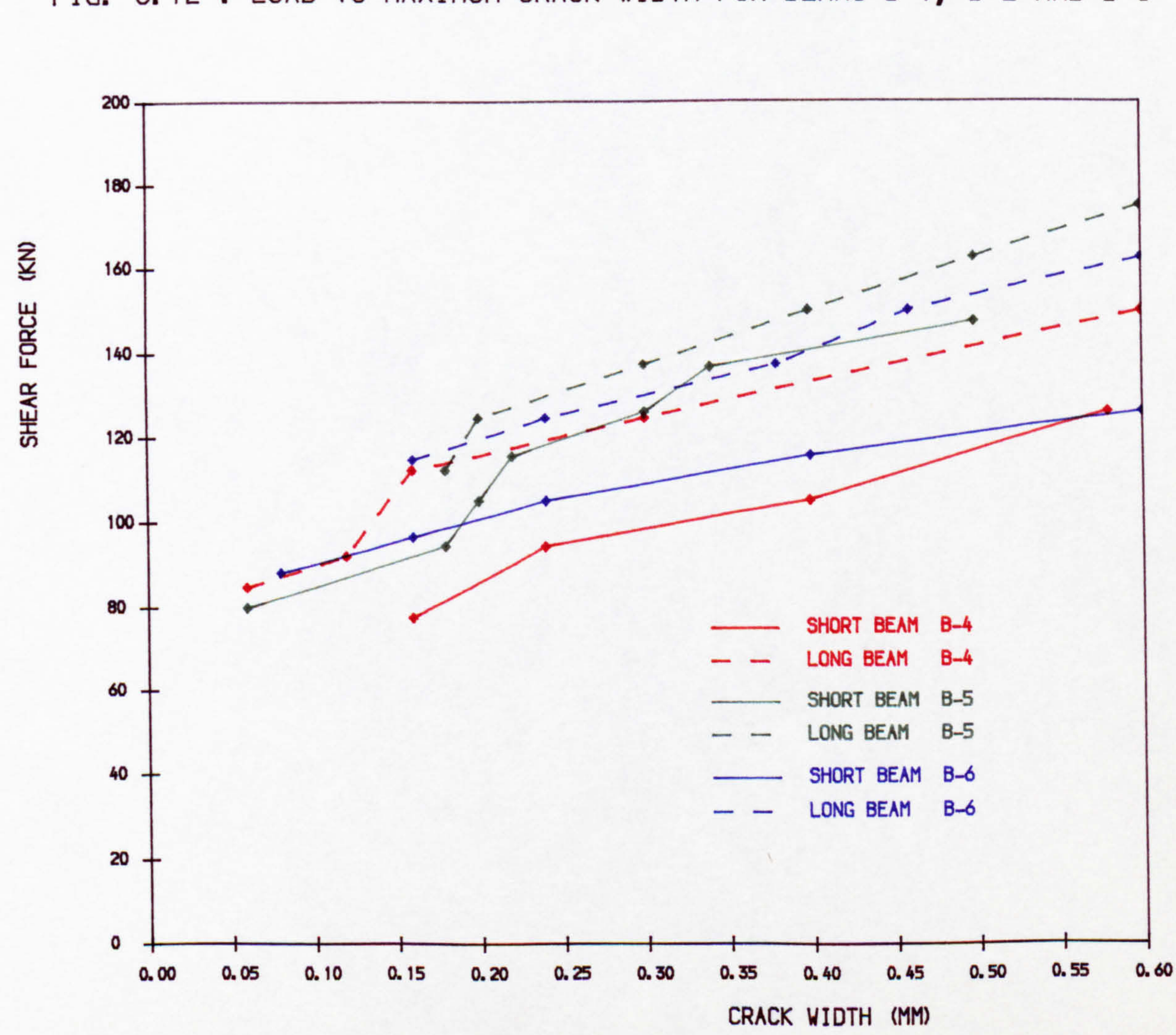

FIG. 8.13 : LOAD VS MAXIMUM CRACK WIDTH FOR BEAMS B-4, B-5 AND B-6

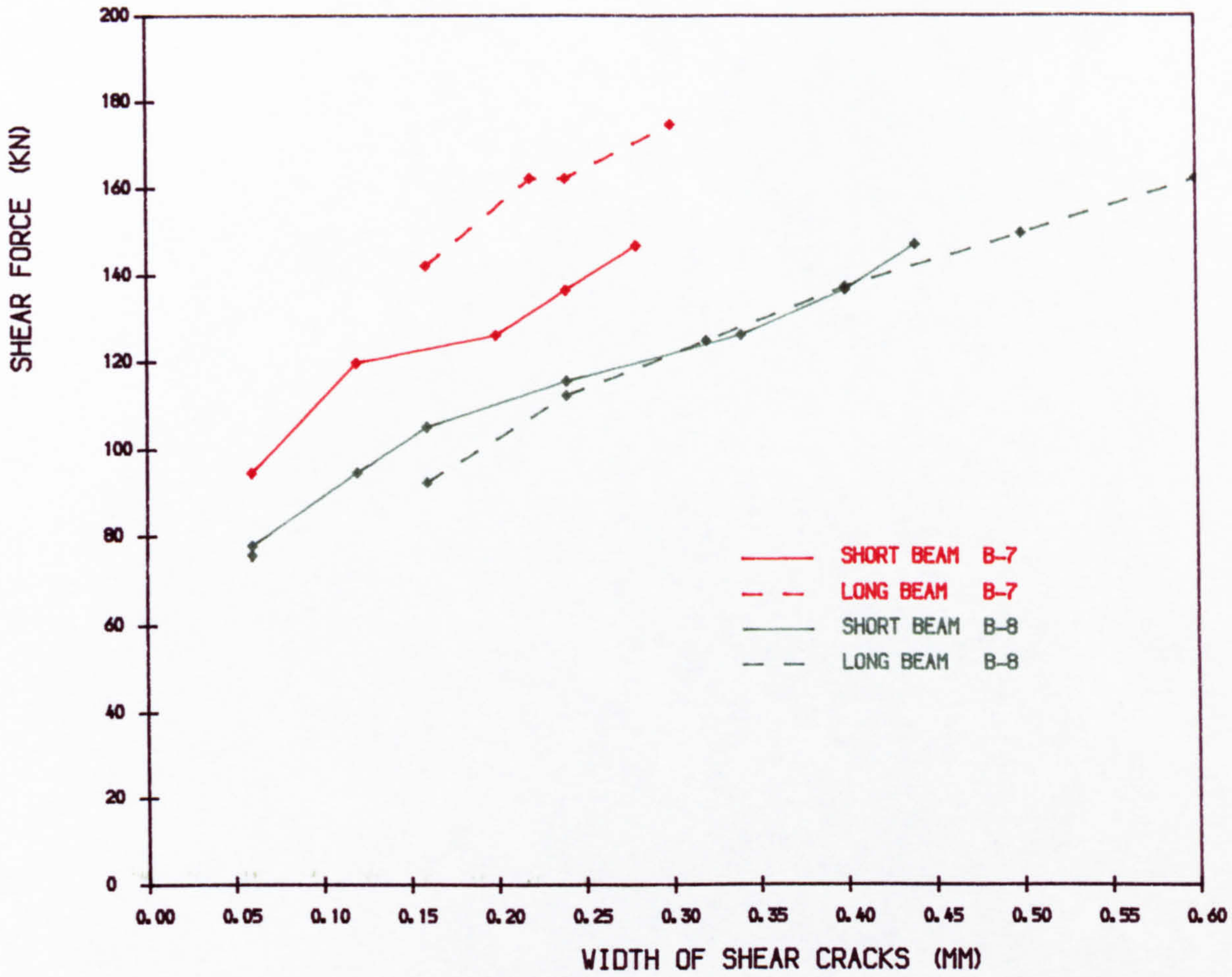

FIG. 8.14 : LOAD VS MAXIMUM CRACK WIDTH FOR BEAMS B-7 AND B-8

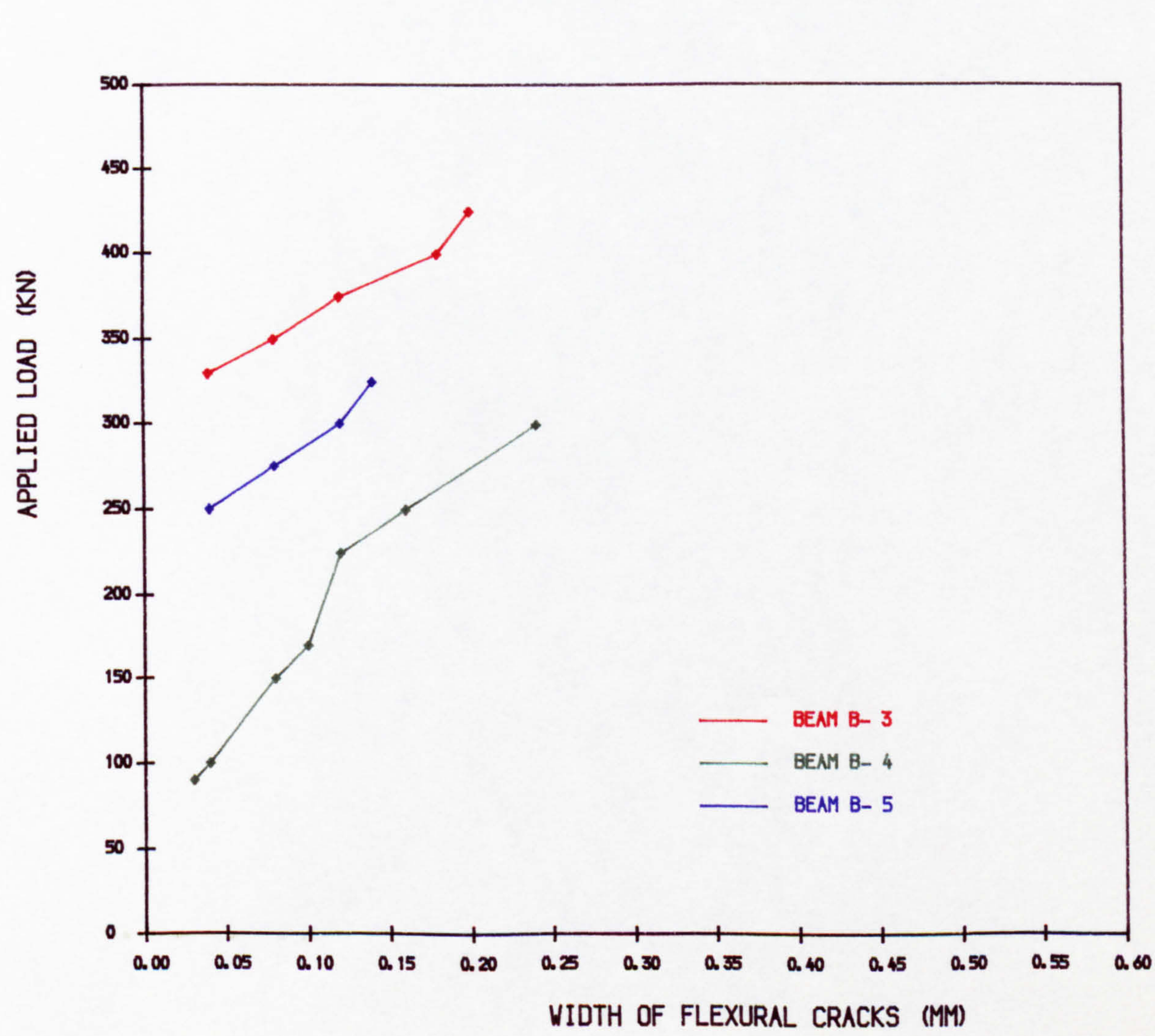

FIG. 8.15 : LOAD VS WIDTH OF FLEXURAL CRACKS FOR B-3, B-4 AND B-5

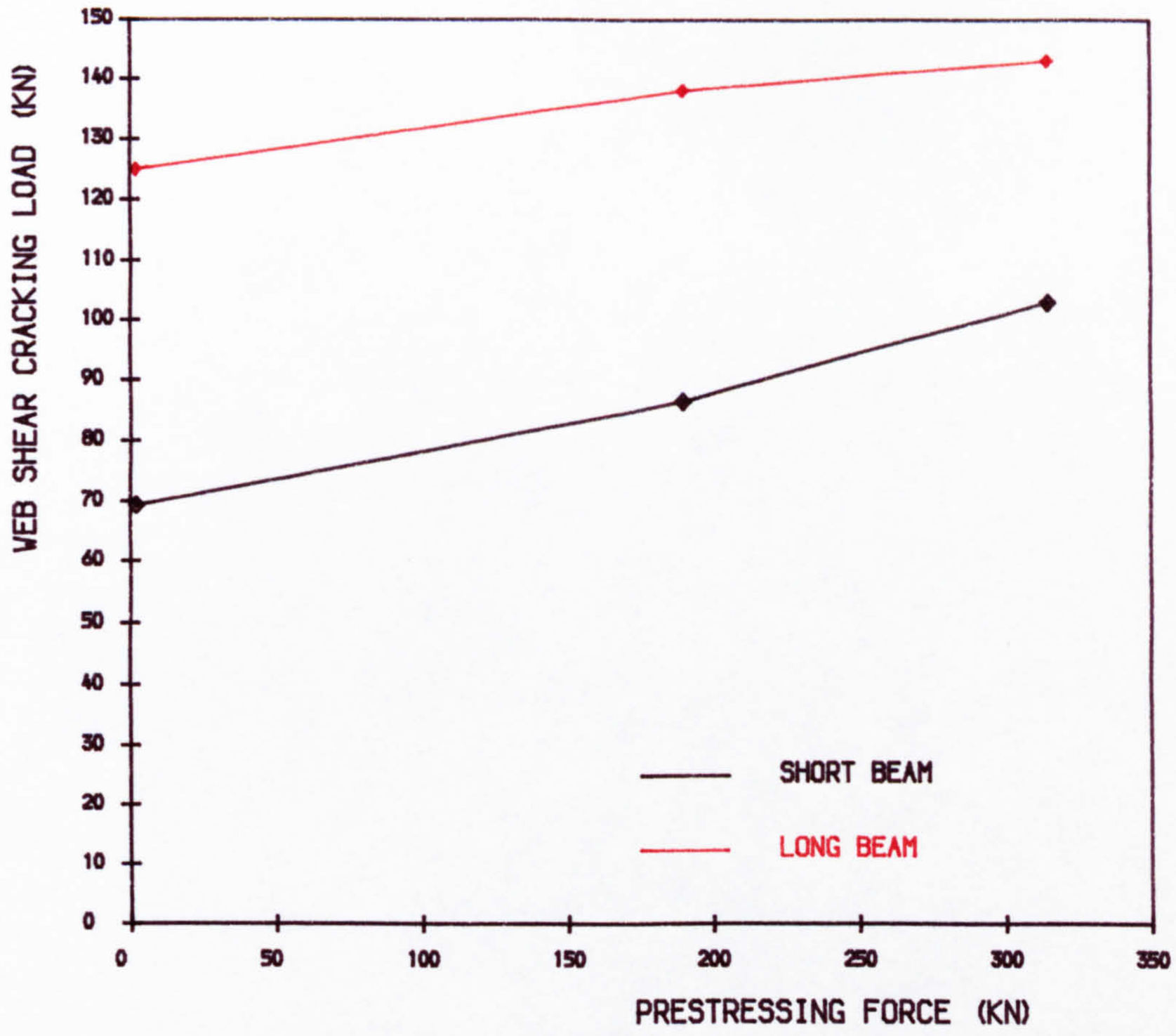

FIG. 8.16. VARIATION OF WEB SHEAR CRACKING LOAD WITH PRESTRESS IN THE SLAB

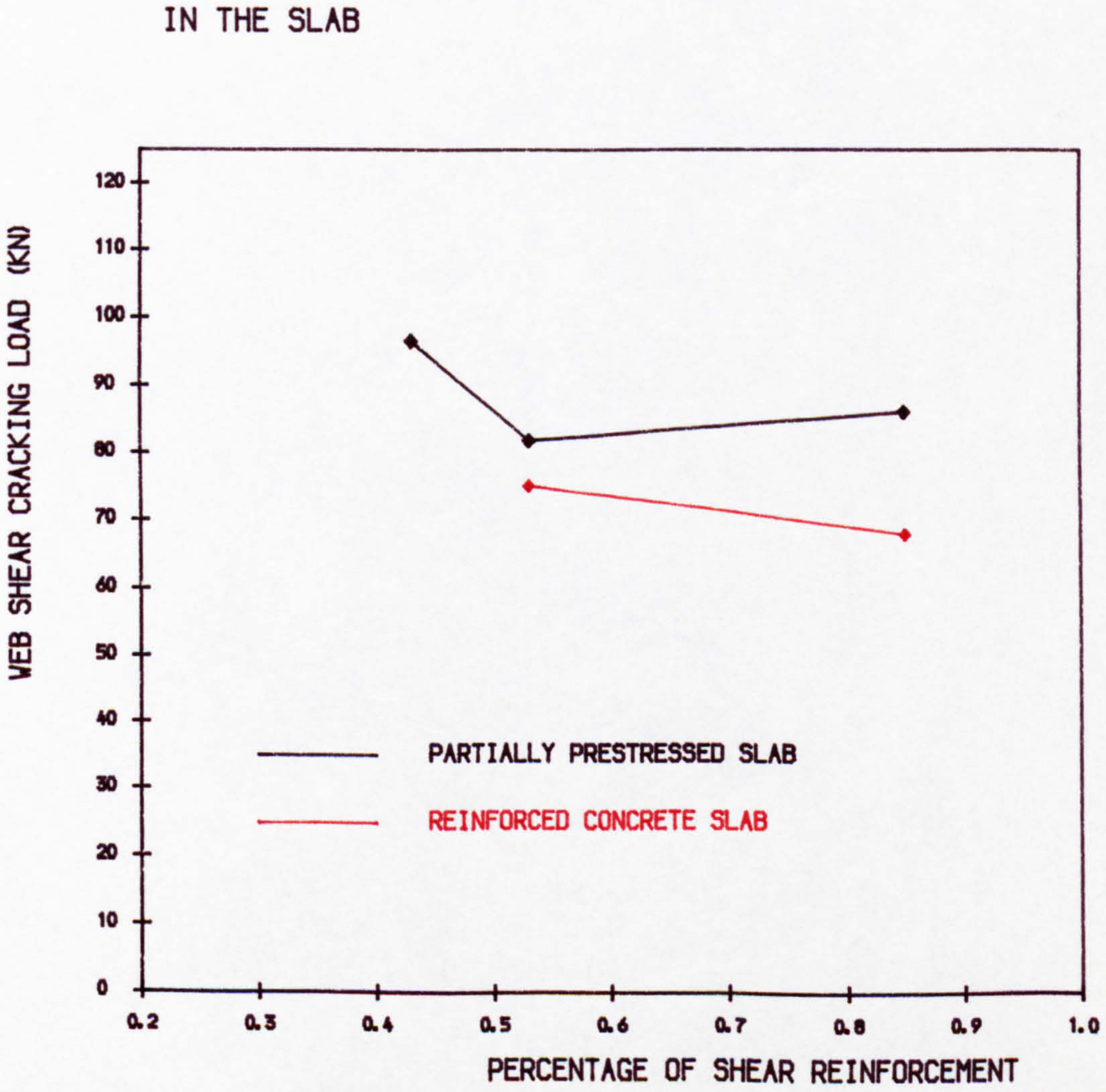

FIG. 8.17 : VARIATION OF WEB SHEAR CRACKING LOAD WITH SHEAR REINFORCEMENT PERCENTAGE

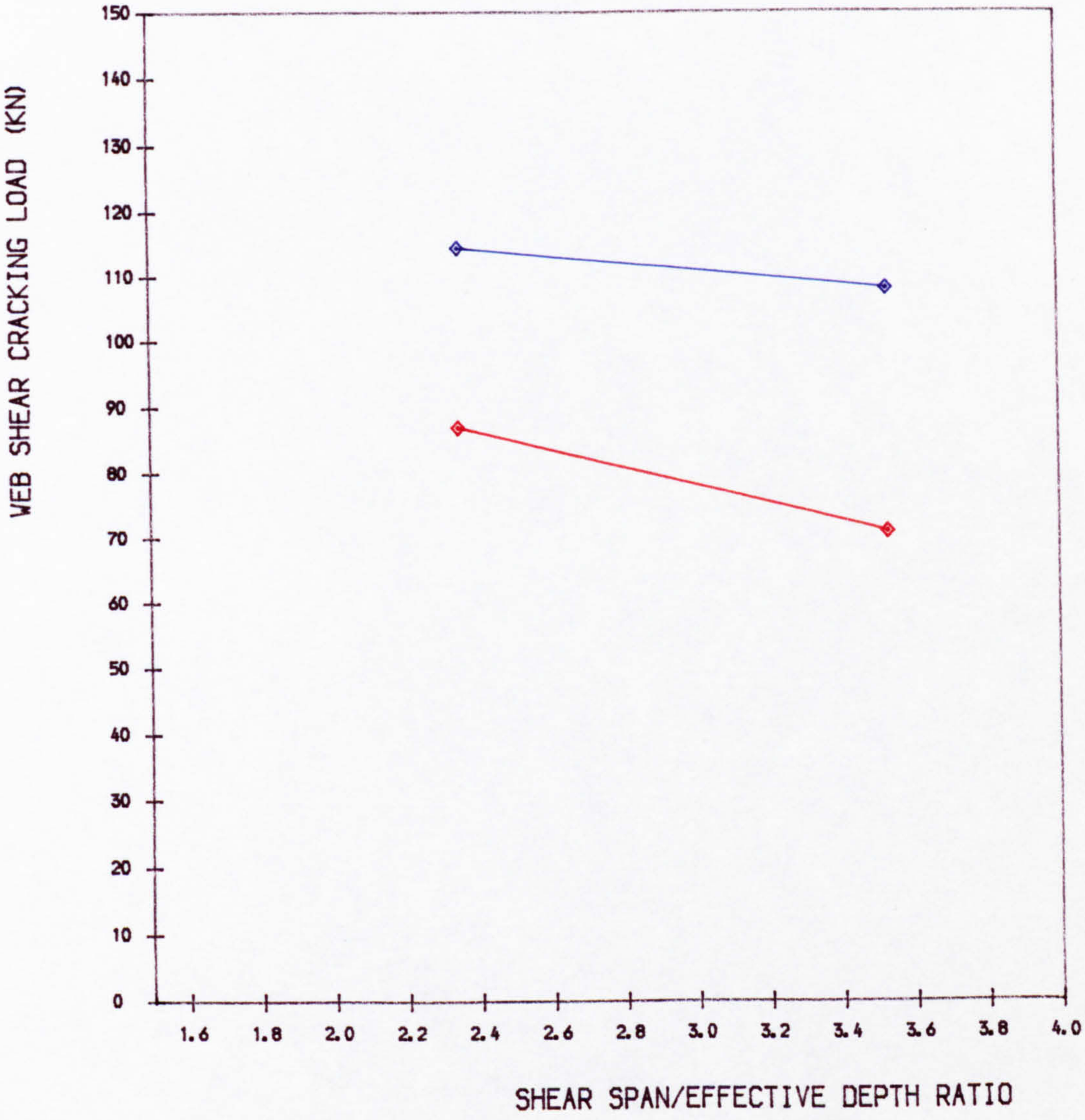

FIG. 8.18 : WEB SHEAR CRACKING LOAD VS SHEAR SPAN/EFFECTIVE DEPTH RATIO

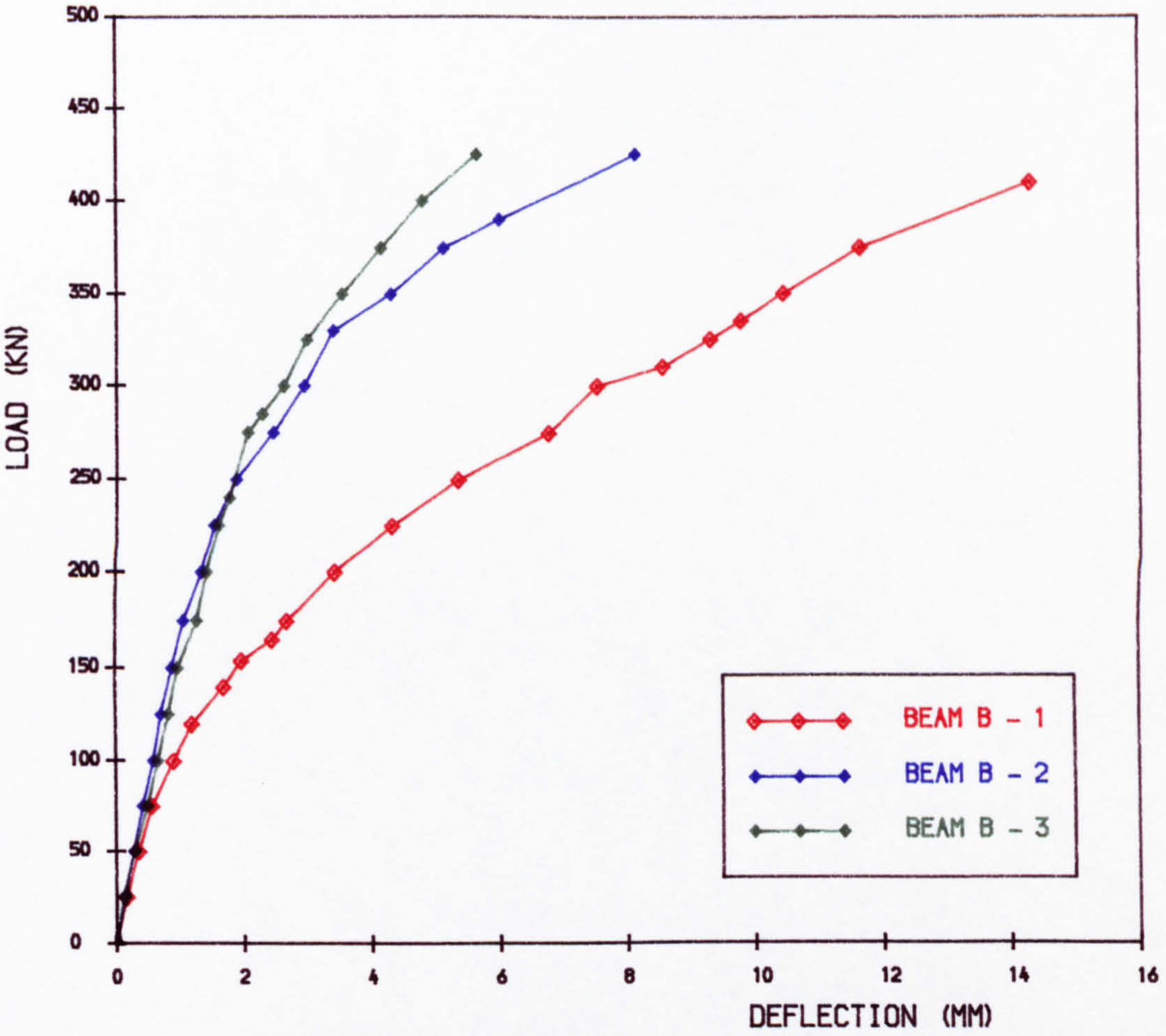

FIG. 8.19 : LOAD VS DEFLECTION CURVES OF BEAMS B-1, B-2 AND B-3 AT THE END OF CANTILEVER

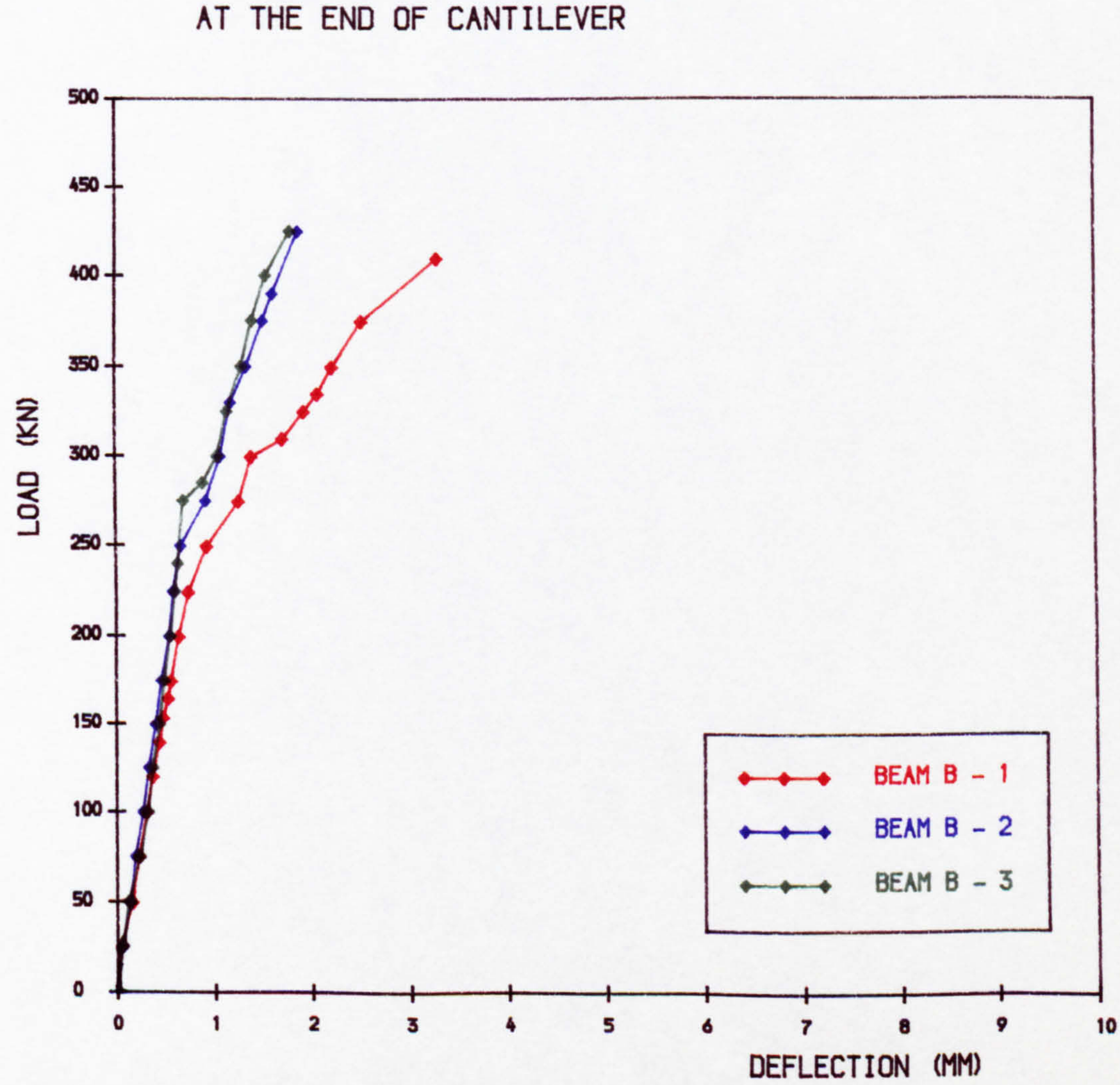

FIG. 8.20 : LOAD VS DEFLECTION CURVES OF BEAMS B-1, B-2 AND B-3 AT THE POINT LOAD ON LONG BEAM

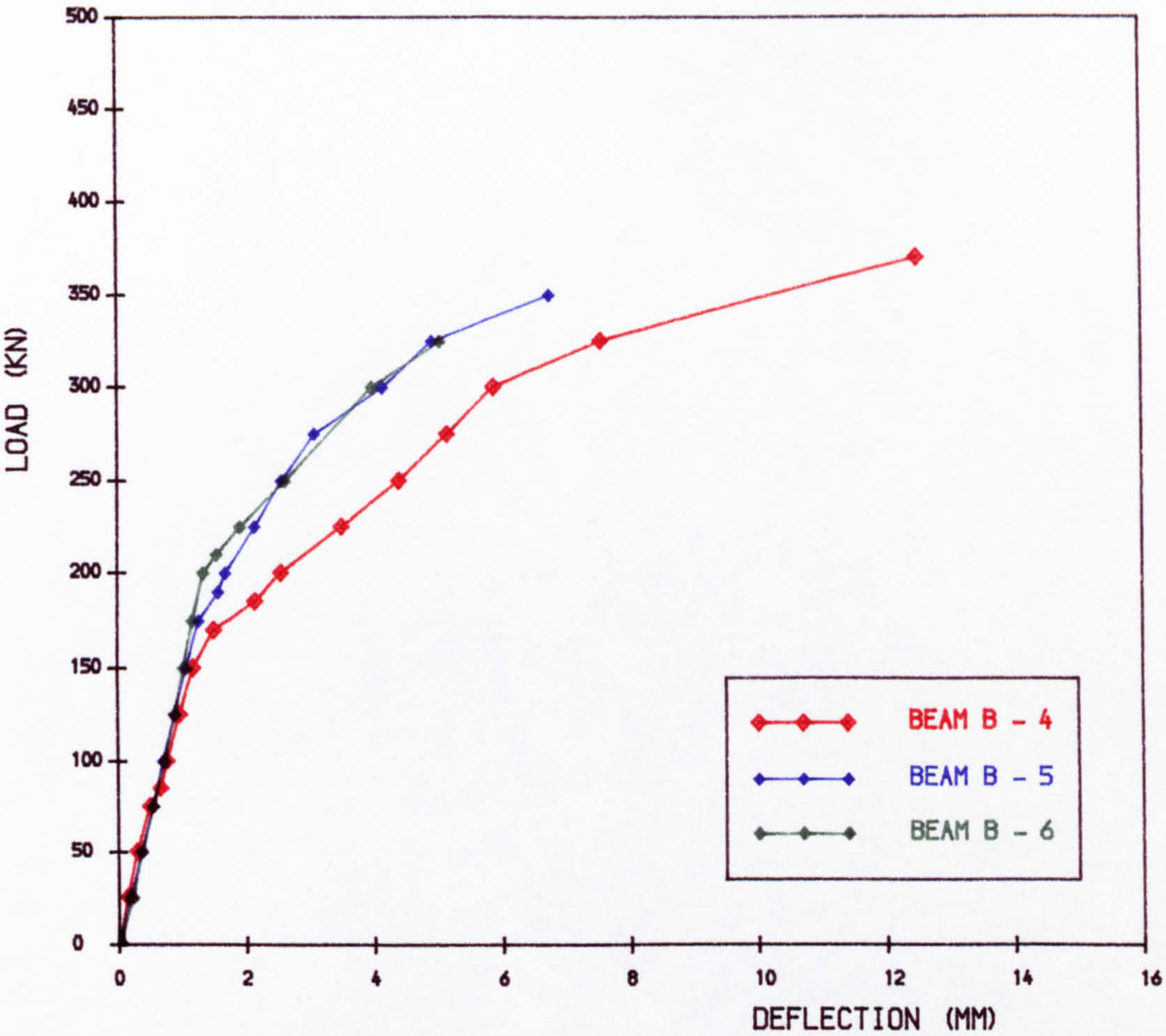

FIG. 8.21 : LOAD VS DEFLECTION CURVES OF BEAMS B-4, B-5 AND B-6 AT THE END OF CANTILEVER

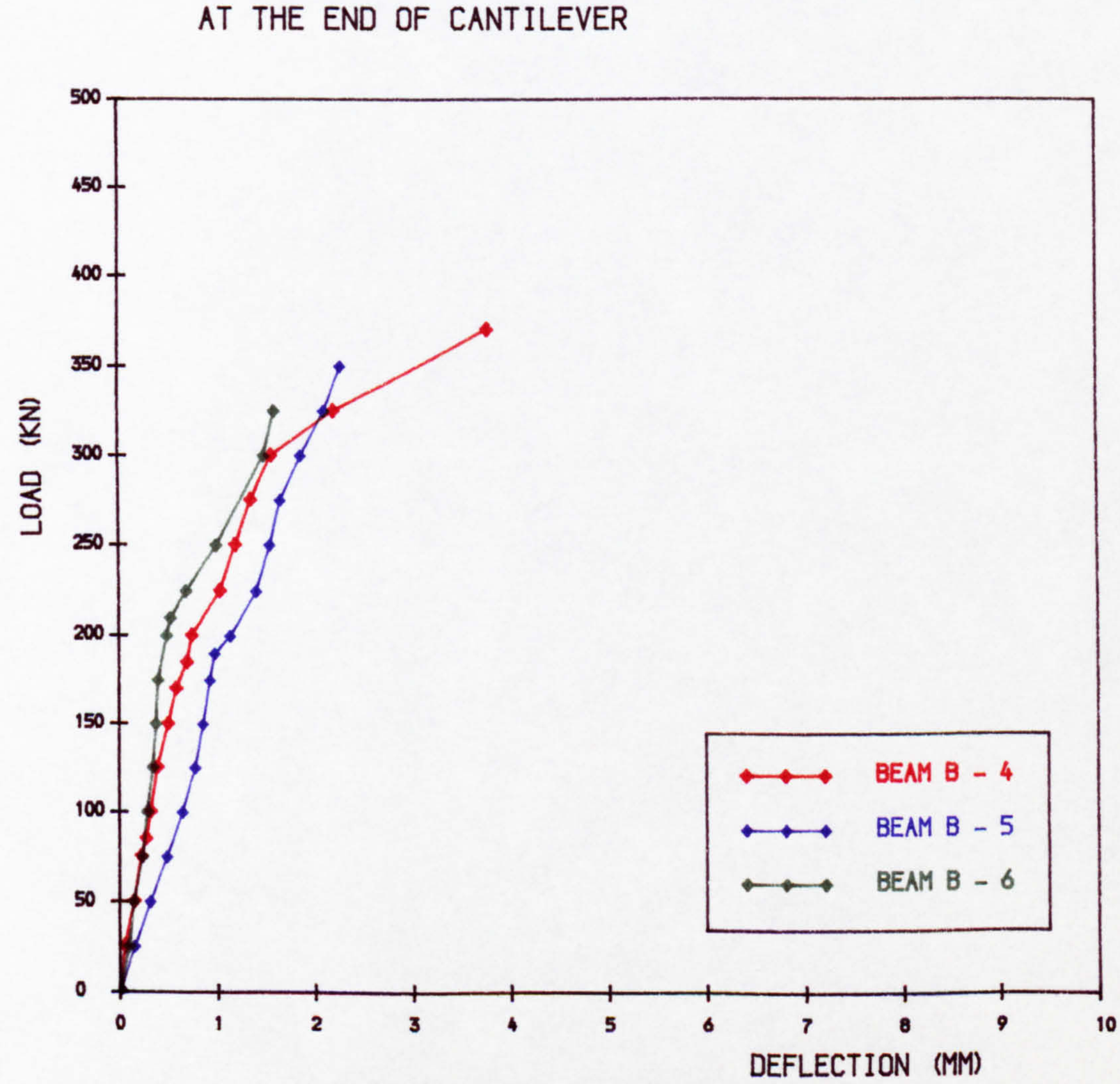

FIG. 8.22 : LOAD VS DEFLECTION CURVES OF BEAMS B-4, B-5 AND B-6 AT THE POINT LOAD ON LONG BEAM

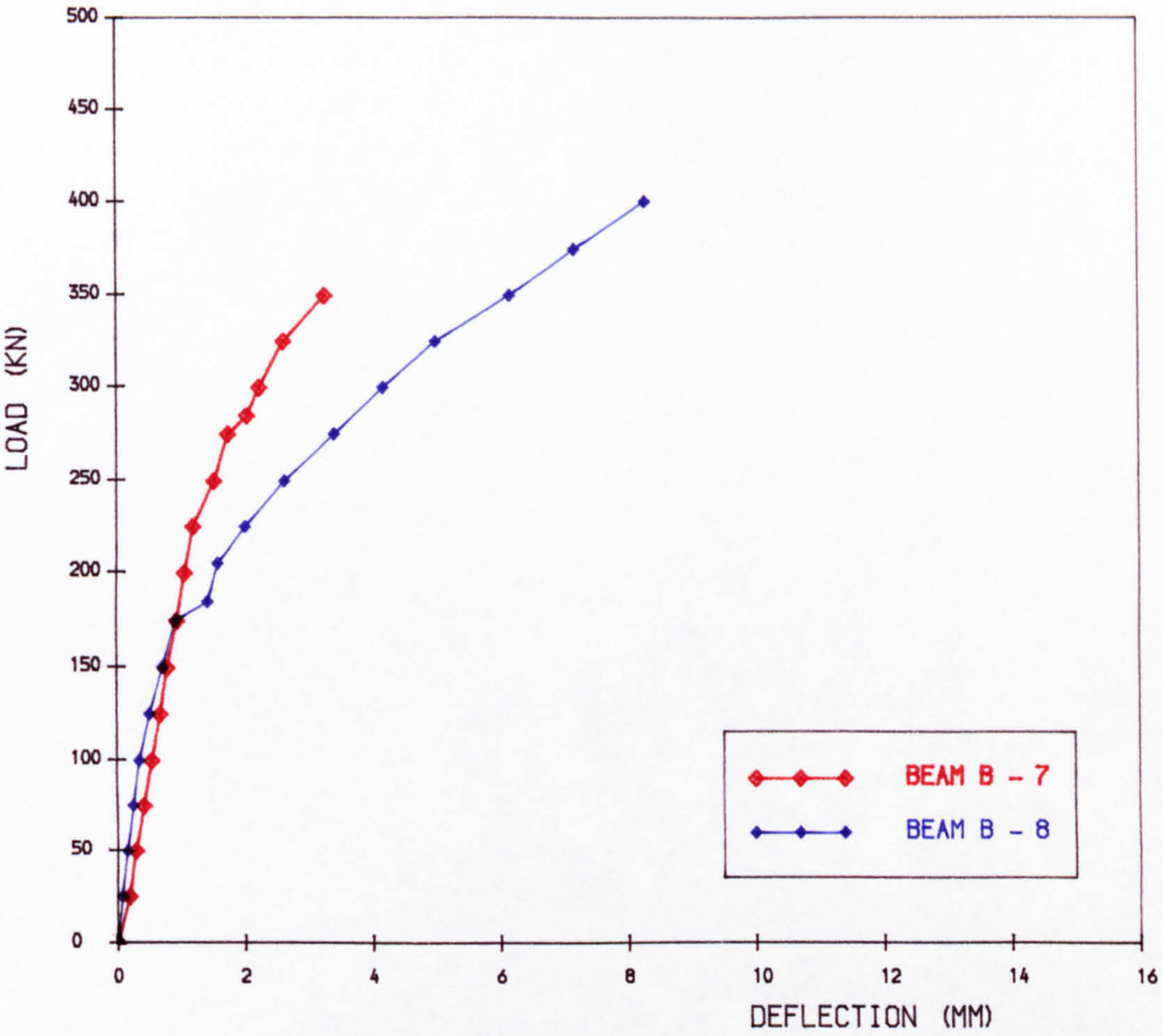

FIG. 8.23 : LOAD VS DEFLECTION CURVES OF BEAMS B-7 AND B-8 AT THE END OF CANTILEVER

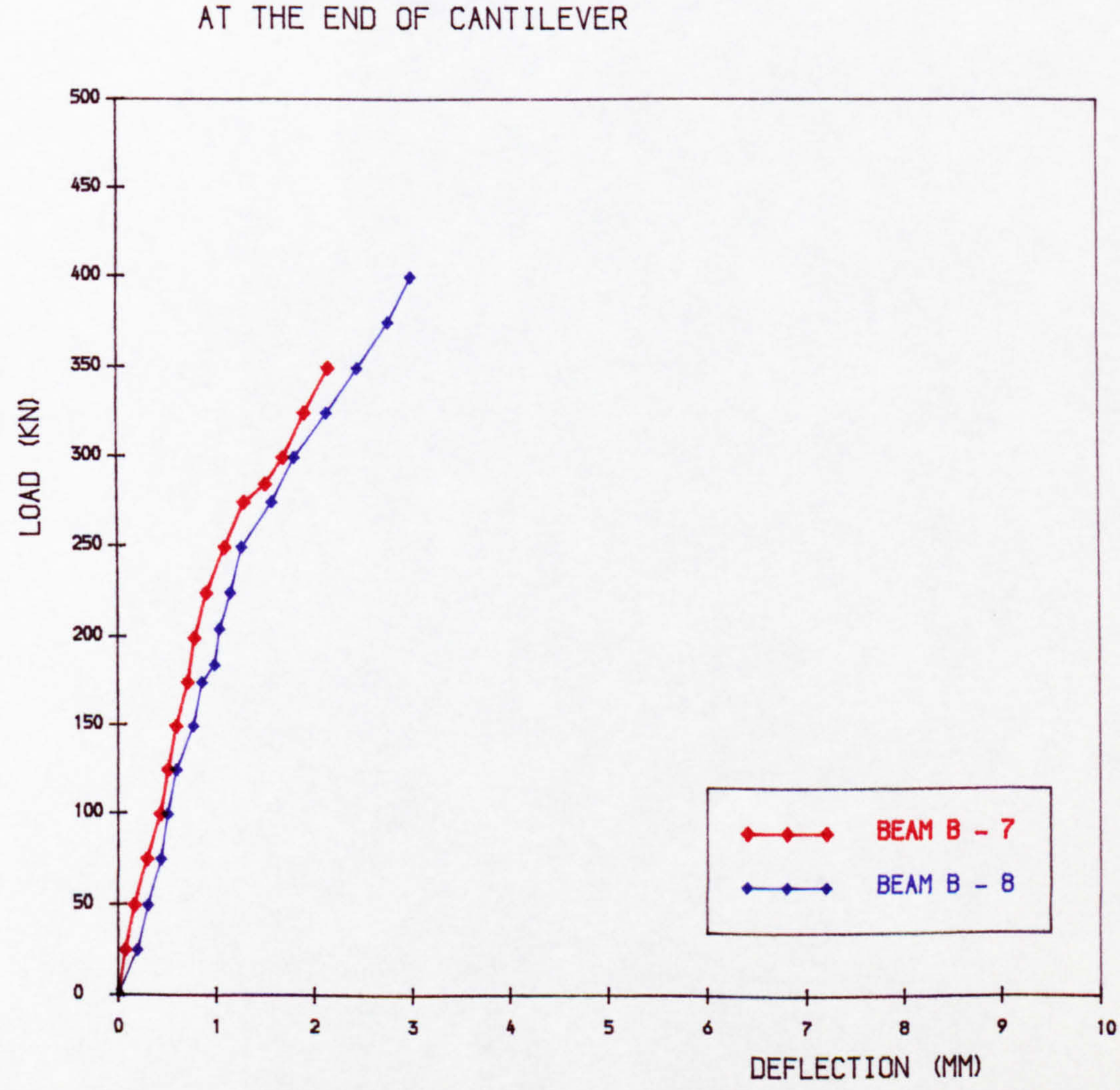

FIG. 8.24 : LOAD VS DEFLECTION CURVES OF BEAMS B-7 AND B-8 AT THE POINT LOAD ON LONG BEAM

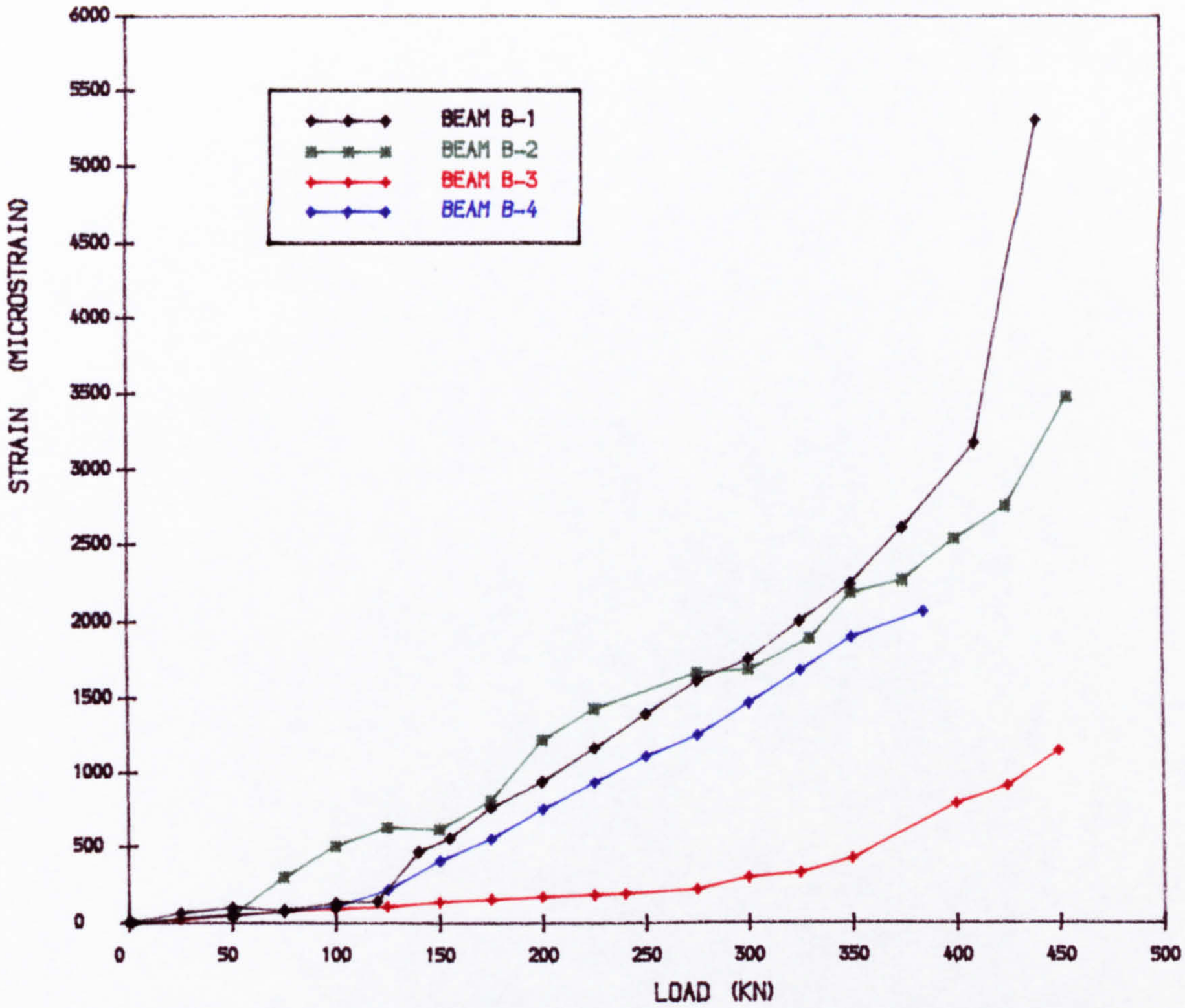

FIG. 8.25 . VARIATION OF STRAIN IN LONGITUDINAL REINFORCING BARS IN THE TOP SLAB OF BEAM B-1, B-2 ,B-3 AND B-4

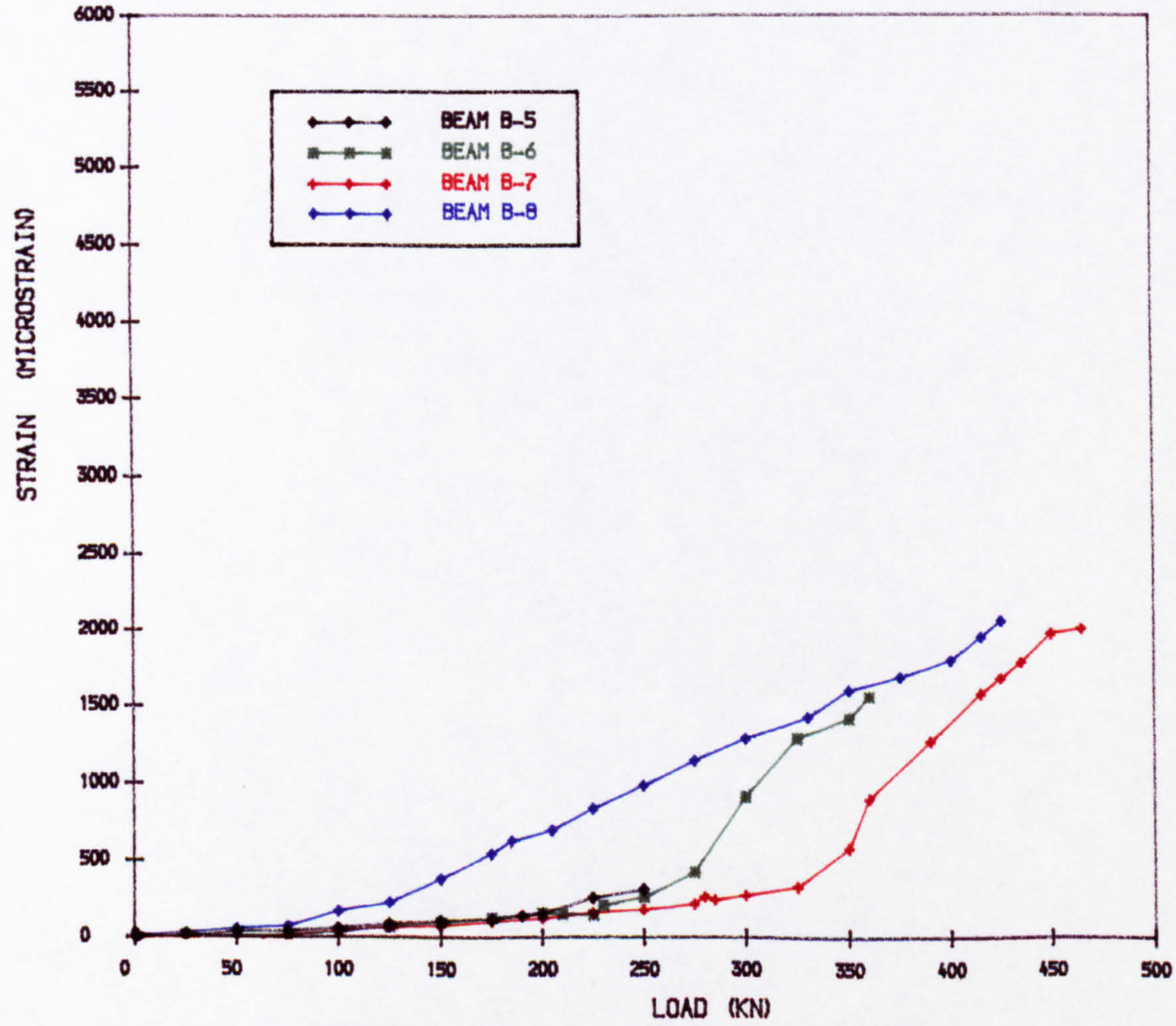

FIG. 8.26 . VARIATION OF STRAIN IN LONGITUDINAL REINFORCING BARS IN THE TOP SLAB OF BEAM B-5, B-6, B-7 AND B-8

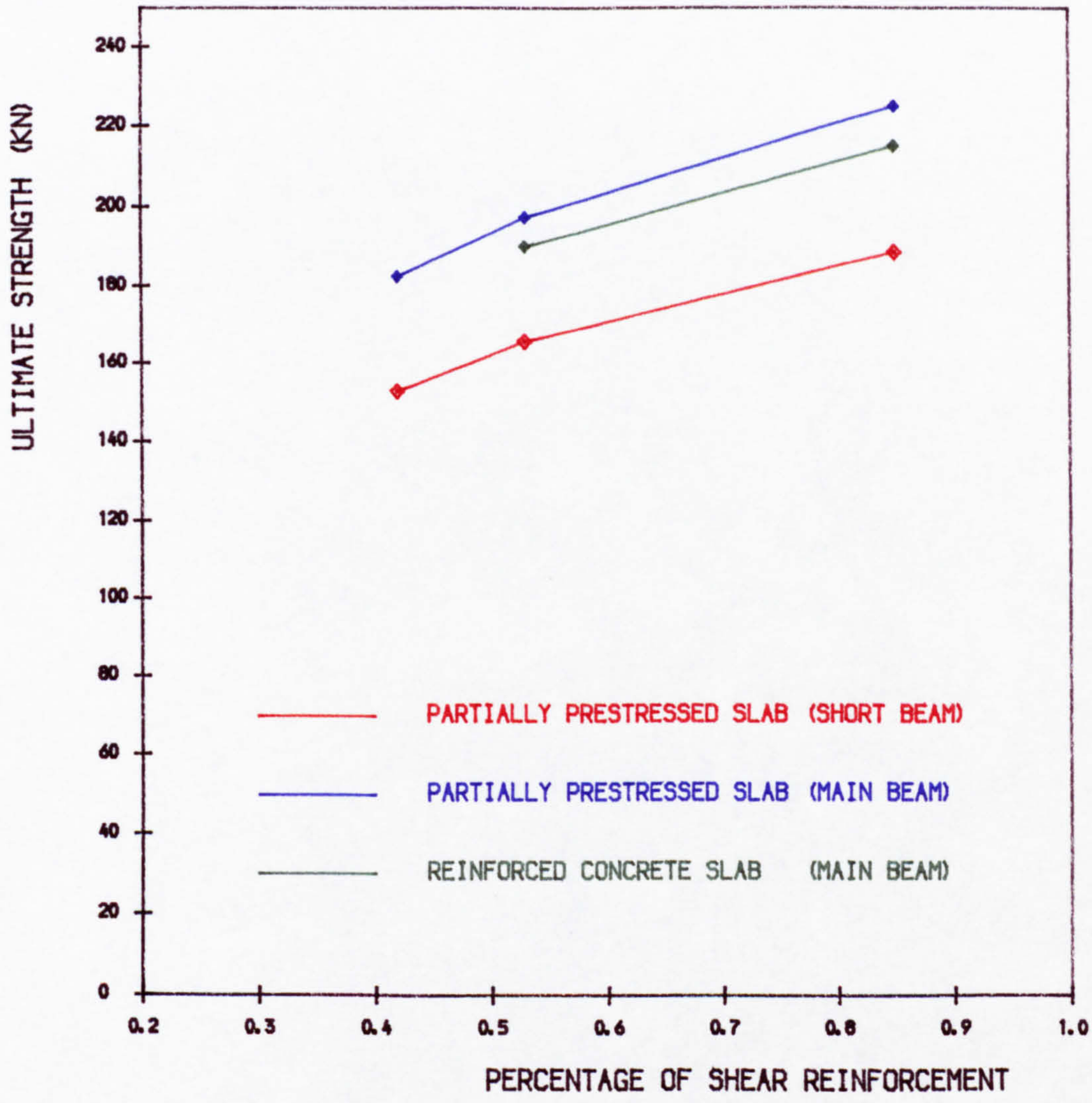

FIG. 8.27 . VARIATION OF ULTIMATE STRENGTH WITH PERCENTAGE OF SHEAR REINFORCEMENT

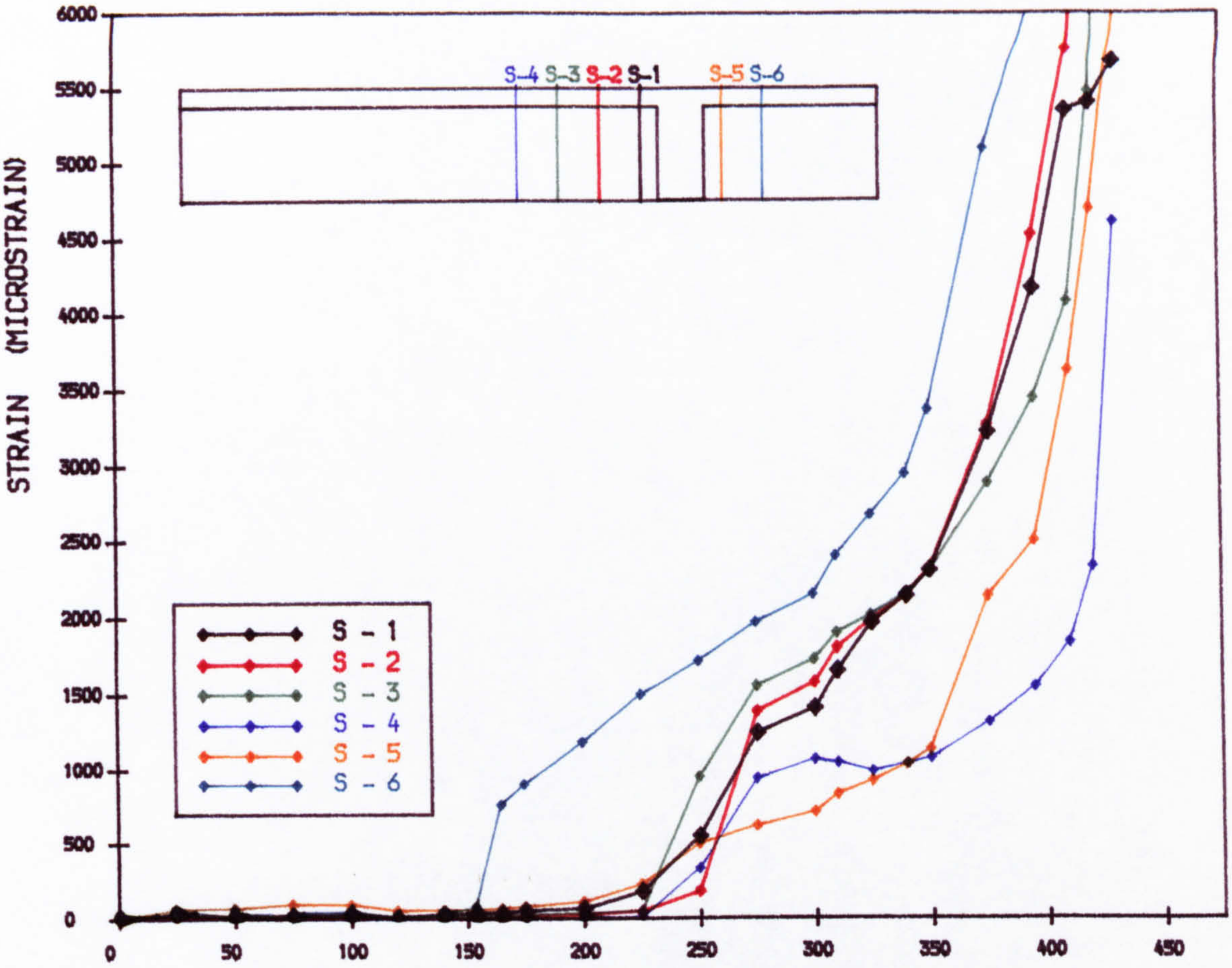

FIG. 8.28 : VARIATION OF STIRRUP STRAIN WITH LOAD - BEAM B-1
(r = 0.84%)

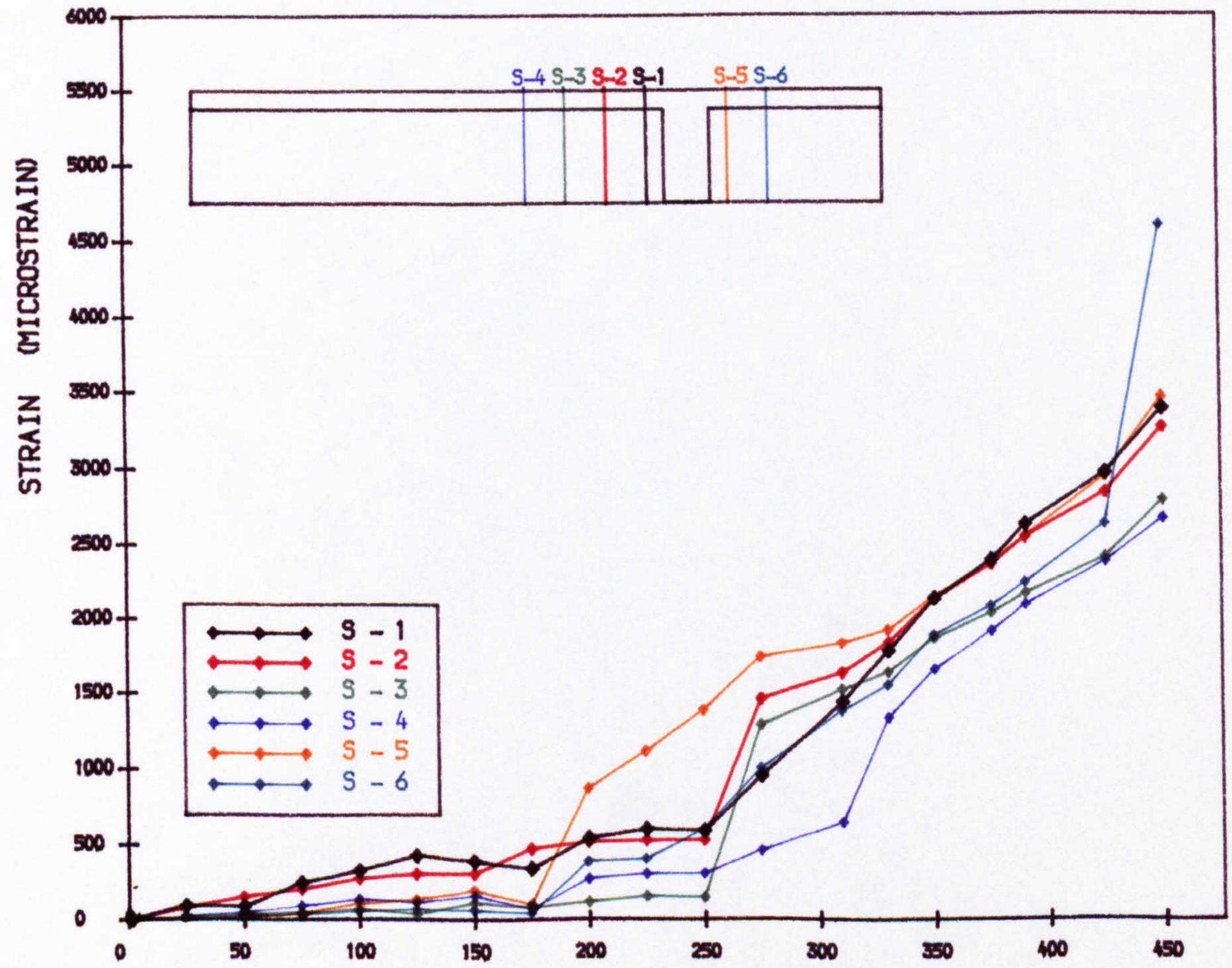

FIG. 8.29 : VARIATION OF STIRRUP STRAIN WITH LOAD - BEAM B-2
(r = 0.84%)

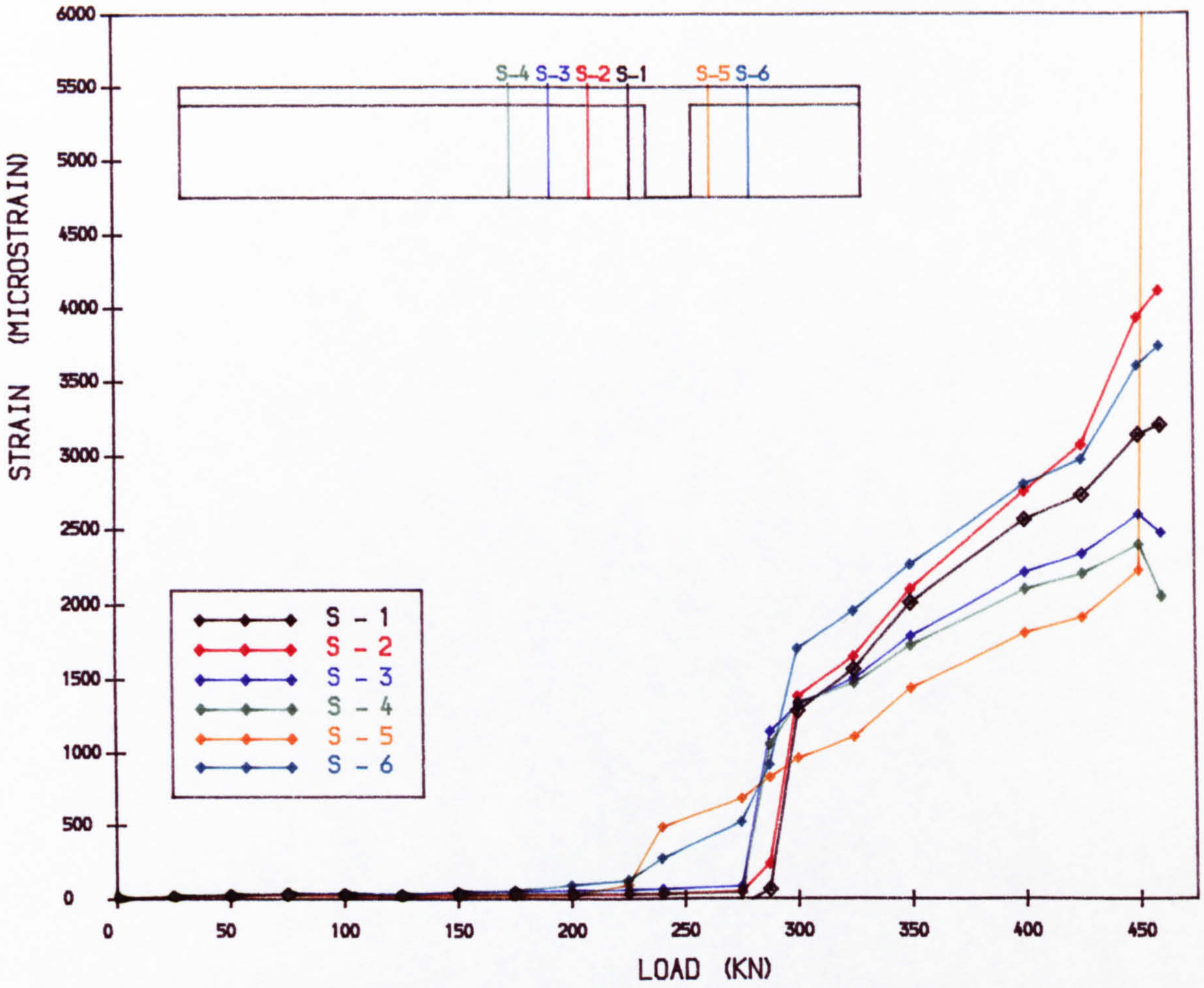

FIG. 8.30 : VARIATION OF STIRRUP STRAIN WITH LOAD - BEAM B-3
(r = 0.84%)

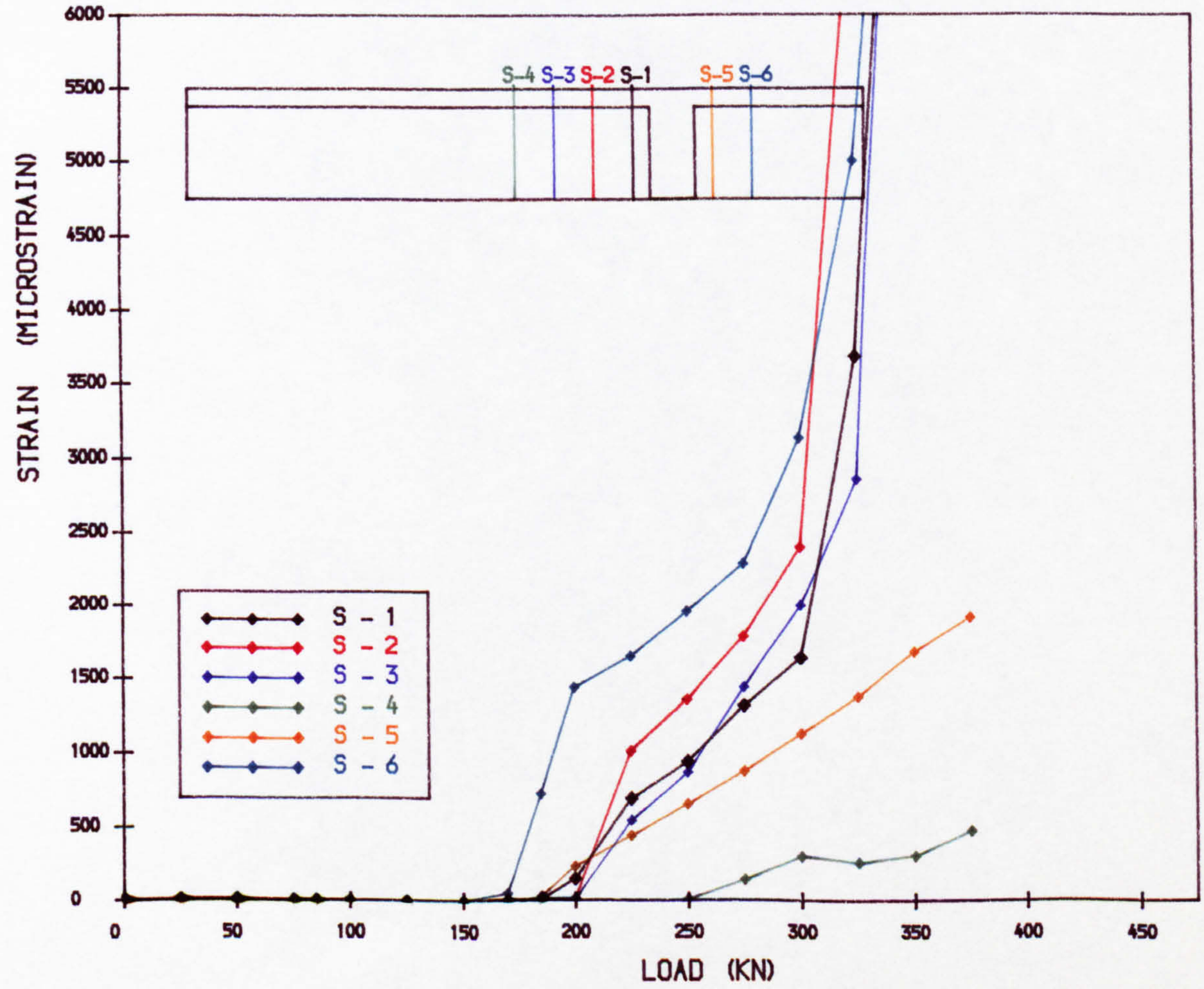

FIG. 8.31 : VARIATION OF STIRRUP STRAIN WITH LOAD - BEAM B-4
(r = 0.53%)

277

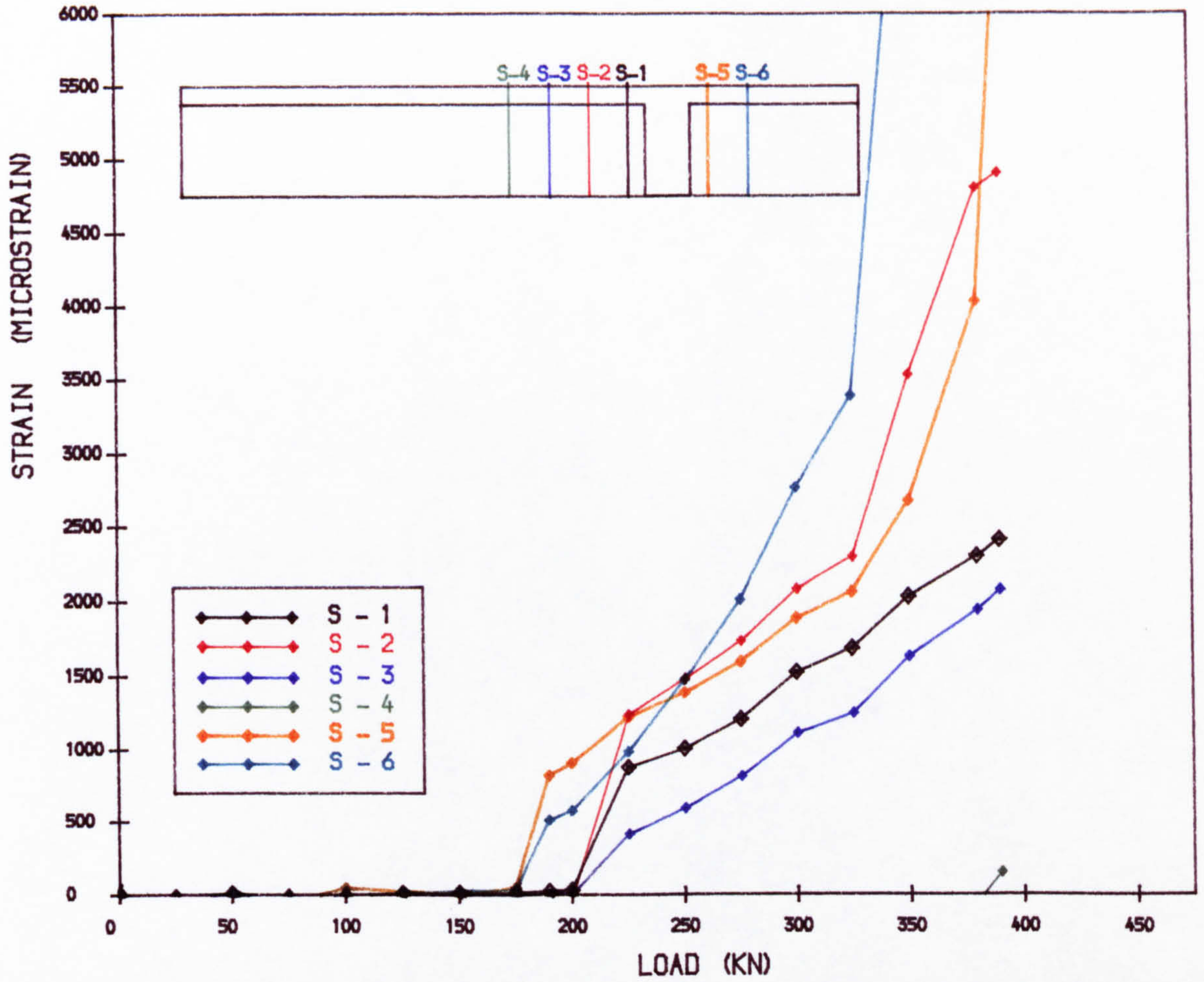

FIG. 8.32 : VARIATION OF STIRRUP STRAIN WITH LOAD IN BEAM B-5
(r = 0.53%)

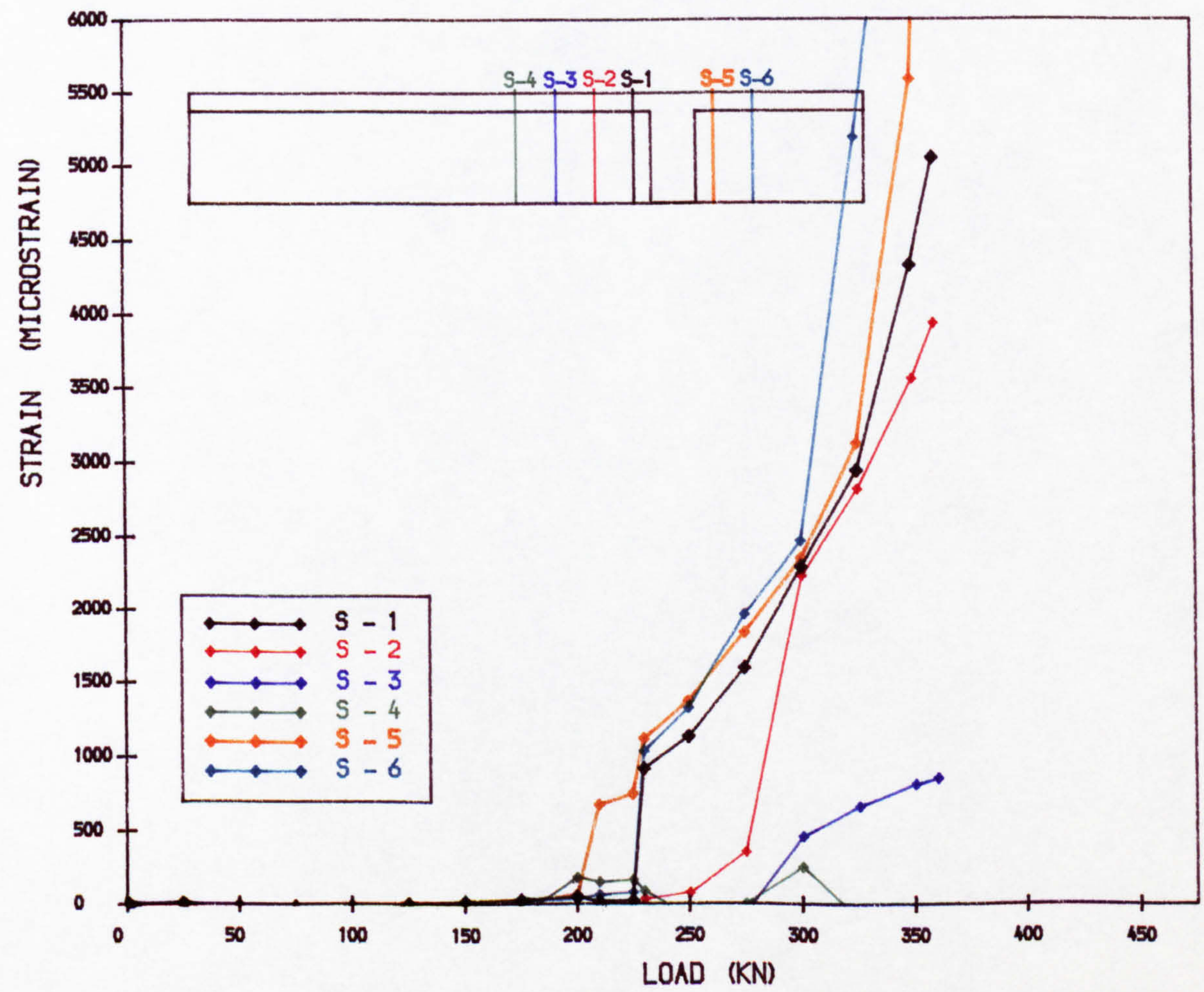

FIG. 8.33 : VARIATION OF STIRRUP STRAIN WITH LOAD IN BEAM B-6
(r = 0.42%)

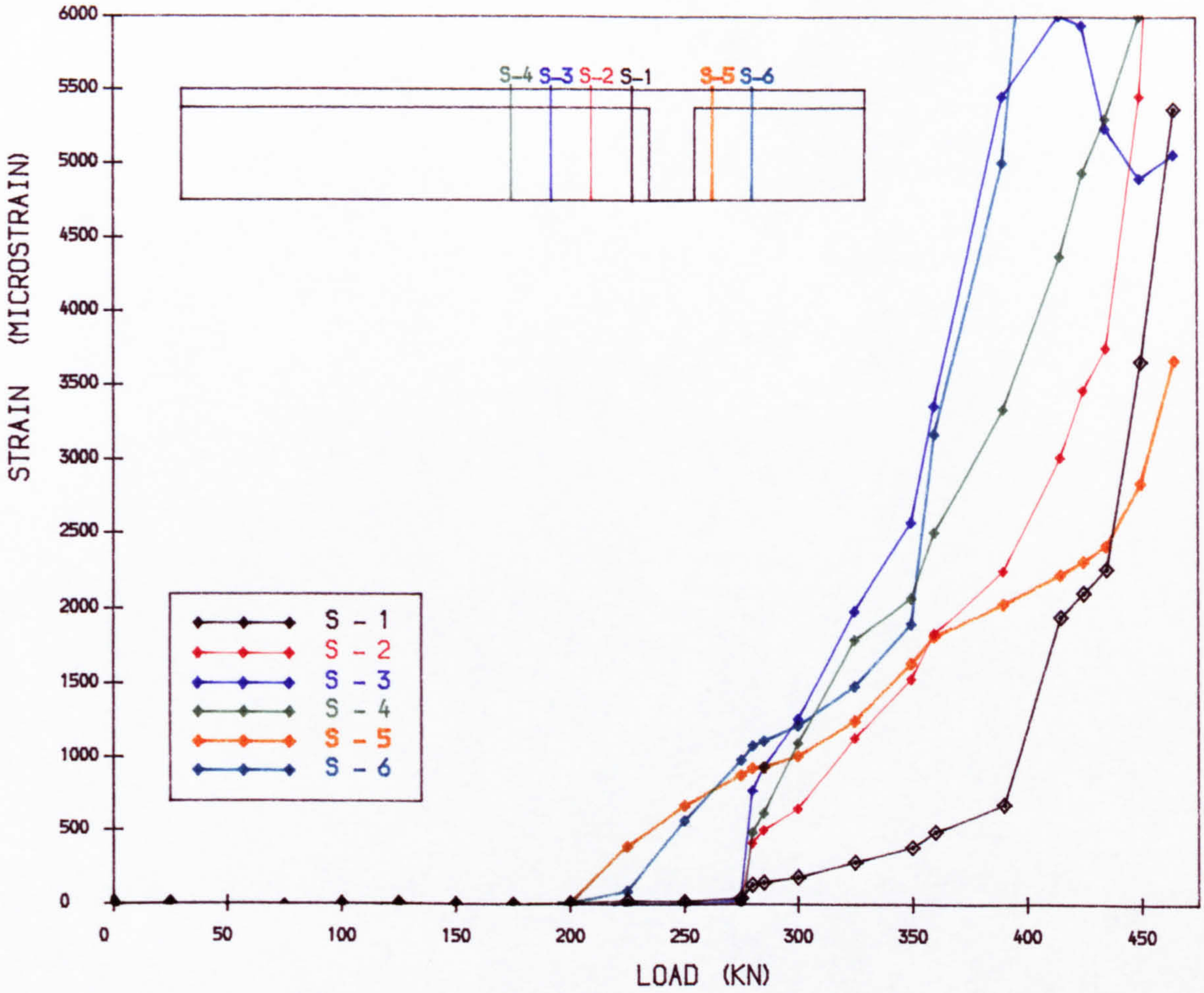

FIG. 8.34 : VARIATION OF STIRRUP STRAIN WITH LOAD IN BEAM B-7
(r = 0.53%)

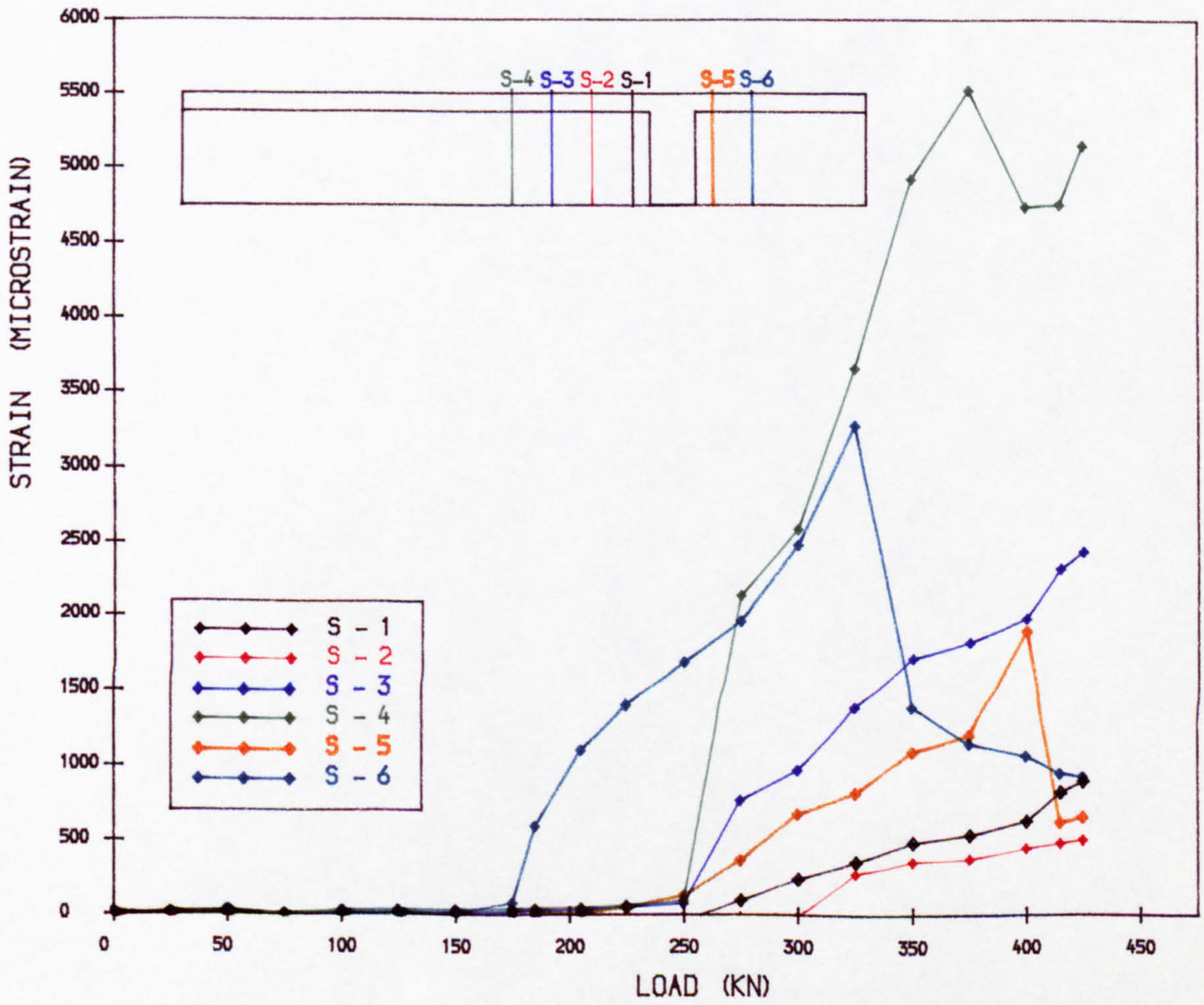

FIG. 8.35 : VARIATION OF STIRRUP STRAIN WITH LOAD IN BEAM B-8
(r = 0.53%)

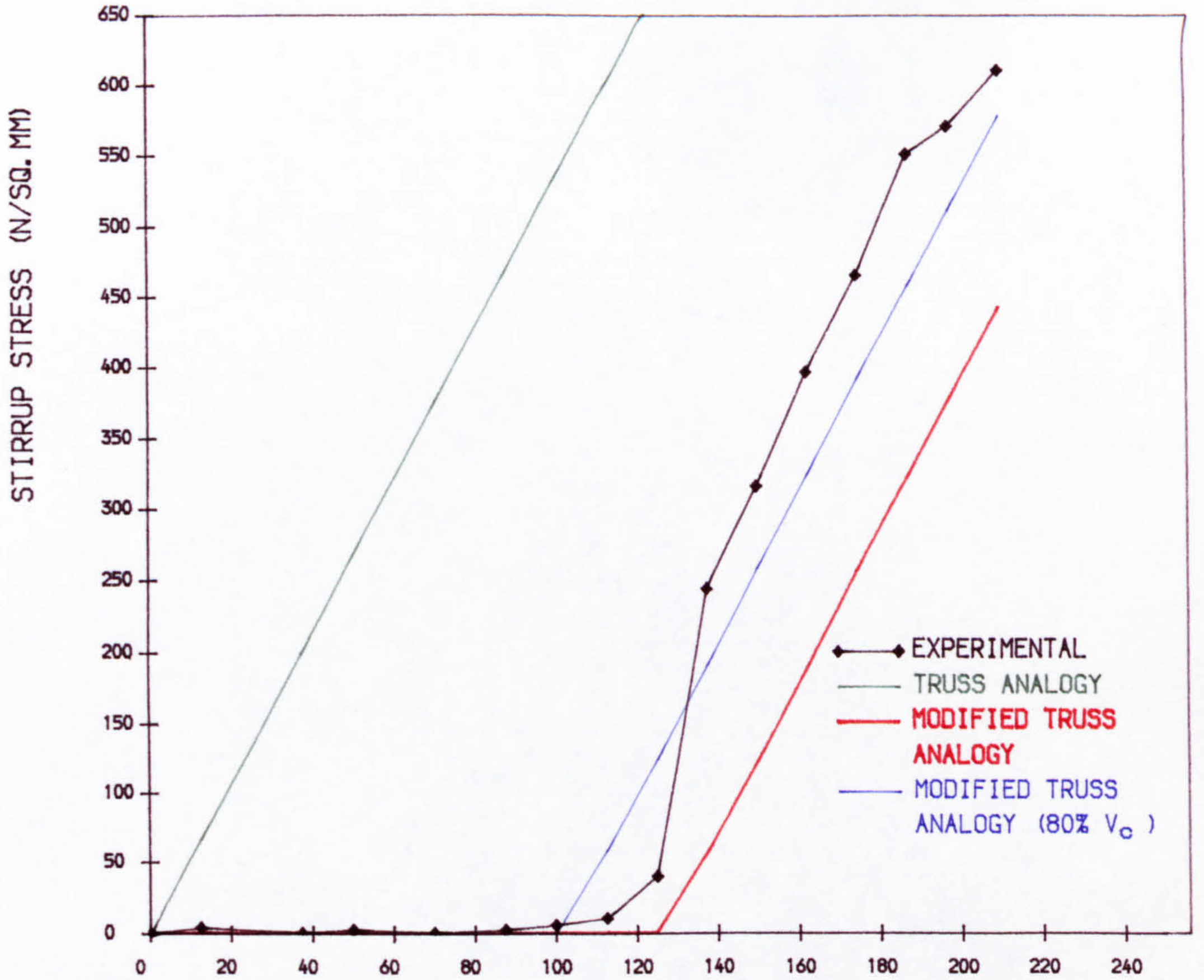

FIG. 8.36 : LOAD VS STRESS IN SHEAR REINFORCEMENT (BEAM B-1) S-1

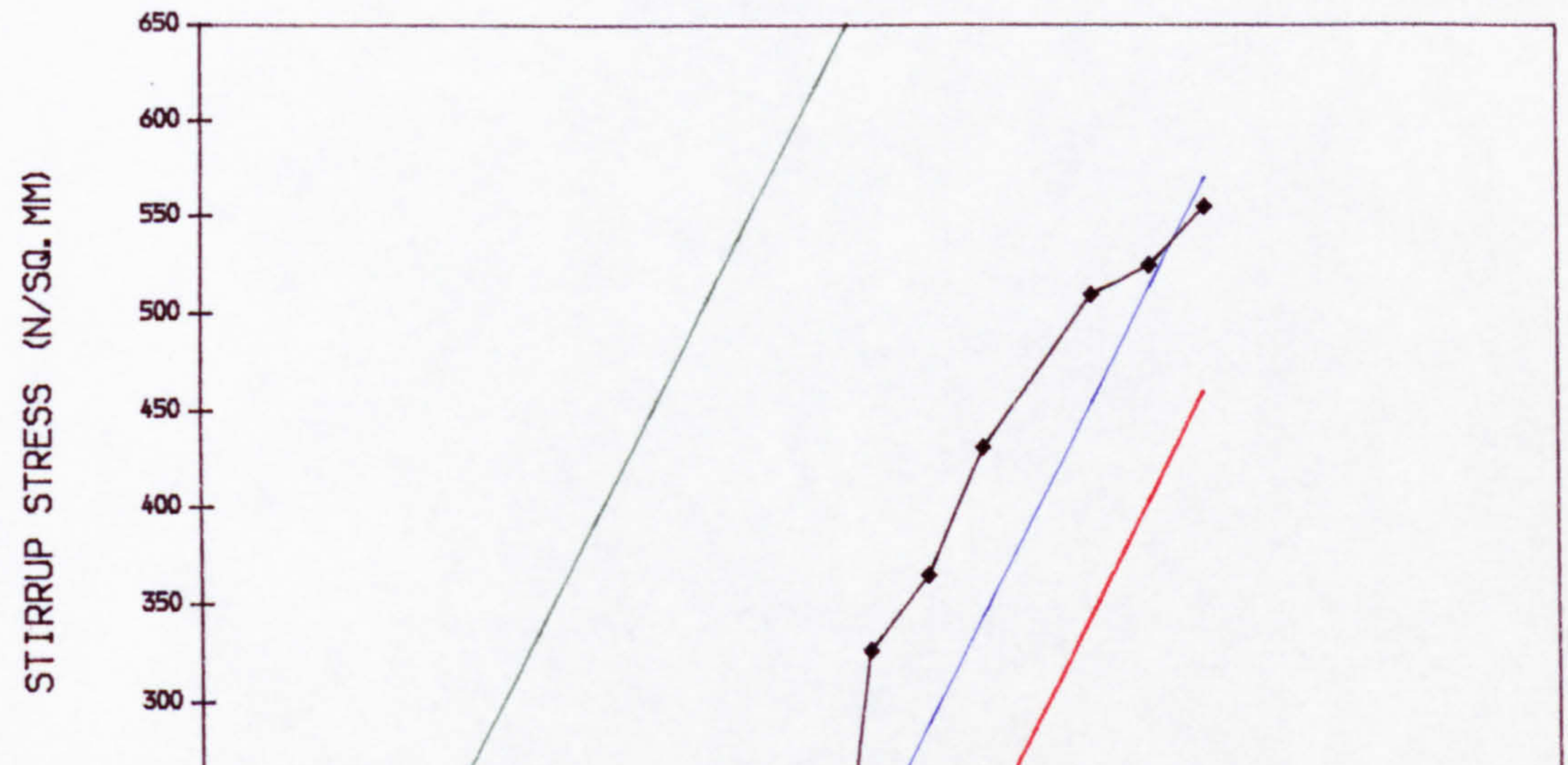

FIG. 8.37 : LOAD VS STRESS IN SHEAR REINFORCEMENT (BEAM B-3) S-6

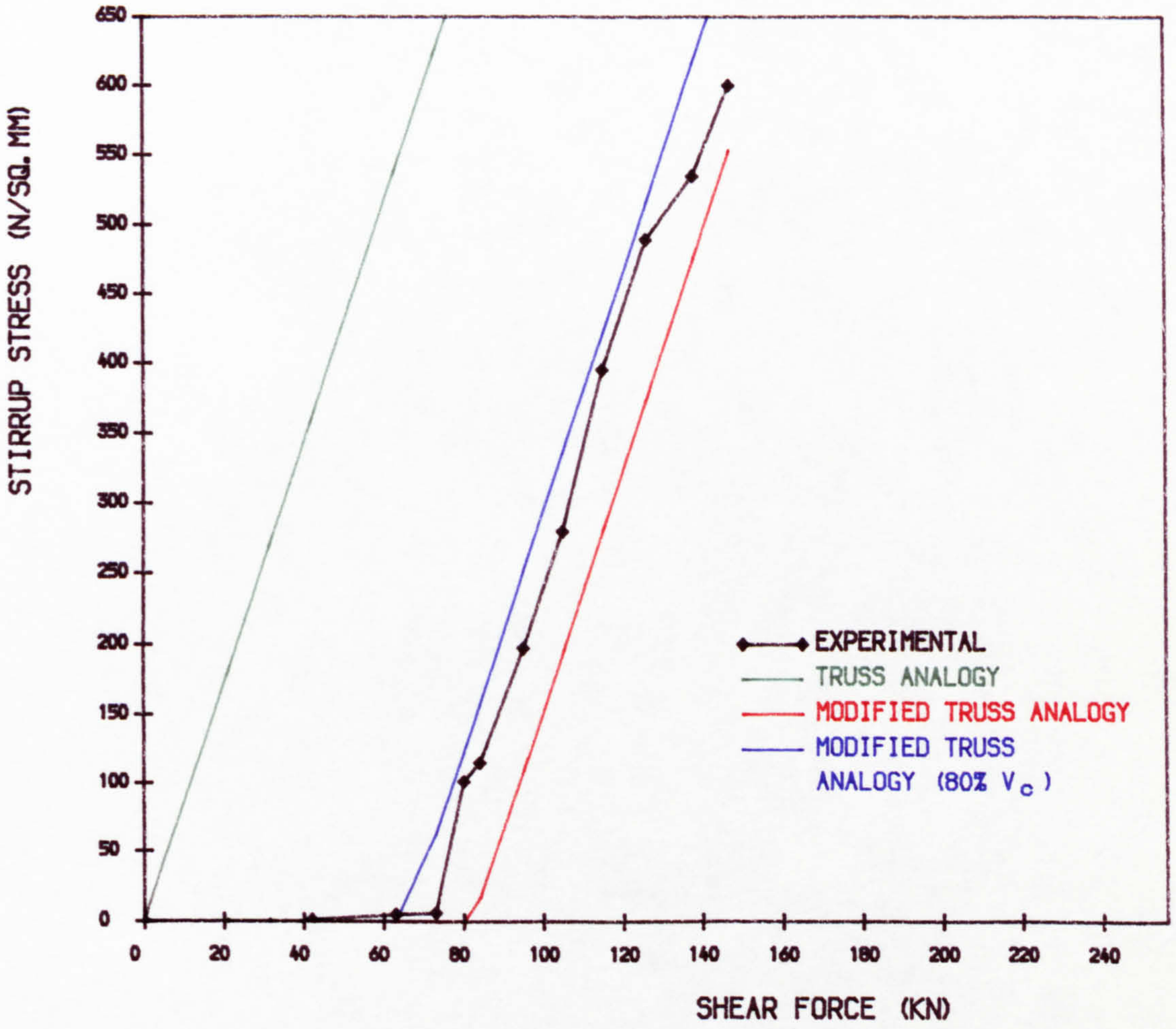

FIG. 8.38 : LOAD VS STRESS IN SHEAR REINFORCEMENT (BEAM B-5) S-6

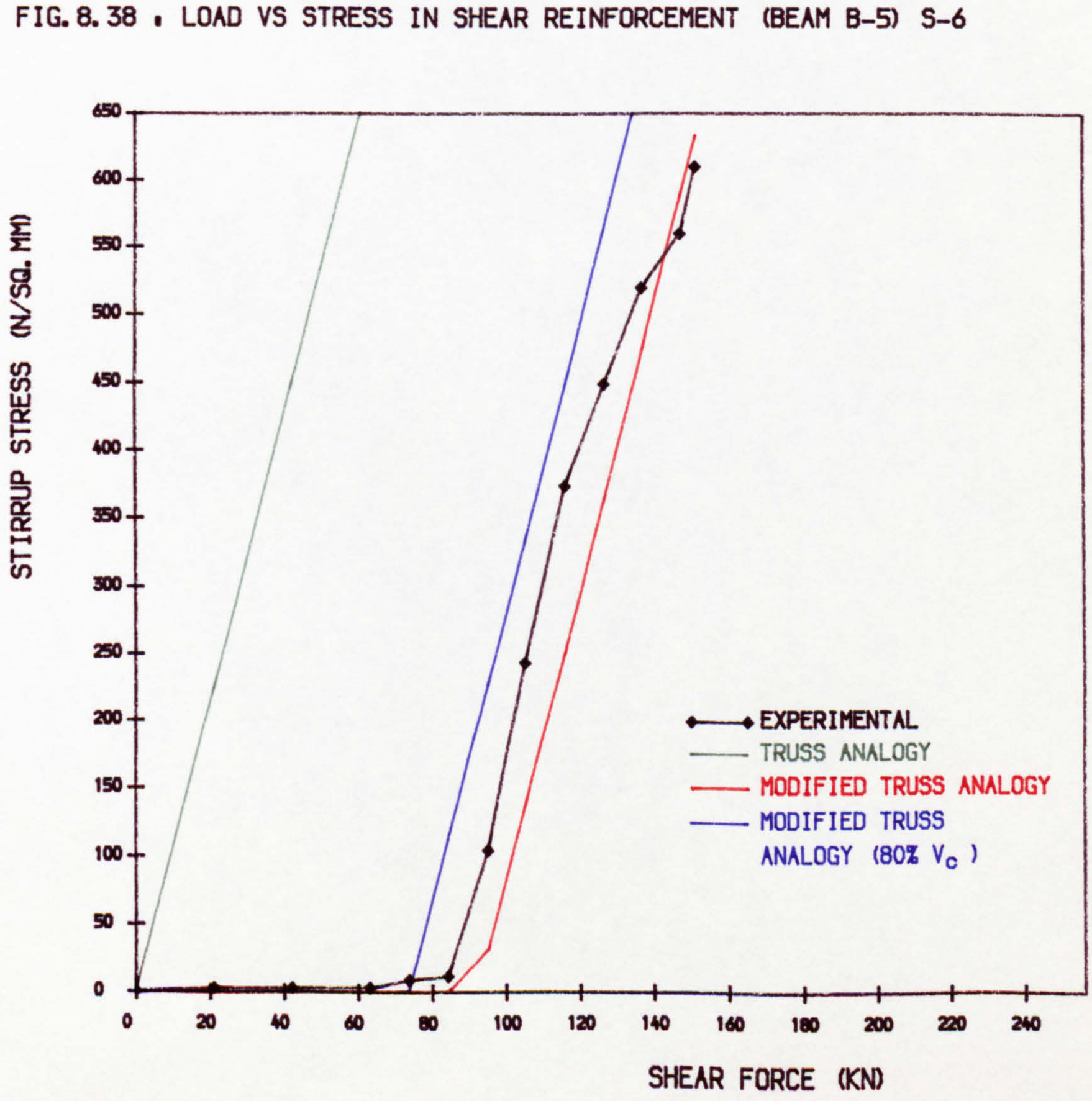

FIG. 8.39 : LOAD VS STRESS IN SHEAR REINFORCEMENT (BEAM B-6) S-5

CHAPTER 9

CONCLUSIONS AND RECOMMENDATIONS FOR FUTURE RESEARCH

9.1 Analytical Comparison Between Continuous Bridge Decks with Prestressed or Reinforced Concrete Slabs

9.1.1 Crack Control

The main advantage of the proposed method of using a prestressed slab to develop continuity between precast bridge girders is that, in addition to developing continuity and composite action, it improves the durability of bridge decks by controlling cracks in the top slab which may be subjected to long term severe exposure conditions. The development of continuity itself, of course, also means that the bridge deck remains essentially joint free throughout its length. In addition, any cracking which may occur under full service moments will close up on removal of live load and provide a crack free top slab.

In the design of multi-span continuous bridge decks with either a fully prestressed slab, a partially prestressed slab or a reinforced concrete slab in the hogging moment region, the top slab can be designed to remain in compression under the action of permanent loads and a part of live load by applying an appropriate amount of prestress. In an analytical study, 50% of the applied live load was considered for a bridge deck with a partially prestressed slab in which the applied prestress ensured a crack free slab under the total service load considered in the design. In contrast, the same bridge deck with a reinforced concrete slab at the interior support will develop flexural cracks under one third of service live load (assuming the flexural tensile strength of concrete to be $0.45\sqrt{f_{cu}}$). The superiority of the prestressed slab in this respect will be more

predominant when a live load of greater magnitude is considered (45 units of HB vehicle compared to the 37.5 units considered in this study)

A comparison of bridge decks with a fully prestressed slab and a partially prestressed slab shows that the partially prestressed slab is more economical and practicable while providing a good crack control, and is therefore recommended for practical applications.

9.1.2 Effect of Two Stage Construction of Top Slab on Support Moment

When prestressed slabs are used in the hogging moment regions of composite beams, the slab has to be cast in two stages. The portion of the slab to be prestressed is cast first and the remainder of the slab is then cast after post-tensioning the first stage construction of the slab. An additional moment is thus produced which does not exist in bridge decks constructed just with reinforced concrete slabs. This additional moment at the interior support, due to the weight of slab cast in second stage increases the amount of prestress required in the slab.

9.1.3 Effect of Secondary Moments due to Prestress in the Slab

A drawback to the application of prestress in the top slab within the hogging moment region is that it induces negative secondary moments and thus reduces the applied prestressing moment at the support. This secondary effect increases with the ratio (α) of the length of the prestressed section of the slab to the overall span itself. Therefore, the length of prestressed portion must be kept as small as possible. A value of α greater than 0.30 should be avoided for two span composite bridge decks as secondary moments then become significant. For most

practical cases, a value of α between 0.20 and 0.25 would be satisfactory in keeping the secondary effects small and to provide prestress over the critical region of the hogging moment. The secondary effects will be less significant when the number of spans is increased.

The secondary effects also depend on the ratio of the stiffness of the composite section to the precast section with a higher ratio resulting in smaller secondary moments.

9.1.4 Effect of Prestressed Slab on Positive Span Moment

The two stage construction of the slab and the secondary effects due to prestress in the slab nevertheless have a beneficial effect on the span moment. Due to the two stage construction, a greater part of the weight of the slab is applied after the development of composite action and continuity at the interior support. Therefore, the moment applied on the precast beam in the mid-span region, due to the weight of the slab, is reduced. Also, negative secondary moments induced by the prestress in the slab reduce the span moment. The combination of these two effects results in a considerable reduction in the service moment carried by the precast section alone, and in the compressive and tensile stresses at the top and bottom of the section. The reductions in the service moment applied on the precast section alone for beams with a fully prestressed slab and a partially prestressed slab are 34% and 31% respectively compared to that of the beam with a reinforced concrete slab. The service moment applied to the composite section in the mid-span region, however, is essentially the same for all three types of slabs.

9.1.5 Reduction in the Prestress Required in the Precast Beam

Due to the reduction in the service moment on the precast beam and the resulting reduction in the tensile stress at the bottom of the precast girders, the amount of prestress required in the precast girders themselves, with a prestressed slab, is smaller than that with a reinforced concrete slab. A comparison of three types of slabs considered in the study shows that the number of prestressing strands required in the precast beam for bridge decks with a fully prestressed slab, a partially prestressed slab and a reinforced concrete slab are 19, 21 and 29 respectively. The saving in prestressing steel for precast beams in the bridge deck with a partially prestressed slab compared to a reinforced concrete slab will be more than sufficient to provide the prestressing steel required for the top slab. The reduction in the number of strands in the beam itself reduces the prestress loss in the mid-span region and becomes advantageous at the ends of the beam where debonding has to be carried out.

9.1.6 Increase in the Span Range for Precast Beams

For the two-span bridge example considered, the M-8 section composite beam with a reinforced concrete slab was just sufficient to carry the flexural stresses, with a very high prestress, for the span (30 m) and the loading (37.5 HB units) considered. On the other hand, the same M-8 section was satisfactory in a bridge deck with a prestressed slab, to carry even larger live loads at the span of 30 m (which is greater than the recommended limit of 27 m) and with a beam spacing of 1.25 m, providing shear does not become critical.

9.1.7 Positive Moment Reinforcement

In continuous composite bridge decks with a reinforced concrete slab, it is often necessary to provide reinforcement at the bottom of the section at the support to resist any sagging moment that may develop due to creep effects when live load is not on the bridge deck [24,38]. Such reinforcement may not be necessary when the continuity is developed using this new method as the weight of the slab cast in the second stage generates a permanent hogging moment at the support which may counteract sagging moment which develops due to creep effects even when live load is not acting. However, more experimental data is required on the long term effects of prestressed slabs before any firm conclusions are made.

9.1.8 Section for the Design of Prestress in the Slab

In the case of bridge decks with a prestressed slab, the critical section for the design of the prestressing force for the slab is at the diaphragm. However, it is uneconomical to base the amount of prestress required in the slab on the diaphragm section which is of relatively short length and of rectangular section. Therefore it is recommended that the adjoining composite section should be considered in the design.

9.1.9 Compressive Stress in the Bottom Flange of Precast Beams

It can be seen from the design of two bridge decks with prestressed slabs that the prestress applied to the slab does not cause any increase in the bottom flange where it is not required. The stress at the bottom due to prestressing force in the slab was nearly zero in the bridge models with both fully prestressed and partially prestressed slabs.

9.2 Conclusions of the Flexural Tests

9.2.1 Cracking Load

The flexural cracking loads of the beams with a partially prestressed slab and a fully prestressed slab were 3.0 and 4.6 times that of beam with the reinforced concrete slab. Cracking occurred well below the service load for the beam with the reinforced concrete slab while no cracks appeared in the beams with prestressed slabs under service load. The measured cracking load of beams with prestressed slabs gave close agreement with the calculated cracking load using the test results for modulus of rupture.

9.2.2 Crack Width

Crack widths were smaller at their first appearance in the prestressed slabs than in the reinforced concrete slab, and these cracks completely closed after unloading in the beams with prestressed slabs. In the beam with the partially prestressed slab, the width of reopened cracks at service load in the second stage of loading was very small (0.05 mm) while reopening of cracks did not occur in the fully prestressed slab under service loads. In comparison, crack widths in the beam with a reinforced concrete slab under service loads exceeded the limiting crack width given in BS 5400 : Part 4 [27].

Improved crack control expected for the prestressed slabs in the composite beams is confirmed by these observations.

9.2.3 Cracking In Diaphragm Section

It was observed in the three tests that the first flexural crack tended to

appear in the diaphragm section or very close to it. However, these cracks did not become critical with increase in load. This justifies the recommendation given in Section 9.1.8 for selection of the prestress in the slab.

9.2.4 Load-Deflection Characteristics

Due to the increase in the cracking load, the deflection of composite beams with prestressed slabs were smaller than those in the beam with the reinforced concrete slab. Up to the cracking load, a linear load-deflection relationship was obtained for all three beams.

When the beams with the prestressed slabs were unloaded and then reloaded after the first flexural crack, the load-deflection curves for the second stage were very similar to those in the first stage indicating that such beams behave as uncracked beams after the removal of overload which caused the initial cracking. The residual deflections were also smaller in those beams. Beyond the cracking load, the load-deflection relationship of the three beams was similar.

The ductility of the composite beams did not seem to be affected by the application of prestress as all three beams underwent large deflections and gave ample warning of failure.

9.2.5 Methods of Calculation of Deflection

Both BS 8110 method (based on curvature) [28] and ACI method(I_e method) [35] which are given mainly for monolithic beams are satisfactory in predicting short-term deflection of continuous composite beams similar to those tested in this study. The ACI method gave a better agreement with measured values, and for this method, the use of an approximate formula for second moment of area of the cracked section as given in PCI Handbook [53] was found to be sufficient.

9.2.6 Analysis of the Cracked Section

The use of linear methods for the analysis of the cracked composite section at the diaphragm gave satisfactory results for all three beams up to yielding of steel. For the beams with prestressed slabs, the method given in the Concrete Society Technical Report 23 [37] predicted the steel stress and gave close agreement with the measured values, especially for the beam with the partially prestressed slab. However, such agreements with measured values for the three beams were obtained only when tension stiffening effects were considered.

9.2.7 Tension Stiffening

For both deflection and steel stresses calculated using the methods described above, better agreements with the measured values were obtained when tension stiffening effects were considered. For composite beams in negative bending, it is important that the tension carried by the concrete is included in the calculations as the tensile zone of the concrete has a significant area (top slab). These effects can be conveniently included by considering an approximate tensile distribution such as that given in British codes [27,28].

9.2.8 Ultimate Behaviour

9.2.8.1 Mode of Failure

The beams tested in the series failed in tension. This would be the mode of failure for most practical cases of partially continuous composite bridge beams. Even though the steel areas provided in the slab were small, the beams failed only after developing large cracks and deflections, and carried considerable additional

load after the commencement of yielding of steel which occurred at about 70% of the failure load. The ratio of ultimate load to cracking load for the three beams with the reinforced concrete slab, the partially prestressed slab and the fully prestressed slab were 4.6. 2.46 and 2.30 respectively. The above ratios for the beams with prestressed slabs are more than sufficient to ensure that sudden failure does not occur immediately after cracking.

9.2.8.2 Increased Strength of Diaphragm

The diaphragm section of the deck, being made of concrete of lower strength and subjected to the greatest bending moment, showed increased strength compared to the composite section, and failure always occurred just outside the diaphragm. The increase in strength of the diaphragm can be attributed to the action of point loads on the diaphragm and which restrained the propagation of any critical crack.

From these observations together with results of tests reported by Kaar et al [8] and Rostasy [15], it can be concluded that the the composite section adjacent to the diaphragm can be considered to be the critical section for the ultimate strength of continuous composite beams at the interior support.

9.2.8.3 Ultimate Strength

The ratio of measured ultimate strength to calculated ultimate strength (ignoring prestress in the precast beams) for the beams with the reinforced concrete slab was 0.92 while an increased ratio of 1.23 and 1.33 were obtained for the beams with the partially prestressed slab and the fully prestressed slab. When 20% of the prestress in the girders was considered, the ratio for the prestressed slabs reduced slightly. However, as full prestress in the girder will

not develop at the critical section and the above ratio for the partially prestressed slab is not significantly above unity, it is suggested that the prestress effects in the girders in the design of interior support sections of bridge decks with prestressed slabs be ignored.

It can be concluded that the continuity and composite action developed by prestressed slabs is structurally efficient at all levels of loading.

9.3 Conclusions of Shear Test Series

9.3.1 Inclined Cracking

In all eight beams, only web shear cracks developed in the web due to the high principal tensile stresses produced. Flexural shear cracks did not develop in these beams which had a shear span/effective depth ratio of 2.35 and 3.5, and b_w/d ratio of 0.125. Even when flexural cracks did appear before the inclined cracks in beams with a reinforced concrete slab, they were too close to the diaphragm to develop into flexural shear cracks. No flexural crack developed before inclined cracking in the beams with prestressed slab. However, flexural shear cracks appeared in the three beams of the flexural test series which had a shear span/effective depth ratio of 5.6. For composite beams with prestressed slabs, it is the web shear cracking load which will be critical in the design for vertical shear at interior supports when the shear span/effective ratio is less than 4.0.

9.3.2 Region of Inclined Cracking

In the majority of the beams tested, the first web shear crack appeared close to the diaphragm. The centre of these inclined cracks was between 200 mm and 250 mm from the support. Therefore, checking web shear strength at a

section at a distance of the centroidal height from the end of bearing, as implied by BS 8110, seems to be satisfactory.

9.3.3 Principal Stresses in the Web

Theoretical analysis showed that the critical level for the maximum principal tensile stress, for the prestress and the loading arrangement used, occurred at the top of the web up to about 350 mm from the support. Beyond that, the difference between the stress at the top of web and the centroid of the composite section became smaller.

The principal stresses determined from the strain rosette readings tended to be greater than the calculated values. The maximum principal tensile stress so determined before inclined cracking was in the range 2.9 to 4.8 N/mm^2 while the range for the principal compressive stress was 10.3 to 18.2 which corresponded to about 0.23 f_{cu}. Therefore, any adverse influence on principal tensile strength of concrete from the compressive stress was minimal.

9.3.4 Inclined Cracking Under Serviceability Shear Force

In two beams with a reinforced concrete slab, inclined cracking developed below the serviceability shear force considered for the beams, and the cracks at the serviceability shear force in these beams were 0.20 mm wide. All beams with a prestressed slab were free of inclined cracks under service conditions indicating the advantage of having prestressed slabs in the hogging moment regions.

9.3.5 Influence of the Prestress in the Top Slab on Inclined Cracking Load

When the level of prestress in the top slab was increased during the first three tests, it resulted in a considerable increase in the web shear cracking load. The beams with the partially prestressed slab and the fully prestressed slab had a 25% and 48% greater inclined cracking load than the beam with reinforced concrete. The same trend was observed in the tests of beams with a partially prestressed slab and a reinforced concrete slab when the effects of other variables were studied. This means that a reduction in the amount of shear reinforcement can be achieved in beams with prestressed slabs near the interior support.

9.3.6 Influence of Other Variables Considered on the Inclined Cracking Load

Of the two other variables considered, the shear reinforcement percentage did not show any definite effect in influencing web shear cracking load. Therefore, its influence on inclined cracking load can be considered to be insignificant.

The inclined cracking load reduced slightly for beams with a partially prestressed slab and a reinforced concrete slab, when the shear span/effective depth ratio was increased from 2.35 to 3.53. However, a greater reduction was observed when the results of other beams in which the shear reinforcement percentage was changed were also considered. Therefore, it can be concluded that the increase in shear span/effective depth ratio tends to reduce the inclined cracking load of continuous composite beams.

9.3.7 Prediction of Web Shear Cracking Load by Design Codes

The comparison of measured web shear cracking load for the shear span of the main beam with the values calculated using different code equations indicates that British and American codes equations will give a safe prediction when the entire composite section is considered at the recommended distance from the support, even when the top slab is flexurally cracked. As specified in codes, the vertical component of the prestressing force for inclined tendons can be included in the web shear cracking load V_{co}. When the top slab was ignored by considering only the precast section as carrying total shear force, very conservative results were obtained even for the beams with reinforced concrete slabs. The CEB-FIP code equation was also found to be very conservative.

The best prediction of the web shear cracking load was obtained when the basic principal tensile stress equation (Eqn. 7.6) was applied at the centroid of the composite section while considering actual sectional properties. For composite beams with a prestressed slab, it gives a safe prediction when the actual partial safety factors for f_t and f_{cp} are applied. This method slightly overestimated V_{co} for two of the three beams with a reinforced concrete slab. Therefore, for the continuous composite beams with a reinforced slab, the more conservative British Code equation is recommended for use considering the entire composite section.

9.3.8 Prediction of the Flexural Shear Cracking Load

For the three beams in the flexural test series which developed flexural shear cracks, a comparison between the measured and calculated (according to BS 8110 and ACI Building Code) cracking load was made and the results show that the BS 8110 equation for V_{cr} gives the best prediction of the three methods considered

for the composite beams with prestressed slabs when the entire composite section is considered. The corresponding equation of the ACI Building Code was found to be slightly unsafe. Also, the calculation of M_o for BS 8110 equation based on the stress at the top of precast beams was found to be unsafe.

9.3.9 Ultimate Shear Strength of Beams

9.3.9.1 Mode of Failure

All eight beams failed in web crushing in one of the shear spans. The failure could be described as gradual rather than sudden at the time of failure, and the shear reinforcement in the failure zone reached yield stress before web crushing. The web crushing was mainly observed in the upper part of the web and therefore did not agree with the hypothesis proposed by Mattock and Kaar[23] that inclined struts fail in combined action of bending and shear at the base of the web.

9.3.9.2 Variation of Ultimate Strength with Prestress in the Slab

The results of the first three beams tested showed slight increase in ultimate shear strength when the level of prestress varied from zero to full prestress. Therefore, it can be concluded that the prestress in the top slab has no significant influence on the ultimate strength of thin webbed composite beams failing in web crushing. The advantage of having a prestressed slab at the support lies in the increased inclined cracking strength.

9.3.9.3 Prediction of Web Crushing Strength by Different Codes

Of the maximum limit for the shear stress given in different codes, ACI code gave the best prediction for the web crushing strength with a mean ratio of

observed to predicted web crushing strength of 1.12. The British codes were more conservative with BS 5400 giving a mean ratio of 1.33 while BS 8110 prediction having a higher ratio of 1.54. Both Standard and Accurate methods of CEB-FIP methods were unsafe in predicting web crushing strength.

9.3.9.4 Variation of Ultimate Strength with Shear Reinforcement Percentage

Although all beams failed in web crushing, ultimate strength increased with the increase in shear reinforcement percentage. The stirrups in the beams with smaller shear reinforcement percentages failed after undergoing very high strains after yielding. Relatively smaller stirrup strains in beams with the highest percentage (0.84%) after yielding suggests that this value is near the upper limit for web reinforcement for the composite section considered.

The results also indicated that the modified truss analogy approach used in British and American codes does not give an accurate prediction for such a high amount of shear reinforcement. Considering the contribution of concrete at ultimate limit state is 80% of inclined cracking load will give a better prediction with truss analogy for such cases.

9.4 Recommendations for Future Research

In this study, the effects of prestressed slabs on the flexural and shear behaviour of the continuity connection were investigated. Further investigations are required in the following areas.

(1) Conditions at the ends of the prestressed portion of the slab under different loading arrangements to obtain an optimum value for the ratio of length of prestressed slab to overall span.

(2) Effects of prestress on the precast beam at sections away from the support region.

(3) Secondary effects of prestressing the slab.

(4) Redistribution of moments in a continuous composite beam with a prestressed slab at the interior support.

(5) Behaviour of the continuity connection under cyclic loading.

(6) Long-term creep and shrinkage effects of prestressed slabs in a continuous beam.

(7) Shear tests on continuous composite beams with shear span/effective depth ratios between 3.0 and 6.0 to evaluate the accuracy of design approaches for flexural shear cracking.

(8) Effect of variation of prestress in the precast beam on shear strength.

(9) Effect of prestressed slab in hogging moment regions of composite beams with greater web width to effective depth ratio.

REFERENCES

1. **Manton B. H. and Wilson C.B.**

   MoT/C & CA Standard Bridge Beams.

   Cement And Concrete Association Publication 32.012, March 1971

2. **Prestressed Concrete Association**

   Publication on Standard Prestressed Concrete Bridge Beams. January 1984

3. **Naaman A.E.**

   Prestressed Concrete Analysis and Design: Fundamentals. McGraw-Hill, 1982

4. **Tilly G.P.**

   Durability of Concrete Bridges. Journal of the Institute of Highways and Transportation, Vol. 35, No. 2, February 1988, pp. 10-19.

5. **Loveall, C.L.**

   Jointless Bridge Decks. ASCE Civil Engineering, Vol. 55, No. 11, November 1985, pp. 64-67.

6. **Lin, T.Y. and Burns, N.H.**

   Design of Prestressed Concrete Structures. John Wiley & Sons, New York, Third Edition, 1982 .

7. **Leonhardt, F.**

   Prestressed Concrete: Design and Construction. Wilhelm Ernst & Sonh, Berlin, Second Edition, 1964.

8. **Kaar, P.H., Kriz, L.B. and Hognestad, E.**

   Precast-Prestressed Concrete Bridges; (1) Pilot Tests of Continuous Beams. Journal of Portland Cement Association Development Department, Bulletin D34, May 1960

9. **McHenry, D and Mattock, A.H.**

   Development of Continuity in Precast Prestressed Construction. Final Report, IABSE Sixth Congress (Stockholm), 1960, pp. 399-412 .

10. **Burns, N.H.**

Development of Continuity between Precast Prestressed Concrete Beams. Journal of PCI, Vol. 11, No.3, June 1966, pp. 23-36.

11. **Mirtalaie, K.**

Shear Transfer between Precast Prestressed Bridge Beams and In-Situ Concrete Crosshead in Concrete Structures. Ph. D Thesis, University of Leeds, April 1988.

12. **Freyermuth, C.L.**

Design of Continuous Highway Bridges with Precast Prestressed Girders. Journal of PCI, Vol. 14, April 1969, pp. 14-39.

13. **Anderson, C., Houdeshell, D.M. and Gamble, W.L.**

Construction and Long-Term Behaviour of 1/8th Scale Prestressed Concrete Bridge Components. Illinois University Department of Civil Engineering, Structural Research Series 384, October 1972 .

14. **Gamble, W.L.**

Overload Behaviour of 1/8 th Scale Three Span Continuous Prestressed Concrete Bridge Beams. Illinois University, Department of Civil Engineering, Structural Research Series, No. 478, May 1980, p 87.

15. **Rostasy, F.S.**

Connections in Precast Concrete Structures-Continuity in Double-T Floor Construction. Journal of PCI, Vol. 7, August 1962, pp. 18-48.

16. **Poston, R.W., Carrasquillo, R.L. and Breen, J.E.**

Durability of Post-tensioned Bridge Decks. ACI Materials Journal, Vol. 84, July-August 1987, pp. 315-326.

17. **Poston, R.W., Carrasquillo, R.L. and Breen, J.E.**

Design Procedures for Prestressed Concrete Bridge Decks. Research Report No. 316-3F, University of Texas, Austin, November 1985.

18. **Basu, P.K., Sharif, A.M. and Ahmed, N.U.**

Partially Prestressed Continuous Composite Beams 1. Journal of Structural Engineering, Vol. 113, No. 9, September 1987, pp.1909-1925.

19. **Basu, P.K., Sharif, A.M. and Ahmed, N.U.**

Partially Prestressed Continuous Composite Beams 2. Journal of Structural Engineering, Vol. 113, No. 9, September 1987, pp. 1926-1938.

20. **Kennedy, J.B. and Grace, N.F.**

Prestressed Decks in Continuous Composite Bridges. ASCE Journal of Structural Division, Vol. 108, November 1982, pp. 2394-2410.

21. **Hanson, N.W.**

Precast-Prestressed Concrete Bridges; Part 2. Horizontal Shear Transfer. Journal of PCA Development Department, Bulletin D35, May 1960.

22. **Mattock, A.H. and Kaar, P.H.**

Precast-Prestressed Concrete Bridges; Part 3. Further Tests of Continuous Girders. PCA Development Department, Bulletin D43, September 1960.

23. **Mattock, A.H. and Kaar, P.H.**

Precast-Prestressed Concrete Bridges; Part 4. Shear Tests of Continuous Girders. PCA Development Department, Bulletin D45, January 1961.

24. **Mattock, A.H.**

Precast-Prestressed Concrete Bridges; Part 5. Creep and Shrinkage Studies. PCA Development Department, Bulletin D46, May 1961.

25. **Mattock, A.H. and Kaar, P.H.**

Precast-Prestressed Concrete Bridges; Part 6. Test of Half Scale Highway Bridge Continuous over Two Spans. PCA Development Department Bulletin D51, September 1961.

26. **British Standard Institution**

BS 5400 : Part 2 (1978) Specification for Loads on Steel, Concrete and Composite Bridges.

27. British Standard Institution

BS 5400 : Part 4 (1984) Code of Practice for Design of Concrete Bridges.

28. British Standards Institution

BS 8110 : Part 1(1985) Structural Use of Concrete.

29. Hand book to BS 8110(1985)

Structural Use of Concrete. Palladian Publication, London, 1987.

30. Kirkpatrick, J., Long, A.E. and Thompson, A.

Load Distribution Characteristics of Spaced M-Beam Bridge Decks.

The Structural Engineer, Vol. 62 B, No. 4, December 1984, pp. 86-88.

31. Jaeger, L.G. and Bahkt, B.

The Grillage Analogy in Bridge Analysis. Canadian Journal of Civil Eng,

Vol. 9, Part 2, January 1982, pp.224-235.

32. West, R.

C & CA / CIRIA Recommendations on the Use of Grillage Analysis for Slab and Pseudo-Slab Bridge Decks. C & CA Research Report 41.021, 1973, London.

33. Cusens, A.R. and Pama, R.P.

Bridge Deck Analysis, Wiley, London 1976

34. Department of The Environment, Highway Engineering Computing Branch.

HECB B/9 GRIDS., Program for the Analysis of Slab and Pseudo-Slab Bridge Decks. 1975.

35. American Concrete Institute.

Building Code Requirements for Reinforced Concrete (ACI 318-83), 1983.

36. American Concrete Institute, Committee 318.

Commentary on Building Code Requirements for Reinforced Concrete, 1983.

37. Concrete Society.

Partial Prestressing, Technical Report No. 23, 1983.

38. Clark, L.A.

Concrete Bridge Design to BS 5400. Construction Press, London, 1983.

39. American Association of State Highway and Transportation Officials (AASHTO)

Standard Specifications for Highway Bridges. Thirteenth Edition, 1983.

40. CEB-FIP

Model Code for Concrete Structures. English Edition, Paris, 1978.

41. FIP Recommendations

Practical Design of Reinforced and Prestressed Concrete Structures.

Thomas Telford, London, 1984.

42. Sabnis, G.M.

Handbook of Composite Construction Engineering. Van Nostrand Reinhold, New York, 1979.

43. Nilson, A.H. and Winter, G.

Design of Concrete Structures. McGraw-Hill, Tenth Edition, 1986.

44. Carreira, D.J. and Chu, K.

Stress-Strain Relationships for Plain Concrete in Compression.

ACI Journal, Proceedings Vol. 82, No. 6, Dec. 1985, pp. 797-804.

45. British Standards Institution.

CP 110: Part 1 (1972). The Structural Use of Concrete.

46. Beeby, A.W.

The Design of Sections for Flexure and Axial Load According to CP 110.

C & CA Development Report 2, December 1978.

47. Sabnis, G.M. and Mirza, S.M.

Size Effects in Model Concretes. Journal of Structural Division, Proceedings of ASCE, Vol. 105, June 1979

48. Blackman, J.S. , Smith, G.M. and Young, L.E.

Stress Distribution Affects Ultimate Tensile Strength. Journal of ACI,

Vol. 30, N0. 6, December 1958, pp. 679-684.

49. Beeby, A.W.

Short-term Deformations of Reinforced Concrete Members. C & CA Technical Report 42.408, March 1968.

50. Leonhardt, F.

Cracks and Crack Control in Concrete Structures. PCI Journal, Vol. 33, No. 4, July-August 1988, pp 124-143.

51. Clark, L.A. and Speirs, D.M.

Tension Stiffening in Reinforced Concrete Beams and Slabs Under Short-Term Load. C & CA Technical Report 42.521, July 1978.

52. Allen, A.H.

Reinforced Concrete Design to CP 110- Simply Explained. C & CA Publication 12.062, 1974.

53. Prestressed Concrete Institute

PCI Design Handbook : Precast Prestressed Concrete. Chicago, 1978.

54. Branson, D.E.

Design Procedures for Computing Deflections. Journal of ACI, Vol. 75, No. 9, September 1968, pp. 730-742.

55. Branson, D.E. and Trost, H.

Unified Procedures for Predicting the Deflection and Centroidal Axis Location of Partially Cracked Non-Prestressed and Prestressed Concrete Members. ACI Journal, Vol. 79, N0 2, March-April 1982, pp 119-130.

56. Shaikh, A.F. and Branson, D.E.

Non-tensioned Steel in Prestressed Concrete Beams. PCI Journal, Vol. 15, N0. 1, February 1970, pp. 14-36.

57. ACI Committee 435

Proposed Revisions by Committee 435 to ACI Building Code and Commentary Provisions on Deflections. ACI Journal, Vol. 75, No.6, June 1978,

Provisions on Deflections. ACI Journal, Vol. 75, No.6, June 1978, pp. 229-238.

58. **British Standards Institution**

BS 1881 (1983) Testing Concrete.

59. **Warwaruk, J., Sozen, M.A. and Siess, C.P.**

Investigation of Prestressed Reinforced Concrete for Highway Bridges, Part 3, Strength and Behaviour in Flexure of Prestressed Concrete Beams. University of Illinois, Engneering Experimentation Station Bulletin No.464, August 1962.

60. **Janney, J.R., Hognestad, E. and McHenry, D.**

Ultimate Flexural Strength of Prestressed and Conventionally Reinforced Beams. Journal of ACI, Vol. 52, February 1956, pp. 601-620.

61. **Olesen, S.O., Sozen, M.A. and Siess, C.P.**

Investigation of Prestressed Reinforced Concrete for Highway Bridges, Part 4: Strength of Beams with Web Reinforcement. University of Illinois Engineering Experiment Station Bulletin 493, July 1967, p 46.

62. **Bennett, E.W.**

Shear Strength of Prestressed Concrete Bridge Beams Type 61. Final Report Proposed for the West Riding County Council, Univ. of Leeds, August 1971.

63. **Bennett, E.W.**

Full-Scale Tests on Two Types of Stirrup in Motorway Bridge Beams. Report Prepared for Leonard Fairclough Ltd., Univ. of Leeds, April 1972.

64. **Clarke, J.L. and Evans, D.J.**

Vertical Shear Strength of Composite Beams. C & CA Technical Report 556, March 1983.

65. **Tay, C.J.**

Shear Strength of Full-Sized Prestressed Concrete Composite Bridge Beams, Ph.D thesis, University of Leeds, December 1983.

66. **MacGregor, J.G., Sozen, M.A. and Siess, C.P.**

Effect of Draped Reinforcement on Behaviour of Prestressed Concrete Beams. Journal of ACI, Vol. 57, No. 6, December 1960, pp. 649-677.

67. **Bresler, B. and MacGregor, J.G.**

Review of Concrete Beams Failing in Shear. Journal of Structural Division, Proc. of ASCE, Vol. 93, Feb. 1967, pp. 343- 372.

68. **Sozen, M.A., Swoyer, E.M. and Siess, C.P.**

Investigation of Prestressed Concrete for Highway Bridges, Part 1: Strength in Sherar of Beams Without Web Reinforcement. Engineering Experiment Bulletin 452, University of Illinois, Urbana, April 1959.

69. **Leonhardt, F.**

Shear and Torsion in Prestressed Concrete. Proceedings, Sixth Congress of FIP, Session 4, Prague, 1970, pp. 137-135.

70. **ACI-ASCE Committee 326**

Shear and Diagonal Tension. Proceedings of ACI, Vol. 59, Jan., Feb., and March 1962, pp. 1-30, 277-334 and 353-396.

71. **Bennett, E.W.**

Structural Concrete Elements. Chapman and Hall, London, 1973.

72. **Mlingwa, G.**

Vertical Prestressed Tendons as Shear Reinforcement in Prestressed Concrete Beams, Ph.D Thesis, University of Leeds, August 1978.

73. **Reynolds, G.C., Clarke, J.L and Taylor, H.P.J.**

Shear Priovisions for Prestressed Concrete in the Unified Code, CP 110.

C & CA Technical Report 42.500, 1974.

74. **Balasooriya, B.M.A.**

The Diagonal Compression Mode of Shear Failure in Reinforced and Prestressed Concrete Beams, Ph.D Thesis, University of Leeds, August 1969.

75. Bennett, E.W. and Balasooriya, B.M.A.

Shear Strength of Prestressed Beams with Thin Webs Failing in Inlined Compression. ACI Journal, Vol. 68, N0. 3, March 1971, pp. 204-212.

76. Arthur, P.D.

The Shear Strength of Pre-tensioned I-Beams with Unreinforced Webs. Magazine of Concrete Research, Vol. 17, No.53, Dec. 1965, pp.119-210.

77. Hicks, A.B.

The Influence of Shear Span and Concrete Strength upon the Shear Resistance of Pretensioned Prestressed Beams. Magazine of Concrete Research, Vol. 12, No. 30, November 1958, pp. 115-122

78. Evans, R.H. and Hosny, A.H.

The Shear Strength of Post-tensioned Prestressed Concrete Beams. Third Congress of FIP, Section 1, Paper No. 11, Berlin 1958, pp. 112-132

79. Elzanaty, A.H., Nilson, A.H. and Slate, F.O.

Shear Capacity of Prestressed Concrete Beams Using High Strength Concrete. Journal of ACI, Vol. 83, May-June 1986, pp. 359-368.

80. MacGregor, J.G., Sozen, M.A. and Siess, C.P.

Strength of Prestressed Concrete Beams With Web Reinforcement.

Journal of ACI, Vol. 62, No.12, Dec. 1965, pp. 1503-1519.

81. ACI-ASCE Committee 426

Shear and Diagonal Tension - The Strength of Reinforced Concrete Members.

Journal of Structural Divsion. Proceedings of ASCE, Vol. 99, No. ST6, June 1973, pp. 1091-1187.

82. Sozen, M.A. and Hawkins, N.M.

Discussion of a Paper by ACI-ASCE Committee 326. Shear and Diagonal Tension. ACI Journal, Proceedings, Vol. 59, Sep. 1962, pp. 1341-1347.

83. Rangan, B.V.

Shear Strength of Partially and Fully Prestressed Concrete Beams. Civil

Engineering Transactions, The Institute of Engineers, Australia, 1979.

84. **Thurlimann, B.**

Shear Strength of Reinforced and Prestressed Concrete- CEB Approach, ACI Special Publication SP 59, June 1979, pp. 93-115.

85. **Acharya, D.N. and Kemp, K.O.**

Significance of Dowel Forces on the Shear Failure of Rectangular Beams with Web Reinforcement. Proccedings, ACI, Vol.62, Oct.1965, pp. 1265-1278.

86. **Fenwick, R.C. and Paulay, T.**

Mechanisms of Shear Resistance of Concrete Beams. Journal of Structural Division, Proc. of ASCE, Vol. 94, October 1968, pp. 2325-2350.

87. **Taylor, H.P.J.**

Investigation of Forces Carried Across Cracks in Reinforced Concrete Beams in Shear by Interlock of Aggregate. C & CA Technical Report 42.477, 1970.

88. **Taylor, H.P.J.**

Investigation of Dowel Shear Forces Carried by the Tensile steel in Reinforced Concrete Beams. C & CA Technical Report TRA 431, November 1969.

89. **Kani, G.N.J.**

A Rational Theory for the Function of Web Reinforcement. Journal of ACI, Vol. 66, No. 3, March 1969, pp. 1069-1091.

90. **Swamy, R.N., Andriopoulus, A. and Adepegba, D.**

Arch Action and Bond in Concrete Shear Failures. Journal of Structural Division, Proc. of ASCE, Vol. 96, ST6, June 1970, pp. 1069-1091.

91. **Walraven, J.C.**

Tests on Partially Prestressed T-Beams Subjected to Shear and Bending. Eigth International FIP Congress (London), Heron, Vol. 23, No. 1, 1978.

92. **Braestrup, M.W.**

Plastic Analysis of Shear in Reinforced Concrete. Magacine of Concrete Research, Vol. 26, No. 89, December 1974, pp. 221-228.

93. Nielsen, M.P. and Braestrup, M.W.

Shear Strength of Prestressed Concrete Beams without Web Reinforcement. Magazine of Concrete Research, Vol.30, No.104, Sept. 1978, pp. 119-128.

94. Lyngberg, B.S.

Ultimate Shear Resistance of Partially Prestressed Reinforced Concrete I Beams. Journal of ACI, Proc., Vol. 73, No. 4, April 1976, pp. 214-222.

95. Leonhardt, F.

Reducing the Shear Reinforcement in Reinforced Concrete Beams and Slabs. Magazine of Concrete Research, Vol. 17, No. 53, Dec. 1965, pp. 187-198.

96. Clarke, J.L. and Taylor, H.P.J.

Web Crushing, A Reveiw of Research. C & CA Technical Report TRA 509, 1975.

97. Leonhardt, F. and Walther, R.

The Stuttgart Shear Tests 1961: Contribution of the Treatment of the Problems of Shear in Reinforced Concrete Construction. C & CA Library Translation No. 111, London 1961.

98. Rezai-Jarobi, H. and Regan, P.E.

Shear resistance of Prestressed Concrete Beams with Inclined Tendons. The Structural Engineer, Vol. 64B, No. 3, Sept. 1986, pp. 63-75.

99. Department of Environment, London

Technical Memorandum (Bridges) BE 2/73 : Prestressed Concrete For Highway Structures. February 1973.

100. Saemann, J.C. and Washa, G.W.

Horizontal Shear Connection Between Precast Beams and Cast-In-Place Slabs. ACI Journal, Vol. 61, No. 11, Nov. 1964, pp. 1383-1409.

101. Badoux, J.C. and Hulsbos, C.L.

Horizontal Shear Connection in Composite Concrete Beams Under Repeated Loads. ACI Journal, Vol. 64, No.12, Dec. 1967, pp. 811-819.